World Renewable Energy Congress – Sweden

8–13 May, 2011
Linköping, Sweden

Editor

Professor Bahram Moshfegh

Copyright

Linköping Electronic Conference Proceedings, 57
Linköping University Electronic Press
Linköping, Sweden, 2011

http://www.ep.liu.se/ecp_home/index.en.aspx?issue=057
ISBN: 978-91-7393-070-3
ISSN 1650-3740 (online)
ISSN 1650-3686 (print)

Volume 5

Goethermal Applications

Table of Contents

Energetic performance evaluation of an earth to air heat exchanger system for agricultural building heating

Onder Ozgener[1,*], Leyla Ozgener[2]

[1]*Solar Energy Institute, Ege University, Bornova, Izmir, Turkey*
[2]*Department of Mechanical Engineering Faculty of Engineering,*
Celal Bayar University, Muradiye, Manisa, Turkey
** Corresponding author. Tel: +90 232 3111232, Fax: +90 232 3886027, E-mail: Onder.Ozgener@ege.edu.tr*

Abstract: The main objective of the present study is to investigate the performance characteristics of an underground air tunnel (**E**arth to **A**ir **H**eat **E**xchanger) for greenhouse heating with a 47 m horizontal; 56cm nominal diameter U-bend buried galvanized ground heat exchanger. This system was designed and installed in the Solar Energy Institute, Ege University, Izmir, Turkey. Based upon the measurements were made in the heating mode. The system COP was calculated based on the amount of heating produced by the air tunnel and the amount of power required to move the air through the tunnel.

Keywords: *Energy, earth to air heat exchangers, COP, sustainable resources*

Nomenclature

COP, heating coefficient of performance of the system
D *pipe diameter*
f *fraction losses coefficient*
$h_{a,i}$ *specific enthalpy at underground air tunnel inlet*
$h_{a,0}$ *specific enthalpy at underground air tunnel outlet*
$h_{b,i}$ *specific enthalpy at blower input*
$h_{b,o}$ *specific enthalpy at blower output*
$h_{v,i}$ *specific enthalpy of water vapor at underground air tunnel inlet*

T_f *arithmetic average temperature of air flowing in buried pipe*
U *Velocity*
V *volumetric flow rate of air*
w_i *absolute humidity at underground air tunnel inlet (kg moisture per kg dry air)*
w_0 *absolute humidity at underground air tunnel outlet (kg moisture per kg dry air)*

$\dot{W}_b$ *work input rate to the blower*
$h_{v,0}$ *specific enthalpy of water vapor at underground air tunnel outlet*
$\bar{h}_a$ *convective heat transfer coefficient of air*
k *coefficient of thermal conductivity of pipe*
L *pipe length*
$\dot{m}_a$ *mass flow rate of air*
Nu *Nusselt number*
Pr *Prandtl number*
Re *Reynolds number*
$\dot{Q}_r$ *extracted heat (underground air tunnel load)*
T_w *measured temperature of pipe surface.K, ºC*

Greek letters

η_{mec} *mechanic efficiency of fan*
ΔP *pressure loss*
ζ *particular resistance losses of pipe line*
ρ *density of air*

1. Introduction

Although various studies [e.g., 1-6] were undertaken to evaluate the performance of underground air tunnel, as described previously, to the best of authors' knowledge, except authors' previous works [1-5] no studies on the performance testing of an underground air tunnel with a 47m, 56cm nominal diameter U-bend horizontal galvanized ground heat exchanger for greenhouse cooling have appeared in the open literature under Turkey's conditions. This study consists of an alternative to heating greenhouses with the utilization of an underground air tunnel system. The present study undertakes performance evaluation of underground air tunnel systems –earth to air heat exchangers (EAHE)- and applies to a local one in Turkey. Namely, thermodynamics performance of an EAHE has been evaluated in a demonstration in Solar Energy Institute of Ege University, Izmir, Turkey.

2. System Description

2.1. Experimental set-up

This system mainly consists of two separate circuits: (i) the fan (blower) circuit for greenhouse cooling, and (ii) the ground heat exchanger (GHE) (underground air tunnel). The underground air tunnel system studied was installed at the Solar Energy Institute of Ege University (latitude 38^o 24' N, longitude 27^o 50' E), Izmir, Turkey. Solar greenhouse was positioned towards the south along south-north axis. The greenhouse will be conditioned during the summer and winter seasons according to the needs of the agricultural products to be grown in it. A positive displacement type of air (twin lobe compressor) blower of 736 Watt capacity and volumetric flow rate of 5300m^3/h was fitted with the suction head positioned in the southwest corner of the greenhouse [1-5].

2.2. Measurements

Experiments were performed at the Ege University, Izmir, Turkey. A galvanized pipe of 56cm in diameter 47m in length was buried in the soil at about 3m in depth, a galvanized pipe of 80cm in diameter 15m in length. The three main reasons for this (i) air blowing speed is advised to be 0-3m/s in greenhouses in terms of efficient grow crop from unit area, (ii) blower power consumption rate was reduced due to low pressure losses, and (iii) pipe works as a heater. It is well known that increasing surface area of heater leads to increasing convection heat transfer rate. Due to the reasons listed, pipe diameter was selected as large. The soil at site was a mixture of clay, sand and small rocks. A sample of the soil taken from 3m depth was tested for thermal properties. Thermal conductivity was estimated to be 2.850W/mK.Temperatures of air, galvanized pipe surface, and soil at different locations was measured using PT-100 resistant thermometers. The temperatures of the air were measured at distances of 0, 4.2m, 8.4m, 12.6m, 16.8m, 21.2m, 25.6m, 29.8m, 34m, 38.2m, 42.4m, and 47m from the inlet end. Since the resistant thermometers used to measure the air temperature in the pipe were not shielded, there would be a small error in the air temperature measurement because of infra red radiative transfer between the resistant thermometers and the pipe surface and line voltage drop between measuring point and display. To measure soil and pipe surface temperatures, the resistant thermometers was positioned in the soil at the 25.6m length of the pipe. Air velocity in the pipe measured about 1m from the entrance; these measurements were subject to error because of entry length. To minimize the errors, air velocity was at several points on four different points and then averaged [1-5].

3. Analysis

In this context, two different ways of formulating heat extraction rate. The first form of the rate of heat extraction by the underground air tunnel in the heating mode $\dot{Q}_r$ is calculated from the following equation [1-5]

$$\dot{Q}_r = \dot{m}_a\left(h_{a,i} - h_{a,o}\right) \qquad (1)$$

where

$h_{a,i} = \left(h_a\right)_i + w_i\left(h_v\right)_i$ and $h_{a,o} = \left(h_{a,o}\right) + w_o\left(h_{v,o}\right)$.

Note that here; the values of $h_{a,i}$ and $h_{a,o}$ can be directly obtained from the psychometric chart. The second form of the rate of heat extracted by the underground air tunnel can be written as follows:

$$\dot{Q}_r = \bar{h}_a A\left(T_w - T_f\right) \qquad (2)$$

with

$$\bar{h}_a = \frac{Nuk}{D}, \qquad (3)$$

$$Nu = 0.023\,\mathrm{Re}^{0.8}\,\mathrm{Pr}^{1/3}, \qquad (4)$$

where $\bar{h}_a$ is the convective heat transfer coefficient of air, A is the surface area of the underground air tunnel (galvanized pipe), T_w is the temperature of pipe surface, T_f is average temperature of air flowing in buried pipe (U-tube), k is the coefficient of thermal conductivity of the pipe, and D is the pipe diameter. The convective heat transfer coefficient " $\bar{h}_a$ " in the above equations depends on the Reynolds number, the shape and roughness of the pipe for turbulent flow. The work input rate to the blower is

$$\dot{W}_b = \frac{\dot{m}_a\left(h_{b,i} - h_{b,o}\right)}{\eta_{mec}} \qquad (5)$$

or

$$\dot{W}_b = \frac{\Delta P V}{\eta_{mec}} \qquad (6)$$

where ΔP is the pressure loss, V is the volumetric flow rate of air, and η_{mec} is the mechanic efficiency of the blower. ΔP is written as follows:

$$\Delta P = 0.5 f \frac{L}{D}\rho U^2 + \Sigma\zeta \qquad (7)$$

where U is the velocity, f is the fraction losses, ζ is the particular resistance losses and L is the pipe length. Hence, the COP of the system can be calculated as

$$COP = \frac{\dot{Q}_r}{\dot{W}_b} \qquad (8)$$

The coefficient of performance of the overall heating system *(COP)* is the ratio of the greenhouse heating load (heat extracted by the underground air tunnel, $\dot{Q}_r$) to work consumption of the blower ($\dot{W}_b$). It can be noticed that the heat generated by the fan goes into the heated space.

4. Results and Discussion

In the present study, the results obtained from the experiments were evaluated to determine the overall performance of the system. The minimum ambient air temperatures varied between 4.7 and 13 ^{o}C during the experimental studies. If the system is operated, the maximum greenhouse temperatures changes between 13.1 and 25.2 ^{o}C. The average values of the temperature for the ambient air and the greenhouse are obtained to be 12.98 ^{o}C and 20.2 ^{o}C, respectively. When the system operates, the greenhouse air is at a minimum day temperature of 13.1^{o}C with a relative humidity of 32%. The maximum COP of the underground air tunnel system occurred at approximately 07:31 AM on November 29, 2009. For example, the maximum heating power of 4.5 kW could be realized at 07:31 PM for the buried pipe with the radius of 0.28m. Fig. 1 shows the COP and heating capacity variations of the underground air tunnel system of 0.28m radius, and illustrates the hourly variations of COP for the period studied. The maximum heating coefficient of performance of the underground air tunnel system is about 6.42, while its minimum value is about 0.98 at the end of a cloudy and cold day and fluctuates between these values at other times. The total average COP in the heating season is found to be 5.16.

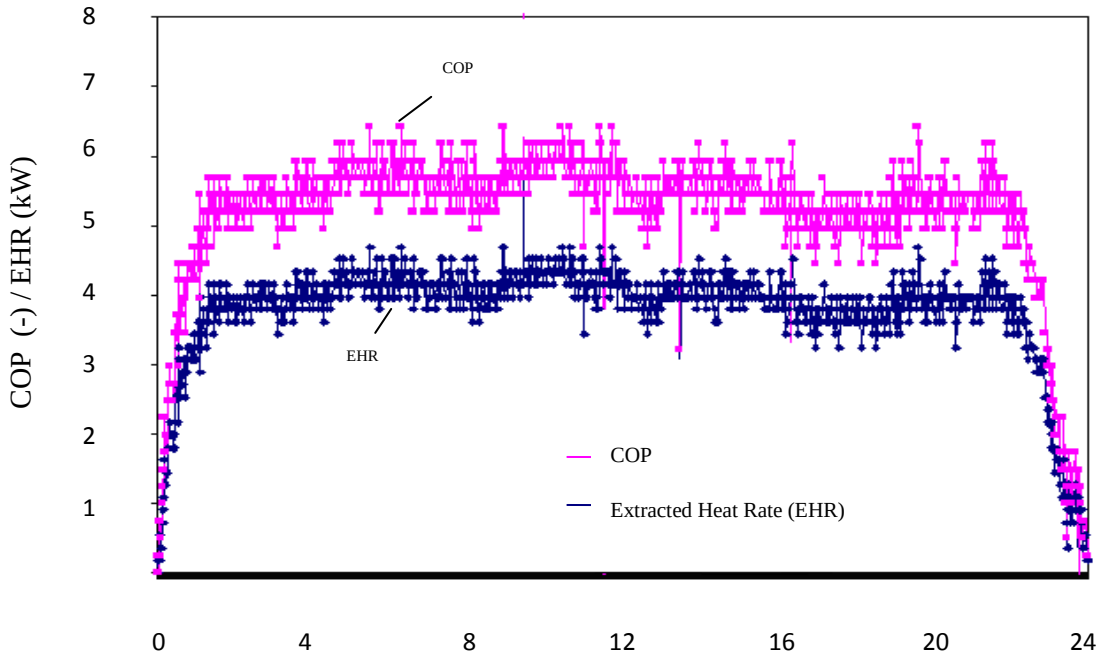

Fig. 1. Hourly variations of heating capacity and COP of the underground air tunnel system [4]

5. Conclusions

The experimental results indicate that this system can be used for greenhouse heating in the Mediterranean and Aegean regions of Turkey. During this test the underground air tunnel was able to provide 60.8 percent of the design heating load cold winter days. In spite of difficulties primarily encountered in coupling geothermal energy with conventional space heating and cooling equipment, underground air tunnels seem to be an exciting alternative [4].

Acknowledgements

The authors are grateful to Ege University Research Fund due to their financial supports.

References

[1] O. Ozgener, L. Ozgener, Exergoeconomic analysis of an underground air tunnel system for greenhouse cooling system, International Journal of Refrigeration 33(5), 2010, pp. 995-1005.

[2] O. Ozgener, L. Ozgener, Exergetic assessment of EAHEs for building heating in Turkey: A greenhouse case study, Energy Policy 38(9), 2010, pp. 5141-5150.

[3] L. Ozgener, O. Ozgener., Experimental study of the exergetic performance of an underground air tunnel system for greenhouse cooling, Renewable Energy 35(12), 2010, pp. 2804-2811.

[4] L. Ozgener, O. Ozgener, Energetic performance test of an underground air tunnel system for greenhouse heating, Energy 35(10),2010, pp. 262-268.

[5] O. Ozgener, L. Ozgener, D.Y. Goswami, Utilization of earth air heat exchangers for solar greenhouses pre heating and performance analysis. Project no: 09GEE003, supported by Ege University Research Fund , 2009, Continuing Project

[6] D.Y. Goswami, S. Ileslamlou, Performance analysis of a closed loop climate control system using underground air tunnel. Journal of Solar Energy Engineering 112, 1990, pp. 76-81.

An adaptive design approach for a geothermal plant with changing resource characteristics

M. Imroz Sohel[1,*], Mathieu Sellier[2], Susan Krumdieck[2]

[1] *Scion, Te Papa Tipu Innovation Park, 49 Sala Street, Rotorua, New Zealand*
[2] *Department of Mechanical Engineering, University of Canterbury, Private bag 4800, Christchurch, New Zealand*
** Corresponding author. Tel: +64 7 3435730; fax: +64 7 3435375; E-mail address: mohammed.sohel@scionresearch.com*

Abstract: Geothermal power plants are designed for optimal utilization of geothermal resource. However, geothermal fields typically undergo significant changes in resource characteristics such as pressure, temperature and steam quality over their life span. With appropriate reservoir modelling it is possible to predict the future resource characteristics of a geothermal field to a reasonable degree of accuracy. We propose a new adaptive design approach that would allow geothermal power plants to take into account the change of resource characteristics that occur over a 30-40 years time horizon based on the results of reservoir modelling. Currently, it is difficult and expensive to modify or renovate an existing plant due to space constraints, piping arrangements, transportation of machinery etc. The adaptive design approach would allow cost effective modifications in operation and equipment to adjust to changes in resource characteristics in the future. A simple model for a typical combined cycle geothermal power plant is considered as a test case for the adaptive design approach. Simulation is carried out using changes in both wellhead specific enthalpy and mass flow rate. There are four case studies presented in this paper that analysed various possible options of the hypothetical power plant depending on the changes in resource characteristics. Taking into account the results of the simulation, alternative plant designs are presented and improvements in performance are discussed. Although, the initial investment cost might go up as a consequence of adaptive design, over the life span of the plant the total benefit may be greater.

Keywords: *Geothermal power, resource characteristics change, adaptive design, low temperature power source.*

1. Introduction

We are at a point of time when on one hand, the negative effects of anthropogenic atmospheric alteration are more evident than ever, and on the other, the demand for energy is ever increasing. Although it claimed that there exists a vast reserve of fossil fuel, field by field petroleum production is decreasing [1]. The huge challenge of emission reduction, growing energy demand and peak oil can be approached in two ways. Firstly, by improving energy conversion efficiency of traditional energy sources and secondly, switching to more and more renewable energy sources. Unfortunately, most renewable energy sources are dependent on climatic variation and are not suitable for base load operations. Geothermal energy, on the contrary, provides a clean, reliable source of renewable energy. Energy concentration in geothermal sources is much higher than in many other renewable sources. Moreover, geothermal power plants are considered to have significant lower CO_2 emissions than a standard combined cycle power plant or a pulverized coal fired power plant [2].

Current research and development trends towards geothermal power generation, specifically, low temperature power cycles are noticeable [3-12]. Geothermal power plants are generally designed based on constant resource characteristics. However, it has been observed in many plants that the resource characteristics change significantly throughout the lifetime of the plant [13]. Consequently, deterioration of plant performance and unplanned design changes occur. However, geothermal power plants are very capital intensive and it is not very easy to change a plant to adapt to resource characteristics different from the original design.

By appropriate reservoir modelling, it is possible to predict future resource characteristics depending on various parameters including the rate of resource utilization, the percentage of brine reinjection etc [14]. In this paper we propose an adaptive design approach where provisions are kept for a plant to adapt to resource characteristics changes at the time of building which may save a great deal of effort and money in the long run. We have presented several case studies to demonstrate the benefit of the adaptive design approach.

2. Methodology

We have taken a hypothetical combined cycle geothermal power plant for our study. The geothermal fluid is a mixture of steam and brine. Steam is separated from the brine in a suitable separator then used to power a steam turbine. The exhaust steam from the steam turbine is used to power bottoming organic Rankine cycle units (BOT-ORC). The separated brine is also used in other organic Rankine cycle units (BRN-ORC). After the heat recovery, both condensed steam and geothermal brine are mixed together and reinjected to the reservoir. Pentane is used as the working fluid in the binary cycles. Fig. 1 shows a schematic of the hypothetical power plant. The base case considered here has four BOT-ORCs and two BRN-ORCs as presented in Fig. 1.

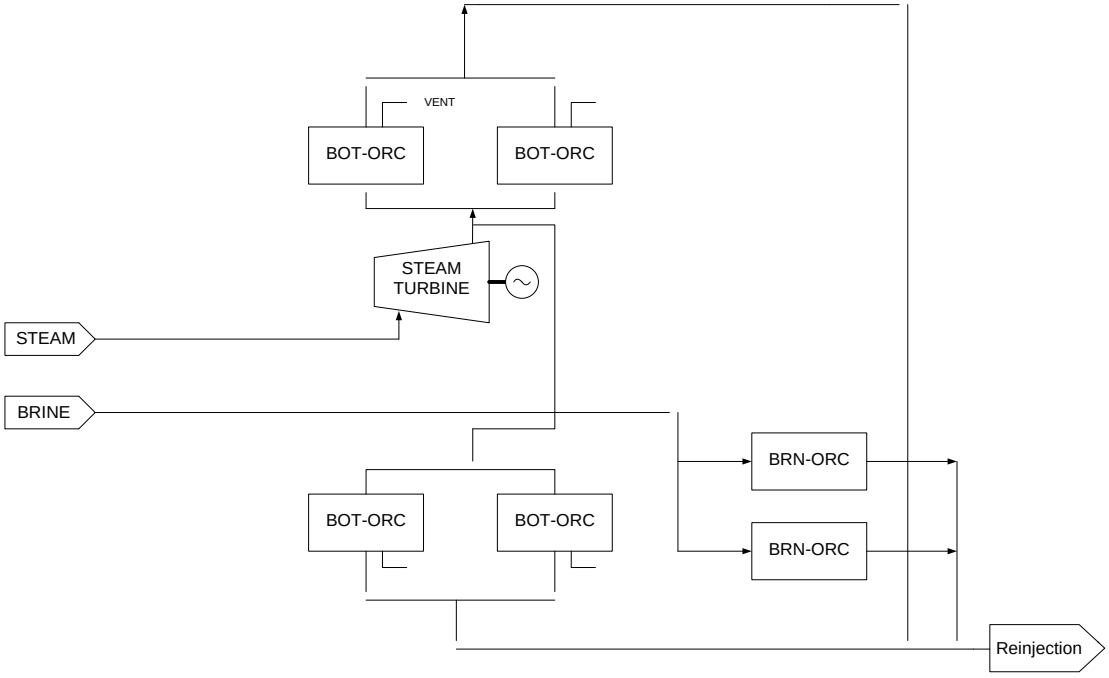

Fig. 1. Schematic diagram of the combined cycle geothermal power plant.

2.1. The component model

Simple models have been used for the analysis presented here. Independent component modules are developed in Matlab/Simulink [15] which can be connected later to develop a system model. The thermo-physical properties are calculated using the REFPROP [16] database. The working fluid flow round the cycle and each process may be analysed using the energy conservation, mass conservation and entropy generation applied to a system boundary around each system component. Changes in kinetic energy and potential energy may be neglected and equilibrium conditions can be assumed at the cross-sections of both inlet and outlet. Detailed discussion on the modelling of these ORCs is available in our previous work [9].

2.2. The Resource Affected Performance Model

A geothermal field passes through four different phases or periods [13]: (1) development, (2) sustainment, (3) decline and (4) renewable. During the last phase, a geothermal resource approaches the ideal of a sustainable and renewable resource. To attain this pahse requires prudent management of the resource. In a Resource Affected Performance Model (RAPM) we change the geothermal resource characteristics and observe the effect on plant performance. We assume that the reservoir modelling predicts that the geothermal resource enthalpy will increase from about 1400 kJ/kg to 2000 kJ/kg over the life time of the power plant. An adaptive design approach is discussed here which keeps provision for this change in resource characteristics.

Applying conservation of mass at the well head

$$\dot{m}_T = \dot{m}_b + \dot{m}_s \tag{1}$$

where, $\dot{m}_T$ is the total mass flow rate at the well head, $\dot{m}_b$ is the brine mass flow rate and $\dot{m}_s$ is the steam mass flow rate. Dividing Eq. (1) with $\dot{m}_T$ yields

$$1 = C_b + C_s \tag{2}$$

where, C_b is defined as brine content and C_s is defined as steam content. It is advantageous to express resource characteristics as steam content (C_s). Applying energy balance at the well head

$$\dot{m}_T h_R = \dot{m} h_b + \dot{m} h_s \tag{3}$$

where, h_R is the resource enthalpy, h_b is the enthalpy of the brine (saturated liquid) and h_s is the enthalpy of the steam (saturated vapour). The reinjection temperature is calculated from the energy balance of mixing of brine and condensate before reinjecting to the geothermal field.

$$\dot{m}_T h_{RNG} = \dot{m}_b h_b + \dot{m}_c h_c \tag{4}$$

where *RNG* stands for reinjection, *b* stands for brine and *c* stands for condensate.

From Eq. (2), if the steam content of a geothermal field (C_s) increases, the brine content (C_b) must be reduced and vice versa. If we want to keep $\dot{m}_b$ and h_b unchanged as C_s increases or decreases, we must manipulate parameters of the left hand side of Eq. (3). Since, h_R is the parameter characterised by geothermal resource, we may not want to manipulate it. The only suitable solution would be to control the geothermal fluid flow rate ($\dot{m}_T$). When C_s increases, we can keep $\dot{m}_b$ constant by using condensate recirculation and increased geothermal fluid flow rate ($\dot{m}_T$). If we are interested only on the constant heat transfer in the vaporizer, the reinjection temperature (i.e. brine outlet temperature) can be lowered. The following assumptions are made for the RAPM.

1. Operating state points of the geothermal power plant remain unchanged i.e., the change in mass flow rate in steam and brine are only responsible for the change in overall heat transfer coefficient.
2. To control the vaporizer steam outlet condition, excess steam is vented to the atmosphere.
3. The off-design well-head condition is always within the wet-steam zone i.e., there is no change in temperature at the well head and the geothermal fluid is a mixture of steam and brine.

3. Results

There are four case studies presented which analyze adaptive design approach to address the change in geothermal resource characteristics. These case studies present four possible solutions for the assumed future resource characteristics.

3.1. The base case

Normally, each turbine has an operating limit and for the steam turbine it has been fixed to 37 MW. For the pentane turbine the maximum power is fixed at 7 MW. Fig. 2 shows the plant output in the base case as the resource enthalpy increases. With increasing steam content from about 25% (1400 kJ/kg) to about 35%, the steam turbine reaches its maximum and produces the same power thereafter. Since the steam turbine is unable to utilize the excess steam, the bottoming cycle is receiving condensate at an elevated mass flow rate. Therefore, the power output of the BOT-ORC increases and owing to a lack of brine, the BRN-ORCs are producing much less than their capacity.

3.2. Case study 1: increased geothermal fluid flow rate

The reduced brine flow problem can be tackled in many ways. If one uses excess geothermal brine to reheat the condensate collected from the BOT-ORC, an increased mass flow of brine can be ensured for the BRN-ORC. Fig. 3 presents a schematic diagram of such a design. Here, more power is being produced at the expense of more geothermal fluid, which means the resource is being utilized at a higher rate; not necessarily ensuring optimum utilization. Fig. 4 shows a corresponding improvement in plant performance by adopting this approach. It is noticeable from Fig. 4 that the BRN-ORC produces gradually less power from 25% steam content to 35% then its power production is independent of steam content. Since, it is more efficient to directly expand steam in a turbine to produce power than in bottoming cycle, one should utilize as much steam as possible in the steam turbine within its manufacturing limit. By increasing the geothermal fluid flow rate, the brine reinjection temperature does not change much.

3.3. Case study 2: upgrading the steam turbine

Fig. 5 shows the performance of the geothermal power plant with increasing steam content when the original steam turbine is replaced with a higher capacity. The rated capacity of the new turbine is assumed 42 MW with the maximum power 47 MW. It is evident from the figure that such an upgrade results in significant improvement in power output. However, it is associated with large capital investment.

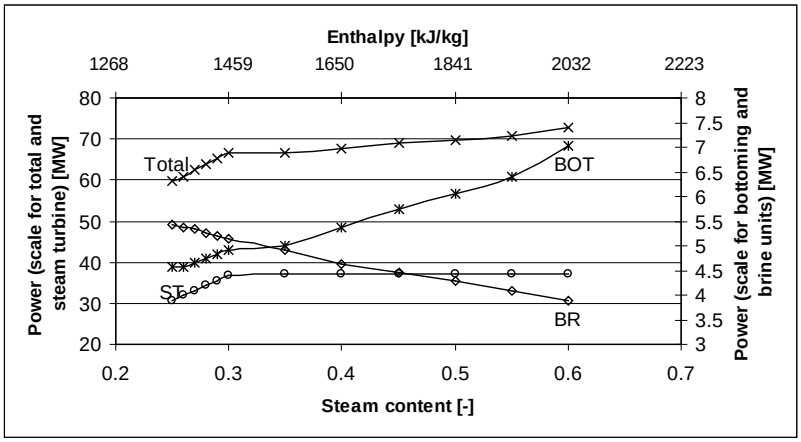

Fig. 2. Theoretical power for the base case as a function of resource enthalpy

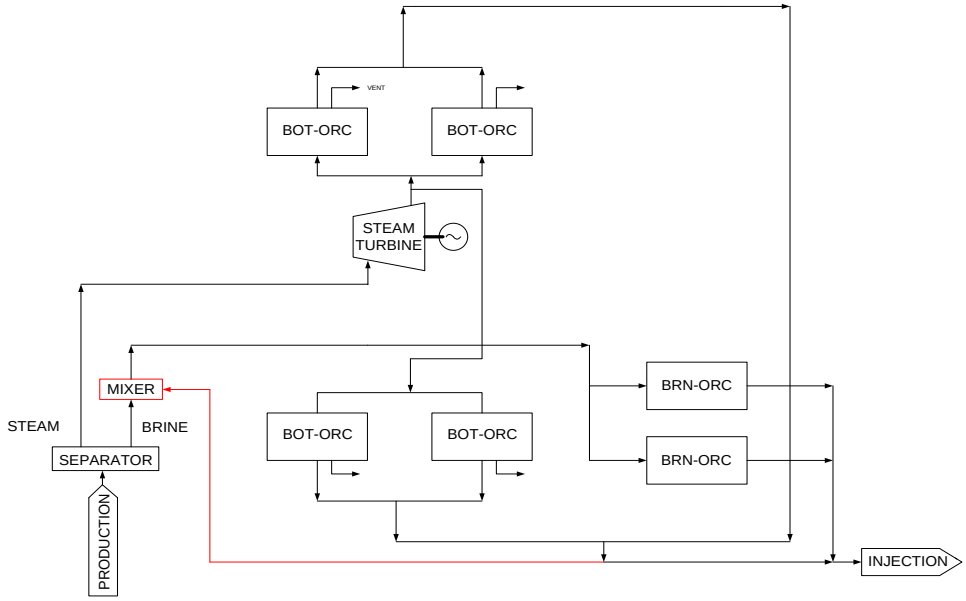

Fig. 3. Adaptive design for an increased flow of geothermal fluid

3.4. Case Study 3: constant flow of geothermal fluid and lowered reinjection temperature

In case 1, more geothermal fluid was used to overcome the problem of reduced brine in BRN-ORCs which results in utilization of the resource at a higher rate. The reinjection temperature of the geothermal brine is not affected much. In the base case, the reinjection temperature is about 125°C. The minimum recommended reinjection temperature of the site is about 80 ºC to prevent silica formation. So there is a possibility of further extracting heat from the reinjected brine.

The alternative design would look the same as Fig. 3. However, the geothermal resource is utilized at constant rate i.e. mass flow of geothermal fluid to the plant is the same as the base case. The plant performance would look like the same as Fig. 4 but the reinjection temperature will change. Fig.6 shows the corresponding reduction in reinjection temperature. It is clear from Fig. 6 that it is possible to stabilize the brine flow rate of the BRN-ORCs and consequently power output by keeping the reinjection temperature within an acceptable limit (80 ºC).

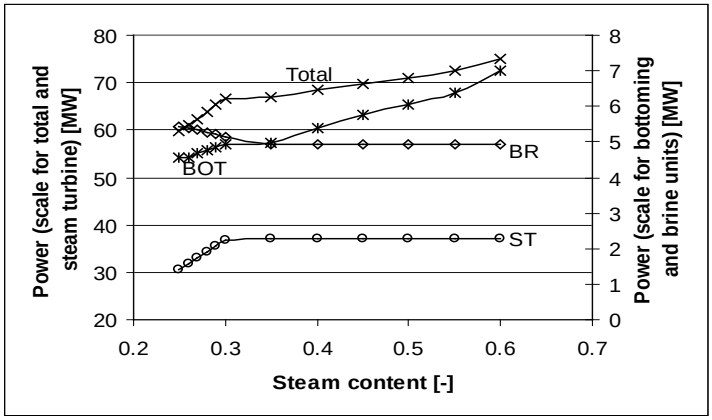

Fig. 4. Theoretical power for base case with increased mass flow of geothermal brine to keep the brine flow rate constant for the BRN-ORC as function of resource enthalpy

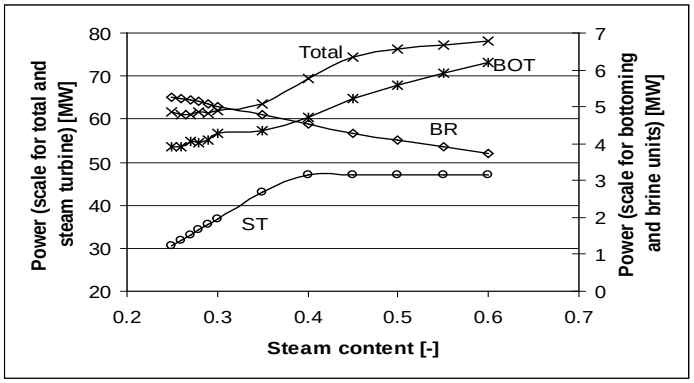

Fig. 5. Theoretical power of the geothermal power plant with a higher capacity steam turbine

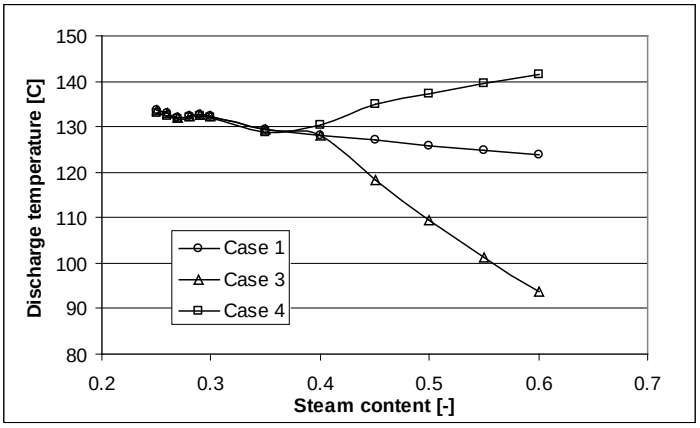

Fig. 6. Theoretical reinjection temperatures for case 1, case 3 and case 4

3.5. Case study 4: constant flow of geothermal fluid with excess steam (50/50)

It was stated earlier that the steam turbine has a power producing limit. Beyond this limit, the steam turbine cannot utilize the excess steam and the consequence is a higher discharge enthalpy. Another possible alternative is depicted in Fig. 7. The excess steam can be bypassed and used to reheat the condensate collected from the BOT-ORCs. The results of mixing excess steam (50%) and condensate (50%) are presented in Fig. 8. It is clear from Fig. 8 that

the reheating of the condensate by excess steam mitigates the reduced brine for the BRN-ORCs. The reinjection temperature is not reduced by this approach (Fig. 6).

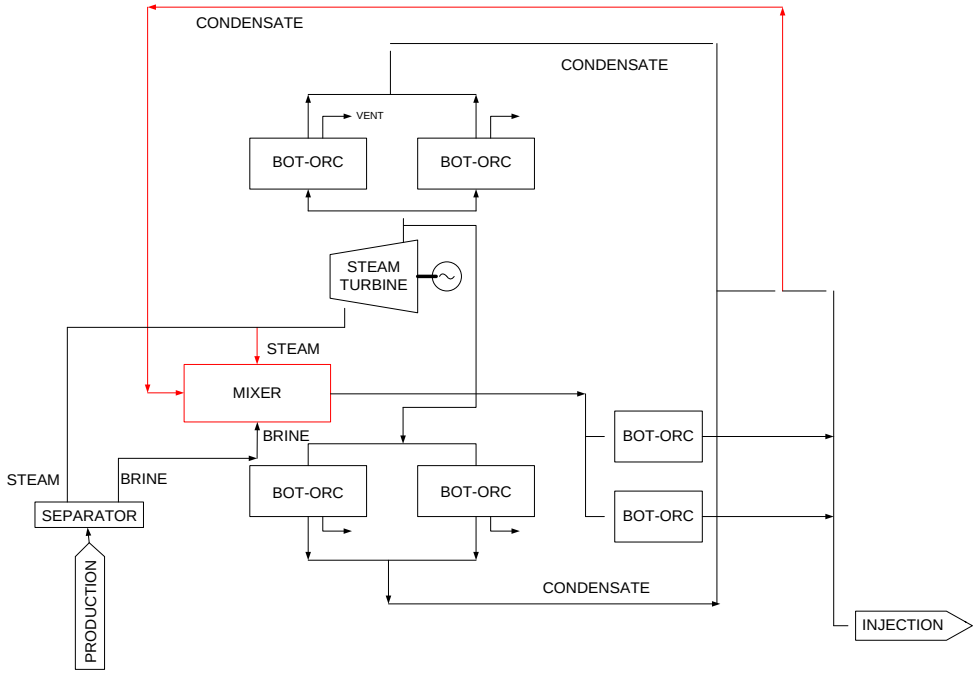

Fig.7. Adaptive design for a constant flow of geothermal fluid and regenerative heating

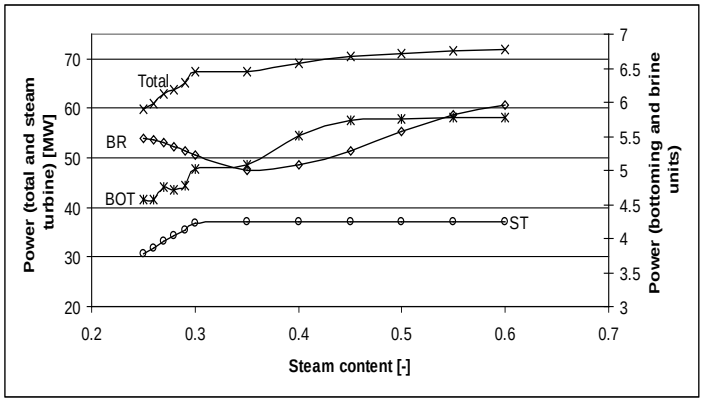

Fig. 8. Theoretical power of the geothermal power plant and constant mass flow of geothermal brine with regenerative heating of the brine by excess steam

4. Discussion and conclusion

This paper has introduced an alternative design approach that takes into account possible changes in future resource characteristics. As geothermal power plants are very capital intensive and it is not very easy to change a plant to adapt to resource characteristics different from the original design, keeping provision for future resource characteristics can be very effective. Although, the initial investment cost might go up as a consequence of adaptive design, over the life span of the plant the total benefit may be greater. A proper cost benefit analysis is necessary to identify the economic benefit. There are four case studies presented in this paper that analysed various possible options of the hypothetical power plant depending on the hypothetical changes in resource characteristics. The results show provisions that could be kept in the plant for future resource characteristics. The next phase is to do a cost benefit

analysis of these options and select the optimum option. In this paper we have only discussed adaptive design approach for increasing resource enthalpy. Similarly, adaptive design for a decreasing resource enthalpy can also be carried out which will provide different provision for the geothermal power plant. One such provision is that one or more of the BOT-ORCs can be designed in such a way that they can be used as BRN-ORCs when geothermal resource enthalpy reduces to utilize the increased brine available.

References

[1] IEA, World Energy Outlook. 2008: International Energy Agency.

[2] Barbier, E., Geothermal energy technology and current status: an overview. Renewable and Sustainable Energy Reviews, 2002. **6**(1-2): p. 3-65.

[3] DiPippo, R., Second Law assessment of binary plants generating power from low-temperature geothermal fluids. Geothermics, 2004. **33**(5): p. 565-586.

[4] Chen, H., D.Y. Goswami, and E.K. Stefanakos, A review of thermodynamic cycles and working fluids for the conversion of low-grade heat. Renewable and Sustainable Energy Reviews, 2010. DOI:10.1016/j.rser.2010.07.006

[5] Bombarda, P. and M. Gaia. Geothermal Binary Plants Utilising an Innovative Non-Flammable Azeotropic Mixture as Working Fluid. in Proceedings 28th NZ Geothermal Workshop. 2006.

[6] Madhawa Hettiarachchi, H.D., et al., Optimum design criteria for an Organic Rankine cycle using low-temperature geothermal heat sources. Energy, 2007. **32**(9): p. 1698-1706.

[7] DiPippo, R., Ideal thermal efficiency for geothermal binary plants. Geothermics, 2007. **36**(3): p. 276-285.

[8] Sohel, M.I. and M. Jack, Efficiency improvements by geothermal heat integration in a lignocellulosic biorefinery. Bioresource Technology, 2010. **101** p. 9342-9347.

[9] Sohel, M.I., et al., An iterative method for modelling the air-cooled organic Rankine cycle geothermal power plant. International Journal of Energy Research, 2010. DOI: 10.1002/er.1706

[10] Sohel, M.I., et al., Dynamic Modelling and Simulation of an Organic Rankine Cycle Unit of a Geothermal Power Plant. Proceedings World Geothermal Congress 2010 Bali, Indonesia, 25-29 April 2010.

[11] Atrens, A.D., H. Gurgenci, and V. Rudolph, Electricity generation using a carbon-dioxide thermosiphon. Geothermics, 2010. **39**(2): p. 161-169.

[12] Atrens, A.D., H. Gurgenci, and V. Rudolph, CO2 Thermosiphon for Competitive Geothermal Power Generation. Energy & Fuels, 2008. **23**(1): p. 553-557.

[13] DiPippo, R., Geothermal Power Plants: Principles, Applications and Case Studies. 2005: Elsevier Ltd.

[14] RJVL, ROTOKAWA GEOTHERMAL DEVELOPMENT Resource Consent Applications and Assessment of Environmental Effects. 2007, Rotokawa Joint Venture Limited, C/- Mighty River Power Limited, 160 Peachgrove Road, PO Box 445, HAMILTON, New Zealand.

[15] MathWorks, www.mathworks.com. 2008.

[16] REFPROP. National Institute of Standards and Technology (NIST), 2007. Available from: http://www.nist.gov/.

Managing Sustainable Design for Geothermal Plants: the Engineer's Perspective

Chun Chin[1,*], Joshua Gunderson[1], Joe Stippel[1], Matt Fishman[1], Gudrun Saevarsdottir[2], William Harvey[2]

[1] *POWER Engineers, Hailey Idaho, USA*
[2] *Reykjavik University, Reykjavik, Iceland*
** Corresponding author. Tel: +001 2087880527, E-mail:cchin@powereng.com*

Abstract: The fast pace of project development, design, and execution of power generation projects, together with the nature of Engineering-Procurement-Construction (EPC) contracts popular in the industry and to banks, often make sustainability considerations a grudging afterthought to the contractor or owner. Although careful consideration of technical, environmental, and social impacts may have been part of the up-front permitting process, the control wielded by skilled engineers during the detailed design process, if implemented in an educated and structured fashion with the owner, and in an EPC environment, with buy-in from the contractor, can result in plant designs that better benefit the local community in dimensions beyond thermal efficiency. This paper will present a structured review process developed by the authors, which is targeted toward the specific considerations of geothermal power projects. This procedure may be applied to other renewable projects, especially those with similarly complex processing systems such as biofuel refineries or solar thermal projects. The review process is performed with the owner and is documented to demonstrate upon completion the project's commitment to sustainable principles. These audit principles provide a platform to educate owners on topics such as alternative methods of construction best suited to the local conditions, workforce, and carbon footprint; project management structures to maximize local content and knowledge transfer, and assessment of all resource and revenue streams from the plant in addition to electrical production. The paper describes the way in which geothermal plants have and require a closer relationship with the local community, and strengthening this relationship is the goal of these processes.

Keywords: *Geothermal, Sustainability reviews, Local content, Project management.*

1. Introduction

The nature of geothermal projects, with their wide range of resource conditions and variety of material and revenue streams, render them more complex cases than many other "plug and play" fossil or renewable generation options. While careful consideration of technical, environmental, and social impacts may have been part of the up-front environmental and local permitting processes, these are often managed by developers and government agencies more focused on establishing the viability of the overall project than optimization of sustainability features. These features may include selection of equipment with lower energy requirements or greater local involvement, such as materials of construction for cooling towers, or use of byproduct streams for maximum benefit, such as recovered sulphur for fertilizers. The time and incentive to focus on sustainability features is diminished by the tendency for many of these projects to be executed under financing structures that discourage value engineering. This paper presents a method to integrate sustainability considerations more systematically into plant design.

This paper presents a structured audit and review process developed by the authors, based on the principles of sustainable development and their experience with geothermal projects, with case studies from locations in the developing world. The review process is targeted toward the specific considerations of geothermal power projects, performed with the owner, and documented to demonstrate upon completion the project's contributions to sustainable principles and community acceptance. These audit principles provide a platform to educate owners on topics such as alternative methods and materials of construction best suited to the

local conditions, best integration of local workforce for initial construction and O&M activities; reducing carbon and land footprint; project management structures to maximize local content and knowledge transfer, and assessment of multiple potential resource and revenue streams from the plant. This process represents a minor investment for the owner, makes best use of the talent available in the design phase, and is executed in the appropriate stage of development for greatest impact at least cost. Pitfalls will be discussed along with ways in which the review can be customized to suit the needs of various owners. Structured sustainability reviews will result in designs that harness the resource more fully, respect the owner's constraints, and contribute to greater project success.

The remainder of the Introduction section will discuss considerations of project execution and financing constraints specific to geothermal plants. The Methodology section will describe the timing and structure of sustainability audits developed by the authors for geothermal projects. The Results section will describe several case studies of how these audit principles have been applied successfully.

1.1. Geothermal Project Development

Geothermal plants, while lacking the aerodynamic sleekness of wind projects or the cutting edge science of photovoltaics, nevertheless can be major contributors to a country's renewable energy portfolio, providing dispatchable, reliable baseload power unaffected by the vagaries of fuel costs and environmental conditions. In developing countries such as Nicaragua and Kenya, geothermal offers the potential to completely displace fossil fuel generation as the lowest cost alternative.

While the capital costs of these projects may be substantial – perhaps $3,000 to $5,000 per kW of installed capacity – they also include the up-front "fuel costs" of well drilling. This high initial cost is further mitigated by the fact that geothermal plants operate at high capacity factors, routinely exceeding 90%.

A typical geothermal project encompasses three major areas:

- the reservoir, from which the hot geofluid (steam or water) is drawn and spent fluid returned,
- the gathering system, where the collected geofluid is conveyed from production wells to the plant and returned to injection wells, and
- the power plant, where power is generated from the geofluid by a variety of methods, most commonly flash (directly driving steam through a turbine) or binary (using the geofluid to vaporize a secondary working fluid, often a hydrocarbon, which passes through the turbine).

The characterization and exploration of the geothermal reservoir is a task that may take years and require the efforts of a dedicated team of geoscientists. Even with the best estimates, the production capacity of a geothermal field is generally uncertain until several wells have been drilled and proven. Until sufficient capacity has been proven, often to a significant percentage of the required plant capacity and typically above 50%, banks are generally unwilling to finance the project. For this reason, exploration is generally funded with equity from a developer which may amount to a considerable sum; a typical 50 MW plant may require an investment of $15 million of equity before loans can be obtained [1]. However, with proven wells and the requisite permits in place, the developer turns quickly to the challenge of designing and financing the project in preparation for construction.

1.2. Project Structures for Execution

The traditional structure for utility projects has historically been a Design-Bid-Build (D/B/B) approach, where the Owner will engage an Engineer to carry out the detailed design. The Owner and Engineer work collaboratively to define the design criteria, design the process, and specify equipment. Purchase orders for equipment are placed by the Owner. After approximately 60% of the design is complete, construction specifications for bidding by Contractors are prepared, where the Contractor will place orders for bulk materials and carry out the requisite work. The advantages of the D/B/B approach are that the Owner maintains firm control over the design process, avoids Contractor markups on major equipment, and the project schedule can be shorter than alternative project delivery methods. One disadvantage is that the firm project cost is not known until later in the process, which makes D/B/B less appealing for financiers. The Engineer might prefer a D/B/B approach because it leaves more room for value engineering and sustainability considerations in collaboration with the Owner. However, narrowly focused financial considerations are leading to an increase in projects that must be executed under an "EPC" approach, discussed next.

An Engineering-Procurement-Construction (EPC) approach is more favored by financiers, although the financial benefits are balanced by certain complications. The Owner begins by preparing a fairly detailed performance specification. An EPC Contractor then gives a firm lump sum bid backed by schedule and performance guarantees. This process is time intensive, leading to EPC projects generally being at least 4-6 months longer than a well executed D/B/B approach. Next, the Contractor engages an Engineer to perform the detailed design and the Contractor places the purchase orders for major equipment. The advantage of the EPC approach is ease of financing due to the Owner's financier having a firm price and performance/schedule guarantees at the beginning of the project. Disadvantages include less Owner control over the evolution of the design, since it is constrained only by the initial specifications; higher cost, due to additional markups and risk burden on the Contractor; and generally longer schedule due to the lengthier contract negotiations and some redundancy in design effort between the Owner and Contractor.

The initial phase of conceptual design by an EPC Contractor/Engineer team generally consists of several months of equipment specification and procurement, the goal being to award purchase orders for the critical path items that define the overall project schedule and impact the design of foundations and supporting subsystems. These major plant items include the turbine/generator, condenser, cooling tower, non-condensible gas removal system, and major pumps. These all will be ordered generally within four to six months after EPC contract award.

The opportunity to explore plant improvements that would improve sustainability attributes can be inhibited by the EPC approach. The contract is generally awarded to the lowest bidder; discouraging the search for solutions that may have greater long-term value. After award, the Contractor generally faces liquidated damages for schedule delays, hence they and the Engineer are considerably motivated to avoid proposing investigation of upgrade opportunities. Finally, the lump sum contract would require renegotiation in the event that the Contractor proposes investments in upgrades. All these, along with the rapid pace of design and construction, are disincentives to thoughtful plant optimization under the EPC approach.

2. Methodology

2.1. Timing of the Sustainability Review

The Engineer faces the challenge of how to incorporate sustainability considerations swiftly, appropriately, and in a win-win approach with the Owner and Contractor, which may have competing interests. The methodology developed by the authors incorporates a Sustainability Review into a natural Owner and Contractor design review process that generally occurs after 3-4 months for a typical project. In this design review the conceptual-level documents are reviewed for adequacy and conformance with the project specifications. At this time it is also common to hold a Process Hazard Analysis (PHA), or Hazard and Operability Study (HAZOP), which is a structured "what-if" review of the conceptual documents to explore the possibilities to improve safety. HAZOP reviews were originally developed for the chemical industry, and conducting these is often an Owner or regulatory requirement for a complex processing plant, such as a geothermal project, with its multitude of fluids and flows. The expansion of 'binary' technologies, which can be used in geothermal, ocean thermal, and solar thermal projects, generally call for HAZOPs since they often incorporate hydrocarbon working fluids. The Sustainability Review we have developed is scheduled at the same time and has a similar structure to the HAZOP.

2.2. Objectives of the Sustainability Review

The Bellagio Principles [3] are used as guidance, which emphasize among others clear goal setting, a holistic perspective, considerations of economic and non-economic principles, local and regional effects, short and long-term effects, and a focus on practical goals. The objective of the Sustainability Review is to emerge from the process with:

- Clear direction from the Owner and agreement with Contractor on any specification, contract, or schedule modifications required to enhance sustainable attributes.
- Written documentation describing the steps Owner, Contractor, and Engineer have taken to be mindful of sustainability considerations, in a format suitable for dissemination to the public if the Owner so chooses.
- An expectation that future changes will be minimized so as to protect the Contractor's project schedule and ongoing design.

2.3. Structure of the Sustainability Review

The proposed Sustainability Review process can be submitted to proposed EPC clients as part of the proposal documentation for consideration according to their green values. This is treated as a value-adding cost option, so that it is appreciated in its own right, and yet does not jeopardize winning an EPC project by building in costs that other bidders may not have allocated. If the project is a win, the Engineer works with the Owner and Contractor to make selections consistent with their philosophy on sustainability.

During the initial conceptual design phase, a preliminary project sustainability report is generated; typically at around the 3 month time frame and prior to the Design Review/HAZOP/Sustainability Review sessions. This provides an agenda and some suggested topics of discussion for the Review. Each proposed aspect should be developed with the following considerations in mind:

1. The Engineer's role is to educate and inform; the Owner and Contractor will be the final arbiters.
2. Must be mindful of the client's own sustainable charter.

3. Must sell on its own merit such that cost benefits, positive environmental impacts, better integration with the surrounding community and other intangible benefits make the program attractive.
4. Must be easy to understand, clearly defined (can be organized by system, discipline or combination thereof) and practical for implementation.
5. Positive impacts to the environment as well as a business case and cost justification must be measurable and presentable to both the Owner and Contractor
6. Flexibility in the program will allow clients to have the freedom to choose the weighted aspects of sustainability they want their project to possess.
7. Conduct risk assessments and comparative studies to show how an innovative technology compares with traditional technologies.

Following the Sustainability Review, a Sustainability Report is generated as part of the project record documentation, identifying the areas of positive impact and stating both one time and recurring benefits.

The effort involved in preparing for and executing the Sustainability Review is not inconsiderable, but the impact on even small subsystems can be substantial. Compare a scenario where 10 workdays are spent in preparation, 20 workdays for an attendance of ten representatives for two days of the review, and 10 workdays for preparation of the summary report. This may come to some tens of thousands of dollars for a dedicated review. Yet, identifying even small efficiency upgrades or locally, less expensive materials can be tremendously impactful. Plant output may be assessed with net present values in the $4000/kW range, meaning a 1% identified efficiency improvement on a 1000 kW pump/motor may cover the cost of the study. Similarly, the cost of a single imported stainless steel large diameter flange may exceed $20,000; alternative materials, layouts, or suppliers permitted by the Owner may result in significant cost savings. Also, design modifications that reduce environmental impact may have long term value for the Owner in terms of local acceptance of the project.

2.4. Methodology of the Sustainability Review

Similar to a HAZOP study, the Sustainability Review is designed to promote discussion and generation of ideas by being open ended. Specific suggestions may be covered in the preliminary report, if some research is required, but other ideas may be generated by the participants during the meeting. A full and comprehensive review meeting may last for several days and require an interdisciplinary and interparty team of 5-15 people, but an abbreviated review can be performed with a smaller group of stakeholder participants.

Natural divisions consistent with plant design may be used to facilitate an organized search for potential sustainability features. Primary divisions may be based on engineering disciplines such as Architectural, Civil, Structural, Mechanical, Electrical, and Controls. Each discipline brings to the review key deliverables such as Process Flow Diagrams, Electrical One-Line Diagrams, or General Arrangement Drawings. A set of key plant areas, systems, or equipment that merits study is developed. The team brainstorms to come up with alternative configurations within the area/system/equipment. Then each alternative is evaluated with regard to sustainability attributes and metrics. The following are sample parameters to be discussed and assessed with a weighted score.

- Environmental: Green/LEED structures, provide animal crossings, minimize chemical waste streams or improve disposal practices.

- Social: Use local labor and locally supplied materials. Innovative designs that appeal to the public while improving sustainability (geothermal heating, energy efficient lighting, passive solar, novel waste heat utilization), reduce noise levels.
- Health & Safety: Minimize use of hazardous materials. Use safer construction practices and materials.
- Diversity: Consider how alternatives may contribute to the diversity of organisms or institutions that benefit from its application.
- Natural Resources: Minimize land use. Minimize water use. Utilize waste streams.
- Human Resources: Make changes to facilities to improve workforce morale (covered walkways, breakrooms, better maintenance access ways, etc.)
- Engineering and Procurement: Increase efficiency due to alternative materials, equipment type, layout, or other design parameters. Improve off-design and turndown capabilities. Shorten the procurement cycle.
- Construction: Compress project schedule with changes to equipment, layout, materials, etc. Use locally available materials and construction techniques.
- Availability: Add equipment redundancy where appropriate. Review single points of failure.
- Operations: Consider alternatives to improve operator experience, ease of troubleshooting, etc.
- Maintenance: Evaluate impact on maintenance frequency, cost, need for specialists.

A typical Sustainability Review process is outlined in the appendix. Each suggestion for improvement is reviewed against the tender specifications to verify that it is not already a mandatory requirement. The cost of any suggested enhancement is assessed or tagged for further study. Within several weeks the facilitator prepares a report of the suggested upgrades, the proposed costs, and any schedule adjustments. Those options that are implemented and other observations such as plant benefits to the local community are documented in the report in a manner sufficient for use by the Owner to demonstrate their commitment to sustainable principles. The usefulness of this procedure would not necessarily be limited to powerplants; other similar renewable energy projects such as a biofuel synthesis facility could be studied with these techniques.

3. Case Studies

Through reviews such as these, several modifications leading to improved sustainability aspects have been successfully implemented in geothermal projects around the world.

Darajat II, Indonesia: This 110 MW geothermal plant houses the world's largest single pressure geothermal turbine. During reviews between the Owner, Contractor, and Engineer of the Darajat II project, it was revealed that several workers had died during the construction of the Darajat I concrete cooling tower some years earlier by a different team. Although a change in the style of construction of the tower was not a contract requirement, the Contractor and Engineer shifted from a cast-in-place concrete cooling tower to a precast design, where forms were set on grade and pieces lifted into place similar to the erection of a massive log building. This had not been attempted before on a geothermal project, and posed POWER Engineers and the cooling tower manufacturer, SPX, with several new challenges. Nevertheless, the tower was constructed without a major construction incident. Ironically the Contractor's project manager, who proposed the modification, lost his life due to illness during the project; the tower is a memorial of sorts.

Germencik, Turkey: This 47.4 MW unit is the largest geothermal plant in Turkey. A decision was made in the design phase to maximize the use of local subcontractors and materials, with consideration that in Turkey little geothermal-specific design expertise existed. A division of labor for the systems was developed that allowed specialist firms to design such items as the powerhouse layout and structural steel required to support equipment and piping, given certain critical loads, while Turkish firms familiar with locally available architectural styles and fixtures completed the detailed design of the façade. A list of structural shapes commonly available in Turkey was provided to POWER Engineers and preferentially used in the steel design to minimize the need for importation [4].

San Jacinto II, Nicaragua: These 2 x 38.5 MW flash plants currently under construction will add 10% of renewable capacity to Nicaragua's total generation of 750 MW, displacing about one million barrels of diesel fuel per year. Due to challenging construction conditions and a local scarcity of construction equipment such as augers, several modifications were made to reduce the size and depth of foundations associated with the major pumps, shortening the construction period and reducing concrete quantities. A shift was made from galvanized steel structures to wider use of painting to resist corrosion, in a desire to reduce imports due to a local scarcity of galvanizing facilities.

4. Conclusion

The rushed pace of project execution, especially for EPC contracts, make incorporation of sustainability considerations a challenge for the engineer. However, the customization of each geothermal plant, required due to the unique nature of each resource, means some time should be allocated to explore new opportunities for each project. Addressing these at the appropriate time during the conceptual design phase or early detailed design phase, and doing so with a structured process between the Owner, Contractor, and Engineer, is necessary for the right ideas to find expression in the plant design. The metrics to be applied and the appropriate weightings are parameters that may change for each project; better quantifying and handling of these is an avenue for future work. Documenting the decisions made and the potential positive impacts the plant can bring to the local community can improve the relationship between the Owner and local resources including workers and policy makers, making ongoing plant modifications or expansions (a common occurrence when new fields are incrementally developed) a smoother process. The review process suggested here is intended to bring more of these considerations into the awareness of the various parties, and may be extended for use to other sorts of analogous renewable projects.

References

[1] Deloitte, Geothermal Risk Mitigation Strategies Report, Prepared for the DOE Office of Energy Efficiency and Renewable Energy Geothermal Program. 2008.

[2] P. Hardi and T. Zdan, Assessing Sustainable Development: Principles in Practice, International Institute for Sustainable Development, 1997.

[3] International Hydropower Association, Sustainability Assessment Protocol, 2006.

[4] T. Dunford, M. Fishman, K. Wallace, M. Ralph, and W. Harvey, Engineering Local Value: Case Studies from Olkaria and Beyond. GRC Transactions, Vol. 34, 2010, pp. 186-190.

Appendix: Sample Sustainability Audit Process

1 DEFINING REVIEW AREAS

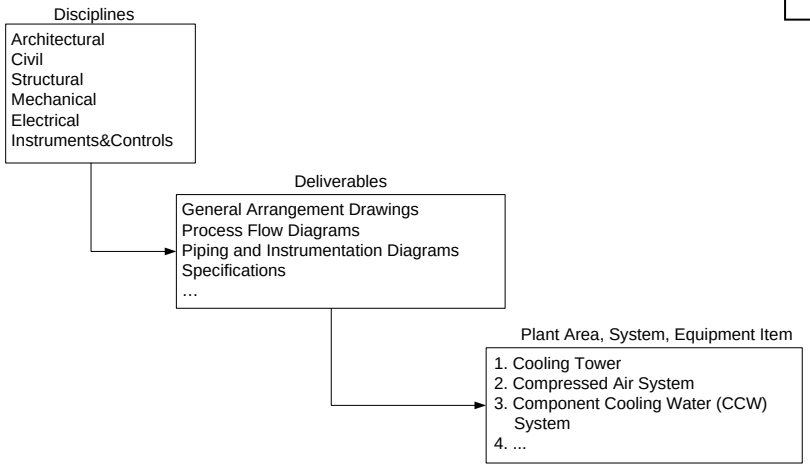

2 IDENTIFYING ALTERNATIVES

ID	Base Case	Alternative Design	Primary Incentive
S01	Fixed speed CCW pumps with control valves	VFD CCW pumps	Increased efficiency and reduced LCC for increased capital cost
S02	Restrictive Orifice used for CCW pump recirculation	Replace Restrictive Orifice with Control Valve	Increased efficiency and reduced LCC for increased capital cost
S03	Standard routing of CCW return to cooling tower	Reroute CCW through parking lot to melt snow in winter	Worker, visitor, community satisfaction and increased safety for increased capital cost
S04	…		

3 ASSESSING ALTERNATIVES

Project No./Name:	Sample Geothermal Project
Base Case:	Traditional CCW Routing
Alternative Design:	Route CCW through parking lot for winter snow melting

Category	C	Q	Description
Environmental			Reduced emissions by snow removal equipment, reduced water used at cooling tower in winter
Social			Will be appreciated by visitors, public relations during startup
Health & Safety			Increased safety in winter
Diversity			
Natural Resource			Reduced fossil fuel use by snow removal equipment, increased materials used for piping, increased equipment use during construction.
Human Resource			Workers will appreciate lack of snow accumulation in lot
Engineering and Procurement			Increased costs, increased engineering effort to properly size system
Construction			Increased costs, pipe must be buried shallow requiring additional protection from surface loads.
Availability			Slight increase in failure probability due to surface loads and increased pipe run length
Operations			
Maintenance			Reduced access to piping under parking lot
Totals (Σ_C,Σ_Q)			

C = Costs (Quantitative Impacts)
Q = Qualitative Impacts

4 SUMMARY AND ACTIONS

ID	Alternative Design	Σ_C	Σ_Q	Proposed Action
S01	VFD CCW pumps			
S02	Replace Restrictive Orifice with Control Valve			
S03	Reroute CCW through parking lot to melt snow in winter			
S04				

Numerical simulation of Northwest Sabalan geothermal reservoir, Iran

Younes Noorollahi[1*], Ryuichi Itoi[2]

[1]*Dep. of Environmental and Energy, Sciences and Research Branch, IAU, Pounak, Tehran, Iran*
[2]*Dep. of Earth Resources Engineering, Kyushu University, Fukuoka, Japan*
** Corresponding author. Tel: +98 21 44865320, Fax: +98 21 44865002, E-mail: hashtroudi@srbiau.ac.ir*

Abstract: A three dimensional numerical model of the northwest Sabalan geothermal system was developed on the basis of a conceptual model drawn from the analysis of the available field data. A numerical model of the reservoir was expressed with a grid system of a rectangular prism of 12km × 8km with 4.6km height, giving a total area of 96km^2. The model has 14 horizontal layers ranging in thickness between 100m to 1000m extending from a maximum of 3600 to -1000m a.s.l. Fifteen rock types were used in the model to assign different horizontal permeabilities from 5.0×10^{-18} to 4.0×10^{-13} m^2 based on the conceptual model. Natural state modeling of the reservoir was performed, and the results indicated good agreements with measured temperature and pressure in wells. Numerical simulations were conducted for predicting reservoir performances by allocating production and reinjection wells at specified locations. Two different exploitation scenarios were examined for sustainability of reservoir for the next thirty years. Effects of reinjection location and required number of makeup wells to maintain the specified fluid production were evaluated. The results showed that reinjecting at Site B is most effective for pressure maintenance of the system.

Keywords: *Geothermal, Reservoir, Simulation, Capacity, Sabalan, Iran*

1. Introduction

In this study, simulation for natural state and capacity assessment of the reservoir were undertaken for the primary purpose of predicting and assessing the response of the NW Sabalan geothermal reservoir to the planned development scenarios. The computer codes of TOUGH2 [1] and AUTOUGH2 [2] were used with the equation of state of water and steam (EOS1). Different production scenarios were examined by numerical simulations for evaluating the reservoir responses, and consequently the optimum future development scenario was defined. Three exploration wells, NWS1, NWS3 and NWS4, were drilled in the study area based on the results of geological, geochemical and geophysical studies. According to the geophysical surveys, deep geothermal reservoir may extend from northeast to southwest where exploration wells were drilled along this suitability area [3, 4, 5].

2. Conceptual model of NW Sabalan reservoir

Before a numerical simulation model of a given geothermal field being set up, a conceptual model must be developed. The model is usually represented by sketches showing a plan view and vertical sections of the geothermal system. On these sketches the most important features such as geothermal surface manifestations, hydrological boundaries, main geologic features such as faults and geological layers, zones of high and low permeabilities, location of deep inflows and boiling zones need to be involved. Thus, developing a conceptual model requires the synthesis of information from a multi-disciplinary team. The geological map of the Sabalan area with main surface manifestation, geological structures shown in Figure 1. A conceptual model of the study area was drawn along AB line in Figure 1, with 12km length, from north to south. Three drilled exploration wells were projected on the AB line [6] and Subsurface geology of the area is described along cross section AB, using geological data and information from three deep and two shallow exploration wells. In the central part of the model, Dizu formation presents and extends to the depth of about 200m a.s.l. This formation clearly exposed in the area where Wells NWS1 and NWS3 are located throughout the Valhezir formation reaches to the surface in the east of Well NWS4 and extends to 700 m

depth in the whole study area from top or below Dizu formation. In the northern part of the area where Well NWS3 was drilled, geological unit is comprised of andesitic lava flows, tuff and tuff breccia that belong to Dizu formation of Neogene to Quaternary and Mejendeh metamorphics of Paleozoic in descending order down to 1000 m below sea level. Magnetotelluric (MT) survey was carried out in 1998 with 212 stations [6]. Nineteen measurement stations were located along the AB line, and the results were analyzed which shows two anomalies of low resistivity in south and north part and a high resistivity in the central part which can represent the location of an intrusive body beneath Well NWS4. Temperature contours are drawn using measured temperatures in exploration wells. The temperature increases from north to south which suggests that an upflow zone of high temperature fluid likely presents in the southern part of the field. Thus, Faults NW3, NNW5, NE5, NNW2 and NW4 play as upflow zone of the system. By integrating the subsurface geology from the wells with resistivity and temperature data, the conceptual model of the system can be illustrated in Figure 2. Differences of subsurface geology revealed from drilling between Wells NWS4 and NWS3 support the presence of Fault NE2. Temperature profiles of these two wells also show differences, which implies that Fault NE2 plays as an impermeable or low permeable boundary. The presence of slightly high resistivity zone beneath Site B can be interpreted as the existence of a diorite porphyry intrusive body. It has been assumed that geothermal fluids ascend through Faults NW3, NNW5, NE5, NNW2 and NW4. This faulted area can be an upflow zone of the system. The fluids would ascend through this fault zone to higher elevations and then flow horizontally in shallow layers to the northward due mainly to gravitational force and discharge through hot springs in lower elevations.

3. Development of numerical model

3.1. Grid system and rock type and properties

The NW Sabalan geothermal system was modeled with a rectangular prism 12km long, 8km wide and 4.6km depth. The model has 14 horizontal layers, AA to PP, ranging in thickness between 100 to 1000m extending from a maximum of 3600 to -1000m a.s.l with 2595 grid blocks in total. For neglecting water-air unsaturated zone, first two top layers, AA and BB, were discarded from the model. Each layer has 192 grid blocks 500×500 and 1000×1000m. The exploration drilling area is located in the center of the model, covering an area of 3×5km. Permeability values were given to the model in ranges from 5.0×10^{-17} to 4.0×10^{-13} m^2**,** with the maximum value in the shallow permeable horizon on depth between 1900 and 1400 m a.s.l (Figure 3). Sixteen rock types were used mainly for assigning different permeability. Porosity, rock density and thermal conductivity were 0.1, 2500kg/m^3 and 2.5W/$m^{2\circ}$C to all rocks. Rock parameters corresponding to the optimum natural state model are summarized in Table 2. The rock types CAP01, TOP01 and TOP02 with lowest permeability were assigned to layers CC, DD and EE which represent the cap rock of the system. The MAKH0 with low permeability was assigned to the northern part of the field below Site C to layers FF, GG, HH, and II. The rock LOW01 was given to the deep part in C area from 1400-500m a.s.l. corresponding to the metamorphosed rocks appeared in Well NWS3. The TOP04 was assigned to the area beneath Site B and surroundings for representing the conductive temperature profile observed in Well NWS4. This rock types appears in elevation from 2000-1400m a.s.l. belong to the layers EE, FF, GG, HH and II. The MAKH1 rock type with high permeability was for the layer MM in Site B. The MAKH2 was assigned to the layers EE, FF, GG, HH and II from elevation of 2000-1400m a.s.l. according to information from Wells NWS1 and NWS4 as high permeable rock formations were found in these horizons. The LOW02 was used to the grid blocks in the layers KK and LL in the southern and central part and represent low permeability between two high permeable layers. The UPFLO rock type indicates the upflow zone with high vertical permeability. Six grid blocks (500×500m) in

southern part were assigned with this rock type from layer PP to GG. Information from two wells, NWS1 and NWS4 indicates that there are two main permeable horizons in the reservoir: a shallow zone between 1800 and 1400m a.s.l. in southern part, and a deeper zone between 500m a.s.l. and sea level in both wells. In the computational grid system, the uppermost high permeable horizon in the reservoir was therefore subdivided into four layers (FF, GG, HH and II). The layer MM denotes the deep permeable horizon. The layers AA and BB represent the unsaturated zone, which were discarded from computing. This geothermal field is located in an arid area and two top layers are unsaturated. We can model such condition by using EOS3 with all layers or EOS1 be neglecting unsaturated zone.

Table 1 Rock parameters of the best natural-state model

Rock type	Density (kg/m^3)	Porosity (%)	Permeability (m^2)			Thermal cond. ($W/m^2°C$)	Specific heat ($J/kg°C$)
			Kx	Ky	kz		
ATMOS	2500	99	2.5×10^{-14}	2.5×10^{-14}	2.5×10^{-14}	2.50	9.0×10^{5}
CAP01	2500	10	2.0×10^{-16}	2.0×10^{-16}	7.0×10^{-17}	2.50	1.0×10^{3}
BASE1	2500	10	6.0×10^{-15}	6.0×10^{-15}	3.0×10^{-15}	2.50	1.0×10^{3}
BOND1	2500	10	9.5×10^{-16}	9.5×10^{-16}	6.6×10^{-16}	2.50	1.0×10^{3}
TOP01	2500	10	5.5×10^{-16}	5.5×10^{-16}	1.1×10^{-16}	2.50	1.0×10^{3}
TOP04	2500	10	5.0×10^{-15}	5.0×10^{-15}	1.1×10^{-15}	2.50	1.0×10^{3}
BASE3	2500	10	1.0×10^{-17}	1.0×10^{-17}	5.0×10^{-18}	2.50	1.0×10^{3}
LOW01	2500	10	6.0×10^{-14}	6.0×10^{-14}	1.0×10^{-14}	2.50	1.0×10^{3}
MAKH3	2500	10	2.0×10^{-13}	2.0×10^{-13}	5.0×10^{-14}	2.50	1.0×10^{3}
MATRX	2500	10	5.0×10^{-15}	5.0×10^{-15}	1.0×10^{-15}	2.50	1.0×10^{3}
TOP02	2500	10	5.0×10^{-16}	5.0×10^{-16}	2.0×10^{-16}	2.50	1.0×10^{3}
MAKH0	2500	10	5.0×10^{-15}	2.0×10^{-15}	5.5×10^{-16}	2.50	1.0×10^{3}
LOW02	2500	10	7.0×10^{-16}	7.0×10^{-16}	1.5×10^{-16}	2.50	1.0×10^{3}
MAKH1	2500	10	1.0×10^{-15}	1.0×10^{-15}	5.0×10^{-16}	2.50	1.0×10^{3}
MAKH2	2500	10	4.0×10^{-13}	4.0×10^{-13}	7.0×10^{-14}	2.50	1.0×10^{3}
UPFLO	2500	10	3.0×10^{-13}	3.0×10^{-13}	3.0×10^{-13}	2.50	1.0×10^{3}

3.2. Initial and boundary conditions

The peripheral boundaries are impermeable for mass and adiabatic for heat. Grid blocks were filled with 15°C of water and pressure was equilibrated as an initial condition. High temperature fluid recharges at a rate of 90kg/s of 1159kJ/kg from the bottom layer was given through regional faults in the southwest region. The temperature of inflow geothermal fluid was calculated using geochemical geothermometers [6] and also slightly changed by trial and error manner through iterative process of natural state simulation. According to a vertical temperature distribution across AB cross section using data from the wells an upflow zone may present about 2.5 km to the southeast of Well NWS1. The recharge was assigned to the grid blocks of 89, 92, 103, 105, 109 and 111 in PP layer. A flow rate of 8kg/s of low temperature, 130°C, inflow was assigned to the grid 4 in northwestern part to simulate the temperature and pressure condition of the northern part close to Well NWS3. Natural discharge from the field was modeled using deliverability method. The productivity index (PI) was calculated on deliverability model [1] and well bottom pressures (P_{wb}) were obtained by trial-and-errors manner. Mass flow rate on deliverability is proportional to the pressure difference between the grid block and a prescribed pressure that is lower than that of the block. There are several hotspring with surface temperatures from 25 to 85°C and the flow rate of about 50kg/s. In order to reproduce the hot spring activity in the numerical model,

fluid production based on deliverability was utilized in three blocks in layers FF (51, 78, and 183) and one block in layer II (130). Heat flux was given to the blocks in the bottom layer, PP, of the model as a conductive heat supply. A heat flux of 200mW/m^2 was used as the initial basis for calculating the heat inflow in southern and central parts.

3.3. Wells data matching and model validation

The validation process normally involves comparing the computed results against measured temperature and pressure in three wells. This pressure are measured as stationary pressure measurement of single major feed zone during well testing. The matches between the measured and computed values were improved primarily by adjusting the permeability, fluid flow rate and specific enthalpy of the high-temperature recharge assigned to the bottom six grid blocks. Also the lower temperature in Well NWS3 was reproduced in the model by assigning an inflow from grid block 4 in the northwestern part.

4. Production prediction simulations

Once a reasonable numerical model of the natural state of reservoir has been developed, it can be used as an initial model for future prediction performances upon various exploitation scenarios. Main concern of prediction in terms of reservoir management is to examine whether the reservoir can produce required steam for specified period of the present state or is able to produce more steam within acceptable effects or changes in reservoir conditions. Two different exploitation scenarios are designed and then examined for future reservoir performances in this field. Wells on deliverability have been used for evaluating production rate of wells during prediction calculations. The well productivity depends on the well bottom pressure (P_{wb}) where the reservoir pressure will decreases during production, and if the reservoir pressure draw down to equal to the P_{wb}, the well cannot produce the fluid. Numerical simulations were carried out using the AUTOUGH2 simulator for 30 years from year 2015. Numerical simulations were conducted for predicting reservoir performances by assigning production and reinjection wells. The production zones are located in the southern area on Sites A, D and E (Figure 1). These areas situated in a junction of Faults NNW2, NNW3, NNW5, NE5, NE6, NW3, NW4 and NW5 where high permeable fractured zones can be developed along these faults. The northern part of the field with lower elevation was recommended for reinjection. Reinjecting geothermal waste water to these localities with different arrangement was examined on production scenarios. The simulations were run for 30 years of production. The recharge flow rate of the high temperature fluid to the system may increases upon production due to reservoir pressure drop. In prediction simulations, however, constant recharge flow rate was assumed as same as the natural state (98 kg/s). Prediction for NW Sabalan geothermal projects was simulated for two different cases for two power output scenarios; **Scenario II: 50MW; Case 1**: with drilling makeup wells and; **Case 2**: without drilling makeup well and; **Scenario III: 100MWe; Case 1**: with drilling makeup wells and **Case 2**: without drilling makeup well. In these scenarios, declines of pressure, temperature, enthalpy and mass rates of fluid and steam productions of wells were evaluated. The mass production rates of fluid and steam were calculated from fluid discharges of production blocks at a separator pressure of 5.5bar. The reinjection rate of wastewater and its enthalpy into reservoir were given as that of the separator pressure and temperature of 155°C. On the basis of discharge data from Well NWS4, required amount of geothermal fluid for a proposed single flash power plant was calculated [7]. The input parameters are; produced fluid enthalpy 985kJ/kg, separation pressure 5.5 bar, condenser pressure, 0.1bars, outlet temperature 46°C and isentropic efficiency of the turbine 0.78. By assigning these inputs and output information, required production rate of geothermal fluid for different scenarios and number of wells are summarized in Table 2.

4.1. Scenario II: 50 MWe power production

In this scenario for 50MWe generation, total amount of 690kg/s of the geothermal fluid is required. This amount of geothermal fluid was assigned to produce initially from 13 production wells which are fed from the layer MM. For reinjection of the wastewater, seven wells were allocated in the northern and central parts (Site B area) of the field. Two different cases in this scenario were simulated and the effects of production on total mass and steam productions, reservoir pressure, temperature, average flowing enthalpy and natural discharge rates were evaluated. To optimize the production scheme two production and injection cases were designed for this scenario including; **Case 1** : 50 MWe steady power production with makeup wells and **Case 2**: 50 MWe power production without makeup well.

Table 2 Characteristics of the production scenarios

Item	Scenario II Case1	Scenario II Case2	Scenario III
Power output (MWe)	50	50	100
Total production (kg/s)	690	690	1380
Steam production (kg/s)	106	106	212
Brine production (kg/s)	584	584	1168
Number of prod. well	13	13	35
Number of reinj. well	7	7	16
makeup wells	7	0	5

In Case 1; the base level was designed to produce 50MWe over 30 years. Because of pressure drop during production, steam flow rate as well as total production rate decrease. When the steam production rate decreases to 90% of the designated level or power generation drop below 45MWe, new makeup wells start to production for maintaining the total production rate. In Case 2 no makeup well was assigned and the production from 13 wells was maintained over 30 years and the behavior of the reservoir was monitored. Table 5 summarizes the production and reinjection flow rates and grid blocks.

4.1.1. Steam flow rates

Steam flow rates versus time for two cases in Scenario II are presented in Figure 4. In early times, production rates rapidly decease with time in both cases. In Case 1, steam production rate decreases below 95kg/s after 3 years of production and then a makeup well starts to production. This new well can keep the power production more than 45MWe for two years and another new makeup well was required. In this scenario seven makeup wells in total were required in years at 2018, 2020, 2023, 2026, 2029, 2033, and 2038 to keep the power generation of 45MWe for 30 years. In Case 2 the makeup well was not assigned and production was continued by 13 initially drilled wells over 30 years. The steam production rate decreases rapidly in the first 5 years with an average of 3.5% per year. From the year 2020 to 2030 the decline rate is moderated to 1.2% per year and in the next 15 years (2030-2045) the steam flow reduces only 0.31% per year. It can be concluded that the production rate eventually stabilize after 15 years of production. In this case, total production rate drops by 34% in 30 years.

4.1.2. Predicted pressure and temperature

Pressure and temperature changes of the reservoir were monitored while running this production scenario for 30 years. Changes of the pressure and temperature from their initial

values at shallow and deep layers are evaluated. Temperature drops in layers HH and MM for Case 1. In Layer HH temperature drop is less than 1°C. In the main producing layer of MM, cooling occurs in the northern part of the reservoir in reinjection area. Decrease amount of temperature shows up to 60°C in the central part of the reinjection zone and the area of 10°C cooling extends over 4.5km^2. Low temperature front moves from reinjection area to the southward of production zone. Actually, the temperature drop in production zone is only about 1°C. As shown in the figures cooling in main production and reinjection layer, MM, is more apparent than layer HH. Pressure changes also occurred in layers HH and MM. Pressure drops at layer HH are in the range of 4-11 bard . Largest pressure drop occurs in the main production zone in the southern part. In Layer MM the pressure drop in production zone is larger than that in Layer HH, and reaches up to 12 bar of pressure drop in the central part of the production zone. In reinjection area, pressure increases up to 50bar due to reinjection of large amount of the waste water.

4.2. Scenario III: 100 MWe power production

The largest power generation of 100MWe was examined for Scenario III. This requires a production of 1380kg/s of the geothermal fluid. For this scenario, total number of 35 production and 16 reinjection wells were assigned. The grid number corresponding to each production and reinjection wells and assumptions of the scenario is presented in Table 5. However, thirty five production wells is a large number, and it causes higher cost per kW of electricity generation. This scenario was given to evaluate the maximum production capacity of the field. As one well can be assigned in one grid, the maximum number of production wells being allocated is forty in the production zone. Thus, five wells can be allocated as the maximum number of makeup wells. One makeup well was allocated every 5 years for this scenario.

4.2.1. Total flow rate and flowing enthalpy

Figure 5 presents the total production rate with time. By starting the simulation with total flow rate of 1380kg/s the flow rate declines rapidly in both cases in 5 years. The result clearly indicates that adding five makeup wells do not increase the total production rate. The total production rate decreases to 600kg/s after 10 years. This corresponds to steam production for electricity generation of 47MWe. Based on the currently available subsurface information this field can produce 100MWe electricity for a short period, 5 years, and then decline to about 50MWe in following years. Total number of 35 production wells of 3000m depth makes the total length of 100km of drilling in this field. Consequently, electricity generation rate can be 1MWe per one kilometer of drilling in early stage of the production, but it is predicted to be decreased in the later years. World average rate is 2-5 MWe/km [8,9] which is much higher than this value. To evaluate the effects of total number of wells on average well output the simulations were carried out with different number of wells, from 5 to 35 wells. The results show that average production rate of each well decrease with an increase of the total number of the wells. Figure 6 illustrates relationship between average well output and the total number of the production well. For 5 to15 wells the average well output is 1.3MWe/km, which is still lower than the world average but output reduces to 0.8MWe/km by increasing the number of wells. This is considerably low and results in an increase of the electricity production cost. The simulation was run for 100 years to find out the reservoir capacity that can deliver steam at stabilized rate. Results show that after 20 years the steam flow rate reaches stable with rate of 98 kg/s which can generate 45-50MWe of electricity over 100 years. The flowing enthalpy does not change significantly during simulation period in both cases and the average flowing enthalpy of the produced fluid shows 998 kJ/kg.

4.2.2. Predicted pressure and temperature

The temperature and pressure changes for scenario III were examined for Layers MM. Cooling occurs in the northern part of the reservoir where reinjection wells locate. Temperature drops by 80°C from the initial in the central part of the reinjection zone, and more than 10°C cooling can be seen over an area about 7km^2 which is 4.5km^2 in Scenario II. In Layer MM the pressure drop in the production zone is large and shows up to 30bar in the central part of the production zone. This pressure drops can cause the production rate decline. Larger pressure drop in Layer MM occurs in a wider area compared with that of Scenario II. In the reinjection area, pressure increases due to the reinjection of large amount of waste water. In reinjection area pressure increases up to 80bar.

5. Conclusions

A three dimensional numerical model of the NW Sabalan geothermal field was developed and calibrated by numerical simulations. Prediction simulations of reservoir behaviors were also carried out using the numerical model developed. Two hypothetical development scenarios were evaluated for production capacity assessment and reinjection effects on fluid production. The conclusions are summarized as follows:

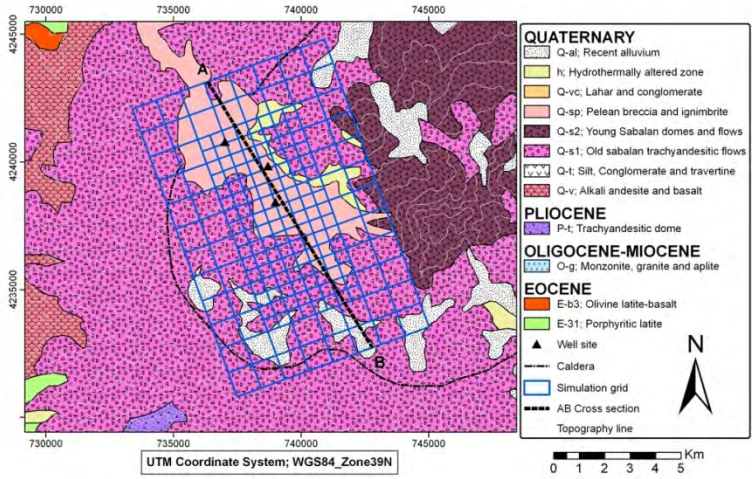

Figure 1 Geological map of the Sabalan area with grid system

The results of natural state simulation using the AUTOUGH2 simulator indicated good agreements in temperature and pressure profiles of three deep wells with measurement. Reinjection of the waste water is effective for moderating reservoir pressure drop. The immediate adjacent area, north to the production area, named as Site B is recommend for locating reinjection wells because of more effective on the pressure support compared with reinjection at further north area, Site C. Based on existing data and assumptions reservoir can sustain steam production equivalent to 50 MWe of electricity for 30 years or more. The reservoir can produce in maximum capacity for production of 90-100MWe for short period of time (5 years), but the production rate decreases gradually to the level of 50MWe after 20 years. The reservoir can sustain steam production for 50MWe over 100 years.

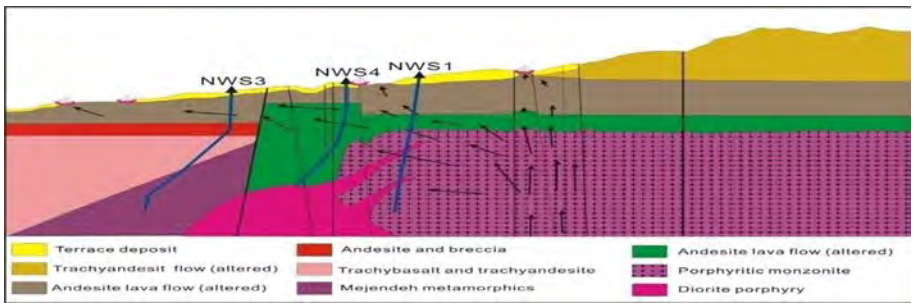

Figure 2 Conceptual model of the NW-Sabalan geothermal field

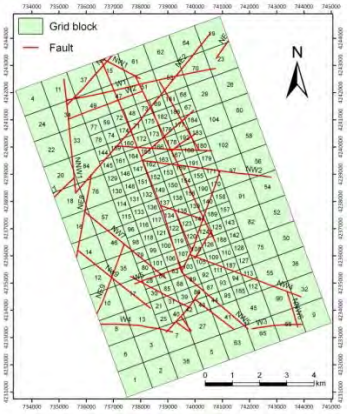

Figure 3 The grid system and faults in study area

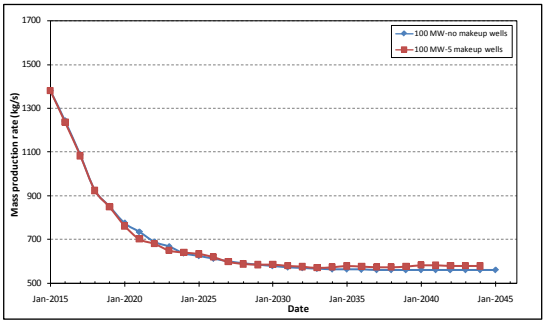

Figure 5 Total production rate over 30 years for Scenario III

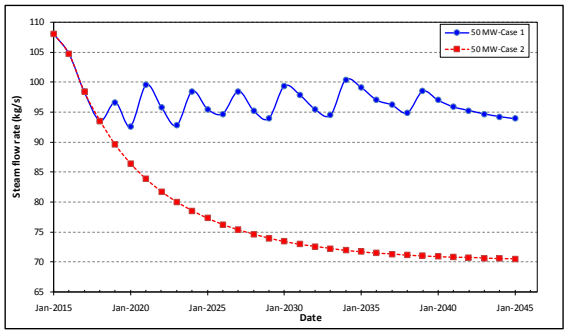

Figure 4 Steam flow rate change with time for Scenario II

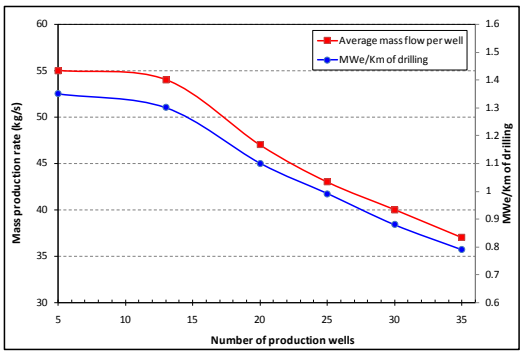

Figure 6 Relationship between average well-output and power generation per km of drilling and number of the production well

References

[1] Pruess, K.,TOUGH2-A General Purpose Numerical Simulator for Multiphase Fluid and Heat Flow, Earth Science Division, Lawrence Berkeley Laboratory, Berkeley,1991,102p

[2] O'Sullivan, MJ., AUTOUGH2 Notes, Department of Engineering Science, University of Auckland, 2000,18 pp

[3] SKM, Report on completion tests and heat up surveys of well NWS1, SUNA Co., 2004a

[4] SKM, Well NWS3 drilling completion report, SUNA Co., 2004b,47 pp

[5] SKM, Well NWS4 drilling completion report, SUNA Co., 2004c, 43 pp

[6] SKM, Sabalan geothermal project, Stage1- surface exploration, final exploration report, report number. 2505-RPT-GE-003, SUNA Co., 1998,83 pp

[7] Beckman, W. and Klein, S., Engineering Equation Solver Professional Versions user manual, F-Chart Software, 2007, pp. 312

[8] Stefansson. V., Investment cost for geothermal power plants, Geothermics, Vol. 31, 2002, 263-272

[9] Stefansson. V., Success in geothermal development, Geothermics, Vol. 21, 1992, 823-834

Utilisation of hydrogeothermal energy by use of heat pumps in Serbia – current state and perspectives

Dejan Milenic[1*], Ana Vranjes[1]

[1]*Univesity of Belgrade, Faculty of Mining and Geology, Department for Hydrogeology, Belgrade, Serbia*
[*]*Tel/fax: +381 11 3346 000, , E-mail: dmilenic@yahoo.ie*

Abstract: The development strategy of the energy sector in Serbia anticipates the intensive utilisation of renewable hydrogeothermal energy sources by using energy efficient technologies. The main aim of the paper is to perceive, for the first time, quantities and possibilities of the utilisation of available hydrogeothermal energy accumulated in groundwater with the temperature up to 30 ^{o}C in the concept of the substitution of fossil fuels by renewable en ergy sources in the Republic of Serbia. The available quantities of groundwater have been observed by regions whose borders correspond with hydrogeological characteristics of the terrain and conditions of groundwater formation. The territory of the Republic of Serbia is divided into eastern part, to which there belong estimated quantities of about 7400 $l \cdot s^{-1}$, namely the available heat power amounts about 200 MW, central and western parts of the territory (to which the capital city Belgrade also belongs) have about 14900 $l \cdot s^{-1}$, which is adequate to about 400 MW of heat power, and northern part of the territory with available 6600 $l \cdot s^{-1}$, namely about 180 MW of heat power. If we take into account the territory of the whole Republic, the available resources of subgeothermal energy amount about 28$m^3 \cdot s^{-1}$, namely over 770MW of heat power.

Keywords: *Hydrogeothermal energy, Subgeothermal energy, Groundwaters, Serbia*

1. Introduction

According to development plans in the field of energetics and energy efficiency of the Republic of Serbia, hydrogeothermal resources belong to renewable energy sources whose application and utilisation, namely the verification of reserves is in its initial phase. The potential and reserves are not examined and explorations of this kind of renewable energy have become significant lately. The strategy of energy development in Serbia anticipates the intensive utilisation of renewable hydrogeothermal energy sources, especially low temperature groundwater via the energy efficient technologies by using heat pumps.

The main aim of the paper is to perceive, for the first time, quantities and possibilities of the utilisation of available hydrogeothermal energy accumulated in groundwater with the temperature up to 30 ^{o}C (subhydrogeothermal energy) in the concept of the substitution of fossil fuels by renewable energy sources in the Republic of Serbia. In the past three years subhydrogeothermal energy resources have been classified in Serbia for the first time (Milenic et.al. 2010, V ranjes 2008), as well as the valorisation of available resources of subhydrogeothermal groundwaters (Stevanovic et al.2010). Hydrogeothermal resources of low enthalpy (fluid temperature to 100ºC) have been classified as the sub(hidro)geothermal energy (fluid temperature to 30ºC) and hydrogeothermal energy in the narrow sense (fluid temperature from 30ºC to 100ºC). Further in the text, for the sake of simplification, the notion: "sub(hydro)geothermal energy" will be used as subgeothermal energy.

On the basis of the mentioned explorations, the definition of subgeothermal energy sources has been deduced: "subgeothermal energy sources are a kind of hydrogeothermal energy of low enthalpy accumulated in groundwaters of the temperature scope to 30 ^{o}C, a nd whose exploitation and utilisation are conditioned by the application of geothermal heat pumps".

Consequently, groundwaters with the temperature of 30^{o}C are significant subgeothermal resources, especially in alluvial plains and Neogene basins in the Republic of Serbia. On the basis of classifications stated in this way, the scientific-research project initiated in the year

2008 (Stevanovic et al.2010), evaluated the availability of groundwater resources which can be used as sources of subgeothermal energy (SGTE) as a kind of hydrogeothermal energy of low enthalpy.The obtained results point out the enormous potential of groundwater in the concept of utilisation as a renewable energy source. However, a small number of subgeothermal systems worked out so far points out the necessity of wider engagement of both the state and independent experts in the sense of awareness are using of the significance of this kind of renewable energy.

The significance of explorations and the utilisation of subgeothermal energy can be seen in the following: groundwater is "easy" for taping and the energy resource is inexpensive for development and exploitation, a l ocally available resource is used via relatively simple technology, the conservation of fossil fuels (oil, natural gas) by the renewable energy source, the increase of self-sufficiency and the sustainability of energy consumption, the increase of environmental quality through the decrease, namely the reduction of the emission of hazardous gases, such as CO_2 (up to 75% in relation to a conventional heating procedure) the improvement of image in public, financial savings due to the reduced purchase of fossil fuels, and the introduction of the principle of "sustainable development".

2. Applied methodology

Hydrogeological and hydrogeothermal explorations in this field are of a highly multidisciplinary character and imply the engagement of researchers from the field of hydrogeology (geothermal resource provision), mechanical engineering (thermo engineering part, the utilization of SGTE), and architecture (the increase of energy efficiency and the correct utilization of SGTE in building).

Hydrogeological explorations imply the evaluation of resource availability, as to:

1. Quantity defining:
    i) hydrogeological regionalisation of the territory of Serbia
    ii) defining of aquifer types within each hydrogeological region
    iii) carrying out of pumping tests at the existing wells within the particular aquifer type
    iv) yield measurements at springs within the particular aquifer type
    v) collecting and synthesis of results of past explorations in the field of hydrogeology
2. Defining of aquifer hydrodynamic characteristics:
    i) calculation of environmental basic parameters
    ii) workingout of aquifer hydrodynamic model
3. Defining of physic-chemical characteristics:
    iii) determining of ground water temperature regime
    iv) determining of qualitative regime
    v) basic chemical composition of ground water
    vi) water aggressiveness (corrosiveness /inscrutability)

After available quantities of subgeothermal energy had been defined, the data obtained in additional explorations were used in discussions, first of all:

Thermodynamic and energy explorations, i.e. calculation of required energy quantity for the heating building / buildings (building energy consume) and techno-economical analyses, i.e. the economical analysis of the investment cost-efficiency in the utilisation of renewable

energy resources comparative analysis of expenses for various fuels and the period of investment cost-efficiency.

The aim of the work methodology set in this way was, first of all, hydrogeological. The paper did not deal, in details, with the efficiency of the utilisation of heat pumps, the analysis of COP, etc. As regards that the utilisation of heat pumps in Serbia is in its initial state, it is not possible to give any detailed analyses of the mentioned parameters of the heat pump work.

3. Survey of subgeothermal potential in Serbia

The Republic of Serbia is pronouncedly rich in hydrogethermal resources (Fig.1a). The waters of Vranjska Banja Spa (96^{o}C), Josanicka Banja Spa (78^{o}C) and some others have the highest temperature. Groundwater with the temperature over 30^{o}C is relatively well utilised. Unlike them, groundwater with temperatures up to 30^{o}C (subgeothermal energy) has not been the subject of explorations from other points of view, except for the needs of water supply. Development of heat pump systems, their growing commercialisation and application in the world, have resulted in increased possibilities of multipurpose utilisation of this water.The availability of subgeothermal groundwater resources is mainly related to depth up to 200m from the surface of the terrain and, on the territory of Serbia it is not evenly spaced. The largest quantities of this kind of energy are related to alluvions of big rivers, especially in towns they run through. Due to the heat island effect, temperatures of groundwater in towns are higher in relation to rural environment, thus the energy potential is higher. On the basis of carried out preliminary explorations of the assessment of groundwater resources with the temperature up to 30°C, the territory of the Republic of Serbia is a highly prospective one, from the point of view of the utilisation of subgeothermal energy. The available quantities of groundwater have been considered by regions, whose boundaries are adequate to hydrogeological characteristics of the terrain and conditions of groundwater formation. Available heat power of low enthalpy hydrogeothermal energy was calculated from the following equation (Eq.1):

$$E = C_p \cdot Q \cdot \Delta T \qquad (1)$$

where:

E - available heat power (KW, MW)

C_P - the specific heat of water (constant, $4.2 KJ \cdot kg^{-1} \cdot °C^{-1}$)

Q - yield of the wells ($kg \cdot s^{-1}$, the same as $l \cdot s^{-1}$)

ΔT - temperature reduction which can be realised in the heat pump (^{o}C)

The areas of big towns in Serbia have special potential, which due to the hot island effect have the most favourable subgeothermal characteristics with raised temperatures of groundwater even to 5^{o}C in relation to the remaining territory. The "heat island" effect is a consequence of urbanisation, leading to micro climatic changes expressed as air temperature raising. This temperature increase can reach 5^{o}C, in relation to inurbane suburbs. Being highly urbanised the City of Belgrade (the city core covers an area of over 10km^2, with more than 1,500.000 inhabitants) has all predispositions for heat island effect occurrence. The geological characteristics of the Belgrade area conditioned the existence of significant quantities of ground waters where heat effect is induced as temperature anomaly.

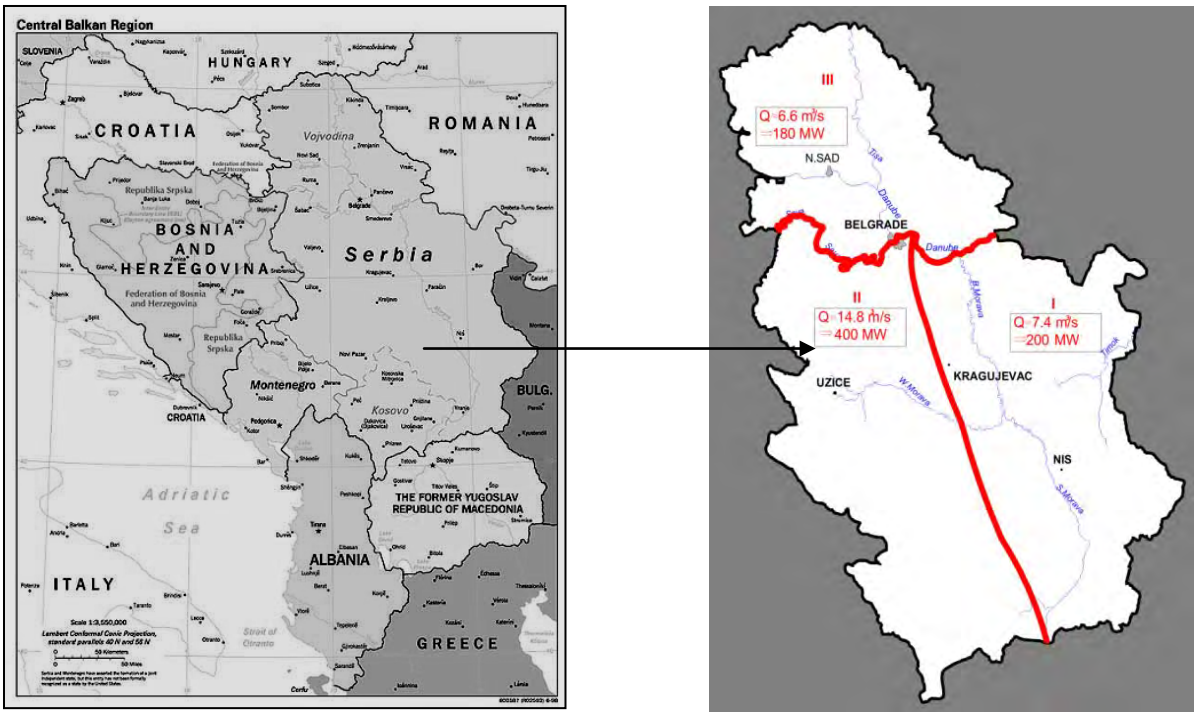

Fig. 1. a)Geographical position of the study area, b)Partition of the investigation area

The available energetic potential of ground water on carried out test exploited wells in New Belgrade goes over 0.5 MW for an individual well. This record was obtained by using minimal well yield of about 1,000- 1,500 m^3/daily and minimal temperature of ground water of 13 to 15°C. Hydroisotherms point out clearly that the groundwater temperature in lesser urbanised areas amounts 13-14°C. Moving to central and highly urbanised parts of New Belgrade the groundwater temperature reaches even 20°C (in summer months), i.e. the groundwater temperatures are higher from 3 to 6 °C. Fig 2.

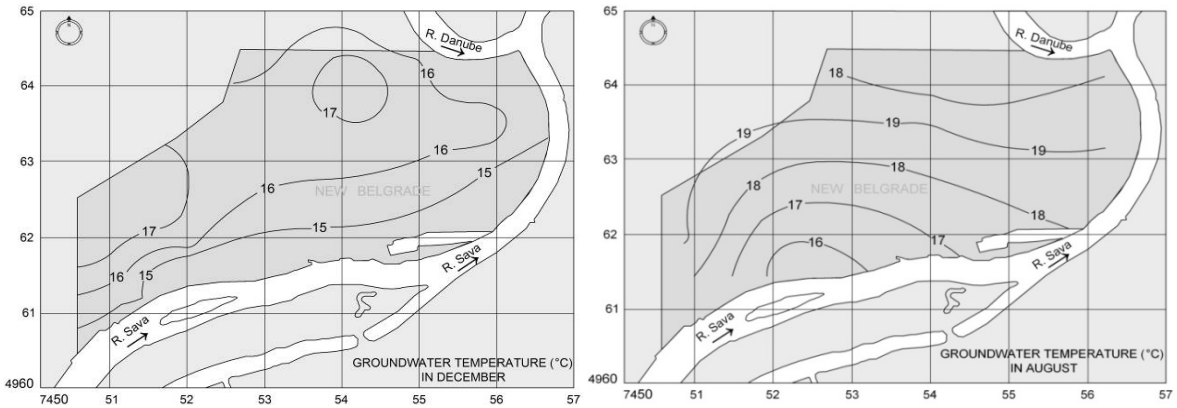

Fig. 2. Hydroisotherm maps of the territory of New Belgrade

The available quantities of groundwater have been observed by regions whose borders correspond with hydrogeological characteristics of the terrain and conditions of groundwater formation. The territory of the Republic of Serbia is divided into eastern part, central and western parts of the territory (Table 1).

Table 1.

	Estimated quantities of groundwaters for all purposes ($l \cdot s^{-1}$)			Total ($l \cdot s^{-1}$)	Total* heat power (MW)	Available quantities for SGTE ($l \cdot s^{-1}$)			Heat power for SGTE (MW)
	Groundwater temperature (°C)					Groundwater temperature (°C)			
	10-16	16-22	22-30			10-16	16-22	22-30	
	1	2	3	4	5	6	7	8	9
Eastern Serbia									
Alluvial deposits	15750	0	0	15750	388	5510	0	0	138
Neogene aquifer	2090	340	200	2630	73	730	155	105	34
Karstic aquifer	5080	130	50	5260	110	725	48	25	23
Fractured aquifer	200	60	50	310	11	71	28	25	5
TOTAL	23120	530	300	23950	582	7036	231	155	200
Central and western Serbia (Including Belgrade)									
Alluvial deposits	29000	0	0	29000	728	10150	0	0	255
Neogene aquifer	4700	350	320	5370	159	1645	150	140	60
Karstic aquifer	7000	380	130	7510	205	2450	150	45	73
Fractured aquifer	250	90	60	400	15	88	45	30	7
TOTAL	40950	820	510	42280	1107	14333	345	215	395
Northern Serbia									
Alluvial deposits	12100	0	0	12100	304	4235	0	0	107
Plioquaternary deposits	5100	200	100	5400	146	1785	100	50	54
Neogene aquifer	800	200	100	1100	38	280	100	50	16
Karstic aquifer	0	0	0	0	0	0	0	0	0
TOTAL	18000	400	200	18600	617	6300	200	100	177
TOTAL TERRITORY	82070	1750	1010	84830	2306	27669	776	470	770

***** Groundwater temperature 10-16 °C, ΔT=6 °C
Groundwater temperature 16-22 °C, ΔT=12 °C
Groundwater temperature 22-30 °C, ΔT=18 °C

4. Discussion

As can be seen from Table 1, the territory of the Republic of Serbia is divided into eastern part to which there belong estimated available quantities for SGTE of about 7400 $l \cdot s^{-1}$, namely the available heat power amounts about 200 MW, central and western parts of the territory (to which the capital Belgrade also belongs) have about 15000 $l \cdot s^{-1}$, which is adequate to about 400 MW of heat power, and northern part of the territory with available 6600 $l \cdot s^{-1}$, namely about 180 MW of heat power. Taking the whole territory of the Republic into account, the total estimated quantities of groundwaters for all purposes amount about 85 $m^3 \cdot s^{-1}$, the total heat power is about 2306 MW, the available resources of subgeothermal energy amount about 29 $m^3 \cdot s^{-1}$, namely over 770MW of heat power (Figure 1b).

If the obtained data are crossed according to types of water bearing structures, it can be seen that intergranular environments in alluvial deposits are far the most abundant. The positions-locations of the biggest towns in Serbia correspond with these environments, thus the possibilities of applications in them are the highest.

If the temperature of groundwater is observed as a parameter, it can be seen that groundwaters with the temperature range of 10-16^oC are most widely distributed. Waters of this temperature in the areas of big towns can be affected by the heat island effect being the most convenient ones for the use of heat pumps.

Utilisation has been mostly related to the territory of the city of Belgrade so far occurring individually, not organized. According to recorded users on the territory of Belgrade, for the needs of climatization of buildings, overall 100 $l \cdot s^{-1}$ of groundwater of 12ºC to 16ºC has been used, while on the territory of whole Serbia the quantities do not exceed 250 $l \cdot s^{-1}$ (overall about 100 users).

On the basis of the stated data, the great potential of subgeothermal resources in Serbia is obvious. The current energy crisis and increasing costs of fossil fuels used for heating(it is primarily related to natural gas whose price rises every year) impose the necessity to take seriously into account the utilisation of subgeothermal resources instead of ignoring it.

The significance of such a way of heating/cooling (by utilisation of SGTE) in building has been highly recognized in the EU. At the end of the last century the member states of the EU completed projects of rehabilitation of the existing housing in order to save energy tending to consume energy for heating lower than 80-100 $kWh \cdot m^{-2}$ annually. In Serbia, the state is still significantly different. The existing buildings are one of the highest consumers of energy in the Republic. Almost 50% of the consumed energy in Serbia is used in buildings, among which 65% for building heating. Almost the third of overall energy needs of Serbia is related to heating of residential and office buildings. According to estimation, the annual energy consumption for residential heating in Serbia ranges from 150 to 250 $kWh \cdot m^{-2}$ depending on the age and the state of buildings. The structure of energy consumption is exceptionally unfavourable: 26% of flats are connected to heating plants; 30% of households use electrical energy; 20% of them use firewood; 15% coal; <6% gas.

Consequently, for the lowest level of consumption (heating) the most qualitative energy (electrical energy) is mostly consumed. The aim of the applied measures is to achieve the reduction of energy consumption in office buildings and public facilities of 80-100$kWh \cdot m^{-2}$ / annually and in individual houses to 70-90$KWhm^2$/ annually, and in flats for collective dwelling to 65-80 $kWh \cdot m^{-2}$ /annually.

Buildings in Serbia are real energy wasters. Over 70% of existing residential buildings were constructed before passing the first serious regulations on thermal protection in the eighties of the last century. Bearing in mind that, annually, only 1% of the existing residential buildings is constructed, it is obvious that the basic resource for applications of energy efficiency measures of any sorts are the existing residential buildings. If only urban area is rehabilitated, i.e. 1.6 million of flats, in the period of the following ten years, that is the work worth 4.5 milliard € or 450 million € annually. Such a wide action would result in the fast creation of conditions for the application of SGTE for due to considerably reduced needs for energy far larger number of facilities could use these resources.

Accordingly, there also goes the comparative analysis of expenses required for the production of 1 MWh of heat energy in relation to the kind of the energy resource, the price of the energy resource, and the manufacturing price in the Republic of Serbia in the season 2010/2011 indicating the highest cost-efficiency of the subgeothermal energy utilisation (Table 2). The analysis has been carried out in relation to the following parameters: natural gas is imported from Russia, the kind of coal is lignite, the approximate price of a pellet is 140 € /t, hydrogeothermal energy is from heat pumps with the approximate COP 1:4, and the price of electrical energy of 0.05 € /KWh.

Table 2. Comparative analysis of expenses required for production of 1MWh of heat energy in relation to kind of energy resource, price of energy resource, and manufacturing price in Republic of Serbia in December 2010

Kind of energy resource	In relation to energy resource price (€)	Manufacturing price (€)
Natural gas	52	72
Mazut	48	68
Coal	32	52
Pellet	38	58
Hydrogeothermal energy (SGTE)	15	35

Nowadays, in Serbia, about 50-55% of overall energy consumption is used in building and about 70% out of that for heating and cooling. By correct investment, with energy savings, energy consumption could be even halved, with invested money refund in the period of five years. The first step is the reduction of loss with final consumers -in flats. The energy rehabilitation of an average flat in Serbia with the surface of 70 m^2 requires about 3000-4000 €. By such investment from 100 to 150 $kWh \cdot m^{-1}$ would be saved annually, meaning 400-600 € annually at nowadays' prices. In this way such investment is repayed in the period of four to seven years.

In order to establish economic justifiability of the SGTE system in new buildings it should be compared to conventional heating systems with regard to initial investment, maintenance expenses, system duration, and cost price of heating resources. Experiences indicate that initial investment in subgeothermal systems (capable to deliver 1 KW of thermal power) ranges within the scope of 850 € per kWh for heating, and up to 1000€ per kWh for combined heating and cooling systems. The initial investment prices in conventional systems are generally lower to some extent than in hydrogeothermal ones being about 40% in heating systems, namely 20% in combined cooling and heating systems. It should be stated that in recent years the prices of STGE systems have dropped significantly approaching those of conventional ones. Unlike the initial investment, the maintenance prices are lower in hydrogeothermal systems, about 50% in combined cooling and heating systems. The use of STGE in Serbia is not charged, once obtained licence for groundwater exploitation is renewed

every five years. Taking into account significant raising of prices of all kinds of fossil fuels, the economic cost-efficiency of this kind of heating is obvious.

Besides, we should bear in mind the reduction of CO_2 emission into atmosphere. As Serbia has signed the Kyoto Protocol, via the system of "quota trade" compensation financial means are obtained on behalf of "preserved" thousand tonnes of CO_2 emission into atmosphere. The current Law on Energetics introduces categories of privileged users, namely legal persons using renewable energy resources anticipating a set of benefits and facilities for them (tax free import of heat pumps, etc.).

References

[1] Milenic, D., Vasiljevic, P., Vranjes, A.: Criteria for use of groundwater as renewable energy source in geothermal heat pump systems for building heating/cooling purposes, Elsevier, Energy and Buildings, 2010, pp. 649-657

[2] Milenic, D., Vranjes, A., Savic, N., Veljkovic, Z.: Indicators of impact of heat island effect on ground water energetic potential on the territory of New Belgrade, Serbia, Europe, Proceedings of the XXXVI IAH Congress,Toyama, Japan,2008

[3] Milenic, D., et al: Exploration and application of renewable subgeothermal groundwater resources in the concept of energy efficiency increase in building, Project Number 33053, Strategic project for technological development for R.Serbia, 2011-2014 (in Serbian)

[4] Stevanovic, Z., Milenic, D., Dokmanovic, P., Martinovic, M., Saljnikov, A., Komatina, M., Antonijevic, D., Vranjes, A., Magazinovic,S.,: Optimization of energy utilization of subgeothermal water resources, Project Number 18008, Strategic project for technological development for R.Serbia, 2008-2010 (in Serbian)

[5] Vranjes, A., 2008: Hydrogeothermal resources of the city of Belgrade territory, phD project, University of Belgrade, Faculty of Mining and Geology

[6] Water management basics of Serbia, 2000

Geothermal Energy Utilization in the United States of America

J. Lund

National Renewable Energy Laboratory, Golden, Colorado, USA
**Tel: +1 541-891-2977, Fax: +1 541-885-1320, E-mail: john.lund@nrel.com*

Abstract: Geothermal energy is used for electric power generation and direct utilization in the United States. The present installed capacity (gross) for electric power generation is 3,087 MWe with about 2,024 MWe net delivering power to the gird producing approximately 16,600 GWh per year for a 94% net capacity factor. Geothermal electric power plants are located in Alaska, California, Hawaii, Idaho, Nevada, New Mexico, Oregon, Utah, Wyoming. The direct utilization of geothermal energy including the heating of pools and spas, greenhouses and aquaculture facilities, space heating and district heating, snow melting, agricultural drying, industrial applications and ground-source heat pumps. The installed capacity is approximately 12,610 MWt and the annual energy use is about 56,550 TJ or 15,700 GWh. The largest application is ground-source (geothermal) heat pumps (84% of the energy use). The largest direct-use (excluding geothermal heat pumps) is fish farming (34%), spa and swimming pool heating (28%), and space and district heating (23%). The energy savings from all geothermal use is about 48.5 million barrels (7.3 million tonnes) of equivalent fuel oil per year and reduces air pollution by about 6.65 million tonnes of carbon annually (compared to fuel oil).

Keywords: *geothermal energy, electric power, direct-use, geothermal heat pumps*

1. Introduction

Geothermal resources capable of supporting electrical generation and/or direct use projects are found primarily in the Western United States, where most of the recent volcanic and mountain building activity have occurred. The San Andreas fault running through California from the Imperial Valley to the San Francisco area, and the subduction zone off coast of northern California, Oregon and Washington along with Cascade volcanism are the source of much of the geothermal activity in the United States. However, geothermal (ground-source) heat pumps extend the utilization to all 50 states. The total identified potential for electrical production is estimated at 21,000 MWe (above 150^{o}C) and 42 EJ (between 90^{o} and 150^{o}C) of beneficial heat [1], and a recent estimate by the U.S. Geological Survey estimates a mean probability of electrical power generation from identified geothermal resources in12 western states during the next 30 years of 8,866 MWe, which would nearly triple the existing electrical capacity. Currently, the geothermal electrical generation installed capacity is 3,048 MWe (gross), 2,024 MWe (net), and the annual energy produced is 16,603 GWh/yr.

Geothermal direct-use is currently estimated at 9,152 TJ/yr (2,542 GWh/yr) with an installed capacity of 611 MWt. Geothermal heat pumps contribute 47,400 TJ/yr (13,167 GWh/yr) with an installed capacity of 12,000 MWt. The total of all direct utilization in the United States is 56,552 TJ/yr (15,709 GWh/yr) with an installed capacity of 12,611 MWt. A total of 20 new direct-use projects have come on line over the past five years, but this increase has been partially offset with closing of one agricultural drying plant and two small district heating projects. Geothermal heat pumps have seen the largest gain, growing at slightly over 10 percent a years with installed units.

This paper is based on material present at the World Geothermal Congress 2010, Bali, Indonesia [2].

1.1. Summary of Electric Power Generation

Even though the United States is the world leader in geothermal electric power generation, geothermal energy remains a small contributor to the electric power capacity and generation in the United States. In 2009, geothermal plants constituted about 0.27 percent of the total operable power capacity, and those plants contributed an estimated 0.48 percent of the total generation.

Since 2005 gross geothermal electrical production capacity has increased in the United States by approximately 500 MWe to a total an installed capacity of 3047.7 MWe and a net running capacity of 2,023.5 MWe due to derating of plants in The Geysers, producing 16,603.4 GWh/yr for a gross capacity factor of 0.62 and a net of 0.94. The low net value is due to plants, especially in The Geysers, operating in a load following mode rather than in a base load mode and due to a reduction in pressure and output of the steam field. The geothermal electric power generation accounted for 4% of the total renewable based electricity consumption in the United States. On a state level, geothermal electric generation is a major player in California and Nevada. The period 1990-2004 also saw a reduction at The Geysers geothermal field in northern California from 1,875 to around 1,529 MWe installed capacity and 945 MWe running capacity. Today, the installed capacity is 1584 MWe and 844 MWe running capacity. This was due to the closing of four units and a reduction in the steam availability. Some capacity has been restored due to the construction of two effluent pipelines, one from Clear Lake and the other from Santa Rosa, that brings about 72,000 tonnes of water per day (19 million gallons/day) to The Geysers for injection. This has restored an estimated 200 MWe of capacity to the field.

1.2. Summary of Direct Utilization

Direct-use, other than geothermal heat pumps, has remained static with increases being balanced by closing of some facilities. The main increases has been in expanding the Boise City District Heating System from 48 to 58 buildings; adding additional wells for space heating in Klamath Falls; expanding the snow melting system on the Oregon Institute of Technology campus from 316 m^2 to 3,753 m^2, increasing the amount of aquaculture product being produced, mainly Tilapia; starting two biodiesel plants; adding an absorption chiller for keeping the Ice Museum at Chena Hot Springs in Alaska intact during the summer months, and adding additional space heating to the Peppermill Casino in Reno. Losses have been the closing of the district heating systems at the California Correctional Center (now using natural gas) and the New Mexico University heating system (due to difficulty with maintenance), and the closing of the Empire onion dehydration plant (due to competition with imported garlic from China) near Gerlach, Nevada.

Geothermal heat pumps have seen the largest growth, increasing over the past five years from an estimated 600,000 to 1,000,000 equivalent 12 kW installed units. The estimated installation rate is from 100,000 to 120,000 units per year, or about a 12 to 13 percent annual growth, with most of the growth taking place in the mid-western and eastern states. A few states have tax rebate programs for geothermal heat pumps, and Congress has established a tax credit of 30% of costs up to $1,500 for installations. Otherwise, there is little support for implementing direct-use projects.

1.3. Enhanced (Engineered) Geothermal Systems

Enhanced (Engineered) Geothermal Systems (EGS) is the current R&D interest of the U.S. Department of Energy, Office of Geothermal Technologies as part of a revived national geothermal program. EGS includes the earlier hot dry rock technology, but now includes any

other method in which to improve geothermal reservoir performance. EGS is associated with both magmatic and high heat producing crustal sources of geothermal energy commonly at depths of about 4 to 5 km to reach 200^{o}C, but also having applications with normal gradient resources. However, EGC projects are currently at an early experimental demonstration stage. Several technological challenges need to be met for widespread efficient use of EGS. The key technical and economic changes for EGS over the next two decades will be to achieve economic stimulation of multiple reservoirs with sufficient volumes to sustain long term production, with low flow impedance, limited short-circuiting fractures and manageable water loss [3].

2. Production of Electricity

The total geothermal electrical installed capacity at the beginning of 2010 was 3,048 MWe producing 16,603 GWh/yr from a running capacity of 2,024MWe. A total of about 514 MWe has been installed in the last five years, amounting to a 20 percent increase or 3.7 percent annual increase.

2.1. Installed and Future Capacity Update

2.1.1. Alaska

Alaska's first geothermal power plant came online in 2006 in Chena Hot Springs. It is a small organic Rankine cycle (ORC) unit (250 kW gross) and produces electricity from the area's low temperature (74^{o}C) geothermal resource. Since coming online the power plant has added another 250 kW unit as well as a 280 kW unit, bringing total production capacity to 730 kW (gross).

Alaska currently has 70 to 115 MW of planned geothermal production coming down the pipeline. Of projects with potential to come online, the Southwest Alaska Regional Geothermal Energy Project 25 MWe, is in an exploratory drilling and resource confirmation phase. Other notable projects are Tongass (20 MWe), Unalaska (10–50 MWe), Pilgrim Hot Springs (10 MWe), and Chena Hot Springs II (5-10 MWe).

2.1.2. California

Current geothermal electricity grossproduction capacity in California is approximately 2497 MWe (1,627 MWe net). In 2010, 4.5% of California's electricity generation came from geothermal power plants, amounting to a net total of 13,605 GWh. The 50 MW North Brawley facility is the state's most recent geothermal power plant addition. Generally, geothermal power generation remains concentrated in California with the majority of production occurring at The Geysers in the north and Imperial Valley in the south.

California has approximately 1,555 – 19,39 MWe of planned geothermal resource production in various stages of development. Production drilling and facility construction are underway at Western GeoPower Corp.'s Unit 1 (35 MWe) at the Geysers as well as CHAR, LLC's Hudson Ranch I (49.9 MWe). Final permitting and PPA's are being secured for Ormat Technologies East Brawley project (30 MWe), Calpine Corporations Buckeye-North Geysers (30 MWe) and Wildhorse-North Geysers (30 MWe) projects, and CalEnergy's Black Rock 1, 2, and 3 units (53 MWe each).

2.1.3. Hawaii

There is only one geothermal power plant in all of Hawaii. Located on the big island, the Puna Geothermal Venture facility has a 35 MWe nameplate capacity and delivers 25–35 MWe of energy on a continuous basis and supplies 20% of the electricity needs of the big

island. Ormat is in the process of securing a PPA and final permitting for an 8 MWe expansion of its Puna project. The 10 units consist of a flash steam plant with a binary bottoming cycle plant.

2.1.4. Idaho

Idaho's first geothermal power plant, Raft River, came online in January 2008. Raft River is a binary plant that uses a 150^{o}C resource and has a nameplate production capacity of 15.8 MWe. Current net production output is between 10.5 and 11.5 MWe. US Geothermal is securing a PPA and final permitting for a 13 – 26 MWe expansion of the Raft River plant.

Another geothermal company, Idatherm, is developing a number of projects throughout Idaho. Idatherm has begun exploratory drilling and resource confirmation operations for its Willow Springs project (100 MWe). It is also planning to develop its China Cap (100 MWe), Preston Area Project (50 MWe), and Sulfur Springs (25 – 50 MWe) resources but is still in the process of conducting initial exploratory drilling and securing rights to resource. Total potential geothermal production for Idaho is 238 to 326 MWe.

2.1.5. Nevada

In 2008 Nevada had 18 geothermal power plants with a total nameplate capacity of 333 MWe and with a total gross output of 10,791 MWh/yr. In 2009 Nevada increased its installed geothermal capacity with the addition of the Stillwater (ENEL, 47.3 MWe), Salt Wells (ENEL, 18.6 MWe), and the Blue Mountain "Faulkner 1" (Nevada Geothermal Power, 49.5 MWe) power plants. Currently Nevada has more developing projects than any other state and it is expected that gross capacity will increase significantly in the future. The following companies have begun production drilling and facility construction at various project sites: Vulcan Power (Salt Wells, 175 – 245 MWe), Presco Energy (Rye Patch, 13 MWe), and US Geothermal (San Emidio "Repower" Project, 8.4 MWe), Ormat (Jersey Valley, 18 – 30 MWe). Many other companies are in the process of securing PPA's and final permitting for a number of projects and other companies are in the early exploratory stages of developing numerous geothermal resources. Nevada currently has 1,776 to 3,323 MW of geothermal capacity in development.

2.1.6. New Mexico

In July 2008, a 0.24 MWe pilot installation project came online at Burgetts Greenhouses near Animas. The pilot installation is part of a larger project known as Lightning Dock that aims to bring a 20 MWe capacity geothermal power plant online in 2011.

2.1.7. Oregon

While there is only one small unit producing geothermal electricity, significant developments are forthcoming. The Oregon Institute of Technology (OIT) has installed a 280 kWe (gross) binary units and is currently producing power for use on campus – the first campus in the world to generate its own power from a resource directly under campus. OIT has also completed production drilling of a 1,600-m deep well and will install a 1.2 MWe binary power unit by 2012 using the 93ºC resource at 158 L/s. Davenport Power, U.S. Renewables Group, and Riverstone are securing a PPA and final permitting for their 120 MWe Newberry Geothermal project as is Nevada Geothermal Power for its 40 – 60 MWe Crump Geyser project. U.S. Geothermal, Inc. successfully completed the drilling of its second full sized production well at Neil Hot Springs (20 – 26 MWe) in October 2009. Overall there are 317 to 368 MWe of potential geothermal power capacity in planning in Oregon.

2.1.8. Utah

Currently, Utah has three power plants online. Unit 1 of the Blundell Plant has a gross capacity of 25 MWe and Unit 2 has a capacity of 11 MWe. Utah's third power plant came online in December 2008 and was the first commercial power plant in the state in more than 20 years. The Thermo Hot Springs power plant, a Raser Techologies operation, came online in 2009 and has a gross capacity of 14 MWe and is expected to generate with a net capacity of approximately 10 MWe. Shoshone Renaissance Geothermal Project. ENEL North America has begun exploratory drilling and resource confirmation operations at its Cove Fort (69 MWe) project site. Other companies have potential geothermal sites that are in the early stages of planning/development and overall Utah has 272 to 332 MWe of planned geothermal capacity for future production.

2.1.9. Wyoming

In August 2008, a 250 kWe Ormat organic Rankine cycle (ORC) power unit was installed at Rocky Mountain Oil Test Site (RMOTC) and a month later it began operating. As of January 2009, the unit had produced more than 485 MWh of power from 413,000 tonnes of hot water annually. The demonstration project is still in operation, and a United Technology Corporation 280 kWe plant is scheduled for operation in 2011. During operation these plants will be an evaluation of how to reduce fluctuations of power and to generate more than 250 kWe.

3. Geothermal Direct Utilization

3.1. Background

Geothermal energy is estimated to currently supply for direct heat uses and geothermal (ground-source) heat pumps 56,552 TJ/yr (15,709 GWh/yr) of heat energy in the United States. The corresponding installed capacity is 12,611 MWt. Of these values, direct-use is 9152 TJ/yr (2,542 GWh/yr) and 611 MWt, and geothermal heat pumps the remainder.

Most of the direct use applications have remained constant or decreased slightly over the past five years; however geothermal heat pumps have increased significantly. A total of 20 new projects have come on line in the past five years.

3.2. Space Heating

Space heating of individual buildings (estimated at over 2,000 in 17 states) is mainly concentrated in Klamath Falls, Oregon where about 600 shallow wells have been drilled to heat homes, apartment houses and businesses. Most of these wells use downhole heat exchangers to supply heat to the buildings, thus, conserving the geothermal water [4]. A similar use of downhole heat exchangers is found in the Moana area of Reno, Nevada [5]. Installed capacity is 140 MWt and annual energy use is 1361 TJ.

3.3. District Heating

There are 20 geothermal district-heating systems in the United States, most being limited to a few buildings. The newest is a small project in northern California [6]. In this rural community of Canby, geothermal heat is used for heating buildings, a greenhouse, and most recently driers and washers in a laundry. The city system in Boise, Idaho has added 10 buildings to their system and will be extended to Boise State University next year. Klamath Falls system has expanded by adding a brewery and an additional greenhouse. Installed capacity is 75 MWt and annual energy use is 773 TJ (215 GWh).

3.4. Aquaculture Pond and Raceway Heating

There are 51 aquaculture sites in 11 states using geothermal energy. The largest concentration of this use is in the Imperial Valley in southern California and operations along the Snake River Plain in southern Idaho. There is a report that some of the facilities in the Imperial Valley have closed, but reliable information is lacking. A large facility at Kelly Hot Springs in northern California has been expanding and now produces slightly over half a million kg of tilapia annually. Two unique aquaculture related projects are in operation in Idaho and Colorado – that of raising alligators [7]. Recent trends in the U.S. aquaculture industry have seen a decline in growth due to saturation of the market and competition from imports. Installed capacity is 142 MWt and annual energy use is 3074 TJ (854 GWh).

3.5. Greenhouse Heating

There are 44 greenhouse operations in nine states using geothermal energy. These cover an area of about 45 ha, have an installed heat capacity of 97 MWt and an annual energy use of 800 TJ/yr (222 GWh). The main products raised are potted plants and cut flowers for local markets. Some tree seedlings and vegetables are also grown in Oregon; however raising vegetable is normally not economically competitive with imports from Central America, unless they are organically grown. One unusual greenhouse product, started recently, is spider mites grown on lima bean plants at Liskey Farms south of Klamath Falls, Oregon. They are grown for their eggs which are then shipped south as feed for predator mites, which in turn are sold to farms to eat spider mites – a complicated process, as the mites and eggs are almost microscopic in size and difficult to see [8]

3.6. Industrial Applications and Agricultural Drying

Industrial applications have increased significantly due to the addition of two biodiesel plants (Oregon and Nevada). These plants primarily use geothermal energy for the distillation of waste grease from restaurants, but one also used canola oil. Small industrial uses include clothes driers and washer installed in Canby, California, and a brewery using heat from the Klamath Falls district heating system for brewing beer and heating the building [9]. The main loss is the closing of an onion/garlic dehydration plant at Empire, Nevada due to competition with imported garlic from China. The installed industrial capacity for these two applications is 40 MWt and the annual energy use 519 TJ/yr (144 GWh/yr) with nine facilities located in three states.

3.7. Cooling and Snow Melting

The two major uses of geothermal energy are for pavement snow melting, on the Oregon Institute of Technology (OIT) campus, and keeping the Aurora Ice Museum frozen year-round at Chena Hot Springs, Alaska. The installed capacity for this application is 4.8 MWt and the annual energy use is 68 TJ/yr (19 GWh/yr).

3.8. Spas and Swimming Pools

This is one of the more difficult applications to quantify and even to find all the actual sites, as most owners do not know their average and peak flow rates, as well as the inlet and outlet temperatures. There are 242 facilities in 17 states, with an estimated installed capacity of 113 MWt and annual energy use of 2,557 TJ/yr (711 GWh/yr).

3.9. Geothermal (Ground-Source) Heat Pumps

The number of installed geothermal heat pumps has steadily increased over the past 15 years with an estimated 100,000 to 120,000 equivalent 12 kWt units installed this past year.

Present estimates are that there are at least one million units installed, mainly in the mid-western and eastern states. The present estimates are that approximately 70% of the units are installed in residences and the remaining 30% in commercial and institutional buildings. Approximately 90% of the units are closed loop (ground-coupled) and the remaining open loop (water-source). The estimated full load hours in heating mode is 2000/yr, and in cooling mode is 1000/yr. The installation cost is estimated at US$6,000 per ton (US$ 1,715 per kW) for residential and US$7,000 per ton (US$2,000 per kW) for commercial. The units are found in all 50 states and are growing 12 to 13% a year. It is presently a US$2 to US$3 billion annual industry. The current installed capacity is 12,000 MWt and the annual energy use in the heating mode is 47,400 TJ/yr (13,168 GWh/yr). The largest installation currently under construction is for Ball State University, Indiana where approximately 4,000 vertical loops are being installed to heat and cool over 40 buildings.

3.10. Conclusions – Direct-Use

The growth of direct use over the past five years is all due to the increased use of geothermal heat pumps, as traditional direct-use development has remained flat. Unfortunately, there is little interest for direct-use at the federal level, as their interests are mainly in promoting and developing Enhanced (Engineered) Geothermal Systems (EGS) and co-produced systems using abandoned oil and gas wells. There are few incentives for the traditional direct-use development, but as mentioned earlier, there are tax incentives for geothermal heat pumps at the federal level and in some states such as Oregon. Since, most direct-use projects are small, there are few, if any, developers and/or investors who are interested in supporting these uses.

4. Energy and Carbon Savings

In total, the savings from present geothermal energy production in the U.S., both electricity and direct-use amounts to 48.5 million barrels (7.28 million tonnes) of fuel oil equivalent (TOE) per year, and reduces air pollution by 6.65 million tonnes of carbon annually. CO_2 reduction is estimated at 18.8 million tonnes.

5. Comparison to Other Countries

Based on data from the WGC2010 [10, 11], the following comparisons with the U.S. geothermal data are made:

5.1 Worldwide Geothermal Electric Power Generation (5 leading countries, except USA)

Country	Installed capacity (MWe)	Running capacity (MWe)	Annual energy produced (GWh/yr)
Philippines	1,904	1,774	10,311
Indonesia	1,197	1,197	9,600
Mexico	958	958	7,047
Italy	843	843	5,520
New Zealand	628	628	4,055
World (24 countries)	10,715	n/a	67,246

5.2 Worldwide Geothermal Direct Utilization (5 leading countries, (except USA.)

Country	Installed capacity (MWt)	Annual energy produced (GWh/yr)	Principal use
China	8,898	20,932	Bathing/district heating

Sweden	4,460	12,585	Geothermal heat pumps
Japan	2,100	7,139	Bathing
Turkey	2,084	10,247	District heating
Iceland	1,826	6,768	District heating
World (78 countries)	48,483	117,778	

As can be calculated compared to the worldwide figures, the United States has 28.8% of the installed capacity, and 24.7% of the annual energy produced for electricity generation; and 26.0% of the installed capacity, and 13.3% of the annual energy use. The low annual energy direct-use percentage for the U.S. is due mainly to the large number of geothermal heat pumps, which have a low capacity factor. In terms of MWe and MWt, the USA is the leader.

References

[1] L. J. P. Muffler (editor), Assessment of Geothermal Resources in the United States – 1978. U. S. Geological Survey Circular 790, U. S. Department of Interior, 1979.

[2] J. Lund, K. Gawell, T. Boyd, D. Jennejohn, The United States of America Country Update 2010, Proceeding World Geothermal Congress 2010, Bali, Indonesia, International Geothermal Association, 2010 (CD-ROM).

[3] J. Tester, B. Anderson, A. Batchelor, D. Blackwell, R. DiPippo, E. Drake (editors), The Future of Geothermal Energy - Impact of Enhanced Geothermal Systems on the United States in the 21st Century, U.S. Department of Energy, 2006, 358 p.

[4] G. Culver, J. Lund, Downhole Heat Exchangers, Geo-Heat Center Quarterly Bulletin 20/3, Oregon Institute of Technology, Klamath Falls, 1999, pp. 1-11.

[5] T. Flynn, Moana Geothermal Area, Reno, NV – 2001 Update, Geo-Heat Center Quarterly Bulletin 22/3, Oregon Institute of Technology, Klamath Falls, 2001, pp. 1-7.

[6] D. Merrick, Adventures in the Life of a Small District Heating Project or The Little Project That Could, Geothermal Resources Council Transactions 26, Davis, CA (CD-ROM).

[7] T. Clutter, Out of Africa – Aquaculturist Ron Barnes Uses Geothermal Water in Southern Oregon to Rear Tropical Fish from the African Rift Lake, Geo-Heat Center Quarterly Bulletin 23/3, Oregon Institute of Technology, Klamath Falls, 2002, pp. 6-8.

[8] L. Riley, Inside the Greenhouse: Geothermal Energy and Spider Mite Production, Geo-Heat Center Quarterly Bulletin 29/3, Oregon Institute of Technology, Klamath Falls, OR, 2010, pp. 15-18.

[9] A. Chiasson, From Creamery to Brewery with Geothermal Energy, Geo-Heat Center Quarterly Bulletin 27/4, Oregon Institute of Technology, Klamath Falls, 2006, pp. 1-3.

[10] R. Bertani, Geothermal Power Generation in the World 2005-2010 Update Report, Proceeding, World Geothermal Congress 2010, Bali, Indonesia (CD-ROM).

[11] J. Lund, D. Freeston, T. Boyd, Direct Utilization of Geothermal Energy 2010 Worldwide Review, World Geothermal Congress 2010, Bali, Indonesia (CD-ROM).

Performance Analysis of a Hybrid Solar-Geothermal Power Plant in Northern Chile

Ignacio Mir[1], Rodrigo Escobar[1]*, Julio Vergara[1], Julio Bertrand[2]

[1] *Departamento de Ingeniería Mecánica y Metalúrgica, Pontificia Universidad Católica de Chile, Santiago, Chile.*
[2] *Empresa Nacional del Petróleo, ENA, Santiago, Chile*
** Corresponding author. Tel: +562 3545478, Fax: +562 3545828, E-mail: rescobar@ing.puc.cl*

Abstract: Chile has introduced sustainability goals in its electricity law in response to increased environmental awareness and the need to achieve higher levels of energy security. In northern Chile, the Atacama Desert has a large available surface with high radiation level, while the tectonic activity along the entire country testifies an ample yet unexploited geothermal resource. The novel concept of hybridizing a geothermal power plant with solar energy assistance is presented here for the particular conditions of Northern Chile. A thermodynamic model is developed to estimate the energy production in a hybrid power plant for two different configurations of solar resource use: adding peak power for a constant geothermal output, and saving geothermal resources for a constant power output. The thermodynamic model considers a single-flash geothermal plant with the addition of solar heat from a parabolic trough field. The solar heat is used to produce superheated steam and to produce additional saturated steam from the separator whenever possible. Results indicate that the energy produced by a geothermal well can be increased up to 11.6% and achieve savings of up to 10.3% in the use of geothermal resources by adding solar assistance when using the single flash geothermal technology. Moreover, the optimal mass flow rate of the geothermal plant is decreased when adding solar assistance. It is recommended to exploit solar energy together with geothermal energy wherever possible, to take advantage of each other's strengths and mutually eliminate weaknesses.

Keywords: *Concentrated solar power, Geothermal Power Plant, Hybrid, Chile*

1. Introduction

Chile exhibits a large diversity of geographical features and climates which has a great impact on the availability of renewable energy sources and their proper assessment. The country has limited energy resources apart from hydroelectric capacity, with a negligible internal fossil fuel production, thus relies on fuel imports to meet its growing energy demand. Renewable energy sources in use by the country comprise only hydroelectricity and wood-based biomass, which combined, only account for 24% of primary energy consumption as of 2008, while non-renewable fossil fuels account for the remaining 76%. Primary energy (Ep) consumption has increased at a yearly rate of 5%, and it is projected to continue doing so as the country further develops [1]. The mechanism that is currently operating in Chile consists in the application of a mandatory renewable energy quota requiring a minimum of 5% of electricity generation starting in 2010 must come from renewable energy sources, excluding large scale hydroelectricity, with a gradual increase of the quota to reach a 10% in the electricity generation mix by 2024 [2]. Given the local distribution of renewable energy sources, northern Chile displays no potential whatsoever for hydroelectricity and biomass since the area is the driest desert in the world. Although there is considerable potential for solar and geothermal energy, none of them is currently contributing to the energy mix, mostly due to the high uncertainty and cost of geothermal exploration and the lack of proper solar radiation databases [3]. Here we propose to integrate both energy sources in a hybrid concept, in order to take advantage of each other strengths and eliminate possible weaknesses. Geothermal resources tend to supply saturated steam and thus are limited in temperature and efficiency, while solar resource is available in daily cycles unless thermal energy storage is used. The goal of the present study is to find the configuration of an hybrid power plant that result in the best combination of solar thermal and geothermal power cycles. The concept of harvesting

solar and geothermal energy together has been proposed in the literature [4, 5] although in those cases the solar energy is used to increase the dryness fraction of the geothermal brine. This approach has been demonstrated as flawed since it makes a less efficient use of the high-exergy, high-cost solar heat. It has been showed previously that the best combination is to utilize the solar energy to increase the temperature of the geothermal fluid by superheating it, with the use of binary cycles also been proposed as a useful alternative for using low-enthalpy geothermal sources [6, 7]. In what follows, we will first describe a power plant configuration with an only-geothermal plant as base case, and then a model of hybridized plant for comparison purposes, aiming to improve the cycle's thermal efficiency and to create synergies between the two energy sources. The results will compare the total electricity produced in a period, and the consumption of geothermal fluid which is related to well depletion.

2. Power plant models

This section presents the plant models under study, focusing on the thermodynamic cycles. First a base case of geothermal-only plant is presented, and then the hybrid Solar-geothermal plant is described.

2.1. Geothermal base cycle

The geothermal power plant model considered for this study consists on a single production well and the basic components of a single flash power plant: a steam separator, turbine, condenser, and re-injection well as shown in Fig. 1. We consider a demonstration plant which is fed by a single well reaching a nominal power of 3.974 MW.

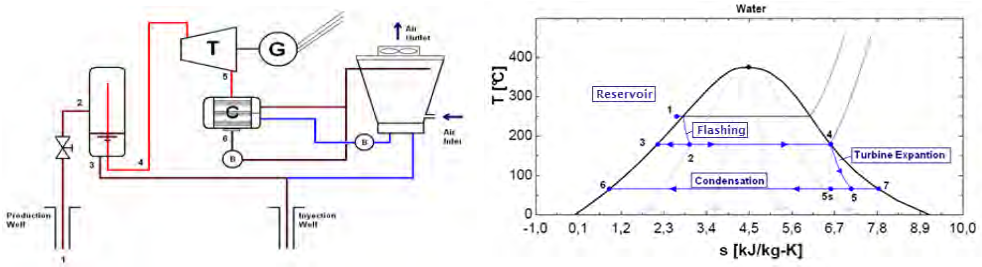

Fig. 1: Single flash plant and T-s diagram.

Numbers in the plant schematic match those from the T-s diagram. The letters T, C, and G stand for turbine, condenser and generator respectively. The conditions at the reservoir are considered to remain constant, while the behavior of the production well is be assumed to follow the productivity curve given by the polynomial expression that relates the mass flow rate with the wellhead pressure [6]:

$$\dot{m} = 44.333 - 0.3363 \cdot P - 0.1357 \cdot P^2 \qquad (1)$$

This fixes the conditions at the cycle beginning. The well head pressure is selected by optimizing the output power as $Max\{x_2 \cdot (h_5 - h_6)\}$, where the index numbers matches those on Fig. 1; therefore, by fixing the working pressure of the condenser, i.e. the pressure at the turbine's outlet, the geothermal power cycle is assumed completely determined. The condenser pressure used here is 0.01234 MPa, equivalent to a condensing temperature of 50°C. For all cases, it is assumed that the reservoir is at a constant temperature of 250°C. The steam fraction after the separator is given by $\dot{m}_{steam} = x_2 \cdot \dot{m}_{total}$, and the specific power from the turbine is $w_t = h_4 - h_5$, where h_5 stands for the enthalpy at the turbine outlet. If we

assume an ideal turbine, then we will have the ideal work produced by the turbine. Thus, we define the isentropic efficiency as the fraction between the real work produced by the turbine and the ideal work at the same conditions, considering h_{5s} as the isentropic enthalpy at the turbine outlet:

$$\eta_t = \frac{h_4 - h_5}{h_4 - h_{5s}} \quad (2)$$

The turbine efficiency is affected by the moisture level present in the steam during expansion. The larger the moisture present, the smaller is the turbine efficiency. This effect can be quantified using the Baumann's rule [8] which proposes that a 1% increase in moisture causes roughly a 1% drop in turbine efficiency. Adopting this rule, the isentropic efficiency is given by:

$$\eta_t = \eta_{td} \cdot \frac{x_4 + x_5}{2} \quad (3)$$

Where η_{td} represents the turbine isentropic efficiency working with dry steam, x_4 is the dryness fraction at the turbine inlet, assumed to be equal to one, and x_5 is the dryness fraction at the turbine outlet. It is assumed that the turbine isentropic efficiency for dry steam is constant and equal to 85%. The dryness fraction at the turbine outlet is calculated as:

$$x_5 = \frac{h_5 - h_6}{h_7 - h_6} \quad (4)$$

Where h_6 and h_7 are the enthalpies of saturated liquid and saturated vapor at the condenser pressure. As the dryness fraction at the turbine outlet depends on the isentropic efficiency, Eqs. (1) to (3) need to be solved simultaneously in order to determinate h_5 and therefore the specific power produced by the turbine. The mechanical power produced by the turbine is then calculated as $\dot{W}_t = \dot{m}_{steam} \cdot w_t$. The model considers that the generator efficiency is equal to 1, and that the parasitic loads are negligible. Finally, the heat rejected by the condenser after the turbine expansion is given by:

$$\dot{Q}_{cond} = \dot{m}_{steam} \cdot (h_5 - h_6) \quad (5)$$

With this the geothermal base cycle is defined and can be solved in order to obtain the steady-state power production.

2.2. Solar Field Modeling.

The solar field for the hybrid power plant is composed of parabolic trough collectors. The solar field sizing considers monthly means of solar radiation and the thermal energy demand. This demand depends on the characteristic of the thermodynamic cycle for each hybrid power plant configuration, depending on steam mass flow rate and the desired maximum temperature of the superheated steam being produced with solar heat. Once the thermal energy demand is determined, the field is sized for satisfying the demand by using a day modeled with the annual average radiation, which in northern Chile is within 20% of the annual maximum value. The sizing procedure includes an energy balance in which the collector area is determined as to ensure that the maximum desired temperature of the superheated steam is met after it passes through the heat exchanger system. The model utilizes Therminol VP1 as the solar field heat transfer fluid (HTF); its properties are obtained from the manufacturer, assuming a maximum working temperature of 400 °C [9]. Heat losses in the

receiver element are modeled based on correlations proposed by NREL [10] as a function of the temperature difference between HTF and the environment:

$$\dot{Q}_{loss} = 0.41 \cdot \Delta T + 1.21 \cdot 10^{-8} \cdot \Delta T^4 \quad (6)$$

A counter flow heat exchanger is used, considering an effectiveness of 95%. The energy balance in the heat exchanger is given by:

$$\eta_{HX} \cdot \dot{m}_{HTF} \cdot Cp_{VP1} \cdot (T_d - T_c) = \dot{m}_{AB} \cdot Cp_{AB} \cdot (T_a - T_b) \quad (7)$$

Where η_{HX} is the heat exchanger effectiveness, $\dot{m}_{HTF}$ is the HTF mass flow rate, C_pVP1 is the HTF heat capacity, T_D is the hot HTF temperature, T_C is the cold HTF temperature, $\dot{m}_{AB}$ is the water or steam mass flow rate, Cp_{AB} is the steam heat capacity, T_A is the sold steam temperature, and T_B is the hot steam temperature. Once the parabolic trough array is sized, it is possible to simulate the operating conditions for each hour of the year by using hourly solar radiation data. The solar field works in a similar way for all cases, varying the mass flow rate of the HTF to keep the outlet temperature constant at the design temperature independent of the actual radiation value. If the solar radiation in a given hour is higher than the design radiation, then it will have a HTF mass flow rate greater than the designed and vice versa. When solar energy exceeds the design value, the extra energy is used to increase the brine dryness factor.

2.3. Hybrid Power Plant

The hybrid Solar-Geothermal power plant consists of a geothermal power plant with assistance from a solar field. Two main scenarios for power production are used; the first aims to produce as much energy as possible without altering the basic operation of the geothermal component of the system, keeping the geothermal optimal mass flow rate from the reservoir fixed and producing extra power as function of solar radiation availability. The second scenario intends to keep the power production constant by reducing the geothermal mass flow rate while supplying extra heat from the solar field. The basic premise here is that saving geothermal fluid could result in extended well and reservoir lifetime, and as a result, decrease make up drilling costs without compromising the energy output rate. The input data are the geothermal well production curve and the solar radiation available (as in Eq. 1), and the prevailing climatic conditions at the chosen plant location. The solar radiation is obtained from pyranometer data available for the general area of Calama (22° 2S, 68° 5 W).

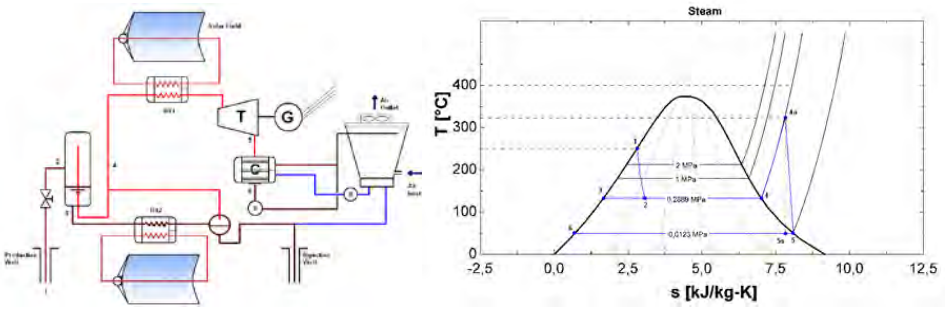

Fig. 2: Single flash Solar-Geothermal plant and T-s diagram.

2.3.1. Hybrid Solar-Geothermal, Scenario 1

A single-flash geothermal power plant is considered, with solar superheating after the separator. This scenario aims to increase production of the plant during the daylight hours

when electricity demand is higher and radiation is available. The geothermal well is kept working at constant mass flow rate, while solar thermal energy is added to increase output power. In this case, a superheating temperature of 320.8 °C is reached according with the thermodynamic conditions. With this temperature, using the radiation data for Calama and assuming an environment temperature of 15 °C, a solar field total aperture area of 4760 m^2 is obtained. If the solar radiation is higher than the design radiation (which is used to size the solar field as previously explained), then the excess is used to evaporate part of the saturated liquid stream from the separator and thus increase the main steam flow. If the solar radiation is lower than the design radiation, point 4a in the T-s diagram does not reach the maximum temperature, but it is instead located closer to point 4. In the limit with no solar radiation available, points 4 and 4a merge and fall in the saturated steam line. When point 4a is below the maximum temperature, expansion within the turbine will occur in two stages; the first is an expansion of superheated steam where the turbine isentropic efficiency is not affected by moisture, and a second stage where the expansion falls into the saturated steam zone, with moisture causing the turbine efficiency to be reduced according to the Baumann´s rule [8].

2.3.2. Hybrid Solar-Geothermal, Scenario 2

The second scenario aims to study a possible configuration that could reduce geothermal steam consumption and thus extend both well and reservoir life cycle. This can be achieved by replacing geothermal energy by solar energy when it is available, reducing the mass flow rate of geothermal fluid from the reservoir, and then using solar energy to compensate for the missing power by keeping the output power equal to the one obtained in the base scenario. The solar field sizing is done by fixing the turbine output at a value of 3.974 MW (equal to the base case, geothermal-only power plant), and then assuming that the design solar radiation is completely available. For this power output, the production curve of Eq. (1) indicates that the lowest extraction pressure is 0.9022 MPa, which results in a steam mass flow rate of 30.25 kg/s from the well, yielding 5.1 kg/s of saturated steam after the separator. The maximum steam temperature is limited to 400 °C, due to the HTF working range. This requires a power of 2505 kW in the heat exchanger number one (HX1, as in Fig. 3) and then a reheating step to take the steam back to 400 °C in the HX2 in order to deliver the 533.7 kW that are needed to reach the base case output power. This gives a total solar contribution of 3038 kW for the design conditions, resulting in a solar field collection area of 3685 m^2 in this scenario.

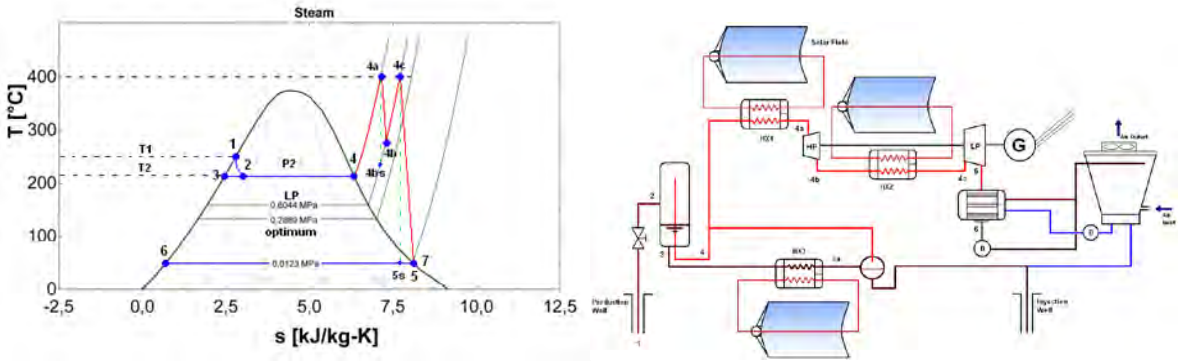

Fig. 3: Single flash Solar-Geothermal plant with reheating and T-s diagram.

An iterative process for the geothermal fluid mass flow rate is performed in order to determinate the thermodynamic states in the power plant model in an hourly basis during a 1-year period. The starting point is a given mass flow rate, which is reduced according to the available solar radiation. A decrease in the well mass flow rate results in a pressure increase at the separator inlet, thus allowing the superheating pressure value to be established. Solving

for the base case output power gives the amount of reheating needed. Again, the procedure is repeated in an hourly basis for the entire 1-year period.

3. Results

The main results obtained in this study are the hourly energy production of the base geothermal-only and the two scenarios of the Solar-Geothermal hybrid power plant, which can be integrated in a 1-year period to obtain the annual energy production of each plant.

3.1. Base Case

The first results correspond to the base case, a geothermal-only plant. By solving the equations that represent the thermodynamic cycle in Fig. 2 for a geothermal power plant, it is possible to obtain the optimum mass flow rate from the reservoir and the pressure at which the separator operates, thus achieving the maximum possible power output. The output power is 3974 kW, the total mass flow rate is 42.22 kg/s, the separator pressure is 0.2897 MPa, the energy produced for the entire year assuming a plant factor of 100% is 34.81 GWh, and the amount of extracted geothermal fluid in a year is 1331500 Tons, parameters which are established as the base case for our comparisons, corresponding to a plant that operates with a single well for a 3.974 MW power output.

3.2. Hybrid Solar-Geothermal, Scenario 1: Increased production

Even though the Chilean Desert offers a large number of clear days throughout the year, the daily radiation is subject to hourly variability as can be seen in days 1, 2, 5, and 9 of the 10-day sequence in Fig. 4. The different peaks in power output allow the plant to produce as much as 5.5 MW, an increase of more than 30% from the base power output. It can be seen that this scenario results in an annual increase of 11.36% on the total energy produced by the plant respect to the base case. An additional advantage of this configuration is that there is no need to regulate the mass flow rate of geothermal fluid from the reservoir, thus resulting in a much simpler plant operation scheme. However, the daily output power profile, where this scenario displays daily power production peaks make the power production variable and not easy to predict, which constitutes a disadvantage in terms of power dispatchability. Even though the difference between daily maximum and minimum varies only around 20%, the power curve is not as attractive as a flat curve. A positive point for these power production profiles is that, in general, the output power peak takes place during peak demand hours, thus resulting in highest spot prices that make this option attractive. The abnormality shown February is due to the altiplanic winter effect, where cloudy periods are present caused by the Amazonia wet season.

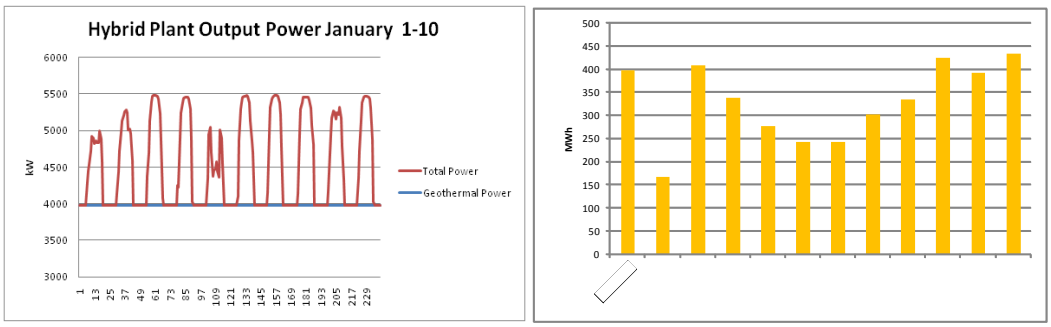

Fig. 4: Daily output power and monthly energy added, Solar-Geothermal plant Scenario 1.

3.3. Hybrid Solar-Geothermal, Scenario 2: Geothermal fluid savings

In this scenario the goal is to produce the same amount of energy as in the base case, by reducing the mass flow rate of geothermal fluid according to the availability of solar radiation, thus using solar heat to compensate for the reduced steam flow while maintaining the power output constant. Fig. 5 shows the power production profile for the same 10-day sequence as in Fig. 4, this time for the conditions corresponding to Scenario 2. The power production remains flat at a 3.974 MW value. The geothermal contribution, however, decreases as solar radiation becomes available. A significant reduction of 10.36% in geothermal fluid mass flow rate can be achieved for this particular conditions, which might translate into longer well and reservoir life, thus reducing the cost of exploring and drilling for new wells to replace those already depleted. An additional benefit is given by the flat power production profile, which makes this plant configuration attractive for sales contracts as is able to supply base load to the Chilean grid. This plant configuration also requires the smallest solar field sizes, due to the reduced solar heat required and the improved thermodynamic efficiency obtained in this scenario. The reduction of mass flow rate from the producing well implies a higher working pressure as per Eq. (1); adding this to the increased steam temperature achieved by the solar-superheated steam increases the efficiency of the thermodynamic cycle. Fig. 5 also displays the monthly total energy produced during a 1-year period. It can be seen that the solar contribution in this scenario is larger than that of scenario 1, thus effectively operating with an increased solar fraction.

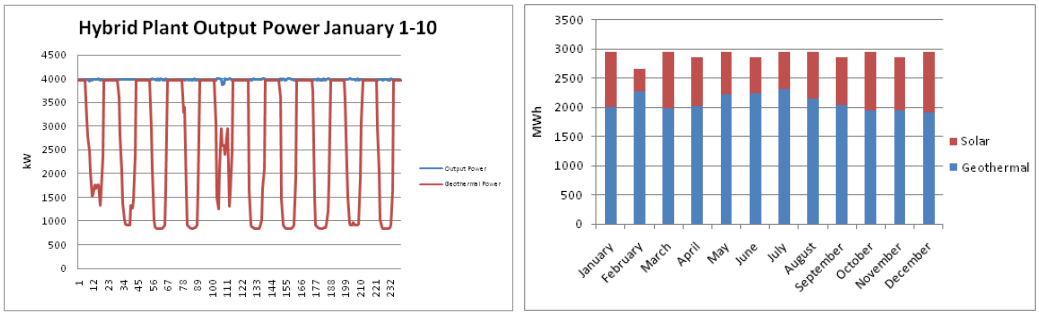

Fig. 5: Daily output power produced by the Solar-Geothermal plant, Scenario 2.

4. Conclusions

Chile faces several energy challenges as a country which is a net energy importer. The country exhibits ample potential for both solar and geothermal energy. Considering the variability of solar energy and the limitations that the use of saturated steam poses to geothermal energy, it is proposed to combine both energy sources into an hybrid power plant concept, with the general goal of taking advantage of each other strengths and mitigate their weaknesses. The hybrid Solar-Geothermal power plant models being presented consider a single flash geothermal plant with the addition of a parabolic trough collector solar field used for steam superheating. In this way the hybrid plant increases its maximum operating temperature and operates with superheated steam expansion in the turbine, as opposed to saturated steam expansion in the original, geothermal-only plant. Simulations of the plant operation in 1-year periods are performed based on hourly databases of available solar radiation for Northern Chile. Two different scenarios are proposed. The first allows the solar heat to increase the power production from the base case geothermal plant, while the second maintains a constant power output, instead utilizing the solar heat to reduce the geothermal fluid mass flow rate. It is found by the authors that the first scenario allows producing as much as 12% more energy than the base case due to the use of solar energy, producing an output power profile with daily peaks following the daily solar radiation availability. These power production peaks coincide with the peak energy demand hours, thus allowing the sale

of electricity at a larger price in the spot market. The main advantage of this generation scheme is the simplicity of its operation, where geothermal components operate the same way they do in a conventional geothermal power plant, allowing the solar radiation to add a contribution whenever available. The second scenario intends to use the available solar radiation as a way to save geothermal fluid mass flow rate. The basic premise is that reducing the well mass flow can result in an extended well and reservoir life, thus saving on exploration and perforation costs. This scenario produces a flat power output profile and therefore the same amount of energy produced than the geothermal-only base case, with lower geothermal fluid utilization. Reductions of more than 10% of geothermal fluid utilization were achieved when comparing to the base case. The operation of a power plant under this scenario requires constant monitoring of the well mass flow rate according to the availability of thermal energy coming from the solar field, which in practice is complex and has never been done before. It is also not known at the present time if the geothermal reservoir can be managed in such a way. The geothermal solar hybrid concept represents an interesting prospect for the Chilean electricity market, with the potential of providing base load energy with a high capacity factor from emissions-free and environmentally friendly sources. Further analyses are being performed for developing an economic model and assess in more detail the feasibility of this concept

Acknowledgements

Proyect FONDECYT 1095166 provided the computational platforms and simulation software, while Project FONDEF D08i1097 provided the solar radiation data.

References

[1] Comisión Nacional de Energía, CNE (2010). Balance Nacional Enegético 2008. Last accessed at http://www.cne.cl/cnewww/opencms/06_Estadisticas/Balances_Energ.html on August 13, 2010.

[2] Ministerio de Economía. Ley general de servicios eléctricos, Decreto con fuerza de ley n°4, Art. único Nº 2, D.O. 01.04.2008. Santiago, February 2007.

[3] Ortega, A., Escobar, R., Colle, S., Abreu, S. (2010). The State of Solar Energy Resource Assessment in Chile. *Renewable Energy*, 35, 11, 2514-2524.

[4] Handal, S., Alvarenga, Y., & Recinos, M. (2008). *Solar* Steam Booster in the Ahuachapán Geothermal Field. El Salvador.

[5] Lentz, & Almaza. (2003). Parabolic troughs to increase the geothermal wells flow enthalpy. Mexico.

[6] DiPippo, R. (2008). Geothermal Power Plants; Principles, Applications, Case Studies and Enviromental Impact, Second Edition. London: Elsevier.

[7] Tester, J. et al, Massachusetts Institute of Technology (MIT) (2006). The future of geothermal Energy. Retrieved Jan, 2010. Last accessed on August 13, 2010 at: http://geothermal.inel.gov/publications/future_of_geothermal_energy.pdf.

[8] Leyzerovich, A. (2005). Wet-Steam Turbines for Nuclear Power Plants. New York: PennWell.

[9] Therminol. (2009). *Therminol*. Retrieved 2009, from www.therminol.com

[10] National Renewable Energy Laboratory *NREL*. (2009). *TroughNet, Parabolic Trough Solar Field Technology* Retrieved 2009, from: http://www.nrel.gov/csp/troughnet/solar_field.html.

Potential use of geothermal energy sources for the production of lithium-ion batteries

Pai-chun Tao, Hlynur Stefansson, William Harvey, Gudrun Saevarsdottir*

[1] *Reykjavik University, Reykjavik, Iceland*
** Corresponding author. Tel: +354 599-6345, Fax: +354 599-6201, E-mail: gudrunsa@ru.is*

Abstract: The lithium-ion battery is one of the most promising technologies for energy storage in many recent and emerging applications. However, the cost of lithium-ion batteries limits their penetration in the public market. Energy input is a significant cost driver for lithium batteries due to both the electrical and thermal energy required in the production process. The drying process requires 45~57% of the energy consumption of the production process according to a model presented in this paper. The model is used as a base for quantifying the energy and temperatures at each step, as replacing electric energy with thermal energy is considered. In Iceland, it is possible to use geothermal steam as a thermal resource in the drying process. The most feasible type of dryer and heating method for lithium batteries would be a tray dryer (batch) using a conduction heating method under vacuum operation. Replacing conventional heat sources with heat from geothermal steam in Iceland, we can lower the energy cost to 0.008USD/Ah from 0.13USD/Ah based on average European energy prices. The energy expenditure after 15 years operation could be close to 2% of total expenditure using this renewable resource, down from 12~15% in other European countries. According to our profitability model, the internal rate of return of this project will increase from 11% to 23% by replacing the energy source. The impact on carbon emissions amounts to 393.4-215.1g/Ah lower releases of CO_2 per year, which is only 2-5 % of carbon emissions related to battery production using traditional energy sources.

Keywords: *Lithium ion battery, Geothermal energy, Energy cost, Carbon emission*

1. Introduction

The exponential growth in the use of portable electronic devices and electric vehicles has created enormous interest in inexpensive, compact, light-weight batteries offering high energy density. Clearly, the lithium-ion battery is one of the most appealing technologies to satisfy this need. It is estimated that the global market for lithium-ion batteries could grow from $877 million in 2010 to $8 billion by 2015[1]. However, cost limits their penetration in the global market. Energy is a significant cost driver for lithium batteries as both electrical and thermal energy is required in the raw materials processing and battery manufacturing and assembly. As energy use is significant in the process, the sustainability of the energy source influences the overall carbon footprint for the battery production. Iceland offers a number of potential avenues for cost and carbon emissions reductions in the manufacturing process, due to readily available medium grade thermal energy from geothermal or industrial sources, access to inexpensive renewable electricity, and a skilled workforce. The purpose of this paper is to quantify the economic advantages and carbon emission reductions to be gained by locating a lithium iron phosphate ($LiFePO_4$) factory in Iceland close to geothermal heat sources, versus sites in other locations where fossil sources of energy must be used. Furthermore, we will also present the sensitivity of profitability to energy cost.

2. Methodology

The presented work consists of three main tasks: 1) Collection of relevant data and information. 2) Estimation of energy consumption and temperature levels at various steps in the production process and 3) Assessment of profitability and impact on carbon emissions. Firstly, the literature review, including interview data, provides us with information to draw a complete production process map of the lithium iron phosphate battery manufacturing process. Unfortunately, detailed energy consumption data from each step in the lithium

battery production is not readily available from factories due to confidentiality reasons in this competitive market. Consequently, we build a theoretical energy consumption model for the drying process based on the thermal properties and moisture content of materials in the batteries, basic physical formulas, and industrial experience. There are some uncertainties in this model, as energy efficiency, and heat loss, are based on educated assumptions. The results from the model are therefore not data from an actual factory, but should be informative none the less. In reality, it could be lower or higher depending on de sign of industrial equipment components. For the profitability assessment, common standards of estimating the profit of an investment, for example, net present value (NPV) and the internal rate of return (IRR) are applied. Consequently, we build a comprehensive profitability assessment model for building a new lithium iron phosphate battery factory in Iceland. Most cost data are obtained directly from suppliers or publicly available information. The main assumptions are listed in Table 2.1. In the model, we make several financial assumptions, such as interest rate, capital structure and discount rate of based on current conditions in Iceland. The profitability calculation and Monte Carlo analysis are performed by Microsoft Excel plug in with @Risk5.7.

Table 2-1 Main assumptions of profitability model

Items	Value
Interest rate of loan	12%
Sale price	1.44 (USD/Ah) with 3% annual decreasing trend
Raw material price	0.69 (USD/Ah) with 2.75% annual decreasing trend
Initial investment	9612 million ISK
Discount Rate	15%
Capital structure	70% loan, 30% equity
Exchange rate	156 (ISK/Euro) 112 (ISK/USD)
Salary for workers	Iceland: 238,000 (ISK/Month) Germany: 1944 (€/Month)

3. Energy consumption of Lithium Iron Phosphate battery production process

3.1. Energy consumption of entire process

Energy consumption in lithium iron battery production is not openly available information from this emerging industry. Lifecycle analysis of lithium iron battery by Mats Zackrisson and Lars Avellán in 2010 claims that the total energy consumption corresponds to 11.7 kWh electricity and 8.8 kWh of thermal energy from natural gas per kg lithium-ion battery [2]. This corresponds to an energy consumption for 1Ah battery of approximately 0.68KWh, assuming that one kg lithium-ion provides 30Ah capacity of battery. In addition, energy consumption data were obtained from Matti Nuutinen, who reported data from a Chinese lithium iron phosphate battery factory and for European Batteries Oy[3]. In this report, Nuutinen shows that 5000kw electric power is required to produce 80MAh battery per year. This equates to energy consumption for producing 1Ah battery is approximately 0.54KWh. Based on these sources the energy consumption could range from 0.54 to 0.68 KWh/Ah according to our investigation.

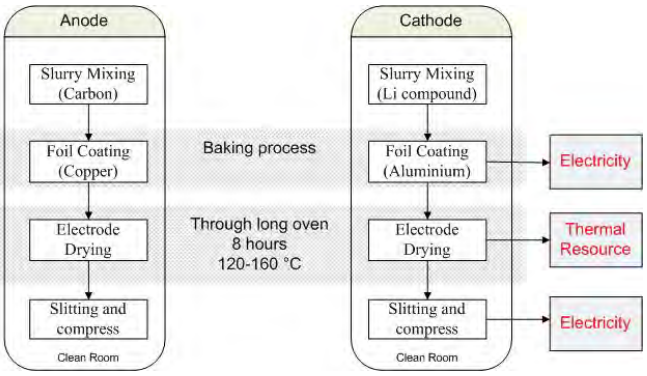

Figure 3-1 Production process map of Part 1

3.2. Production process map

In general, our analysis of the lithium iron battery production process starts with the various raw materials and components from suppliers. The overall process can be divided into two parts: preparation of electrodes and cells assembly. Fig 3-1 shows the main steps in first part of the production process. In first part, the first step is to mix anode and cathode powders with solvent and binder, coat them on the respective foils, and dry them in the vacuum oven at around 120˚C for 8 hours. Traditionally the heat applied at each of the drying steps is obtained by electric heating. However, since the temperature needed in the vacuum oven is relatively low, we might be able to replace electric heating with heat exchangers using geothermal steam as a thermal source. After this drying step the electrode disks would be cut into suitable sizes and compressed thinner by automatic machines. At this stage, the individual electrode is ready for assembly.

Fig 3-2 shows the second part, which is to assemble the various components, such as the separators, internal circuits, anodes and cathode altogether. In this step, the electrodes can be stacked and clamped first and put into a metal packing case. Afterwards, the battery cells are placed in the core drying machines. The purpose of this step is to remove the remaining moisture from electrodes completely. This is the most energy intensive step of the whole process. In principle it would seem feasible to accelerate this drying step by increasing the temperature in the oven. However, the melting point of the binder (PVDF) is around 170°C, so the temperature in the vacuum oven must be kept below 170°C. As an alternative the process is accelerated by lowering the pressure in the oven in order to efficiently remove the vapor formed. Thereby the boiling point of water and solvent is decreased in order to shorten the drying process. In the end, the moisture content rate in the electrodes is reduced to 500ppm [4]. After the core drying process, the electrolyte is injected into cell and it is sealed completely. Since the electrodes are very sensitive to moisture, those processes are usually operated in a room, where the humidity is kept at an acceptable level. In principle, the battery pack is ready for use at this stage. However, most producers test their products several times in order to ensure its performance and collect data before shipping the product to consumers.

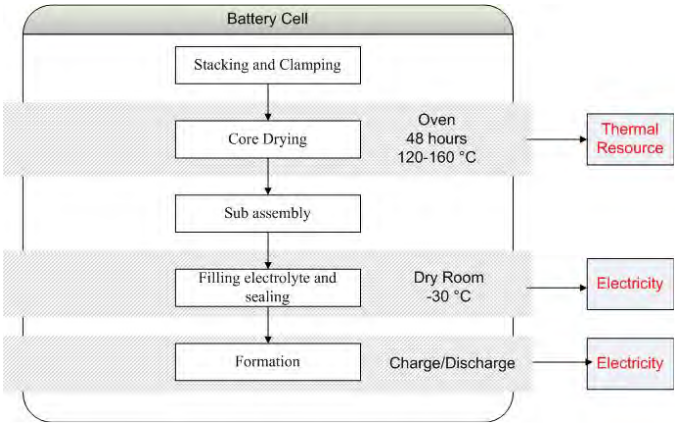

Figure 3-2 Production process map of Part 2

3.3. Energy consumption of the drying process

Through production analysis, the approximate energy consumption figure has been already addressed in the previous text. But, we need to know the energy consumption of the drying process, if we want to consider alternative energy resources for the drying process. Consequently, we build a theoretical calculation model. It is not perfect, but a reasonable approach to figure out the approximate energy consumption of the drying process. The first step of building an energy consumption model of drying is to collect the weight percentage and thermal properties of component materials. Table 3-1, shows the physical thermal properties of each material in the lithium iron battery.

Table 3-1 Physical properties of component material

Information of 1 kg lithium iron battery component material			
Cathode Composition	Weight (g)	Heat capacity	Others
$LiFePO_4$	422 g [2]	C_v: 0.9 J/g-K [2]	Melting point: 223°C
Al foil	19 g [2]	C_P(25°C) 0.89 J/g-K	Melting point: 660.3°C
Carbon black	27 g [2]	C_P(25°C): 0.71 J/g-K	Melting point: 3500°C
Binder (PVDF)	28 g [2]	C_v: 1.9J/g-K [5]	Melting point: 170 °C
NMP solvent	Initial: 244.2 g Outlet: 10g[6]	C_v: 1.76 J/g-K [7]	Boiling point: 202°C Heat of vaporization, 20°C: 550.5 KJ/g [6]
Anode Composition			
Graphite	169 g [2]	C_P(25°C): 0.71 J/g-K	Melting point: 3500°C
Cu foil	46 g [2]	C_p(25°C): 0.385 J/g-K	Melting point: 1084.6°C
NMP solvent	Initial: 116.2 g Outlet: 4.8g [6]	C_v: 1.76 J/g-K [7]	Boiling point: 202°C Heat of vaporization, 20°C: 550.5 KJ/g [6]
Total moisture	Initial: 4.5g Outlet: 0.5g [4]	C_v (25°C): 4.18 J/g-K C_v(100°C, steam): 2.08	Evaporation energy: 2270 KJ/g)

The model predicts how much thermal energy we need in order to remove the moisture and NMP from the electrodes. It is accompanied with the increasing temperature of other materials and some heat lost to environmental. The thermal energy consumption of the drying process calculation could be divided into two parts. (1) The energy for increasing the temperature of all component materials. (2) The energy for evaporating the moisture and NMP away from the feedstock. Through the thermal properties and some basic physical formulas, we obtain theoretical results for both parts respectively. And then, we take the empirical energy efficiency of the vacuum dryer into account to get more realistic data. The energy required for heating the materials to the dryer temperature would is 128.62kJ/kg. The second part is the energy consumption of evaporation. It dominates the energy consumption of drying process. The overall energy consumption of evaporation is 198197.8kJ/kg. The key factors in this calculation are the initial weight and outlet weight of moisture because the heat of evaporation of water and solvent dominates as compared to the sensible heat. However, the energy efficiency is not 100%. Based on the literature we assume that the energy efficiency of the vacuum dryer is 0.6 according to the Handbook of Industrial Drying [8]. In this case, the practical energy consumption would be 0.186/0.6 = 0.26 KWh/Ah. As a consequence the energy required is approximately 0.31 KWh thermal to dry 1Ah of lithium iron phosphate battery. This number does not include the electricity for vacuum machines and drying rooms, which are also part of the drying system. It only focuses on the thermal energy that can be replaced by geothermal steam. According to the energy consumption data in previous research, the whole energy consumption of producing 1Ah lithium battery would raised from 0.54~0.68 KWh. Based on this information 45~57% of the energy consumed by the process can be replaced by an alternative thermal source.

3.4. Alternative drying technology

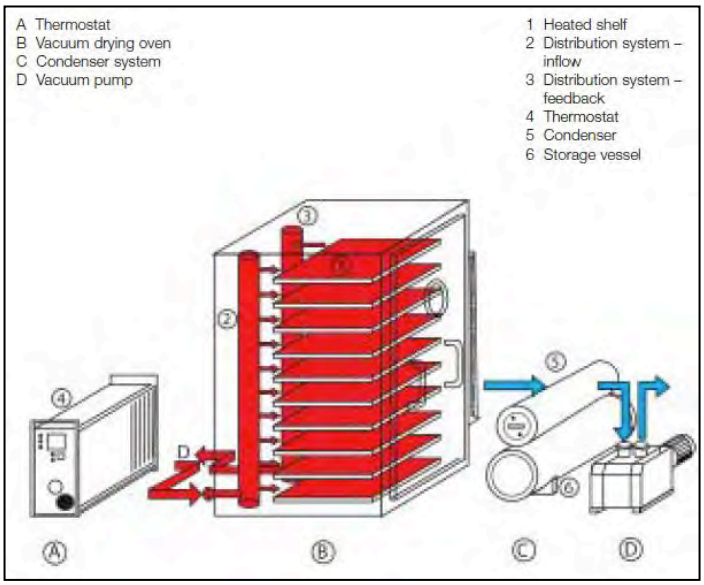

Figure 3-3 Schematic model of vacuum oven could use working fluid as thermal resource [9]

The volatile components targeted in drying are moisture and organic solvent (NMP) that are a part of the cathode or anode paste. The oven provides thermal energy to the feedstock continuously by convection, conduction or radiation in order to remove the targeted compounds from the battery components. In Iceland, geothermal power plants are typically operated with steam at 10-12 bar, but in some cases, a higher pressure up to 18 bar is applied. In this case we consider Reykjanes as a location due to the power plants proximity to a harbor and a developed industrial area, so geothermal steam at 18 bar 207°C is used as a thermal resource for the analysis. However a resource at 9 bar and 173°C, which would be more widely available, is quite sufficient for this process. As the factory is located close to the geothermal power plant, steam from two-phase separators could be applied directly. The power company, Hitaveita Sudurnesja, has offered 20 bar steam to other customers at 4USD/ton and 6 bar at 3 USD/ton in 1995[10]. As a comparison a diatomite processing plant at Lake Myvatn that was in operation until 2004 paid 1 USD/ton for geothermal steam. In this model, a steam price of 4 USD/ton is assumed. In reality, this price highly depends on the negotiation with power companies. The optimal dryer technology for lithium ion battery production is a tray dryer (batch) using conduction heating method under vacuum conditions. Although the geothermal steam from well contains some deleterious materials, most of them would be contained within the liquid phase in the separators. Thus, we would be able to fill the geothermal steam into the entire cavity of shelves directly. As you can see in Fig 3-3, while the feedstock is placed on the shelves, the thermal energy is transferred to products by conduction. In addition to the conduction, it also could be combined with irradiative heating in order to accelerate the drying rate. We assume the new type of dryers will cost 20% more than normal electric dryers. As the cost of dryers is only 14% of production lines, it does not affect the overall cost of production significantly.

4. Reduction in carbon emissions

From the data shown in Table 3-2, we can see that the energy structure of each country has different features. Based on that data, the average emission from electricity generation for each energy profile is calculated. If we build a lithium iron phosphate battery production facility with 10MW power requirement in other countries, it will emit 36247~64771 tons of CO_2 per year depending on the country's electric energy production profile. In Iceland, approximate 50% of energy consumption is still electricity, which emits 23.5 g/KWh CO_2 on average [11]. The rest of the energy consumption will be replaced by geothermal steam, which emits 18g/KWh CO_2 in this case. Thus, the total CO_2 emission in Iceland would be around 1818 tons of CO_2 per year. In summary, this project in Iceland has 393.4-215.1 g/Ah lower CO_2 emission advantage compare to other countries. However, we have to put it in mind that most of carbon dioxide is emitted naturally from geothermal area in Iceland. The

emission from geothermal plants is already part of CO_2 cycle, no new CO_2 is being produced as is in the case of fossil fuel.

Table 4-1 Comparison of carbon emission for Li-ion factories with 10MW power requirement located in different countries [12].

Various Resource	Average CO2 emission (g/kwh)	China	USA	Germany	Japan
Renewable	50	0.4%	2.8%	11.6%	2.7%
Oil	400	0.6%	1.3%	1.4%	12.8%
Gas	430	0.9%	20.9%	13.7%	26.1%
Nuclear	6	1.9%	19.2%	23.3%	23.8%
Hydro	4	16.9%	6.4%	4.2%	7.7%
Coal	925	79%	49%	45.6%	26.6%
Total		100%	100%	100%	100%
Average CO2 emission from electricity (g/kwh)		738.9	552.1	494.2	413.51
Total emission from this project per year (87.66 GWh)		64771.9	48402.3	43321.5	36247.4

5. Profitability assessment

We built a comprehensive model containing cost analysis, investment, operation, cash flow, profitability and sensitivity analysis in order to estimate the profitability of building a lithium iron phosphate battery factory using renewable energy in Iceland. We calculate NPV and IRR based on the current cost data on the market and some financial assumptions. The main results of this model are presented in the following text.

5.1.1. Net present value

Fig 5-1 shows that the NPV of total cash flow (for loan and equity) with 15% discount rate is 48.16 m illion USD after 15 years operation time. Also, NPV net cash flow (only for equity) with 15% discount rate is 52.57 million USD. The value of NPV of total cash flow and net cash flow take 9 and 8 years to turn positive, respectively. From the point of view of NPV, it seems a reasonably profitable business in Iceland. Building the factory at another location in Europe with similar operating environment, the accumulated net present value might turn negative due to much higher prices of industrial electricity. Applying European electric prices, the accumulated NPV of net cash flow will be -20.6 million USD, as shown in Fig 5-1. Other cost contribution might vary slightly depending on location but it is observed that energy price significantly affects net present value. The energy price will play more substantial part of the total variable as raw material prices are predicted to fall in the next 10 years.

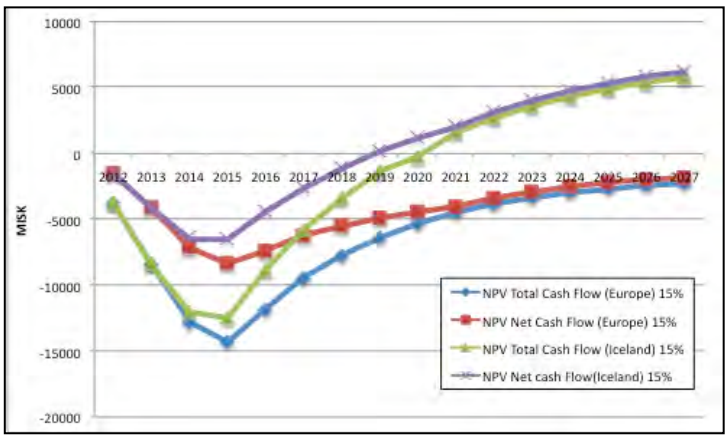

Figure 5-1 Accumulated NPV comparison between Iceland and other European countries.

5.1.2. Internal rate of return

In terms of internal rate of return, it is used in capital budgeting to measure and compare the profitability of the investment. Fig 5-2 shows the internal return rate of total cash flow and net cash flow in Iceland is 22% and 27%, respectively. On the other side, the internal return rate of total cash flow and net cash flow in Europe is 11% and 12%, respectively. Although there is some risk and uncertainty in this project, IRR is higher than the cost of capital in the normal situation in Iceland. To compare to a common investment, it has a relatively high internal rate of return based on the assumption. However, 11~12% of IRR is a normal and acceptable result for an investment project in other European countries.

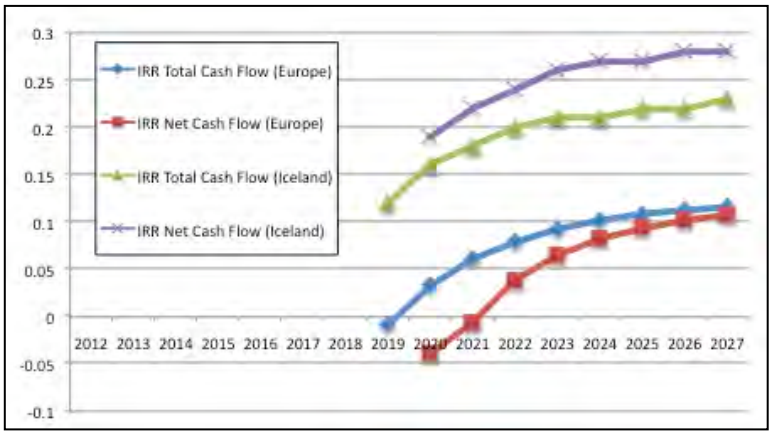

Figure 5-2 IRR comparison between Iceland and other European countries

6. Conclusion

With the anticipated reduction in material cost for Lithium-ion batteries, the energy cost for battery production will play a more important role in the overall cost of lithium ion batteries. According to our investigation, the energy consumption could range from 0.54 to 0.68 KWh/Ah depending on the factory's design and production process. Although we did not get access to first-hand energy consumption data of each step from factories directly, we can infer that the main energy consumption steps in the procedure are drying room, vacuum dryers, and testing equipment from our production process analysis, and create a process model. In locations with access to geothermal heat, such as Iceland, it is possible to replace the electricity used as a heat source for the drying processes by geothermal steam, reducing energy cost in combination with reasonably priced electricity. According to the model, the energy consumption of removing the moisture content in 1 Ah battery is 0.31 KWh, which is around half of the total energy consumption. The variable energy cost in Iceland could be reduced to 0.012 USD/Ah (0.007 USD for electricity; 0.005 for geothermal steam) if geothermal steam is used for drying. In this study Reykjanes in Iceland is considered as a location so geothermal steam at 18 bar 207°C is used as it is the available resource from an existing geothermal power plant. However a resource at 9 bar and 173°C, which would be more widely available, is quite sufficient for this process. In this case, the ideal type of dryer and heating method for lithium batteries would be a tray dryer. A profitability model was built using current cost data based on operating environment in Iceland. According to this model, the accumulated NPV for equity with a 15% discount rate is 52.5 million USD and internal rate of return is 27%. On the other hand, if we move the factory to other European countries with higher energy price (0.18€ /KWh[13]) and the same cost assumption, the NPV for equity will fall down to -20.6 million USD. The internal rate of return will fall from 27% to 11%. Moreover, with current feedstock prices the energy cost is estimated to be 1% with the Icelandic cost structure, while it would amount to 12~15% in other European countries based on average energy prices. The lower energy cost in Iceland results in an NPV less sensitive to fluctuation of energy prices. The geothermal resource seems to have a great economic advantage for lithium ion battery production due to lower energy prices, whether it is electric

energy or direct use of geothermal heat. Another feature of even more importance is that the lower carbon footprint of geothermal heat and renewable electricity, will result in 34429-62953tons lower CO_2 emissions per year from running a battery factory with 10 MW power consumption and 160MAh production capacity, compared to the emissions where a t he electric production profile is more traditional as would be the case in Europe or China. That means that only 2-5% percent of the carbon dioxide would be emitted as a result from this process as compared to traditional energy usage. This could bring some practical carbon emission credit value or an advantageous position on g reen marketing. Although most of battery companies still focus on reducing the cost of raw material at this moment, the energy cost will become more and more critical in the entire cost structure with future price reductions of raw material. The trend for companies planning to develop production in Europe will be a higher emphasis on selecting a location with reasonably priced renewable sources for heat and electric energy. The access to low cost low emission energy sources should be a significant factor when selecting a location for Lithium ion battery production.

References

[1] Pike Research, "Asian Manufacturers Will Lead the $8 B illion Market for Electric Vehicle Batteries", Retrieved 10.01.2010, from Pike Research: http: //www.pikeresearch.com/ newsroom/asian-manufacturers-will-lead-the-8-billion-market-for-electric-vehicle-batteries

[2] Zackrisson M & Orlenius J, Life cycle assessment of lithium-ion batteries for plug-in hybrid electric vehicles e Critical issues. Journal of Cleaner Production, 2010, pp.1517-1527.

[3] Nuutinen, M, Lithium-ion battery factory relocation from China to Finland. Material science and engineering. Helsinki: Helsinki university of technology, 2007, pp.68-69.

[4] She Haung Wu and Yang-Ting Lai, The effects of the moisture content of LiFePO4/C cathode and the addition of VC on the capacity fading of the LiFePO4/MCMB cell at elevated temperatures. The electrochemical Society, 2007.

[5] Dr. Michael Eastman, Smart Sensors Based on Piezoelectric PVDF, 2010, pp-6

[6] LICO Technology Corporation, LHB-108P Hydrophilic Binder, 2008, pp-6

[7] Taminco Co, N-Methylpyrrolidone Electronic grade Technical Data Sheet, 2004, pp-1

[8] Mujumdar A. S, Handbook of Industrial Drying. Taylor & Francis Group LLC, 2006, pp.1108-1109.

[9] Weiss Gallenkamp, Vacuum oven and drying oven VVT, 2010, pp-4.

[10] Invest in Iceland Agency, Doing business in Iceland 8 E dition. Reykjavik: Iceland investment agency, 2010.

[11] Landssvirkjun, Landssvirkjun's carbon footprint, Reykjavik: Landssvirkjun, 2009, pp-11.

[12] World Energy Council, World Energy council. Retrieved 10 1, 2010, from World Energy council:http://www.worldenergy.org/publications/survey_of_energy_resources_2007/geothermal_energy/737.asp

[13] Europe's Energy Portal, Industrial Electricity Rate, November 2009, http://www.energy.eu/#Industrial

Energy and exergy analysis and optimization of a double flash power plant for Meshkin Shahr region

Mohammad Ameri [1,*], Saman Amanpour [2], Saeid Amanpour [3]

[1] *Energy Eng. Department, Power & Water University of Technology, Tehran, Iran*
[2] *Department of Aerospace and Mechanical Engineering, Shiraz University, Shiraz, Iran*
[3] *Department of Electrical Engineering, University Teknologi Malaysia, Johor Darul Takzim, Malaysia*
** Corresponding author. +9821-73932653, Fax: +9821-77311446, E-mail: ameri_m@yahoo.com*

Abstract: One of the most influential improvements in geothermal industries has been the application of double flash power plants which can produce more power in comparison with single flash one. Although it is more expensive, however it is a reasonable option as the additional output power can justify the prices. The aim of this study is to represent a methodology in which a double flash power plant is thermodynamically designed and optimized in order to maximize the output power, and make a comparison with other possible type of geothermal power plant (single flash) for Meshkin Shahr region. Besides it represents the study of exergy and energy analysis for plant components through the optimization process, which can guide one to assess the operating status of plant components. It has been shown that flash vessels are the greatest exergy dissipaters and double flash power plant can be more efficient than single flash for this region.

Keywords: *Double Flash Power Plant, Geothermal Power Plant, Energy Analysis, Exergy Analysis, Optimization.*

Nomenclature

c	*specific heat of water* ..... *J/(kg K)*	*BF*	..... *Brute Force*
$\dot{E}$	*Exergy* ..... *kJ*	*Cond*	..... *condenser*
e	*specific exergy* ..... *kJ/kg*	*cw*	..... *cooling water*
h	*specific enthalpy* ..... *kJ/Kg*	*FV*	..... *flash vessel*
$\dot{m}$	*mass flow rate* ..... *kg/s*	*FUN*	..... *functional*
T	*temperature* ..... *°C*	*lp*	..... *low pressure*
w	*specific work* ..... *kJ/kg*	*t*	..... *turbine*
x	*quality or dryness fraction* ..... $m \cdot s^{-1}$	*W*	..... *work*
ρ	*density* ..... $kg \cdot m^{-3}Q$		

Subscripts

Greek Letters

η	*efficiency*
Δ	*difference*

1. Introduction

Increasing oil price and environmental concerns about pollution and global warming in recent years has doubled geothermal energy use as a clean source of energy [1]. Today three major types of geothermal power plants are being utilized: dry steam plants, flash steam plants and binary cycle plants [2]. DiPippo has presented some information about new geothermal power plant designs [3]. Flash power plants are likely in liquid-dominated fields with temperature greater than 182° C [4]. An important concern in engineering field of geothermal energy is thermodynamic design and optimization of an energy system, especially a power plant, which can reduce the expenses significantly. The application of double flash power plant is not rational for all projects, since the conversion system is more complex and of course more expensive. Stefansson depicted a strategy for the investment costs of geothermal power plants and estimated investment cost level in unknown fields [5]. Therefore, it is important to assess the performance of geothermal plants based on an optimized thermodynamic scheme with respect to the surrounding conditions and thermodynamic state of geothermal reservoir, before putting the plan into action [6]. This can help the designer in better understanding of

the occasion so that a precise decision can be made to select either a single flash or a double flash plant with respect to costs. Ozcan and Gokcen managed a thermodynamic assessment of single flash power plant and studied the effect of non-condensable gases on plant performance [7]. Dagdas et al. carried out a thermodynamic optimization for a geothermal power plant based on real data and results revealed that 93.2% more power can be obtained [8]. Franco and Villani found that optimization of binary cycle power plants can yield to reduction of brine specific consumption in a significant way up to 30-40% [9].

The study of energy and exergy analysis, based on Second Law of Thermodynamics, helps to evaluate the performance of a geothermal power plant in order to eliminate excess energy loss and improve the overall efficiency of the plant [6]. Kanoglu performed an exergy analysis of a binary geothermal power plant using actual plant data and studied the causes of exergy destruction [10]. DiPippo also made comparisons between different cycles of binary plants for low-temperature geothermal fields based on Second Law of Thermodynamics [11].

Bodvardson and Eggers made a comparison between single flash and double flash power plants taking advantage of their exergy tables, as denoted by Yari [1]. Kanoglu and Bolatturk performed an exergy analysis of a binary geothermal power plant, applying actual plant data [2]. Cerci evaluated the performance of a single flash power plant in Turkey by using exergy analysis based on actual plant operation data [12]. He had a debate in the form of response to Serpen who made some comments on performance evaluation of the same project in Turkey concluding that the performance of a geothermal power plant is affected by the chemistry of reservoir [13, 14, 15]. Serpen believed that the design and evaluation of geothermal power plants are subjected to profound study of the geothermal reservoir [13]. Madhawa et al. presented a criterion for cost effective optimum design of organic Rankine cycles based on low temperature geothermal heat sources [16]. Kanoglu et al. did a comprehensive survey on different power cycles including geothermal power plants and presented energy as well as exergy based efficiencies with some illustrative examples [17]. DiPippo also investigated different types of geothermal power generating systems and he applied the exergy analysis to geothermal power systems [3]. Yari did a comparative study of different geothermal power plants based on exergy analysis [1].

This paper represents a two dimensional optimization of a double flash power plant for Meshkin-Shahr region in which the pressure of the first and the second flashing process are optimized by help of a FORTRAN code in order to reach the maximum output power; and the results are sketched in form of 3D surfaces. Moreover, the isentropic efficiency of turbine, brute force and functional efficiency, and exergy dissipation of each plant components are calculated simultaneously in each step of optimization process.

Meshkin-Shahr, a region in the Moil valley which is located on the western slopes of Sabalan Mountain, is a potential geothermal field for power generation. It is the place where the first Iranian geothermal power plant is going to be installed [4]. According to the reservoir type of this region, flash power plants are valid cases for utilization of geothermal energy.

2. Methodology

2.1. Energy and exergy analysis

Exergy analysis is a thermodynamic analysis technique which is based on second law of thermodynamics. It presents a bright way for evaluation and comparison of processes and systems [18]. This method can be used to estimate the performance of any energy system and

the combination of this method with energy analysis can assist in elimination of excess energy loss in order to improve the overall efficiency [6]. All the processes in double flash power plant are assumed to be steady state processes. Therefore, the balance equations can be employed to calculate output power, exergy of flow streams and energy and exergy efficiencies. Neglecting the change in kinetic and potential energies, the First Law of Thermodynamics and mass balance equations can be written as:

$$\dot{Q} - \dot{W} = \sum\left(\dot{m}_e h_e - \dot{m}_i h_i \right) \tag{1}$$

$$\sum \dot{m}_i = \sum \dot{m}_e \tag{2}$$

The second law of thermodynamics for a perfect reversible process and the specific exergy of a fluid stream associated to dead state condition can be stated by Eq. (3) and Eq. (4) respectively. The subscribe "0" represents dead state condition at 20° C and 1 atm.

$$\sum\left(\dot{m}_e s_e - \dot{m}_i s_i \right) - \frac{\dot{Q}_0}{T_0} = 0 \tag{3}$$

$$e = h - h_0 - T_0(s - s_0) \tag{4}$$

2.2. Thermodynamic nature of processes in double flash power plants

Double flash power plant as a choice of energy conversion system for liquid-dominated fields, constitute about 14% of all geothermal plants with the power capacity ranges from 4.7 MW to 110 MW [3]. A T-S schematic diagram of a double flash power plant is shown in Fig. 1.

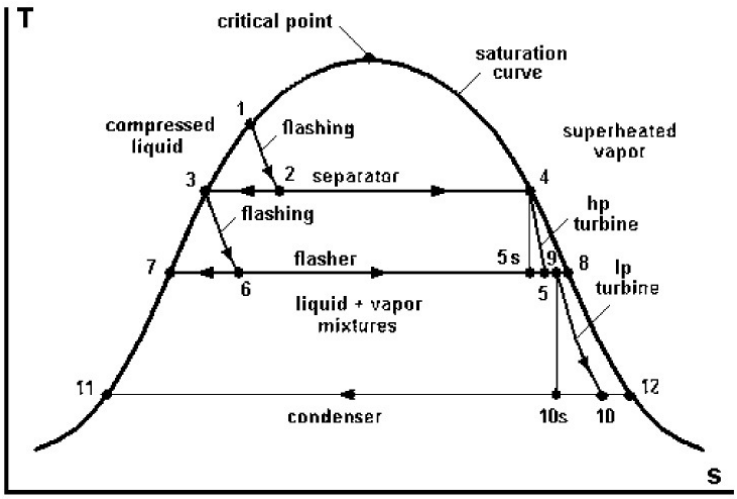

Fig. 1. Temperature-Entropy diagram of a double flash power plant.

Two phase fluid from geothermal wells is pumped to power plant on the ground surface at condition near saturation and it can be assumed as pressurized liquid (point 1 in Fig. 1). The pressurized liquid undergoes the first flashing process by passing through a throttle valve so its pressure falls in an isenthalpic process, where a two phase fluid is produced (point 2 in Fig. 1). These two phases are separated in a high pressure separator where the steam is guided to

drive the high pressure turbine (point 4 in Fig. 1) and the liquid phase undergone the second flashing process (point 3 in Fig. 1) and the two phases are separated efficiently. The low pressure steam of this process is guided toward a dual-admission turbine or it is guided toward a separate low pressure turbine (point 9 in Fig. 1) and the liquid phase is disposed to the injection wells (point 7 in Fig. 1). The two phased mixture of turbine exhaust will be then condensed in a condenser and disposed into injection wells (point 11 in Fig. 1). The enthalpy of actual turbines' processes can be easily calculated by incorporating fluid properties at state 5s and 10s and the efficiency of turbines as well as the Baumann rule. This rule states that since the turbine processes take place in wet region, there would be a 1% drop in efficiency of turbines per every percent of average moisture. Thus for low pressure turbine one may write:

$$h_{10} = \frac{h_9 - 0.425\left(h_9 - h_{10s}\right)\left(x_9 - \dfrac{h_{11}}{h_{12} - h_{11}}\right)}{1 + \dfrac{0.425\left(h_9 - h_{10s}\right)}{h_{12} - h_{11}}} \tag{5}$$

Properties at state 9 can be easily gained by combination of First Law of Thermodynamics and mass conservation and the condensation process is assumed to take place in a constant pressure process, and effects of non-condensable gases are neglected.

2.3. Exergy efficiencies and exergy dissipations of double flash power plant

There are two different approaches for the definition of exergy efficiencies. Brute force efficiency, defined as the sum of all output exergy terms divided by the sum of all input exergy terms, and functional efficiency, defined as the exergy of desired energy output divided by the exergy spent to achieve the desired output [3]. According to Fig.1, exergy dissipations and exergy efficiencies of a double flash power plant's components can be expressed as follows, for brevity we just point out some of the relations and others can be written in a similar way [3].

$$\Delta \dot{E}_{FV2} = \dot{m}_3 e_3 - \dot{m}_7 e_7 - \dot{m}_9 e_9 \tag{6}$$

$$\eta_{FV2,BF} = \frac{\dot{m}_7 e_7 + \dot{m}_9 e_9}{\dot{m}_3 e_3} \tag{7}$$

$$\eta_{FV2,FUC} = \frac{\dot{m}_9 e_9}{\dot{m}_3 e_3} \tag{8}$$

$$\eta_{tlp,BF} = \frac{w_{lp} + e_5}{e_4} \tag{9}$$

$$\eta_{tlp,FUN} = \frac{w_{hp}}{e_4 - e_5} \tag{10}$$

The functional efficiency for condenser can be estimated by two different approaches based on the nature of unit [3].

3. Results

The methodology which is used in this paper is based on assumptions pointed out in table 1 and piping losses are assumed to be negligible. "Equal-temperature-split" rule [3] is a usual method for the selection of temperature (or pressure) of separation process in order to approach the optimum state which leads to maximum output power. This rule cannot define the exact pressure since processes take place in two phase region. However, it can lead one to the verge of best option. The precise pressures require a two-dimensional optimization on vicinity of pressures estimated by "equal-temperature-split" rule. Fig. 2 illustrates a two-dimensional optimization in form of a saddle shaped surface where the maximum vertical point illustrates the maximum output power which is equal to 67793.04 KJ. This power is the total power produced by high pressure and low pressure turbines and it seems that double flash power plant can produce about 13-14% more power than single flash one [6]. The related pressures to this point are 0.67 MPa and 0.1 MPa for the first and second separation processes respectively. It is worth to mention that P2 and P6 in the following figures are adopted from Fig. 1.

Table 1. Fixed and variable parameters.

Parameter	Status	Possible range
Inlet temperature	225˚C (based on reservoir condition)	Temperatures greater than 180˚C [4]
Inlet mass flow rate	700 kg/s	-
Separators' pressure	Variable (optimized)	100-1000 KPa [19]
Condensation pressure	Fixed at 10 KPa	Recommended 8-10 KPa [19]

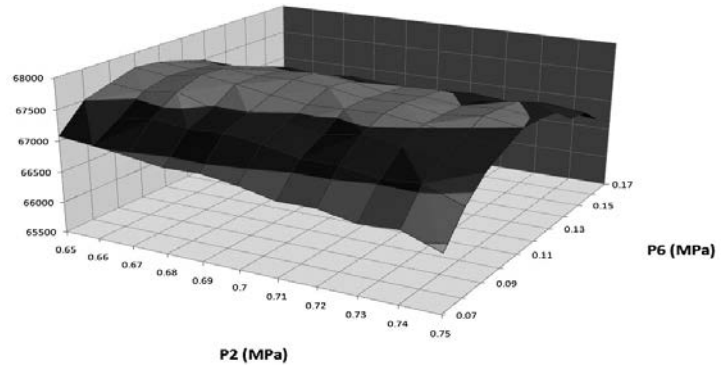

Fig. 2. Two dimensional optimization for output power (KJ).

Fig. 3 shows the effect of pressure change on the isentropic efficiencies of high pressure and low pressure turbines. It is obvious that the effect of separation pressures on isentropic efficiency of high pressure and low pressure turbines is somehow in opposite directions. Total exergy dissipations of turbines, flash vessels and condenser are illustrated in Fig. 4 and Fig. 5. It seems flash vessels are the greatest exergy dissipators in power plant and small changes in pressures can lead to a dramatic change in exergy dissipation of flash vessels.

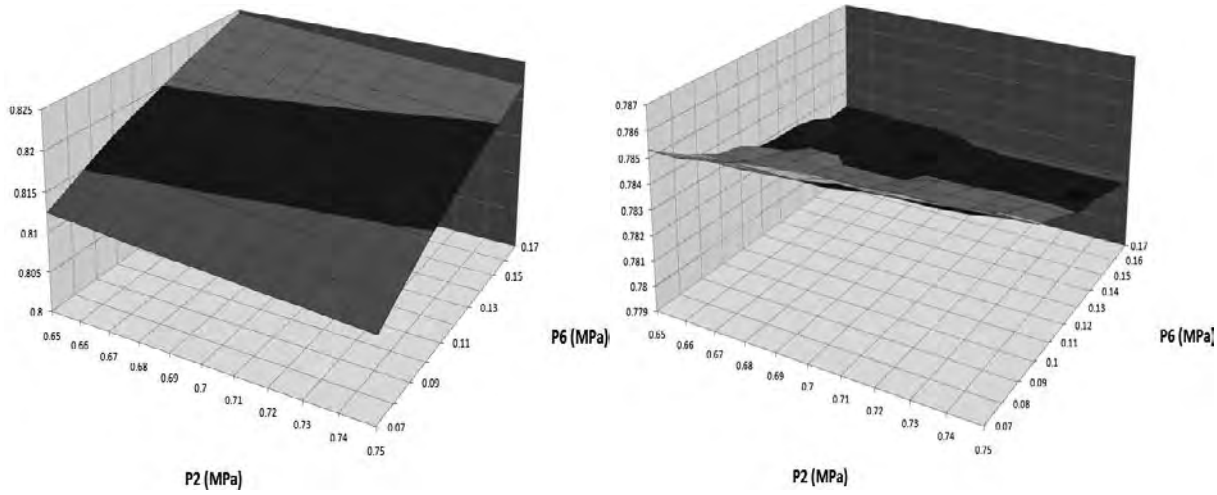

(a) *(b)*

Fig. 3. Isentropic efficiency for (a) High pressure turbine (b) Low pressure turbine.

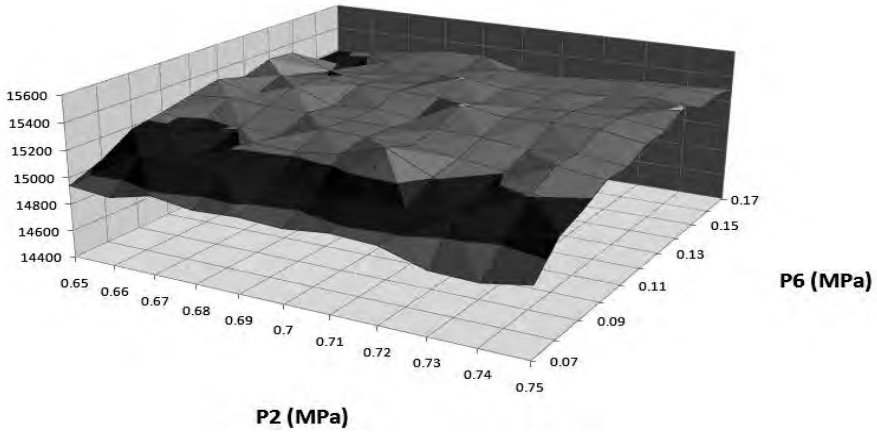

Fig.4. Total exergy dissipation of turbines (KJ).

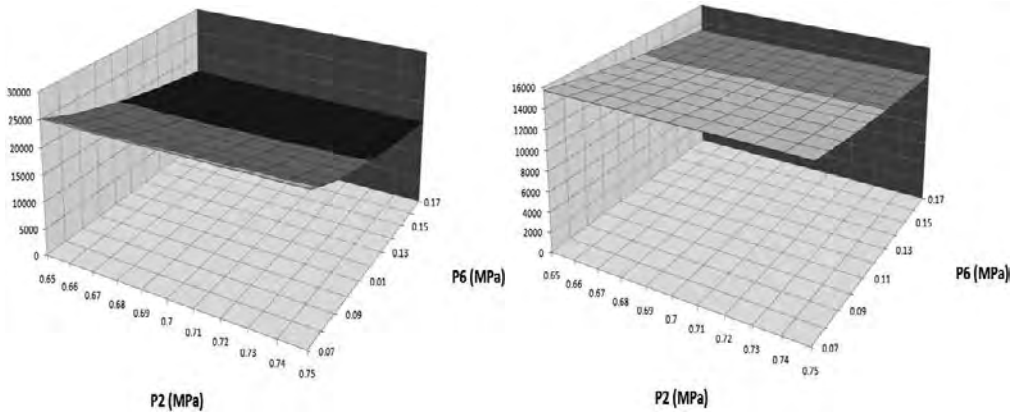

(a) *(b)*

Fig. 5. Total exergy dissipation (KJ) (a) Flash vessels (b) Condenser.

4. Discussion and Conclusions

As there is no data available for Meshkin-Shahr power plant, the validation of this study is done for a geothermal power plant in Turkey [19]. It shows good agreement. However, the validation is limited to annual net output power. The results of our study demonstrate that the exergy efficiencies of high pressure and low pressure turbines change in opposite directions. Brute force efficiency can reveal how much exergy of incoming flow is utilized and how

much is lost. On the other hand functional efficiency can disclose how much of incoming exergy is conserved in flow stream and how much leaves the component.

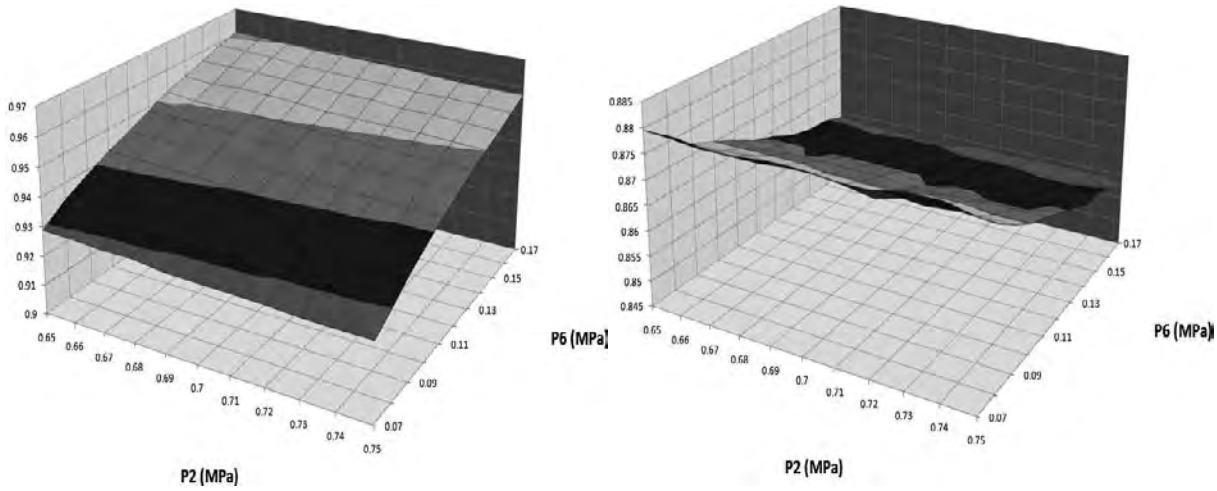

(a) (b)

Fig. 6. Brute force efficiency (a) High pressure turbine (b) Low Pressure turbine.

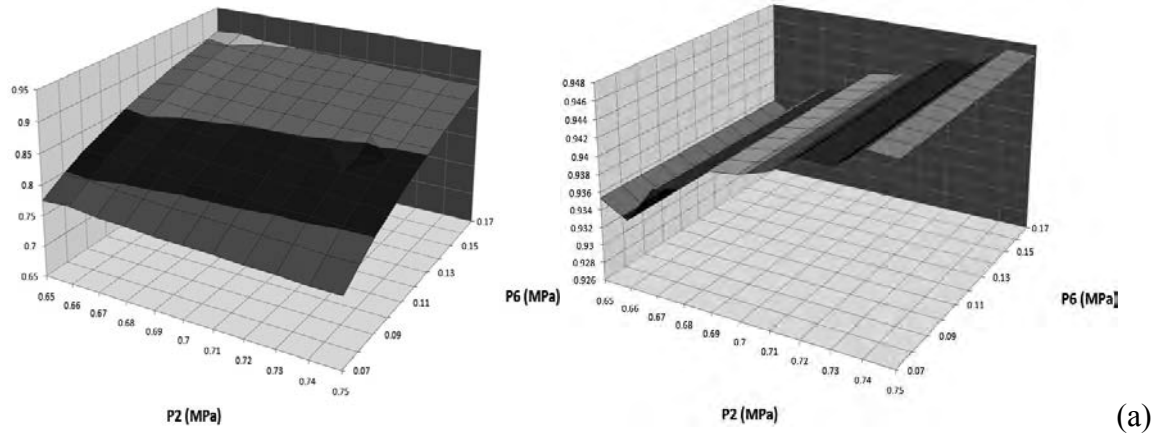

(a)

(b)

Fig. 7. Brute force efficiency (a) Low pressure flash vessel (b) High pressure flash vessel.

The suffered brute force and isentropic efficiencies of low pressure turbine in comparison with high pressure turbine is due to the fact that more amount of incoming exergy has left the turbine. A more profound study of Fig. 6 and having in mind that in double flash power plants low pressure turbines have greater portion in output power production, one can easily find why the optimum point for pressures is situated in the intersection of 0.67MPa and 0.1MPa. Since the pressure of incoming flow to high pressure flash vessel is constant, one can easily understand why the brute force efficiency surface is like sets of stairs.

References

[1] M. Yari, Exergetic analysis of various types of geothermal power plants, Renewable Energy 35, 2010, pp. 112-121.

[2] M. Kanoglu, A. Bolatturk, Performance and parametric investigation of a b inary geothermal power plant by exergy, Renewable Energy 33, 2008, pp. 2366-2374.

[3] R. DiPippo, Geothermal power plants, Elsevier Ltd, 2nd E dition, 2007, pp. 191 -251 & 102-104 & 241-247.

[4] M. Ameri, S.R. Shamshirgaran, M. Pour Yousefi, The Study of Key Thermodynamic Parameters Effect on the Performance of a Flash Steam Geothermal Power Plant, Proceeding of 2nd Joint Int. Conference SEE 2006, Bangkok, 2006, B-004 (O).

[5] V. Stefansson, Investment cost for geothermal power plants, Geothermics 31, 2002, pp. 263-272.

[6] M. Ameri, S. Amanpour, S. Amanpour, Energy and exergy analysis of Mehkin-Shahr single flash geothermal power plant, Proceeding of 10th International Conference on Clean Energy (ICCE-2010), 2010, No. 12-08.

[7] N. Y. Ozcan, G. Gokcen, Thermodynamic assessment of gas removal systems for single-flash geothermal power plants, Applied Thermal Engineering 29, 2009, pp. 3246-3253.

[8] A. Dagdas, R. Ozturk, S. Bekdemir, Thermodynamic evaluation of Denizli Kizildere geothermal power plant and its performance improvement, Energy Conversion and Management 46, 2005, pp. 245-256.

[9] A. Franco, M. Villani, Optimal design of binary cycle power plants for water-dominated, medium-temperature geothermal fields, Geothermics 38, 2009, pp. 379-391.

[10] M. Kanoglu, Exergy analysis of a dual-level binary geothermal power plant, Geothermics 31, 2002, pp. 709-724.

[11] R. DiPippo, Second Law assessment of binary plants generating power from low-temperature geothermal fluids, Geothermics 33, 2004, pp. 565-586.

[12] Y. Cerci, Performance evaluation of a single-flash geothermal power plant in Denizli, Turkey, Energy 28, 2003, pp. 27-35.

[13] U. Serpen, Comments on Performance evaluation of single-flash geothermal power plant in Denizli, Turkey, Energy 29, 2004, pp. 1219-1223.

[14] Y. Cerci, Response to comments on "Performance evaluation of single-flash geothermal power plant in Denizli, Turkey", Energy 29, 2004, pp. 1225-1226.

[15] U. Serpen, Reply to the author's response to comments on "Performance evaluation of single-flash geothermal power plant in Denizli, Turkey", Energy 29, 2004, pp.1227-1229.

[16] H.D. Madhawa Hettiarachchi, M. Golubovic, M. Worek William, Y. Ikegami, Optimum design criteria for an Organic Rankine cycle using low-temperature geothermal heat sources, Energy 32, 2007, pp. 1698-1706.

[17] M. Kanoglu, I. Dincer, A. Rosen Mark, Understanding energy and exergy efficiencies for improved energy management in power plants, Energy Policy 35, 2007, pp. 3967-3978.

[18] I. Dincer, M. Rosen, Exergy, Elsevier Ltd, 2007, pp. 23-24.

[19] N. YILDIRIM OZCAN, modeling, simulation and optimization of flashed-steam geothermal power plants from the point of view of non-condensable gas removal systems, PhD thesis, Graduate School of Engineering and Science of Izmir Institute of Technology, 2010, pp. 82-83 & 149-150.

Thermoeconomic evaluation of combined heat and power generation for geothermal applications

Florian Heberle*, Markus Preißinger, Dieter Brüggemann

University of Bayreuth, Germany
** Corresponding author. Tel: +49 921 557163, Fax: +49 921 557165, E-mail: lttt@uni-bayreuth.de*

Abstract: In this study a thermoeconomic analysis of combined heat and power generation (CHP) for geothermal applications is presented. Different working fluids and power plant concepts are investigated for power generation by Organic Rankine Cycle and additional heat generation. For geothermal conditions in Germany, process simulations of series, parallel and hybrid circuits compared to sole power generation are performed. The results show that for power generation fluids with low critical temperature, like R227ea or isobutane, are suitable. In general, an additional heat generation decreases the averaged costs of electricity generation. In case of a source temperature of 120 °C the costs can be reduced from 25 ct/kWh to 16 ct/kWh compared to power generation. For CHP applications fluids with higher critical temperature and series or hybrid circuits are the most efficient concepts. With increasing temperature of the geothermal water an increase of supply temperature of the heating system has less influence on the costs of electricity generation. A doubling of mass flow of the geothermal water decreases the averaged costs of electricity generation in the range of 28 % and 43 % depending on power plant concept and boundary conditions.

Keywords: *Geothermal energy, Organic Rankine Cycle, cogeneration, thermoeconomic analysis*

Nomenclature

c	*cost of electricity generation* ct/kWh	n	*contract period* a
C	*costs* €	N	*produced amount of electricity* kWh
e	*specific exergy* kJ/kg	p	*pressure* Pa
$\dot{E}$	*exergy flow rate* kW	P	*mechanical power* kW
h	*enthalpy* J/kg	s	*entropy* J/(kgK)
i	*interest rate* %	T	*temperature* °C
$\dot{m}$	*mass flow rate* kg/s	η	*efficiency* %

1. Introduction

Regarding base load capacity, geothermal resources play an important role for renewable energy generation. For temperatures of the geothermal water below 180 °C direct expansion or flash processes are not suitable under thermodynamic and economical aspects [1]. Instead binary power plants like the Organic Rankine Cycle (ORC) or the Kalina Cycle are used. Therefore thermal energy of the geothermal water is coupled with the secondary thermodynamic cycle. Concerning the ORC, there are different possibilities, like selection of the working fluid, supercritical cycle or multi-stage expansion, to raise the electric efficiency [2-5]. Another interesting strategy to improve the second law efficiency and economic aspects is combined heat and power generation (CHP). In case of geothermal applications, previous exergoeconomic and thermoeconomic investigations are restricted to sole power generation or district heating [6-8]. In this study potential ORC fluids, isobutane, isopentane, R227ea and R245fa are investigated for power generation. In case of additional heat generation, parallel, series and hybrid circuit are considered. Second law efficiency and costs of electricity generation are calculated for an assumed heat demand and typical geothermal conditions in Germany. Detailed simulations are performed for variations of mass flow of the geothermal water and supply temperature of the heating system. The results provide basic criteria for fluid selection under thermoeconomic aspects in case of power generation by ORC and CHP.

2. Methodology

2.1. Simulation

Process simulations are done by the software tool Cylce Tempo and fluid properties are calculated by REFPROP Version 8.0 [9,10]. The process scheme of the ORC for sole power generation (SPG) and the corresponding *T,s*-diagram for isopentane at standard conditions are shown in Fig.1.

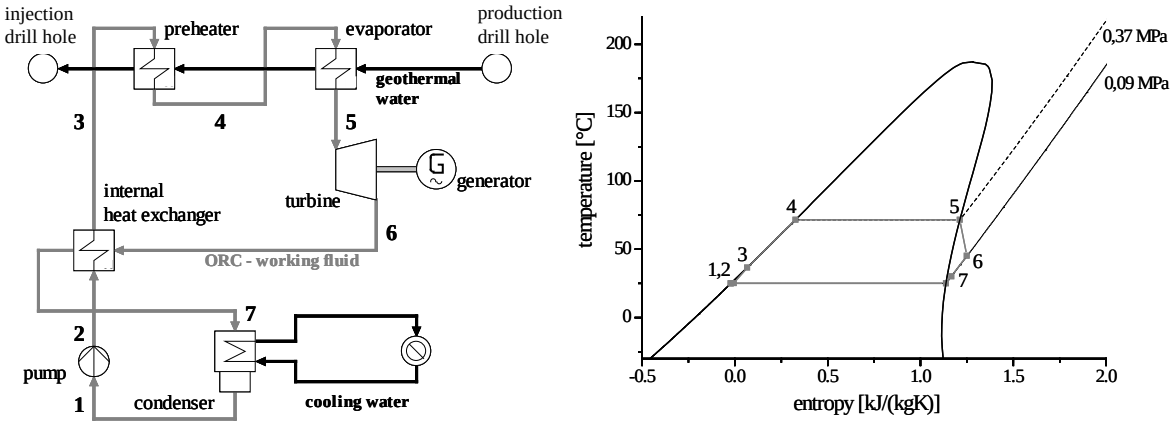

Fig. 1. Scheme of a geothermal ORC-power plant and corresponding T,s-diagram of isopentane.

The liquid fluid is compressed by the pump to maximum process pressure. The heat supply takes place in three steps. First the internal heat recovery, followed by the coupling with the geothermal heat source in the preheater and finally in the evaporator. As the analyzed fluids show a negative slope of the dew line in the *T,s*-diagram, so-called dry fluids, superheating is not necessary [11]. After the expansion the fluid is cooled down in the internal heat exchanger and condensed in the condenser. For the standard case, process parameters and boundary conditions of the heat source and sink are listed in table 1.

Table 1. Standard parameters of the ORC process simulation

parameter	
temperature of geothermal water	120 °C
mass flow of geothermal water	65.5 kg/s
ΔT-pinch-point (evaporation / condensation)	5 K
ΔT of the cooling water	5 K
cooling temperature	15 °C
maximum pressure ORC	$0.8 \cdot p_C$
isentropic efficiency (turbine / feed pump)	0.75

Regarding the additional heat generation, three concepts are investigated. Fig. 2 shows the series (SC), parallel (PC) and hybrid circuit (HC). As standard parameters of the heating system a supply temperature of 75 °C and a return temperature of 50 °C are assumed. The minimum temperature difference between heating system and geothermal water is 5 K. The supposed annual demand of thermal power is simulated in four steps: 10 MW for 1000 operating hours, 7.5 MW for 1500 operating hours, 5 MW for 2500 operating hours and 2.5 MW for another 3500 operating hours.

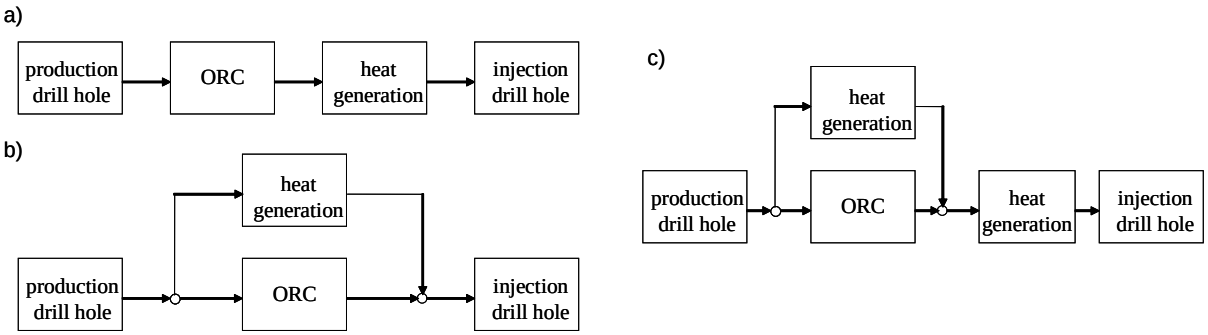

Fig. 2. Series circuit (a), parallel circuit (b) and hybrid circuit (c) as concepts for CHP

In case of series circuit the temperature of the geothermal water at the outlet of the ORC must be adapted to the peak load of the heat demand. For parallel circuit fluctuations in heat demand can be adjusted by varying the ratio of mass flow of the geothermal water. The hybrid circuit describes a coupling of series and parallel circuit.

2.2. Second law analysis

The simulations of the power plant are performed by solving a system of equations, consisting of energy balances of the heat exchangers units. Pressure and heat losses are not considered in the process components and pipes. As an example the energy balance of the preheater is given by

$$\dot{m}_{GW}(h_{GW,in}\text{-}h_{GW,out})_{PH} = \dot{m}_{ORC}(h_4 - h_3) \tag{1}$$

where $\dot{m}_{GW}$ corresponds to the mass flow of the geothermal water, $h_{GW,in}$ and $h_{GW,out}$ to the enthalpy of the geothermal water at the inlet and outlet of the preheater. The mass flow of the ORC is described as $\dot{m}_{ORC}$, h_3 and h_4 correspond to the enthalpies of the working fluid at the inlet and outlet of the preheater. A detailed formulation of the simulation model can be seen in Heberle and Brüggemann [12]. By using a user subroutine the outlet temperature of geothermal water is adapted to the maximum power output of the ORC in case of power generation. The second law efficiency for sole power generation is calculated by

$$\eta_{II,el} = \frac{\left|P_T + P_P\right|}{\dot{E}_{GW}} \tag{2}$$

where P_T is the power of the turbine and P_P corresponds to the power of the pump. The maximum power output of geothermal source, the exergy flow $\dot{E}_{GW}$, is obtained by multiplying the specific exergy e with the mass flow of the geothermal water:

$$\dot{E}_{GW} = \dot{m}_{GW} e \tag{3}$$

The specific exergy is calculated by:

$$e = h - h_0 - T_0(s - s_0) \tag{4}$$

The state variables T_0, p_0 and s_0 are related to ambient conditions. In the case of additional heat generation, the numerator from Equation 2 is extended with the exergetic value $\dot{E}_Q$

$$\eta_{II,tot} = \frac{\left|P_T + P_P\right| + \dot{E}_Q}{\dot{E}_{GW}} \tag{5}$$

where the exergy flow of the thermal energy coupled to the heating system $\dot{E}_Q$ can be calculated by

$$\dot{E}_Q = \dot{m}_{HS}\left(e_{out} - e_{in}\right)_{HS} \tag{6}$$

where $\dot{m}_{HS}$ is the mass flow of the heating system. The specific exergy at the inlet and outlet of the heat transfer unit of the heating system are e_{in} and e_{out}.

2.3. Economic analysis

The assumed parameters for the economic analysis, like exploration costs or specific costs for the ORC module and heating system, are listed in table 2 **[13]**. PRIVATE EQUITY AND STATE FUNDING ARE NOT CONSIDERED FOR THE CALCULATIONS.

Table 2. Economic boundary conditions for geothermal CHP

parameter	
exploration costs	18 000 000 €
other (building, insurance, etc.)	4 000 000 €
power plant (ORC)	4 000 €/kW
heating system	150 €/kW
costs of heating pipeline	150 €/m
heating price	40 €/MWh
rise in price rate (heating price)	1,5 %/a
operating and maintenance (O&M) costs	750 000 €/a
rise in price rate (O&M)	2 %
interest rate *i*	7 %
contract period *n* for consumption of fixed capital costs	20 a

The annual costs C_A of the power plant consist of capital consumption C_C, imputed interest C_I, and O&M costs $C_{O\&M}$. The imputed interest $C_{I,t}$ for the year t is calculated by

$$C_{I,t} = \frac{R_{t-1} + R_t}{2} \cdot i \qquad \text{with } t = 1,\ldots,n \tag{7}$$

where R_t is the residual value and R_0 corresponds to the initial investment costs. The costs of electricity generation c_t at year t are calculated by

$$c_t = \frac{C_{A,t}}{N} = \frac{C_{C,t} + C_{I,t} + C_{O\&M}}{N} \tag{8}$$

where N is the annual produced amount of electricity. In the following the averaged costs of electricity generation c are calculated for the economic analysis by:

$$c = \frac{\sum_{t=1}^{n} c_t}{n} \tag{9}$$

3. Results

3.1. Second law efficiency for power generation

The second law efficiency for sole power generation as a function of inlet temperature of the geothermal water is shown in Fig. 3 for the investigated working fluids.

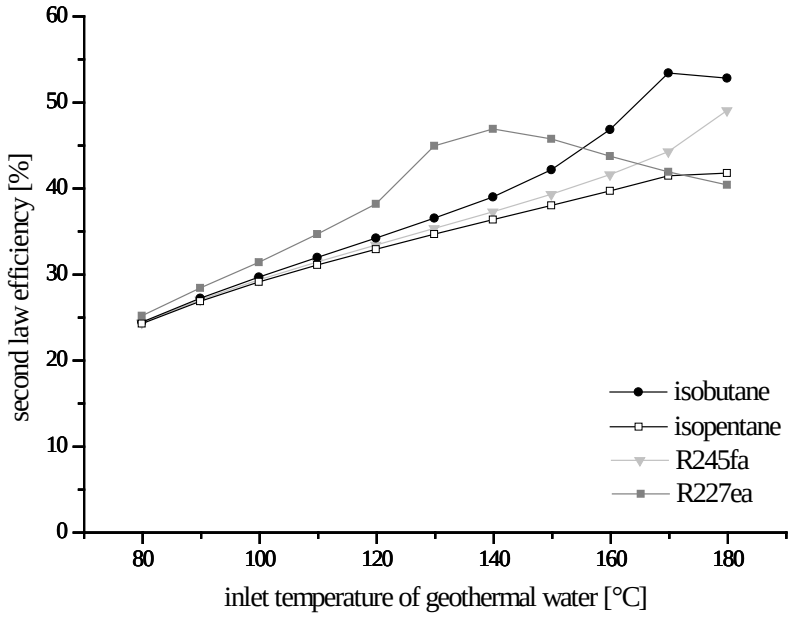

Fig. 3. Second law efficiency for the investigated working fluids as a function of temperature of the geothermal water

The results show obvious differences in efficiency depending on inlet temperatures. For low temperatures R227ea is a suitable working fluid, for temperatures higher than 150 °C isobutane should be favored. The local maxima for R227ea and isobutane are due to the shift of the pinch point from the inlet of the evaporator, state point 4, to the inlet of preheater, state point 3. The effect occurs, because the maximum process pressure of the ORC fluid is reached, which leads to a high amount of thermal energy coupled to the cycle. As a result the outlet temperature of the geothermal water decreases significantly. In case of the less efficient fluids, like R245fa and isopentane, the second law efficiency increases linear with inlet temperatures. For these fluids the outlet temperatures of the geothermal water are higher compared to R227ea or isobutane. At 120 °C inlet temperature isopentane leads to an outlet temperature of 64.3 °C compared to R227ea with 59.7 °C. The difference becomes apparent for 160 °C with outlet temperatures of 73.2 °C and 36.5 °C. A detailed explanation and graphical description of these correlations can be found in Heberle and Brüggemann [12].

3.2. Second law efficiency for CHP

Fig. 4 shows the second law efficiency for CHP as a function of thermal power of the heating system compared to sole power generation at standard conditions for isopentane and R227ea.

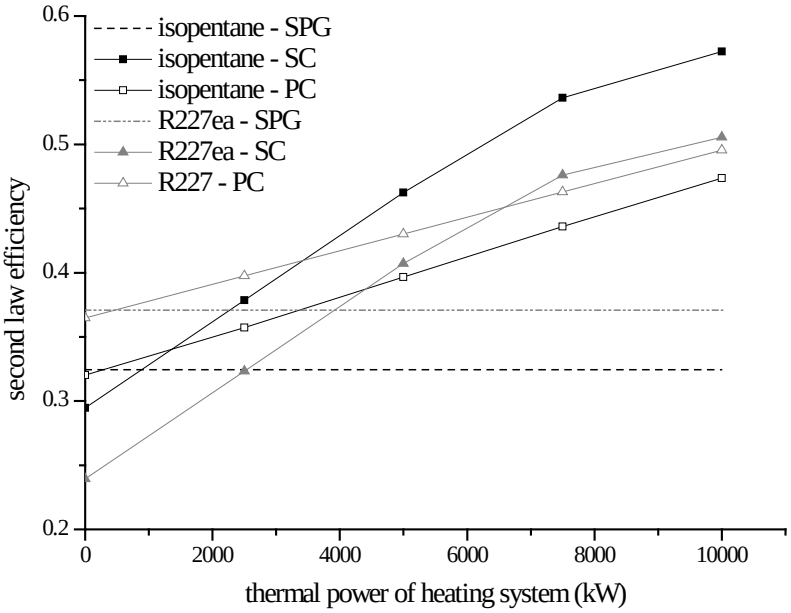

Fig. 4. Second law efficiency depending on thermal power coupled to the heating system

An additional heat generation improves the second law efficiency of the analyzed system. In case of isopentane the efficiency increases up to 24.8 % compared to sole power generation. For R227ea the raise is 15.5 % in case of 10 MW thermal power coupled to the heating system. Another interesting aspect is the comparison of the different concepts and working fluids. In the range of 1 MW to 10 MW thermal power the series circuit is the most efficient concept for isopentane as an ORC working fluid. In case of R227ea only for a thermal power higher than 7 MW the series circuit leads to slightly higher efficiencies compared to parallel circuit. The different behaviour of the working fluids corresponds to the outlet temperatures of geothermal water, which has to be adjusted to the temperatures of the heating system in case of series circuit. For R227ea, this adjustment shows higher losses in power generation compared to isopentane.

3.3. Averaged costs for electricity generation depending on power plant concept

In the following sections only the results for R227ea and isopentane are presented, to guarantee well-arranged analyses. The Southern German Molasse Basin and the Upper Rhine Rift Valley with temperatures of 120 °C and 160 °C for the geothermal water are chosen as geothermal reservoirs. In Fig. 5 the averaged costs of electricity generation depending on power plant concept and geothermal conditions are presented. Corresponding to the second law analysis R227ea is more suitable for power generation in comparison to isopentane. In case of 120 °C the costs are 25 ct/kWh, for 160 °C they are reduced to 15 ct/kWh. The difference to isopentane decreases with increasing temperature of the heat source. In general CHP leads to a decrease of averaged costs of electricity generation. In case of R227ea and 120 °C they are reduced to 18 ct/kWh by parallel circuit. The most economic concept for 120 °C is isopentane in conjunction with series circuit. For 160 °C the working fluid isopentane and the hybrid circuit with averaged costs of electricity generation of 9 ct/kWh should be preferred. In general the hybrid circuit only makes sense for working fluids with high outlet temperatures of the geothermal water, like R245fa or isopentane.

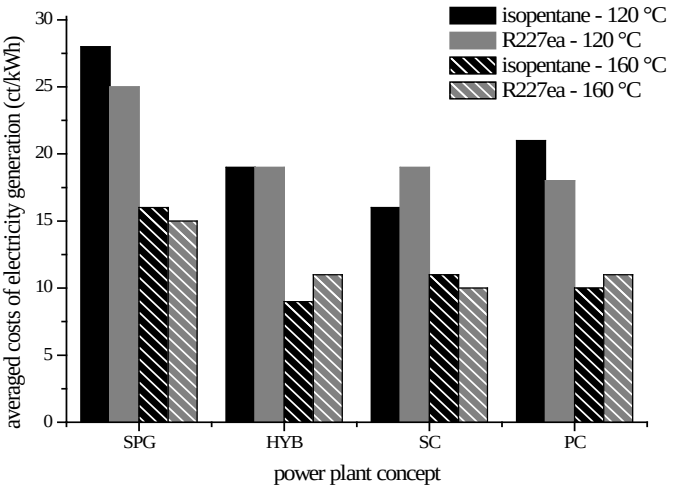

Fig. 5. Averaged costs of electricity generation depending on power plant concept

3.4. Variation of supply temperature of the heating system and mass flow of the geothermal water

Table 3 shows the averaged costs of electricity generation as a function of supply temperature of the heating system and mass flow of the geothermal water for isopentane in case of SPG and SC. In this case the duration curve of heat demand is analyzed more detailed in 11 steps.

Table 3. Averaged costs of electricity generation depending on supply temperature of the heating system and mass flow of the geothermal water

heating system supply temperature	SC – 120 °C (ct/kWh)	SPG – 120 °C (ct/kWh)	SC – 160 °C (ct/kWh)	SPG – 160 °C(ct/kWh)
75 °C	20	28	11	14
85 °C	24	28	11	14
95 °C	32	28	12	14
mass flow				
65.5 kg/s	20	28	11	14
100 kg/s	15	19	8	11
120 kg/s	13	16	8	10

In case of 120 °C an increasing supply temperature has a significant influence on the averaged costs of electricity generation. Since the outlet temperature of the geothermal water has to be increased for higher supply temperatures the losses in electrical power generation rise. For 95 °C supply temperature, the CHP concept leads with 32 ct/kWh to higher costs than sole power generation with 28 ct/kWh. For 160 °C the increase in supply temperature has only a marginal influence on economic aspects. A rise in mass flow of the geothermal water leads to a higher power output and lower costs of electricity generation. At a source temperature of 120 °C an increase from 65.5 kg/s to 120 kg/s leads to a reduction of costs from 28 ct/kWh to 16 ct/kWh in case of power generation and for series circuit from 20 ct/kWh to 13 ct/kWh. In case of 160 °C, costs are reduced up to 28 %.

4. Discussion

A thermoeconomic analysis for combined heat and power generation in case of geothermal heat sources below 180 °C was performed. For power generation the ORC with different

working fluids was investigated. The second law efficiency and the costs of electricity generation were calculated for three concepts of heat generation and two typical geothermal conditions in Germany. The following conclusions can be summarized:

- Second law efficiency and economic aspects can be enhanced by CHP.
- For power generation working fluids with low critical temperatures, at the shift of the pinch point, should be selected.
- R227ea leads with 25 ct/kWh and 15 ct/kWh to low costs for sole power generation.
- In case of CHP, working fluids with higher critical temperatures are suitable.
- Isopentane in conjunction with series and hybrid circuit is the most economic concept for CHP. In case of 120 °C and series circuit the costs of electricity generation are 16 ct/kWh and for 160 °C and hybrid circuit the costs are 8 ct/kWh.

References

[1] R. DiPippo, Small geothermal power plants: design, performance and economics, GHC Bulletin, June 1999.

[2] B. Saleh, G. Koglbauer, M. Wendland, J. Fischer, Working fluids for low-temperature organic Rankine cycles, Energy 32, 2007, pp. 1210-1221.

[3] U. Drescher, D. Brüggemann, Fluid selection for the Organic Rankine Cycle (ORC) in biomass power and heat plants, Applied Thermal Engineering 27, 2007, pp. 223-228.

[4] S. Karellas, A. Schuster, Supercritical fluid parameters in Organic Rankine Applications, International Journal of Thermodynamics 11, 2008, pp. 101-108.

[5] Z. Gnutek, A. Bryszewska-Mazurek, The thermodynamic analysis of multicycle ORC engine, Energy 26, 2001, pp. 1075-1082.

[6] O. Arslan, Exergoeconomic evaluation of electricity generation by the medium temperature geothermal resources, using a Kalina cycle: Simav case study, International Journal of Thermal Sciences 49, 2010, pp. 1866-1873.

[7] O. Arslan et al., Exergoeconomic evaluation on the optimum heating circuit system of Simav geothermal district heating system, Energy and Buildings 41, 2009, pp. 1325-1333.

[8] A. Hepbasli, A review on energetic, exergetic and exergoeconomic aspects of geothermal district heating systems, Energy Conversion and Management 51, 2010, pp. 2041-2061.

[9] N. Woudstra, T.P. van der Stelt. Cycle-Tempo: a program for the thermodynamic analysis. Energy Technology Section, Delft University of Technology, The Netherlands, 2002.

[10] E.W. Lemmon, M.L. Huber, M.O. McLinden. NIST Standard Reference Database 23 – Version 8.0. Physical and Chemical Properties Division, National Institute of Standards and Technology, Boulder, Colorado, US Department of Commerce, USA, 2002.

[11] P. Mago, L. Chamra, K. Srinivasan, C. Somayaji, An examination of regenerative organic Rankine cycles using dry fluids, Applied Thermal Engineering 28, 2008, pp. 998-1007.

[12] F. Heberle, D. Brüggemann, Exergy based fluid selection for a geothermal Organic Rankine Cycle for combined heat and power generation, Applied Thermal Engineering 30, 2010, pp. 1326-1332.

[13] B. Görke, A. Sievers, Gewinnbetrachtung von strom- und wärmegeführten Geothermie-Projekten unter Berücksichtigung der aktuellen EEG Novelle, Tagungsband Geothermiekongress, 2008, Karlsruhe (D), pp. 157-156.

Energy supply in buildings: heat pump and micro-cogeneration

Marta Galera Martínez, Laura Cristóbal Andrade, Pastora M. Bello Bugallo*, Manuel Bao Iglesias

Department of Chemical Engineering and Seminar of Renewable Energy (Aula de Energías Renovables), University of Santiago de Compostela, Spain
** Corresponding author. Tel: +34 881816757, Fax: +34981528050 , E-mail: pastora.bello.bugallo@usc.es*

Abstract: Heat pumps and micro-cogeneration technology for residential applications are an alternative for energy saving and for improving the energy efficiency. Nowadays, several nomenclatures are used for these technologies, creating confusion within this field. This situation causes that the commercial brands could not offer their products clearly to the market as the concepts and terminology they use are usually incorrect. This paper clarifies these concepts using thermodynamics, and provides clear classification criteria considering the heat pump and the power cycle as the starting point. Therefore, this paper provides an update review of heat pumps and micro-cogeneration which could be of great importance in the future for achieving the goals of the European legislation, especially those related to energy supply in buildings. It emphasizes the principles of operation and the advantages of the different devices as well as the consideration of this technology as renewable energy.

Keywords: *Energy Efficiency, Heat Pump, Micro-cogeneration, Distributed Generation*

1. Introduction

Buildings have an impact on long-term energy consumption. According to data from 2010, buildings account for 40% of the total energy use in the European Union (EU) [1]. Around the same percentage of all greenhouse gas emissions in developed countries have their origin in building equipments, where approximately 60% are produced by cooling and heating systems [2]. However, the energy use of any residence largely depends on its architectural design. All these factors are included in the Directive 2002/91/EC on the energy performance of buildings [3], which states that the calculation methodology must take into account insulation, technical and installation characteristics, design and positioning in relation to climatic aspects, solar exposure and influence of neighboring structures, own-energy generation and other factors such as indoors climate, which influences the energy demand. Directive 2009/28/CE on the promotion of the use of energy from renewable sources similarly talks about passive energy systems which use building design to harness energy [4]. This directive also requires that, before the end of 2014, Member States enforce the use of minimum levels of energy from renewable sources in buildings. This requirement may be fulfilled through heating and cooling systems that use a significant percentage of renewable energy sources [4].

Heat pumps (HP) and micro-cogeneration technologies for residential applications are an alternative for energy saving and for improving energy efficiency. Consequently, these technologies allow reducing the greenhouse gas emissions and can reduce energy dependence.

This paper clarifies these concepts using thermodynamics, and provides clear classifications considering the HP and the power cycle as the starting point. Therefore, this paper provides an update review of HPs and micro-cogeneration which could be of great importance in the future for achieving the goals of the European legislation. It emphasizes the principles of operation and the advantages of the different devices.

2. Heat pumps

2.1. Foundations

HP is a system that undergoes a thermodynamic cycle while thermally communicating with two bodies located in the surroundings or thermal reservoirs. They are devices designed to utilize low temperature sources of energy to heat a space to higher temperatures. The low temperature source may be the atmospheric air, the ground or a nearby body of water (lake or river). This energy comes from the solar radiation reaching the surface of the earth and its use constitutes therefore an indirect use of solar energy [5]. On the other hand, the space to be heated corresponds to the circuit for space heating, usually water or air. Net work input is needed to be provided by electricity, though it may also be provided by a mechanical engine. The components of a HP cycle, namely vapor compression HP, are: evaporator, condenser, compressor and expansion valve (Fig. 1).

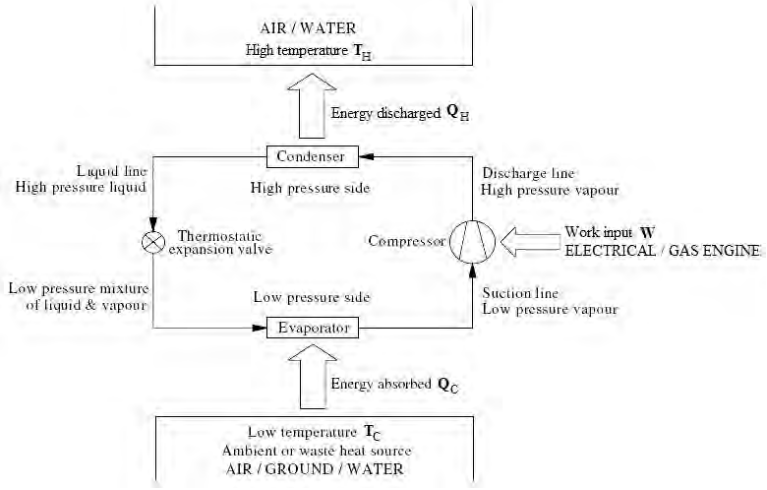

Fig. 1. Typical HP schematic.

$$W = Q_H - Q_C \quad (1)$$

$$COP = \frac{Q_H}{W} \quad (2)$$

$$COP = \frac{Q_H}{Q_H - Q_C} \quad (3)$$

$$COP_{máx} = \frac{T_H}{T_H - T_C} \quad (4)$$

The objective of a HP is to maintain the temperature *above* that of the surroundings. According to energy flows, the energy balance is defined by Eq. (1). Therefore, the Coefficient of Performance (COP) of a HP is calculated as the amount of energy discharged from the cycle system to the hot reservoir by the net work input needed to accomplish this effect (Eq. (2)). As Q_H is greater than Q_C, COP is never less than unity but it is also limited to a maximum value. The maximum COP of a reversible HP cycle is obtained in terms of reservoirs temperatures (Eq. (4)). In any case, and in spite of these limitations, it is desirable to obtain high values of COP.

2.2. Heat pumps classification

2.2.1. Thermodynamic cycle type

The foundations of HPs are used to give a first qualitative classification depending on the thermodynamic cycle. Accordingly, there are mainly three types of HPs (Fig. 2). Vapor-Compression Heat Pumps (VCHPs) are commonly used for space heating applications. Its compressor is mechanical, so it requires mechanical drive energy. Vapor Absorption Heat Pumps (VAHPs) are also used for space heating and require thermal drive energy. Both systems involve changes in phase, whereas in gas refrigeration systems the working fluid stays as a gas throughout. The Brayton refrigeration cycle illustrates an important type of gas refrigeration system [6] and consequently it can be also worked as a HP [7].

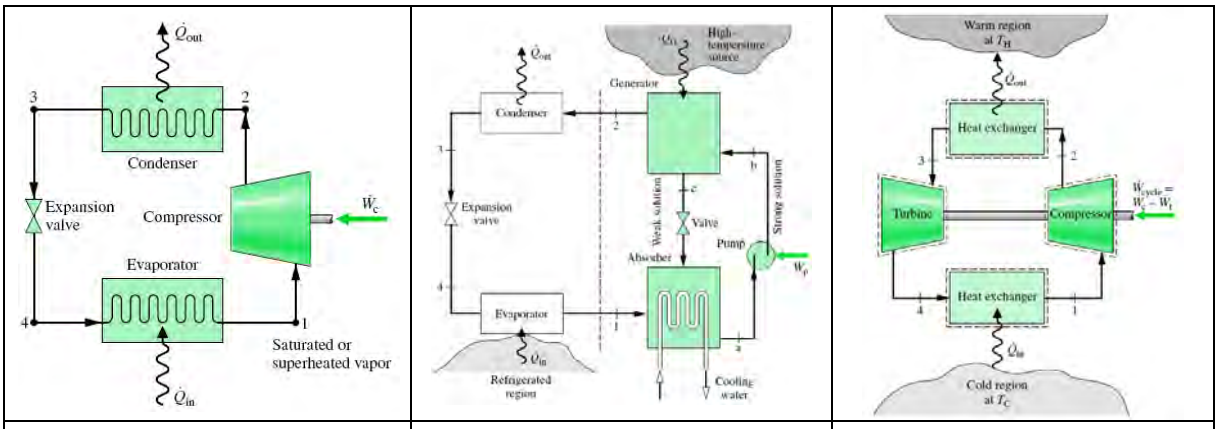

Vapor-compression cycle	Absorption cycle	Brayton cycle

Fig. 2. Diagrams of principal refrigeration or heat pump cycle [6].

2.2.2. Equipment

According to Fig. 1, and depending on the type of equipment that the HP uses to operate, different classifications can be considered.

- Evaporator. Depending on the type of equipment used to evaporate the refrigerant fluid, a classification can be made including any type of heat exchanger, as differently disposed shell-and-tube heat exchangers, solar collectors, etc. That depends on the cold reservoir. As a particular case, the Solar Assisted Heat Pump (SAHP) system mixes HP and solar technology, using solar radiation as evaporating heat source. This allows an improvement of the COP of the HP and, therefore, of the energy conversion efficiency. In Spain, a commercial term "thermodynamic solar cell" appears around 2006. From a commercial point of view, it is more socially impactful taking about "solar cells" than "HP", as solar cell is a term associated with positive connotations (ecologic, renewable, etc), which are not used when talking about HPs. However, the reality is that a "thermodynamic solar cell" is a SAHP. Ozgener et al. [8] have done a classification of SAHP according to the literature: (i) SAHPSs for water heating, (ii) SAHPSs with storage (conventional type) for space heating, (iii) SAHPSs with direct expansion for space heating, and (iv) Solar-Assisted Ground Source Heat Pump Greenhouse Heating System (SAGSHPGHS). Ji et al. [9] proposed in 2007 a novel Photo-Voltaic Solar Assisted Heat Pump (PV-SAHP) system capable of providing space cooling-heating and domestic water-heating. The solar panels are actually an assembly of PV cells laminated onto the evaporator-collector plate, allowing the direct solar energy absorption and, therefore, improving the protection of the evaporator from frosting in winter. Through experiments, the maximum COP (10.4) was obtained when the solar irradiance was also the highest. Then, they concluded that PV-SAHP system is better than the conventional HP systems.

- Compressor. Gas Engine Heat Pumps (GEHPs) have the compressor driven by a gas (natural gas, propane or LPG) fuelled internal by a combustion engine instead of electricity.

- Valve. There are two types: reversible (inverter) and irreversible, depending of the type of valve (four or two-way valves).

2.2.3. Net work input

HPs require energy (net work, W) for operating, so they can be basically divided into Electric-driven Heat Pumps (EHPs) and the Gas Engine Driven Heat Pump (GEHPs).

2.2.4. Cold reservoir

Directive 2009/28/CE enables HPs to use aerothermal, geothermal or hydrothermal heat. HPs are formally classified as air source, ground source or water source depending on the thermal reservoir they use. But there are hybrid HPs which combine, for example, ground source/air source units, and solar assisted and solar boosted air source and water source units.

2.2.4.1 Air-source HPs

The most common type of HP is the air-source HP. This category includes the air-to-air and air-to-water HPs. The solar energy is stored in the air, so this HP indirectly uses solar energy. They operate using fans to draw air across the evaporator. The inconvenient is their efficiency is influenced by the variation in ambient air temperature. If this temperature drops below 4 ºC, ice may appear in the evaporator, so efficiency decreases. The main advantage if compared with Ground Source Heat Pumps (GSHPs) is the relatively low capital cost.

2.2.4.2 Ground-source heat pumps (GSHPs)

GSHPs are also known as Geothermal Heat Pumps (GHPs). Yang et al. [10] classified these systems according to the source where they absorb the energy. This means that the cold reservoir could be the ground, ground water or surface water, and based on the type of reservoir there are basically three categories: (i) Ground-Coupled Heat Pump (GCHP) systems, (ii) Ground Water Heat Pump (GWHP) systems and (iii) Surface Water Heat Pump (SWHP) systems. They may be also classified according the loop: open loop (ground coupled) or closed loop (water source) [8]. The great advantage is the underground temperature remains fairly constant during the year, so this technology offers higher energy efficiency. However, in the case of SWHP the surface water temperature is influenced by weather condition. The pipes are buried in the ground horizontally or vertically. The horizontal system installation is less expensive than vertical one, but it requires much more ground area and it is more influenced by ambient air temperature.

2.2.4.3 Water-source heat pumps (WAHPs)

WAHPs, as the term implies, obtain heat from a large body of water source. As it uses water from the Earth as their energy source, WSHPs are incorporated in ground-source HPs. The classification has been shown before in 2.2.4.2, where SWHP employed a lake loop instead of water wells used in GWHP.

2.2.5. Hot reservoir

It is not usual to classify HPs according to the hot reservoir. It is more common to consider the relation between the cold and hot reservoir, which is explained in the next epigraph.

2.2.6. Cold reservoir-Hot reservoir

The types of HPs are usually determined by the combination of the heat source and the heat sink (where the heat is absorbed and where the heat is discharged) [11]. The cold reservoir is employed as heat source, and it may be the air, the ground or water. Depending on the nature of the hot reservoir, there are two possibilities: air or water, according to the objective. For example, air-to-water HP transfers heat from ambient air, which is used as cold reservoir, to water for space heating (radiators or an under floor heating system) or for domestic sanitary hot water [12]. On the other hand, air-to-air HP works transferring heat from the air outside to inside the building, where it is distributed by moving air. In the same way there are other systems [13]: ground-to-water, ground-to-air, water-to-water and water-to-air. It is observed

that this nomenclature is more used in the commercial sector, though it can also be found in scientific papers. In the commercial sphere there may also be found combinations like sun-water and sun-air, when a solar collector is used to obtain the heat [14].

3. Micro-cogeneration

Micro-cogeneration, also termed Micro-Combined Heat and Power (MCHP) or residential cogeneration, is a technology that has the ability to produce both useful thermal energy and electricity from a single source. Fuel is used more efficiently (Fig. 3), as a heat exchanger recovers waste heat from the engine and/or exhaust gas to produce hot water or steam [15].

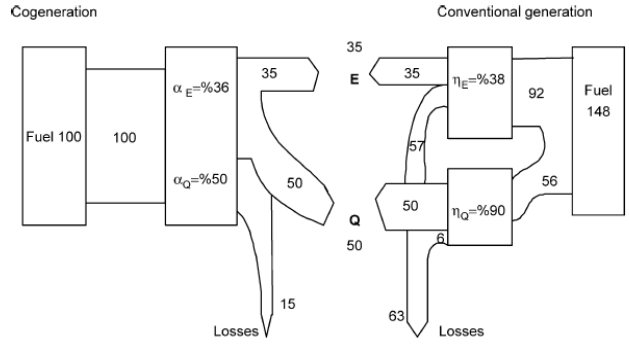

α_E, part of the energy transformed into electricity in a cogeneration unit.

α_Q, part of the energy transformed into usable heat in a cogeneration unit.

η_E, electrical yield of an electrical power plant (electricity production only).

η_Q, yield of a boiler (heat production only).

E, electricity demand.

Q, heat demand.

Fig. 3. Difference of primary energy consumption required for producing the same amount of heat and power using conventional fossil fuel fired electricity generation and boiler system compared to a cogeneration system [14].

The small-scale implementation (<10kW) or cogeneration is a solution that provides all the advantages of cogeneration, as controlled and predictable energy savings and emissions, energetic decentralization, supply security, etc [16].

3.1. Micro-cogeneration classification

A variety of types of cogeneration systems are commercially available (Table 1). The choice of the system depends on factors such as the demand of power and thermal energy, the choice of prime mover, capital installation and maintenance, etc. Some systems have been developed for micro-cogeneration, and their actual conditions are shown in Table 2.

Table 1. Cogeneration technologies [17].

Cogeneration Technology		
Combined cycle gas turbines	Steam turbine plants	Stirling engines
Steam condensing extraction turbine	Gas turbines with recovery boilers	Steam engines
Internal combustion engines	Microturbines	Fuell cells
		Organic Ranking cycles

Table 2. Status of micro-cogeneration technologies [18].

Technology	η_E (%)	η_Q (%)	η_T (%)	Minimal load (%)	T (ºC)	Noise (dB)	Fuel
Gas turbine	15-35	40-59	60-85	75	450-800	62-75	Natural gas
Alternative internal combustion engines	25-45	40-60	70-85	50	300-600	52-56	Gas, diesel, biofuel
Stirling engines	25-50	40-60	70-90	50	300-600	56	All
Fuel cells	35-55	40-60	70-90	No limit	250-550	Low	H_2

η_E: electric yield; η_Q: thermal yield; η_T: total yield; T: temperature

3.1.1. Reciprocating internal combustion engine

Reciprocating internal combustion engines are classified by their method of ignition: compression ignition (Diesel) engines and spark ignition (Otto) engines. Spark ignition engines are used typically for micro-cogeneration due to their heat recovery system producing up to 160°C hot water compared to diesel engines, where the temperature is often lower. Their efficiencies range from 25 to 45%. The main advantage is that their technology is mature and well-understood. It can be designed for different fuels but it needs frequent maintenance. On the other hand, as this technology burns fossil fuel there are emissions of pollutants such as oxides of nitrogen (NOx), carbon monoxide (CO), and volatile organic compounds (VOCs—unburned, non-methane hydrocarbons).

3.1.2. Micro-turbines

The basic components are the compressor, turbine generator and the recuperator. The thermodynamic process involves the pressurization of intake air by the compressor. The compressed air and a suitable fuel are mixed and ignited in a combustion chamber. The resulting hot combustion gas expands turning the turbine, which drives the compressor and provides power by rotating the compressor turbine shaft. With the recuperator, the hot exhaust gas helps pre-heat the air as it passes from the compressor to the combustion chamber. This increases the efficiency of the system. At first, micro-cogeneration competes with HP technologies but actually they may complement each other. For example, the remaining electricity generated from micro-cogeneration system is to meet a portion of the heating and cooling needs through the use of HPs. Ehyaei et al. [19] show how the excess electricity generated by the micro-turbines can to be used in a HP. This technology offers a high-grade of waste heat and other advantages such as a compact size, low weight, low maintenance requirements and lower noise. However, in the lower power ranges, reciprocating internal combustion engines have higher efficiency. It also produces pollutants (but in minor amount than the reciprocating internal combustion engine) as NOx, CO and unburnt hydrocarbons, and insignificant amounts of SO_2.

3.1.3. Fuel cells

Fuel cell technology is an emerging technology with a potential for cogeneration applications and is currently being developed for use in residential applications (3-10 kW). It can run independently or in parallel to a power grid [20]. The electrochemical reaction of hydrogen and oxygen in the presence of an electrolyte produces electricity without combustion and mechanical work. Water and heat are the only byproducts. Fuel cells normally run with hydrogen but can also be used with natural gas, propane or other fuels by external or internal reforming or through the electrolysis of water too. The advantages include low noise level, potential for low maintenance, low emissions and potential to achieve an overall efficiency of 85–90% even with small units. The fuel cell is the most promising technology and gradually becomes available, but it still has a problem with its high cost and relatively short lifetime.

3.1.4. Stirling engine

Stirling engine is an *external* combustion engine operated on the Stirling cycle, not totally developed yet. The cycle consists on four internally reversible processes in series: isothermal compression at constant temperature, constant-volume heating, isothermal expansion at constant temperature, and constant-volume cooling. The Stirling cycle engine can use different types of renewable sources of energy including biomass, solar and geothermal energy [21], so it offers opportunities for high efficiency with reduced emissions. It can be operated with a wide variety of fuels, the maintenance may be low and the life is usually long.

The major disadvantage is its high cost. Stirling engines can be classified according to their arrangement: the Alpha, Beta and the Gamma. This technology and fuel cell for cogeneration systems seem promising for residential and small-scale commercial applications.

4. Conclusions

HPs offer an energy-efficient and economical alternative to HVAC (Heating, Ventilating and Air Conditioning) systems for residential applications. According to recently published European legislation, HP can be considered as a renewable energy technology, since it is based on the essential feature of these unlimited sources, such as the water, air and ground. The micro-cogeneration is an emerging technology that produces useful thermal energy and electricity from a single resource of fuel, in the same place of consumption or close to it. Even though HP and micro-cogeneration technologies require less than conventional devices, they do require energy, usually obtained from the power distribution system where fuel is mainly converted to electrical energy at power plants and the waste heat is discharged to the environment. So it is not exactly correct to state that they are renewable energy technologies. For example in Spain, renewable companies offer geothermic energy for building, but generally is a "false" geothermal energy because it uses solar energy absorbed from the ground surface. Real geothermal energy uses the thermal energy stored into the Earth. Nevertheless, they are really efficient technologies that could involve a great change in the current power distribution system of centralized generation and could give way to distributed generation. This will minimize energy losses due to electrical transmission and distribution system. These will allow having fuel conversion systems close to consumption points, and energy efficiency could become higher. In addition, the waste heat of fuel combustion can be recovered by approximately 80%.

Considering the electrically driven HP technology within power distribution system of distributed generation and renewable supply like photovoltaic solar energy will be a great choice. This may be an alternative for Europe since their solar energy potential [22], especially of Southern Europe.

According to the Spanish regulation, the technologies presented are a good alternative. Moreover, these technologies provide a chance to change the current power distribution system (based on large electrical generation plants far from consumption points) by becoming a generation system where the electricity is generated and consumed in the same site or nearby. The distributed generation has the potential to reduce losses due to electrical transmission and distribution inefficiencies and to alleviate utility peak demand problems.

The possibilities of these technologies that use renewable energy suppose a great chance. The CHP (Combined Heat and Power) plants can be integrated with other fuels/technologies such as biomass, geothermal energy or solar collectors. But this makes no sense outside a bioclimatic construction field.

References

[1] EU, Directive 2010/31/EU on the energy performance of buildings, Official Journal of the European Communities L153, 2010, pp. 13-35.

[2] N. Pardo, A. Montero, J. Martos, J.F. Urchueguía, Optimization of hybrid – ground coupled and air source – heat pump systems in combination with thermal storage, Applied Thermal Engineering, 30, 2010, pp. 1073-1077.

[3] EU, Directive 2002/91/EC on the energy performance of buildings, Journal of the European Communities L1, 2002, pp. 65-71.

[4] EU, Directive 2009/28/EC on the promotion of the use of energy from renewable sources, Official Journal of the European Communities L140, 2009, pp. 16-62.

[5] L. Aye, W.W.S. Charters, Electrical and engine driven heat pumps for effective utilisation of renewable energy resources, Applied thermal engineering, 23, 2003, pp. 1295-1300.

[6] M.J. Moran, H.N. Shapiro, Fundamentals of engineering thermodynamics, Wiley, 5th edition, 2006.

[7] L. Chen, N. Ni, C. Wu, F. Sun, Performance analysis of a closed regenerated Brayton heat pump with internal irreversibilities, International Journal of Energy Research, 23, 1999, pp. 1039-1050.

[8] O. Ozgener, A. Hepbasli, A review on the energy and exergy analysis of solar assisted heat pump systems, Renewable & Sustainable Energy Reviews, 11, 2007, pp. 482-496.

[9] J. Ji, G. Pei, T. Chow, K. Liu, H. He, J. Lu, C. Han, Experimental study of photovoltaic solar assisted heat pump system, Solar energy, 82, 2008, pp. 43-52.

[10] H. Yang, P. Cui, Z. Fang, Vertical-borehole ground-coupled heat pumps: A review of models and systems, Applied energy, 87, 2010, pp.16-27.

[11] HPs as a renewable energy (in Spanish), *El instalador* magazine, 458, 2008, pp. 5-8.

[12] Toshiba, Air to water heat pump system, (available at http://www.toshiba-aircon.jp).

[13] A. Pither, N. Doyle, UK Heat Pump Study, 2005 (available at Energy Efficiency Partnership for Homes, http://www.eeph.org.uk).

[14] H.I. Onovwiona, V.I. Ugursal, Residential cogeneration systems: review of the current technology, Renewable and sustainable energy reviews, 10, 2006, pp. 389-431.

[15] M. Goodell, About the Renewable Energy Institute, Climate Science & America's Clear and Present Danger, 2010 (available at http://cogeneration.net/).

[16] D. Arzoz del Val, Energy saving in buildings by small-scale cogeneration (in Spanish), *El instalador* magazine, 466, 2009, pp. 70-72.

[17] European Commission, Reference Document on Best Available Techniques for Energy Efficiency, Institute for Prospective Technological Studies (IPTS), 2009.

[18] Energylab, Electricity micro-cogeneration: concepts, typology and results (in Spanish), Plenary Conference on the Electricity micro-cogeneration Seminar, 2010.

[19] M.A. Ehyaei, M.N. Bahadori, Selection of micro turbines to meet electrical and thermal energy needs of residential buildings in Iran, Energy and Buildings, 39, 2007, pp. 1227-1234.

[20] US Fuel Cell Council, www.usfcc.com.

[21] D. Scarpete, K. Uzuneanu, N. Badea, Stirling Engine in Residential Systems Based on Renewable Energy, (available at http://www.wseas.us).

[22] M. Šúri, T.A. Huld, E.D. Dunlop, H.A. Ossenbrink, Potential of solar electricity generation in the European Union member states and candidate countries, Solar Energy, 81, 2007, pp. 1295–1305(available at http://re.jrc.ec.europa.eu/pvgis/).

Study on the performance of air conditioning system combining heat pipe and vapor compression based on ground source energy-bus for commercial buildings in north China

Yijun Gao, Wei Wu, Zongwei Han, Xianting Li*

Tsinghua University, Beijing, China
** Xianting Li. Tel: +86 01062785860, Fax: +86 01062785860, E-mail: gaoyj08@mails.tsinghua.edu.cn*

Abstract: After introducing the application status and problems of geothermal air conditioning system in China, a new kind of ground source air-conditioning system (EBCS) is put forward. The system consists of distributed air-conditioners combining heat pipe and vapor compression, fresh air handling unit with large enthalpy difference and ground source water loop. Geothermal energy is transported to the combined air-conditioners for heating and cooling by water loop. The combined air-conditioner can be operated at heat pump condition or heat pipe condition for air conditioning. In winter and transition season, the cooling energy in ground can be directly used for the cooling in inner zone by heat pipe mode, while the recovered heat is used for heating in peripheral zone.

To analyze the performance of proposed system, a commercial building in north China has been taken as the research object, and the annual energy use is simulated. It is shown that the new system can save 21.7% energy compared to the traditional ground source heat pump system, and may be a potential air conditioning system for commercial buildings in north China.

Keywords: *Building energy efficiency, Ground source, Heat pipe, Water loop, fresh air handing unit, air conditioning.*

1. Introduction

The ground source heat pumps (GSHP) are widely used in China. The building areas that use this system exceed 10,000,000 m^2 in 2008, and it continues to keep a rapid growth [1]. The ground source heat pump is a heating and air-conditioning system which uses the shallow geothermal energy on the surface of the earth. The shallow geothermal energy is regarded as a renewable energy source [2]. In summer, the soil temperature is lower than the ambient temperature, which contributes to improve the COP of heat pumps. At the same time, the waste heat of buildings in summer can be stored in the soil to supply heat in winter. Thus, heat is transferred over seasons. The waste building heat rejected in summer and the primary energy demands for heating in winter are decreased greatly, which is good for environment protection. However, the COPs, especially the cooling COPs of many GSHP projects in China are proved to be not higher, or even lower than that of the traditional water-cooled systems with cooling towers. The existing problems in the GSHP systems are analysed and a novel central air conditioning system using geothermal energy is put forward.

2. Analysis on the existing problems in traditional GSHP systems

The traditional GSHP system consists of cooling water pumps, underground heat exchanger, heat pump unit, chilled and hot water pumps and terminal fan-coil units. The GSHP produces chilled water in summer and hot water in winter which is then transported to terminal fan-coil units to realize cooling and heating. At the same time, cooling water, the heat and cold source of the GSHP unit, is transported through underground heat exchanger. In this way, the ultimate energy transfer of the system is realized.

The main problems of traditional GSHP systems are listed as follows:

1) The centralized producing chilled water and hot water in summer and winter increases the energy transfer links of systems. So the improvement of COP is restricted. Besides, it is very common that the COP of heat pump is low under partial load, which leads to huge energy use.

2) In order to transport chilled water and hot water, the energy use of water circulating pumps of GSHP system is very high.

3) In the existing GSHP systems, usually, the switch of cooling and heating is realized by switching the cooling water circulation. The control is difficult because of the complexity of cooling water systems. In winter and transition season, when the cooling and heating is demanded simultaneously, it needs to produce both chilled and hot water.

How to improve the COP of GSHP systems? Based on the analysis above, some factors below should be taken into consideration.

Firstly, the centralized chilled and hot water should be cancelled. Cold or heat in cooling water can be transferred to the room air directly by distributed terminal cooling and heating units. So the energy transfer links are reduced, and the chilled and hot water pumps are cancelled. Consequently, the energy use of water pumps is reduced. On the other hand, the advantage of flexible adjustment of distributed terminal units can improve the cooling and heating COP under partial load.

Secondly, make the best use of the low temperature advantage of geothermal energy. The shallow soil temperature is lower than the demanded room temperature most of the year. So, it will obviously reduce the cooling energy use of a compressor if the temperature difference is used for natural cooling. But the system must be able to flexibly switch between natural cooling and compression refrigeration. When the natural cooling mode cannot meet the demand, it can easily be changed to compression mode.

3. Introduction of the new energy-bus air conditioning system

A new energy-bus central air conditioning system (EBCS) based on ground source is proposed according to the analysis above.

3.1. Composition construction and key equipments of EBCS

The new system, which is put forward by Xianting Li et al [3], professor of Tsinghua University, consists of water loop, water-cooled air conditioners combined with heat pipe, and fresh air handling unit with large enthalpy difference. The cooling water is transported to the terminal air-conditioners combined with heat pipe and fresh air handing units for heating, cooling by the water loop. The terminal air-conditioners combined with heat pipe can realize natural cooling in heat pipe mode or vapour compression cycle in heat pump mode depending on the water loop temperature. The fresh air handing unit with large enthalpy difference has a strong ability of dehumidification, which makes it capable of carrying much more building latent heat load in summer. The key equipments are introduced as follows.

Cooling-only type terminal unit with natural cooling function

The schematic diagram is showed as *Figure 1*. It combines the compression refrigeration circulation and separated heat pipe technique, which can realize switching between the two operating modes. When there is a temperature difference between the water loop and the room air, the compressor can stop working and the heat pipe starts to operate natural cooling circulation. When the water loop temperature is higher than the room air temperature, the

vapour compression refrigeration mode is activated. This unit is suitable for buildings with inner zones that need cooling throughout a year.

Heat pump type terminal unit with natural cooling function

The schematic diagram is showed as *Figure 2*. Compared to the cooling-only type unit, there is an additional four-way valve in heat pump type unit. Thus, the compressor is able to produce heating. So this unit can meet the demand of cooling as well as heating in the peripheral zones all year round.

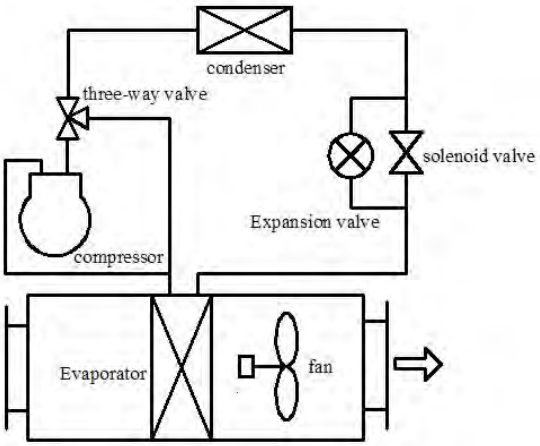

Figure 1 Cooling-only type terminal unit with natural cooling used in inner zone

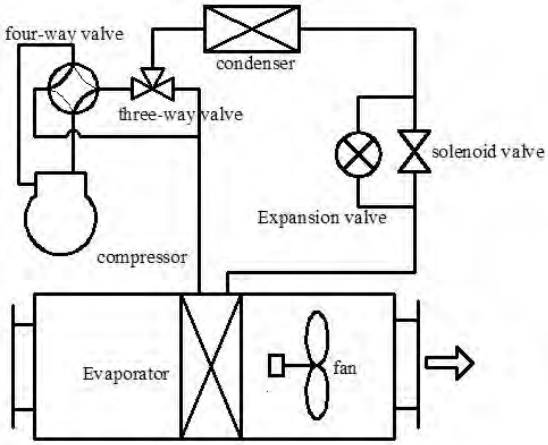

Figure 2 Heat pump type terminal unit with natural cooling used in peripheral zone

Direct evaporative fresh air handing unit with large enthalpy difference

The schematic diagram of direct evaporative fresh air handing unit with large enthalpy difference is showed as *Figure 3*. With the sensible heat exchanger, this unit can realize the sensible heat exchange between the fresh air handled by evaporator or condenser and non-handled fresh air. So the fresh air can be pre-cooled and the refrigeration system mainly carry the latent heating load in summer, which consequently reduces the energy use of the fresh air handling system. In winter, the non- handled fresh air can be pre-heated by the handled hot fresh air so as to solve the problem that compressor cannot work because of too low condensation pressure. It makes sure that the system can still work normally in cold weather.

Compared with the traditional fresh air unit, the fresh air handing unit with large enthalpy difference has a strong ability of dehumidification. So the fresh air handling unit is used to carry the latent load while the heat pipe combined air-conditioner is used to undertake the sensible heat load.

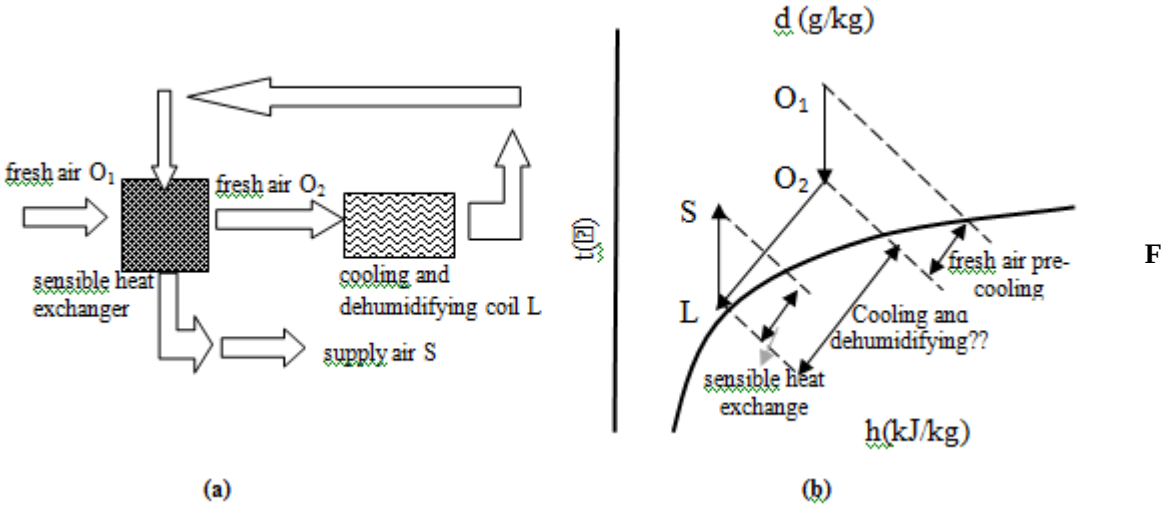

Figure 3 Direct evaporative fresh air handing unit with large enthalpy difference the schematic diagram (b) the psychrometric chart of air handling process notes : O_1 is the outdoor air condition, S is supply air condition Example in chart has no dehumidifying

3.2. The working principals of EBCS

In cooling season, the water-cooled air conditioners combined with heat pipe can realize switch between heat pipe mode (natural cooling) and air conditioning mode. At the beginning of cooling season, the soil temperature is low and the building load is small. So the terminal units can completely provide natural cooling under heat pipe mode. The heat is released to water loop and then stored in the soil through underground heat exchanger. When the heat pipe mode is insufficient to meet the cooling demand and the room temperature is higher than the maximum set value, the air conditioning mode is activated. When the room temperature is lower than the minimum set value, the compressor stops working and the heat pipe mode is activated. The switch between two operating modes can greatly reduce the compressor's working time.

In winter, the natural circulation of heat pipe mode is operated for cooling in the inner zones while the heat pump mode is operated for heating in the peripheral zones. If there is an unbalance between heat released to the soil and absorbed from it, heat compensation is needed. So this system can also recover the waste heat of inner zones for heating.

4. Energy saving and economic analysis of the new system

In order to evaluate the energy saving potential of the new system, a building model is built to simulate the annual energy consumption of the system which starts to operate from the summer cooling term. And then the energy use of the EBCS system and a traditional GSHP system are compared. Beijing, with a year average temperature of 11.4 ℃, is chosen as the simulation city. Both the EBCS and traditional GSHP system use underground heat exchangers as cold and heat source.

4.1. Building model

The building model is obtained from a research office building in Beijing after suitable simplification. There are 5 floors, and the drawing of standard floor is showed as *Figure 4*.

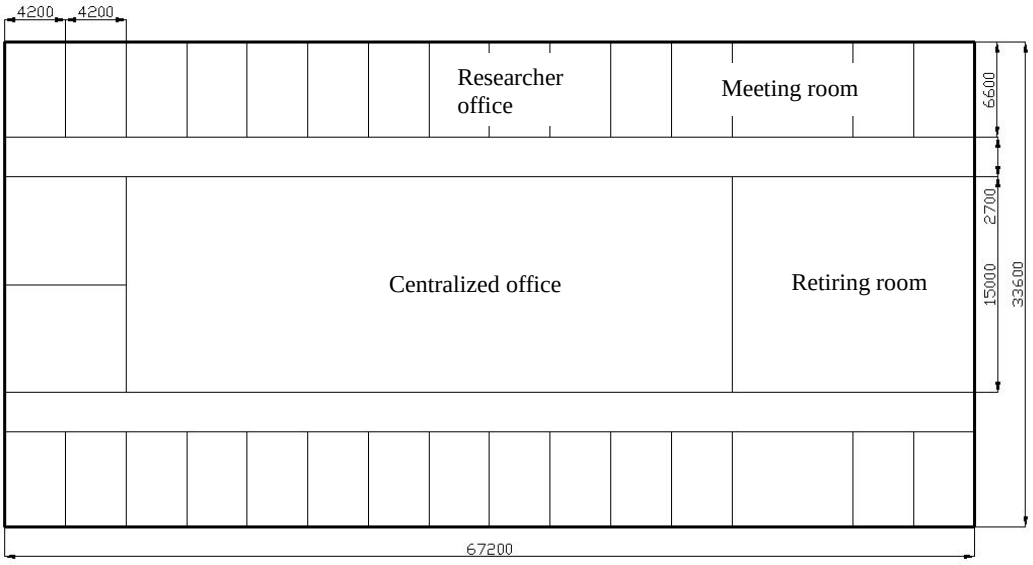

Figure 4 Standard floor of the building model

The area of each floor is 2258 m^2 and the total building area is 11290 m^2. The heat transfer coefficient of outside wall and roof is 0.8 W/m^2·K.The windows are doble-glazed with a 12 mm air layer and its heat transfer coefficient is 3.9 W/ m^2·K. The shading coefficient of the window is 0.83 and the inner shading is used. The window-wall area ratio is 0.65 in the south and north side and 0.9 in the east and west side.

The average minimum fresh air flow rate for each person in the building is 30m³/h. The room temperature is set within 24~26℃ in summer and 20~24℃ in winter. The software DEST-c is used to calculate the whole year hourly building load [4]. The calculation results are showed as *Table 1* and *Table 2*.

Table 1 The total building load

	Load
peak heating load	730.4(kW)
peak cooling load	895.3 (kW)
annual accumulated heating load	787.4 (MWh)
annual accumulated cooling load	844.3(MWh)

Table 2 The peak load of typical room

Typical room	area (m^2)	peak room cooling load (kW)	fresh air cooling load (kW)	peak room heating load (kW)	fresh air heating load (kW)
centralized office in inner zone	630.00	52.68	29.29	-4.90	29.17
office in outer zone	27.70	1.75	0.93	2.05	0.66

Notes: the humidification load is not included.

4.2. Simulation method for the energy use

The GSHP unit, fan-coil unit, fresh air handling unit, air conditioners combined with heat pipe and circulation water pump are chosen based on the total building load and peak cooling and heating load of typical room. The underground heat exchanger is designed to have 105 pipes with a 5.5 m interval and an 80 m depth. The U-bend heat exchanger is used in the simulation. Usually, the average transferring heat per unit of borehole depth is about 56w/m in Beijing. The U-bend is regarded to be equivalent to a vertical single pipe, and is numerically discreted by the inner node control volume method [5].

The method to calculate the energy use of GSHP unit or air conditioners combined with heat pipe is as follows [6] [7]:

$$N_c = \sum \frac{Q_{ci}}{EER_i} + \sum \frac{Q_{hi}}{COP_i} \quad (1)$$

Where N_c is the electricity consumption of GSHP unit or air conditioners combined with heat pipe, kWh. Q_{ci}, Q_{hi} is the building cooling load and heating load respectively in hour i, kWh. EER_i, COP_i is the energy efficiency ratio of GSHP unit/ air conditioners combined with heat pipe unit respectively in hour i.

The method to calculate the energy use of fans is as follows:

The total electricity consumption of fans in each system includes fan consumption in fresh air unit, fan-coil and air conditioners combined with heat pipe unit.

$$N_f = N_m \times \tau \quad (2)$$

Where N_m is the rated power of fans which are chosen based on the peak cooling load. τ is the annual running time of the air-conditioning system.

The method to calculate the electricity consumption of water pumps is as follows:

$$N_s = \sum N_w \times n_i \quad (3)$$

Where N_w is the rated power of a water pump. 3 chilled water pumps, 3 cooling water pumps and 3 hot water pumps are chosen with 2 in usage and 1 as backup. The selection of pumps is based on the peak cooling and heating load in the whole year. n_i is the number of pumps that should run in hour i.

4.3. The simulation results for annual energy use

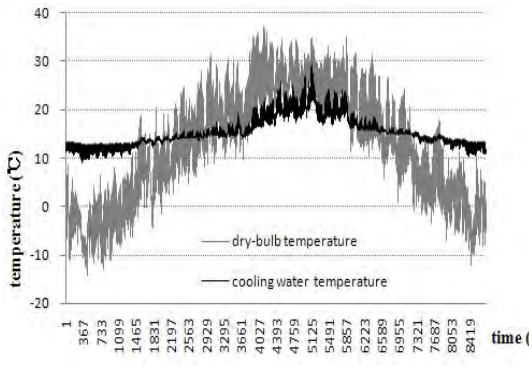

Figure 5 Hourly dry-bulb temperature and cooling water temperature

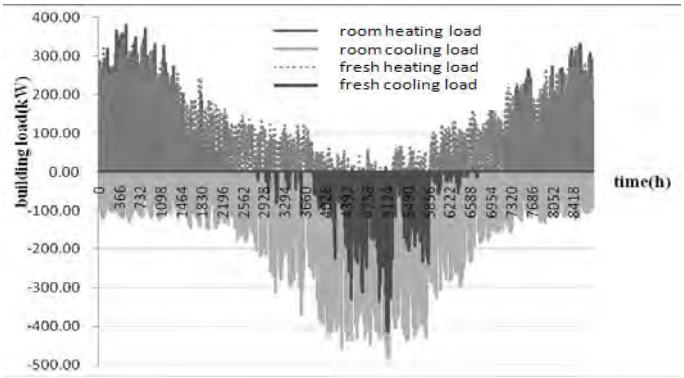

Figure 6 The calculated hourly building load for the whole year

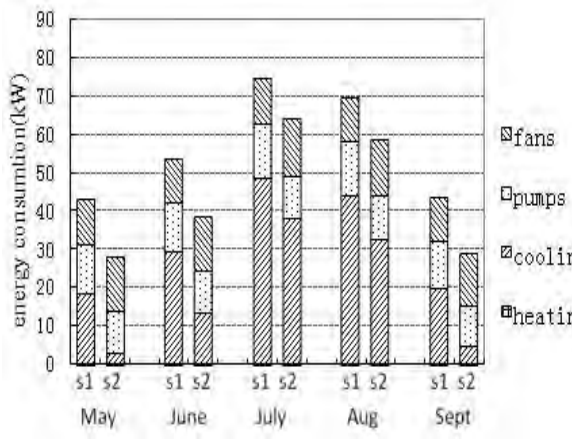

Figure 7 The comparison results of system energy use in summer

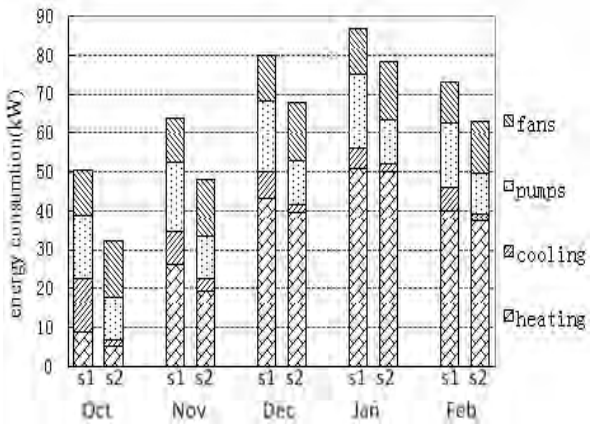

Figure 8 The comparison results of system energy use in winter and transition season

Notes: "s1" represents the GSHP and "s2" represents the EBCS, "heating" is the electricity consumption of compressors and in the GSHP and EBCS for heating, and "cooling" is the electricity consumption of compressors and heat pipe fans in the GSHP and EBCS for cooling.

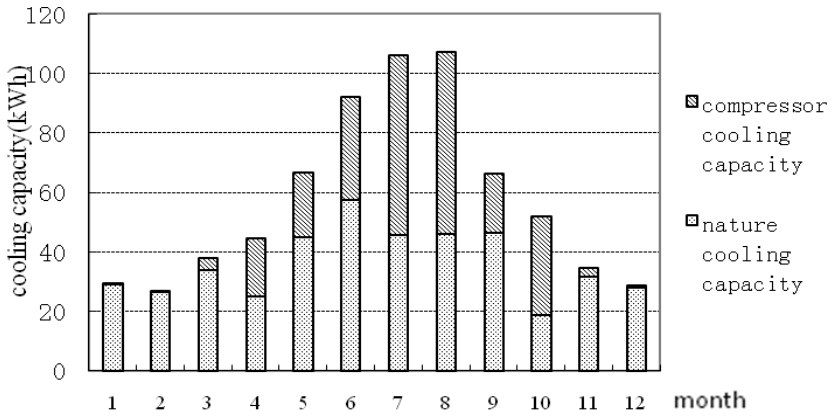

Figure 9 The annual accumulated natural cooling capacity analysis

From the energy use comparison, it can be concluded that:

1) The energy saving potential of EBCS is 21.7% compared to the traditional GSHP system. In EBCS, the air conditioners combined with heat pipe and water pumps use less energy while the fans use a little more energy.

2) Air conditioners combined with heat pipe contribute the most of energy saving because of natural cooling. With the heat pipe, the natural circulation mode can undertake almost all the cooling load in winter and transition season. Even in summer, it can undertake more than 30% cooling load. In the whole year, the natural circulation mode undertakes more than 60% cooling load totally.

3) In heating season, the EBCS has an obvious energy-saving advantage under partial load. It indicates that decentralized heating terminal units have higher energy efficiency at partial load.

4) Since the chilled and hot water pumps are cancelled in the EBCS, the annual electricity consumption of pumps is 30% lower in EBCS, even if the water head of pumps are higher than the cooling pump in the GSHP system.

5. Conclusions

The existing problems of the traditional GSHP systems are analyzed. A novel central air conditioning system based on ground source is proposed. The new system consists of decentralized terminal air conditioners combined with heat pipe, fresh air handing unit with large enthalpy difference and water loop. The chilled and hot water systems are cancelled. And the cooling water is transported to the terminal air-conditioners and fresh air handing units for heating and cooling by water loop. The air conditioners combined with heat pipe have two operating modes: natural cooling circulation and heat pump mode (compression refrigeration/heating). The air conditioners can switch between these two modes. The fresh air handing unit with large enthalpy difference has a strong ability of dehumidification, so it can be used to undertake the major latent load.

Based on the theoretical analysis, the annual energy consumption of an office building in Beijing is simulated. The calculation results show that EBCS can reduce much energy consumption for cooling compared to the traditional GSHP system. That's because the new system can realize natural circulation which can undertake 60% of the annual cooling load in the whole building. At the same time, EBCS also has obvious energy saving advantage in heating and transportation (pumps and fans) consumptions. The total energy saving potential in the whole year can reach 21.7%. Besides, the system form is simple and the control is easy. The terminal units can flexibly realize cooling and heating depending on the room demand, the same as the four-pipe type system. All this advantages can better ensure the temperature and humidity comfort all year round with much less energy use.

References

[1] W. Yang, J. Zhou, W. Xu, and G, Zhang. Current status of ground source heat pump in China. Energ. Policy, vol. 38, 2010: 323-332.

[2] Tao Meng. Yanqing Di, Li Liu, et al. Research of ground heat balance of ground source heat pump. 2009 International Conference on Energy and Environment Technology, 2009: 777-781.

[3] Xianting Li, Yijun Gao, Zongwei Han, et al. A new central air conditioning system combining heat pipe and vapor compression based on energy-bus. HEATING VENTILATING & AIR CONDITIONING, Vol.41, No.2, 2011: 1-6.

[4] Chen Feng, Deng Yuchun, Xue Zhifeng and Wu Ruhong. Toolpack for building environment simulation. HEATING VENTILATING & AIR CONDITIONING, Vol.29, No.4, 1999: 58-63.

[5] Zongwei Han, Maoyu Zheng, Fanhong Kong. Simulation research on solar-assisted ground source heat pump heating system with seasonal soil thermal storage in severe cold area. ACTA ENERGIAE SOLARIS SINICA. Vol.29, No.5, 2008: 574-580.

[6] Liu Tianwei, Du Kai. Research on the energy saving of water loop heat pump system applied to office buildings. HEATING VENTILATING & AIR CONDITIONING, Vol.40, No.3, 2010: 63-67.

[7] Huang Bing,Yang Chang-zhi. Resarch on simulation and economic assessment of ground source heat pump system. FLUID MACHINERY, Vol.38, No.1, 2010: 75-80.

Economic performance of ground source heat pump: does it pay off?

Laura Gabrielli[1,*], Michele Bottarelli[2]

[1] *University of Ferrara, Italy*
[2] *University of Ferrara, Italy*
** Corresponding author. Tel: +39 0532 293671, E-mail: laura.gabrielli@unife.it*

Abstract: A DCF model (discounted cash flow model) is implemented in order to investigate the economic aspects of GSHP (ground source heat pump) for heating and cooling, in comparison to traditional CB (condensing boiler). The DCF model allows the analysis of investment costs, operating costs and revenues of the two different systems in order to understand if the GSHP outperform its conventional counterpart in coming years, explicitly taking account for factors as price/cost growth. The whole analysis is performed adopting a parametric approach, in which all the previous terms are linked to energy labels, degree-days and EMRs (Energy Mix Ratios), the latter obtained as ratio between the full unit cost of electricity and natural gas paid by the householder. Relating to different EMRs, the DPBPs (Discounted Pay Back Periods) are presented in decision support matrixes in which energy labels and degree-days are the row/column variables, to confront the benefits of choosing between GSHP versus CB. Some considerations are also presented in order to express the environmental aspects. The results show that all higher energy labels have a good profitability ratio between costs and payback periods and demonstrate that GSHP system does pay off. Lower labels become interesting when the EMR drops to 0,25 and the gas price goes up 0,70 €/Nm^3.

Keywords: *ground source heat pump, discounted cash flow models, energy mix ratio, decision support matrixes*

1. Introduction

Heat pumps (HPs) are a reliable technology for space heating and cooling in commercial, industrial and residential buildings. In ground source heat pumps (GSHPs), the ground is used as heat source or sink; when compared to external air, it has smaller temperature variations during both heating and cooling season, and more advantageous thermal properties. For these reasons, GSHPs become an attractive alternative to conventional heating and cooling systems [1], owing to their higher energy utilization efficiency and reduction in greenhouse gases emission [2]. Economic evaluations were approached to exploit low temperature geothermal energy for buildings. In [3], the net present value is developed, showing a payback period of just a few years. Here, a discounted cash flow model (DFC) is implemented to assess the payback period for a GSHP application in comparison to traditional condensing boiler (CB), where the ground heat exchanger is the horizontal flat panel presented in [4].

2. Methodology

The goal is to calculate the payback period for a ground GSHP versus a CB, in connection with degree-days and energy building labels. The climate aspect and energy label are taken from the Italian law, but they can be easy extended to any other country setting different degree-days and energy requirements. To define the climate condition, a function was performed for the time series air temperature. Calibrating this function to obtain specific degree-days, it was possible to consider different climate zones. For both air conditioning systems it is supposed the same indoor distribution plant working at the same fixed low temperature (44 °C), keeping the analysis free from this part. The GSHP is supposed a vapor compression type heat pump coupled to a horizontal ground heat exchanger (Fig. 1). The CB is taken as boiler with high performance. For the GSHP, the coefficient of performance (COP) basically depends from the temperature at the evaporator, if the temperature at the condenser is taken fixed, like in this case. Anyway, the evaporator temperature is depending from the climate and the thermal behaviour of the HGHE and surrounding soil, so that this last

behavior is the key to approach correctly the problem. A solution for the HGHE behaviour was fund implementing a numerical model in unsteady state, and adopting a combination of degree-days and energy requirements. The results was achieved forcing the behavior of an exchanger five meters long to reach on average 0 °C in the ground surrounding the exchanger, to exclude groundwater icing. The combination between degree-days and maximum power for exchanger unit length represents the limit that each other combination must respect. So, all the other cases were gathered as different combinations among climate zones and energy requirements. The thermal analysis has made all the results for next economic valuation. Here, installation and operation costs were considered to achieve a full price for unit building volume. The economic analysis was performed adopting different ratio between the full unit cost of natural gas and electricity, and their potential trend, to link the payback and pay off to an energy mix ratio (EMR). In the following sections, the former steps are reported to explain the approach.

2.1. Building energy requirements and thermal behaviour

The Italian law defines the limit for building energy requirements in heating (EP_i), according to a country classification in seven degree-days climate zones (*A,B,C,D,E,F*), and to a building shape ratio (*S/V*). Moreover, the daily heating time is defined for each climate zone, but its observance is difficult to verify. The energy labeling weights the limit energy requirements to define eight energy classes (a^+,*b,c,d,e,f,g*), adopting *K* factors from 0,25 to 2,50 applied to EP_i. Generally, the heat exchange power ($\delta q_V/dt$) in steady state and for unit volume can be estimated for a given thermal difference *dT* occurred in time step *dt*, as:

$$\frac{\delta q_V}{dt} = \frac{1}{V}\frac{\delta Q}{dt} = U \cdot \frac{S}{V} \cdot dT \tag{1}$$

If its integral is extended to the full heating season, the product between *dT* and *dt* would represent the degree-days (*dd*) multiplied by the daily heating hours (*hh*). If as q_V it is taken $K*EP_i$ for a given climate zone and shape ratio, the previous transmittance would give the global behaviour of the whole building, inclusive of all heat exchanges (heat transfer through shell, air ventilation, free heating, …). So, it could be assumed as all-inclusive *"equivalent transmittance"*, and estimated as:

$$\overline{U} = \frac{EP_i}{\frac{S}{V} \cdot dd \cdot hh} \tag{2}$$

The former definition becomes usefully to approach heat transfer in a closed thermodynamic system by lumped parameters. Here, the building could be simplified in a homogenous body, whose internal energy variation occurs owing to the heat transfer belong its shell. The global mass is basically express only from walls, roof and foundation, because the air contribute is absolutely marginally. Knowing the building volume (*V*), the average density (ρ) and specific heat (*c*), and the ratio (*r*) between plenum over building volume, the integral of the energy balance between two time step becomes easy to do, assuming the air temperature independence from this heat exchange:

$$r \cdot \rho \cdot V \cdot c \cdot dT = -\overline{U} \cdot S \cdot \left(T - T^{air}\right) \cdot dt \quad \Rightarrow \quad \int_{T_0}^{T} \frac{d(T - T^{air})}{T - T^{air}} = -\int_{t_0}^{t} \frac{\overline{U} \cdot S}{r \cdot \rho \cdot V \cdot c} \cdot dt \tag{3}$$

where T_0 is the indoor air temperature at time step t_0. The indoor temperature becomes also:

$$T = T^{air} + \left(T_0 - T^{air}\right) \cdot e^{-\frac{\overline{U} \cdot S \cdot (t - t_0)}{r \cdot \rho \cdot V \cdot c}} \tag{4}$$

When the air conditioning plant is turned off, the function (4) calculates the indoor air temperature in time related to the changing outdoor air temperature. When the plant is switched on, a constant target value for the indoor temperature can be assumed, and the heat of the air conditioning plant can be calculated by the equation (1). For simplicity, we assume the plant is able to reach the target temperature in a single time step. To generalize the climate zones, a time series for air temperature was defined, so that knowing its trend during days and seasons, the degree-days are known and also the energy requirements according to the former equation (4) and (1). The time series was conceptualized as a sinusoidal trend, representing the seasonal temperature variation for daily maximum and minimum temperature, with a smaller sinusoidal oscillation superimposed, representing the hourly temperature variation with a daily time shift. In Fig 4 the air temperature is showed for a whole year; for each other details we remand to [4], where the method is presented.

2.2. Defining the Coefficient Of Performance for the heat pump

According to the previous considerations, the minimum fluid temperature leaving the indoor circulating pump is set to 44°C. Hence, it defines the temperature at the heat pump condenser, which can be supposed only few degrees higher (46 °C) than the first one, to perform suitably the heat exchange during condensation process. Neglecting the superheating after the evaporation and considering irreversibility coefficients to take into account the real processes, the thermodynamic cycle only depends from the temperature at the evaporator, which remain linked to the GHE. Therefore, even the COP only is depending to the fluid temperature leaving the GHE. It shouldn't drop too below 0 °C to exclude groundwater icing problem, and shouldn't go up 25÷30 °C, to limit environmental effects. If we adopt the refrigerant R134a, the thermodynamic cycle is laid in the Pressure-Enthalpy chart, where it is easy to estimate working relationships between enthalpy and temperature. According to the Fig.1 and [5], we have estimated the most important functions for the working temperature supposed at the condenser (46 °C), whose saturated pressure is 1,20 MPa. The compressor work is defined by the adiabatic *12* and then correct with a irreversibility coefficient η_{12}. The heat exchange at the condenser can be calculated knowing h_2 and h_3, and adopting a heat transfer coefficient η_{23}. Here, the performance at the compressor and at the condenser are taken 0,85 both. So, the COP becomes i.e. 4,01/5,35 at 0/10 °C. The expressions are reported in Fig. 2 and hold very high variances (R^2 >0,96).

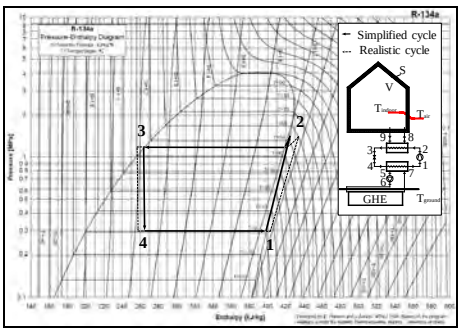

Figure 1: Thermodynamic cycle for R134a (E. Hansen & I. Aartun, NTNU 1999)

Quantity	Temperature at the condenser 46°C
h_1	$-0{,}0013 \cdot T^2 + 0{,}5774 \cdot T + 397{,}3$
h_2	$0{,}0012 \cdot T^2 - 0{,}1988 \cdot T + 426{,}2$
h_3, h_4	265,6
l_{12}	$0{,}0025 \cdot T^2 - 0{,}7762 \cdot T + 28{,}9$
q_{23}	$0{,}0012 \cdot T^2 - 0{,}1988 \cdot T + 160{,}6$
COP^*	$0{,}0012 \cdot T^2 - 0{,}1988 \cdot T + 160{,}4$
COP	$\dfrac{0{,}0012 \cdot T^2 - 0{,}1988 \cdot T + 160{,}4}{0{,}0025 \cdot T^2 - 0{,}7762 \cdot T + 28{,}9}$
	$\eta_{12} \cdot \eta_{23} \cdot COP^*$

Figure 2: Relationships in temperature adopting R134a (ASHRAE Trans., 1988, vol.94)

2.3. Benchmark for geothermal outlet loop temperature

The evaluation of the GHE performance was carried out as reported in [4]. There, the solution was conducted via the implementation of the unsteady-state three-dimensional numerical finite element code FEFLOW®, which allows determining the groundwater flow and temperature fields in saturated/unsaturated porous media, considering both conductive and convective heat transport. The HGHE used herein consists in a flat panel 0.80 m high, 0.02 m wide and 5.0 m long, buried vertically in a trench 6.0 m long, 0.30 m wide and 2.49 m deep. The overall computational domain is subdivided into 23 horizontal layers (Fig. 4) and the groundwater flow was imposed parallel to the HGHE direction with a piezometric gradient of 0,2%. The hydraulic and thermal properties attributed to the different materials constituting the domain (fluid within the panel, backfill, and surrounding soil) are assumed to be homogeneous are typical for sandy silts, bentonitic clay and water, within the ranges usually cited in [4]. Thermal boundary conditions are given at the soil surface in the form of a temperature time series, applying a coefficient at the previous sinusoidal function for air temperature, set to 0,6. The GSHP operation hours are selected to represent frequent working conditions, 5 AM - 9 AM and 5 PM - 10 PM from Monday to Friday, 7 AM - 11 PM on weekends. The heating operation is allowed from October 15th to April 30th, the cooling from June 1st to Septemebr 30th. During on time, the HP is activated in heating/cooling mode to maintain the indoor target temperature (20/26 °C), supplying for each time step the heat estimated according (1) and (4). For simplicity, we assume that this heat and the related power is the same requested at the HGHE, and the compressor works only to raise it to the requested temperature. This hypothesis overrates the heat required from the HGHE for a rate linked to the heat pump COP at the working temperature. The flow rate into the HGHE is calculated for flushing water with 3 °C between the inlet and outlet temperature. To do so, a specific numerical loop was supplied directly from the FEFLOW's producer [6]; this is the most important difference with [4], where the inlet temperature was fixed to 4°C in heating and 35°C in cooling. The resulting temperatures are showed in Fig. 3, with two independent temperatures at 1,4 and 2,5 m deep from soil surface. The minimum temperature at the soil near the inlet reached almost 0 °C at 70th day; no less temperature is accetable without icing problem. It means that no higher power is possible for this configuration, according to initial soil temperature, degree-days, energy requirements and type and length of HGHE. The maximum power was 36 W/m in heating mode for each meter of HGHE; the medium one 27 W/m. The soil volume surrounding the HGHE whose temperature varies by more than 0,5 °C from initial condition is almost 80 m^3.

The run for a full year needed very long computational time (more than six days). To avoid the time for running 29 cases, we examined each configuration according to the previous limit, and assuming the following hypothesis and observations:

1. the maximum heat extractable from the soil for heating time depends from the initial soil temperature and the maximum soil volume involved at same time;
2. the HGHE rate flow depends from the energy balance defined previously;
3. the HGHE outlet temperature for each different case can be estimate scaling the temperature time series resulting from the numerical solution for the limit case, using the difference between the two initial soil temperatures;
4. the difference of soil temperatures between two cases is equal to the difference of the yearly average air temperatures, because the sinusoidal functions are in phase;
5. the major or minor maximum power of a different case requires a proportional HGHE length for getting the same maximum power for unit length of limit case.

So, the heat transfer for each new case *"N"*, only can be equal to that of the limit case *"L"*:

$$c_t\rho_t V_t \cdot \left(\overline{T}_{i,N}^{soil} - \overline{T}_{f,N}^{soil}\right) + c_w\rho_w \dot{V}_N^w \Delta T_e \Delta t_N = c_t\rho_t V_t \cdot \left(\overline{T}_{i,L}^{soil} - \overline{T}_{f,L}^{soil}\right) + c_w\rho_w \dot{V}_L^w \Delta T_e \Delta t_L \quad (5)$$

As the final energy state of the involved soil volume must be the same for both cases, even their final average temperatures must be the same ($\overline{T}_{f,N}^{soil} \equiv \overline{T}_{f,L}^{soil}$), then, recording the phasing $\left(\Delta t_L \equiv \Delta t_N\right)$:

$$\dot{V}_N^w = \dot{V}_L^w + \frac{c_t\rho_t V_t}{c_w\rho_w \Delta T_e \Delta t_L} \cdot \left(\overline{T}_N^{air} - \overline{T}_L^{air}\right) \quad (6)$$

$$T_N = T_L - \left(\overline{T}_N^{air} - \overline{T}_L^{air}\right) \cdot \left(1 - \frac{t}{\Delta t_L}\right) \quad (7)$$

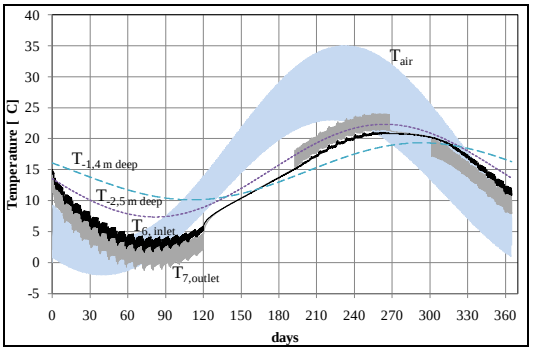

Figure 3: Time series for temperatures

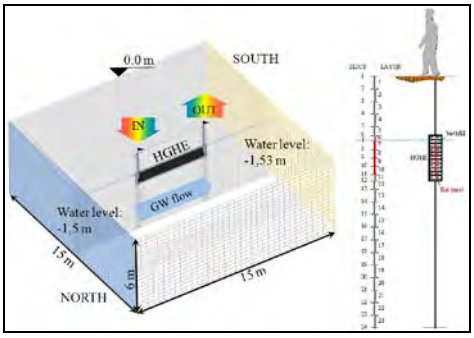

Figure 4: Computational finite elements domain

2.4. Pay back approach in Discounted cash flow analysis

The economic analysis was undertaken using the discounted cash flow (DFC) approach in order to compare the different hypothesis. Typically the investment feasibility calculations are carried out using DCF where all the present and future inflows and outflows are discounted to obtain the net present value (NPV), the internal rate of return (IRR) or the discounted payback period (DPBP). The net present value represents the present value of all incomes and costs during the period of analysis of the investment. If the present value gives us a number larger than zero, then the project can be accepted. If the NPV is negative, the project must be rejected or modified. The IRR is the discount rate that makes the net present value equal to zero, so when the net present value of all costs equals the net present values of all incomes or revenues of the project. Usually the IRR must exceed the cost of capital. The discounted payback period for a project is the time it takes to recover the cost of investment. The cash flows are added up after taking account of the time value of money. The decision is based on comparing the different pay back periods with a predetermined cut off period decided by the decision maker. [7] In our analysis we considered the DPBP in order to verify if the GSHP pays off in comparison to a traditional heating system. To undertake the economic analysis, it needs to identify all the critical variables and assign appropriate values to them based on an analysis of the current market. The variables identified are listed in Tab. 1. Four scenarios (*1*,*2*,*3*,*4*) where tested in order to consider the different cost of electricity and natural gas, which gives us a diverse energy mix ratio (EMR). The energy cost is expected to grow at a rate of 3% per year (in real term), inflation is considered at 2% per year. The rates were extrapolated considering the historical trends in the Eurozone [8]. To discount the future cash flows a weighted average cost of capital approach was used, considering a Debt/Equity ratio of 0.60/0.40; the cost of debt is set at 5% and the cost of equity is assumed at 7%. Sinking

funds formula has been used to build up a sum of money to replace the systems after their usable life. The formula is:

$$a = Ci\frac{r}{q^n - 1} \tag{8}$$

Where *a* is the annual deposit. The final value is used to replace the equipment at the cost *Ci*. All costs were discounted considering an inflation rate plus a growth rate of energy costs, which gave us:

$$C = \sum_{t=1}^{n} \frac{C_t(1+i+g)^t}{(1+r)^t} \tag{9}$$

Where *C* are the costs, *i* is the inflation rate, *g* is the growth rate, *r* is the discount rate. The same approach was used by [3]. The discounted payback period is finally calculated as:

$$DPBP = \frac{(Ci_{GSHP} - Ci_{CB})}{(C_{ECB} - C_{EGSHP})} \tag{10}$$

where:

Ci_{GSHP} : cost of installment (or investment) for GSHP system;
Ci_{CB}: cost of installment (or investment) for CB system;
Ce_{GSHP}: running costs (maintenance and electricity costs) for GSHP system;
Ce_{CB}: running costs (maintenance and natural gas costs) for CB system.

Table 1: Economic data

Description	*Value*	*Units*	*Life cycle*	Scenarios	A	B	C	D	Units
Indoor circulating pump	2,000	€/W_e	*10 years*	NATURAL GAS	1,0	1,0	0,7	1,2	€/Nm^3
GSHP	0,700	€/W_e	*15 years*	ELECTRICITY	0,5	0,25	0,175	0,24	€/kWh
Stack	0,100	€/W_t		EMR	0,50	0,25	0,25	0,20	
CB cost of maintenance	0,100	€/m^3*year		INFLATION RATE (i)	2%	2%	2%	2%	%
GSHP cost of maintenance	0,010	€/m^3		GROWTH (g)	3%	3%	3%	3%	%
CB	0,100	€/W_t	*15 years*	DISCOUNT RATE (r)	5,50%	5,50%	5,50%	5,50%	%
Pollution check	0,100	€/m^3*year							
Major supply cost	0,003	€/W_e*year							
GHE	40,000	€/m	*30 years*						

2.5. Results

The thermal analysis calculated all the necessary data to perform the economic analysis, adopting shape building ratio *S/V=0,5* and excluding climate zone *A* and energy labels *a+* and *g* of the Italian law, as they are very expensive or rare. In Tab. 2 are presented the most important entry data for calculating the payback period. In all next tables, data are given adopting energy labels (*a*/*b*/*c*/*d*/*e*/*f* as 0,37/0,63/0,88/1,13/1,50/2,13 part of EP_i) and climate zones (*B*/*C*/*D*/*E*/*F* as 750/1150/1750/2550/3550 degree-days) for rows and columns ($_L{}^Z$). The primary energy requirements are showed in Tab. 3 and 4, and from Tab. 5 to Tab. 8 payback periods are displayed for different scenarios (*1*/*2*/*3*/*4*). If we consider a predetermined cut off period of 30 years, in scenario *1* a large number of solutions overcame that period (indicated with *nc*). Considering a suitable payback for an householder of 10 years, all scenarios show that *a* energy label is the best option, not depending from the EMR and the gas price. When

we change the EMR from 0,50 to 0,25 keeping the gas price fixed into 0,7÷1,0 €/Nm^3, we can also include the *b* label as good opportunity for the GSHP technology. In scenario *4* almost the solutions give positive results as quicker payback periods, excluding the worst energy label *f*, which do not perform in terms of recovering the initial investments. In Fig. 4 is showed the EMR given by natural gas price for EU27 and used in our scenarios to identify their equivalence with Europe countries. Finally, in Fig. 5 is reported the payback period related to the energy requirements for each scenario, excluding the energy label *f*, for which the Italian low forces a fixed energy requirements. The scenario *1* shows higher slope, which can be taken as sign of instability with energy requirements. The scenario *4* mirrors the opposite case, where the low slope reflects almost the independence between payback period and energy requirements.

Table 2: Climate zones variables, shape building ratio S/V=0,5

Data	*Unit*	*B*	*C*	*D*	*E*	*F*
Daily heating hours	*hours/day*	7.2	8.0	9.0	9.6	10.5
Potential heating days	*day/season*	200	200	200	200	200
EP_i	$kWh_t/m^3 year$	8.1	11.2	15.4	20.4	22.9
Seasonal heating COP	-	6.3	6.1	5.9	5.6	5.3

Table 3: Electricity, kWh/m^3·year

L^Z	*B*	*C*	*D*	*E*	*F*
a	0.552	0.834	1.285	1.647	1.884
b	0.949	1.442	2.194	2.825	3.230
c	1.342	2.030	3.098	3.964	4.503
d	1.742	2.641	4.016	5.148	5.833
e	2.343	3.552	5.397	6.908	7.807
f	3.396	5.146	7.784	9.959	11.182

Table 4: Natural gas, Nm^3/m^3·year

L^Z	*B*	*C*	*D*	*E*	*F*
a	0.305	0.455	0.687	0.858	0.946
b	0.524	0.788	1.174	1.473	1.622
c	0.742	1.111	1.658	2.067	2.262
d	0.964	1.446	2.150	2.686	2.931
e	1.298	1.947	2.892	3.606	3.923
f	1.883	2.824	4.174	5.202	5.621

Table 5: Payback period, scenario 1

L^Z	*B*	*C*	*D*	*E*	*F*
a	0	3	6	10	8
b	4	9	13	20	18
c	7	15	21	nc	31
d	11	21	30	nc	nc
e	17	nc	nc	nc	nc
f	29	nc	nc	nc	nc

Table 6: Payback period, scenario 2

L^Z	*B*	*C*	*D*	*E*	*F*
a	0	3	4	7	5
b	3	6	8	10	8
c	5	9	10	12	10
d	7	11	12	14	12
e	10	14	14	16	13
f	13	17	16	19	15

Table 7: Payback period, scenario 3

L^Z	*B*	*C*	*D*	*E*	*F*
a	0	3	5	7	6
b	3	7	9	12	10
c	9	10	12	15	12
d	8	13	15	18	15
e	11	17	18	21	17
f	16	22	22	25	21

Table 8: Payback period, scenario 4

L^Z	*B*	*C*	*D*	*E*	*F*
a	0	3	4	6	5
b	3	6	6	8	7
c	5	8	8	10	8
d	6	9	10	11	9
e	8	11	11	12	10
f	11	13	12	14	11

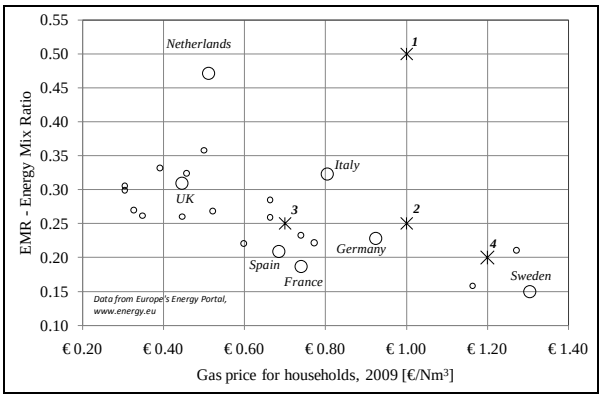

Figure 4: EMR given by gas price in EU27

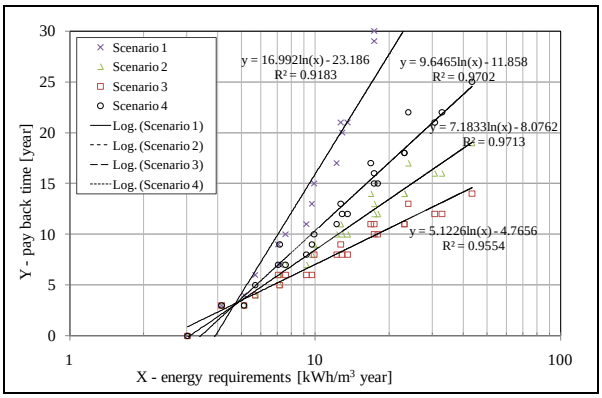

Figure 5: Regression analysis for the scenarios

3. Conclusions

We calculated the payback time for a ground source heat pump (GSHP) in comparison with a condensing boiler (CB), in connection with degree-days, energy building labels and an energy mix ratio (EMR), reflecting energy prices due to different combinations of primary energy. EMR is obtained as ratio between electricity and gas price. A numerical model was used to value the soil temperature modified from the HGHE, and this solution was scaled to approach the other combinations among climate zones and energy labels. The results show that all higher energy labels have a good profitability ratio between costs and payback periods, and demonstrate that GSHP system does pay off. Lower labels become interesting when the EMR drops to 0,25 and the gas price goes up 0,70 €/Nm^3. Further investigations should consider also environmental aspects (reductions of diffuse emissions, urban pollution control), potential raising energy label for retrofit action and different growth rate of energy price.

References

[1] A.D. Chiasson, Advances in modeling of ground-source heat pump systems, M. SC. Thesis, 1999, Oklahoma State University

[2] L. Rybach and W.J. Eugster, Sustainability aspects of geothermal heat pumps, Proceedings of 27th Workshop on Geothermal Reservoir Engineering, 2002

[3] Kulcar B., Goricanec D. Krope J. Economy of exploiting heat from low-temperature geothermal sources using a heat pump, Energy and buildings, 40, 2008, pp. 323 - 329

[4] Bottarelli M., Di Federico V., Adoption of flat panels in soil heat exchange, Proceedings of 11th World Renewable Energy Congress, 2010, pp. 330-335

[5] Y.A. Cengel, Termodinamica e trasmissione del calore, McGraw-Hill, 1st Ed., 1998, pp. 659-663

[6] DHI-WASY GmbH, OpenLoop IFM Module, Copyright 2009, Berlin

[7] G. Brown, G. Matysiak, Real estate investment, a capital market approach, Prentice Hall, 2000

[8] Europe's Energy Portal, 2010, www.energy.eu

Comparing Geothermal Heat Pump System with Natural Gas Heating System

Emin Acikkalp[1], Haydar Aras[2*]

[1]*Department of Mechanical and Manufacturing Engineering, Engineering Faculty, Bilecik University, Bilecik, Turkey*
[2]*Department of Mechanical Engineering, Engineering and Architecture Faculty, Eskisehir Osmangazi University, Eskisehir, Turkey*
** Corresponding author. Tel: +90 222 239 3750 / 3351, Fax: +90 222 239 36 13, E-mail: h_aras2002@yahoo.com, haras@ogu.edu.tr*

Abstract: In this study, approximately 150 m2 of floor space Eskisehir-Turkey have been investigated in a 2-story home. The building is heated with natural gas and heat loss is 24,172 kW. 3000 m 3 / year to meet the heat loss and the cost of natural gas consumed in 1620 U.S. dollars / year. Only the heat pump system under study is replaced by natural gas boilers, home heating system has not been any other changes. Thermodynamic analysis is applied, first, both the system and exergy loss of energy expenditure were calculated. Second, the environmental values were calculated for both systems. Finally, the results were compared between the two systems.

Keywords: *Geothermal heat pump, Exergy and energy analysis, Environmental aspects, Renewable energy*

1. Introduction

Due to the depletion and the environmental damages of the fossil fuels, use of alternative energy sources has become a necessity. Sustainable energy sources are divided into two parts as ground-source and atmosphere-source. Ground-source geothermal energy is stored heat energy in the earth's 0 to 10 km depth. This energy is 245.106 EJ in areas of high flux and 181.106 EJ low flux areas respectively. Considering the use of 1% of this energy is able to meet the world's current energy needs. It is predicted that Turkey has geothermal reserves that provide 50 EJ energy [1]. 31,500 MWh of thermal energy in Turkey and 2000 MWe/year of electrical energy can be achieved with this source. In the world, Turkey is the 5th among the best geothermal energy potential countries. Turkey has the geothermal energy potential to meet 30% thermal or 5% of electrical energy of it [2]. A significant portion of world energy consumption to the domestic heating and cooling is attributable. Heat pump and widely used in many applications are preferred due to their high utilization efficiencies Compared to conventional heating and cooling systems. There are two common types of heat pumps: air-source heat pumps and ground-source heat pumps (GSHPs), also known as geothermal heat pumps (GHPs). Several Advantages over or GHPs have GSHPs air source heat pumps as: (a) They're consumes less energy to operate. (b) They tap the earth or groundwater, a more stable energy source than air. (b) They require supplemental heat during extreme low outside temperature not do. (d) They're less refrigerant use. e) They have a simpler design and consequently less maintenance. (f) Require the unit to be located, where they're not do it is exposed to weathering. Their main disadvantage is the higher initial capital cost, being about 30-50% more expensive than air source units. This is due to the extra expense and effort to bury heat exchangers in the earth or providing a well for the energy sources. However, once installed, the annual cost is less over the life of the system, resulting in a net savings [3].

Eskisehir in Central Anatolia region of Turkey has a continental climate and has rich geothermal resources. Eskisehir water temperatures 25 ^{o}C - 55 ^{o}C has a range from 10 geothermal areas [1]. Geothermal resources in Eskisehir hotels, public baths and hot springs

are also used and not used in another application. This study investigated the geothermal heat source for a building.

2. Methodology

First and second law is basic laws for thermodynamics. First law is conservation of energy and the second law deals with the nature and quality of energy. In this study, heat pump and natural gas systems analyzed for first and second law of thermodynamic, and then environmental impacts of them has been attached and the results were then compared with each other finally.

2.1. Description of Systems

Application made for a house about 150 m^2 floor areas in Eskisehir-Turkey. Home is heated with natural gas and the heat loss is 24.172 kW. The study period was considered to be 6 months. In this time, 3000 m^3 of natural gas has been spent in and it cost $ 1,620 / year. R-134 was used as a refrigerant in heat pump. Natural gas boiler and heat pump system are shown in figure 1 and figure 2.

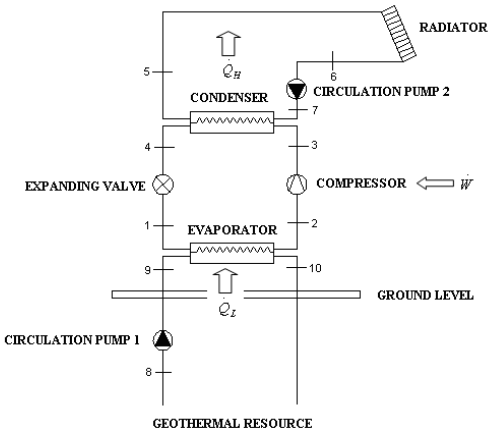

Figure 1. Investigated heat pump system.[3]

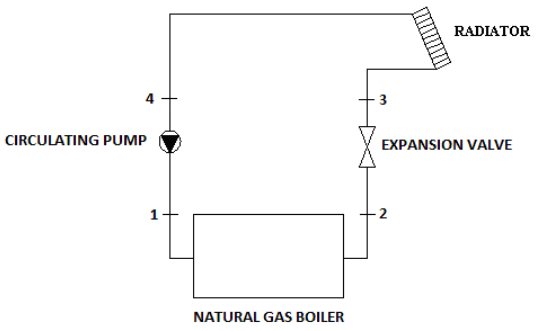

Figure 2. Natural gas boiler system

The assumptions for the system are as follows:

• All systems are adiabatic to the environment.

• Minimal and the average temperature during the heating period for Eskisehir are -12 ^oC and 5 °C respectively.

• Geothermal resource temperature is 40.5 ^oC [4].

• Radiator inlet and outlet temperature are 90 ^oC and 70 ^oC, respectively.

• Geothermal water depth is 79 m [4].

• Average daily heating period is 12 hours.

2.2. Thermodynamic Analysis

In this section, thermodynamic analysis was made detailed for first law (energy terms) and second law (exergy terms), also additional parameters have been added that allows evaluation system of the thermodynamically.

2.2.1. 2.2.1 Energy terms

Energy balances for any control volume at steady state can expressed as following [5],

$$\dot{Q} + \dot{W} = \dot{E}_Q + \dot{E}_W = \sum_o \dot{E}_o - \sum_i \dot{E}_i \quad (1)$$

In the absence of nuclear, magnetism, electricity and surface tension effects in the thermal systems and in this present study, the changes in the kinetic energy and potential energy are assumed to be negligible. The total energy for a flow of matter through a system can be expressed as [6];

$$\dot{E} = \dot{E}_{ph} + \dot{E}_{ch} \quad (2)$$

The physical energy for air and combustion gaseous with constant specific heat may be written as [6];

$$\dot{E}_{ph} = \dot{m}\left(h_{(T)} - h_o\right) \quad (3)$$

Given work to the pumps is;

$$\dot{W}_p = \dot{m}.g.H \quad (4)$$

Fuel's energy is given [5];

$$\dot{E}_F = \dot{m}_f LHV \quad (5)$$

LHV and molecule weight of natural gas is 44661 kJ/kg and 16,28 kg/kmol respectively [7,8]. *COP* of heat pump can be defined as the ratio of the energy output to energy input [6];

$$COP = \frac{\dot{Q}_{cond}}{\dot{W}_{comp} + \dot{W}_{pump,1} + \dot{W}_{pump,2}} \quad (6)$$

The energy efficiencies are calculated by [6];

$$\eta = \frac{\dot{E}_o}{\dot{E}_i} \quad (7)$$

2.2.2. 2.2.2 Exergy terms

Exergy balances for any control volume at steady state can expressed as following [5],

$$\sum\left(1-\frac{T_o}{T_k}\right)\dot{Q}_k+\dot{E}x_W+\sum_i\dot{E}x_i-\sum_o\dot{E}x_o=\dot{E}x_D \tag{8}$$

In the absence of nuclear, magnetism, electricity and surface tension effects in the thermal systems, and in this present study, the changes in the terms of kinetic exergy and potential exergy are assumed to be negligible, the total exergy for a flow of matter through a system can be expressed as [6];

$$\dot{E}x=\dot{E}x_{ph}+\dot{E}x_{ch} \tag{9}$$

The physical exergy of the liquid and gas is calculated by [9];

$$\dot{E}x_{ph}=\dot{m}\left[\left(h-h_o\right)-T_o\left(s-s_o\right)\right] \tag{10}$$

An approximate formulation for the chemical exergy of gaseous hydrocarbon fuels as C_aH_b is given as [10];

$$\frac{\dot{E}x_{ch,NG}}{\dot{m}_{NG}LHV_{NG}}=\gamma_{NG}\cong 1.033+0.0169\frac{b}{a}-\frac{0.0698}{a} \tag{11}$$

γ_{NG} is equal to 1.0308 for the natural gas(NG) composition given in Table 2.
The fuel exergy is equal to chemical exergy of fuel. The exergy efficiencies are calculated by [6];

$$\psi=\frac{\dot{E}x_o}{\dot{E}x_i} \tag{12}$$

2.2.3. Other Thermodynamic Evaluation Parameters

Fuel exergy depletion ratio can be defined as [5];

$$\alpha_k=\frac{\dot{E}x_{C,k}}{\dot{E}x_{TF}} \tag{13}$$

Relative exergy consumption ratio is calculated from [5];

$$\beta_k=\frac{\dot{E}x_{C,k}}{\dot{E}x_{TC}} \tag{14}$$

The exergetic improvement potential can be expressed following [5];

$$ExIP_k = (1-\psi)\, Ex_{C,k} \quad (15)$$

Similar parameters can be defined for energy terms. Fuel energy depletion ratio can be defined as [5];

$$\phi_k = \frac{\dot{E}_{L,k}}{\dot{E}_{TF}} \quad (16)$$

Relative energy loss ratio [5];

$$\Theta_k = \frac{\dot{E}_{L,k}}{\dot{E}_{TL}} \quad (17)$$

Energetic improvement potential [5];

$$EIP_k = (1-\eta)\, E_{L,k} \quad (18)$$

2.3. Environmental Aspects

In this section, environmental impacts were evaluated for CO_2 emissions released into the environment. Combustion equation of natural gas is showed as following;

0.9334 CH_4 + 0.00211 C_2H_6 + 0.00029 C_3H_8 +0.00012 C_4H_{10} + 0.06408 N_2 + 26.675 (0.7448 N_2 + 0.20509 O_2 + 0.0003 CO_2 +0.019 H_2O) 0.9469725 CO_2 + 4.76343 H_2O + 2.425 O_2 +19.93162 N_2 [7,8]

(19)

Rate of CO_2 mass to total mass [11];

$$M_{CO_2} = \frac{0.9469725 CO_2}{M_F} \quad (20)$$

Mass of CO_2 releasing to air [11];

$$M_{CO_2} = \frac{0.9469725 CO_2}{M_F}.m_F \quad (21)$$

3. Results

In this part, results of the energy and exergy values of the systems were submitted firstly. Then the results are presented in terms of environmental impacts.

3.1. Energy and Exergy Results for Both Systems.

Some important results can be summarized as follows. The largest loss of energy for natural gas and heat pump systems is in radiator. The largest exergy destruction is at natural gas system for boiler for natural gas system and at compressor for heat pump. The highest energy efficiencies are at condenser and evaporator for heat pump system and at natural gas boiler for natural gas system. The highest exergy efficiencies are at condenser for heat pump system and at radiator boiler for natural gas system. All thermodynamic values in the two systems can be shown in table 3-6.

Table 1. Heat pump system pressure, temperature, energy rate and exergy rate

Point	Fluid	Temperature (K)	Pressure (kPa)	Mass flow (kg / s)	Energy rate (kW)	Exergy rate (kW)
0	water	278.15	100			
0	refrigerant	278.15	100			
1	refrigerant	282.09	400	0.142	11.56	27.60
2	refrigerant	282.09	400	0.142	27.78	27.83
3	refrigerant	373.15	1400	0.142	38.81	33.01
4	refrigerant	347.15	1400	0.142	14.91	15.99
5	water	363.15	100	0.29	54.546	3.349
6	water	343.15	100	0.29	78.870	7.547
7	water	343.16	100	0.29	78.970	8.020
8	water	313.65	100	0.87	129.35	7.620
9	water	313.75	100	0.87	129.71	7.670
10	water	308.15	100	0.87	109.32	5.500

Table 2. Calculated values for heat pump system in terms of energy

Component	Energy input (kW)	Energy output (kW)	Energy loss (kW)	η	ϕ	Θ	EIP (kW)
Circ. pump 1	0.680	0.360	0.320	0.530	0.010	0.008	0.150
Circ. pump 2	0.142	0.100	0.042	0.700	0.001	0.001	0.012
Compressor	30.000	23.900	6.100	0.800	0.200	0.162	1.220
Condenser	137.300	136.670	0.630	0.990	0.021	0.016	0.006
Evaporator	118.070	117.900	0.170	0.990	0.006	0.004	0.002
Expansion valve	14.860	8.920	5.940	0.600	0.200	0.158	2.376
Radiator	78.870	54.546	24.324	0.691	0.801	0.548	7.516
All system	379.922	342.396	37.542	0.901	1.251	1.000	3.491

Table 3. Calculated values for heat pump system in terms of exergy

Component	Exergy input (kW)	Exergy output (kW)	Exergy destruction (kW)	ψ	α	β	ExIP (kW)
Circ. pump 1	0.680	0.050	0.630	0.080	0.021	0.028	0.630
Circ. pump 2	0.142	0.030	0.112	0.210	0.004	0.005	0.112
Compressor	30.000	17.020	12.980	0.570	0.432	0.571	12.980
Condenser	15.480	15.050	0.430	0.970	0.014	0.019	0.430
Evaporator	7.520	5.890	1.630	0.780	0.054	0.072	1.630
Expansion valve	1.870	0.120	1.750	0.070	0.058	0.077	1.750
Radiator	7.547	3.349	4.198	0.443	0.173	0.228	2.338
All system	63.262	41.509	21.73	0.670	0.752	1.000	7.448

Table 4. Natural gas system pressure. temperature. energy rate and exergy rate

Point	Fluid	Temperature (K)	Pressure (kPa)	Mass flow (kg / s)	Energy rate (kW)	Exergy rate (kW)
0	water	278.15	100			
1	water	343.16	100	0.29	78.97	8.02
2	water	363.15	300	0.29	103.21	13.18
3	water	363.15	100	0.29	103.21	13.18
4	water	343.15	100	0.29	78.87	7.99
Fuel	Natural gas	-	300	0.00065	28.630	29.97

Table 5. Calculated values for natural gas system in terms of energy

Component	**Energy input (kW)**	**Energy output (kW)**	**Energy loss (kW)**	**η**	**ϕ**	**Θ**	**EIP (kW)**
Circ. pump	0.14	0.1	0.04	0.7	0.002	0.002	0.012
Exp. valve	103.21	103.21	0	-	-	-	-
Nat. gas boiler	28.63	24.34	4.29	0.85	0.001	0.001	0.001
Radiator	78.870	54.546	24.324	0.691	0.801	0.548	7.516
All system	210.71	192.196	15.554	0.912	0.543	1.000	1.369

Table 6. Calculated values for natural gas system in terms of exergy

Component	**Exergy input (kW)**	**Exergy output (kW)**	**Exergy destruction (kW)**	**ψ**	**α**	**β**	**ExIP (kW)**
Circ. pump	0.140	0.030	0.110	0.210	0.004	0.004	0.087
Exp. valve	13.180	13.180	0.000	-	-	-	-
Nat. gas boiler	29.97	5.160	24.810	0.172	0.797	0.797	20.543
Radiator	7.547	3.349	4.198	0.443	0.173	0.228	2.338
All system	50.837	21.719	29.118	0.427	0.974	1.000	16.678

3.2. Result of Environmental Aspects

Natural Gas system release 4.64 kg/h CO_2 to air, while heat pump system doesn't release CO_2 emissions to the environment.

4. Conclusions

Considering energy need and environmental troubles, importance of saving large amount energy used heating in the world can be better understood. In this study, natural gas heat and pump systems compared with in terms of energy, exergy and environmental aspects. Some important results obtained are as follows; Heat pump COP value is 4.5, ie 4.5 unit heat energy corresponds to a unit to electrical energy can be obtained. According to energy analysis the energy consuming of natural gas system are 5.46 times more than heat pump system. Heating a building with heat pump is environmentally friendly. Because, using natural gas system causes releasing 4.64 kg/h CO_2 to air, on the contrary, in case heat pump using there is no emission to environment. According to exergy analysis the total exergy destruction of natural gas system are 3.82 times more than total exergy destruction of heat pump system, exergy efficiency heat pump system is 0.67, while 0.47 for the natural gas system. Energy development potential is 3.491 kW for the heat pump system, while 3.522 kW for the natural

gas system and the exergy development potential of the heat pump system is 7.448 kW, while 16.049 kW for the natural gas system.

According to the results seen above, energy, exergy and environmental assessments seems to be more suitable for the use of heat pump system. In addition, a review of the whole system in detail what is the weak and strong aspects of the system clearly seems possible. On this basis, these criteria should be considered when designing systems. Finally, it can be said geothermal source heat pump is suitable for places has rich geothermal resources such as Eskisehir.

References

[1] DPT. Sekizinci bes yıllık kalkınma planı DPT 2609 – ODK 620 (in Turkish) . Madencilik ozel ihtisas komisyonu raporu enerji hammaddeleri alt komisyon jeotermal calısma grubu Ankara. Turkey. 2001

[2] Jeotermal Enerji Derneği. http://www. jeotermaldernegi.org.tr.

[3] Hepbasli A.. Balta Tolga M. A study on modeling and performance assessment of a heat pump system for utilizing low temperature geothermal resources in buildings. Building and environment 42. 2006. pp. 3747-3756

[4] Demirkazıksoy M.A. Eskisehir civarı Jeotermal enerji potansiyeli kullanımı ve gelistirilmesi. A Thesis Submitted to The Graduate School of Natural and Applied of Anadolu University Eskisehir. Turkey; 2004.

[5] Balli O. Aras H. Hepbasli A. Thermodynamic and thermoeconomic analyses of a trigeneration (TRIGEN) system with a gas–diesel engine: Part I – Methodology. Energy Conservation and Management 51. 2010. pp. 2252- 2259.

[6] Moran MJ. Shapiro HN. Fundamentals of Engineering Thermodynamics. Wiley. 5th edition. 2006. pp. 121-315.

[7] Balli O. Aras H. Energetic and exergetic performance evaluation of a combined heat and power system with the micro gas turbine (MGTCHP). International Journal of Energy Research; 37. 2007. pp. 1425-1440.

[8] Balli O. Aras H. Hepbasli A. Energetic analysis of a combined heat and power system (CHP) in Turkey. Energy Exploration and Exploitation 25. 2007. pp. 139- 162

[9] Moran MJ. Sciubba E. Exergy analysis: principles and practice. Journal of Engineering Gas Turbines Power 116. 1994. pp. 285-290.

[10] Moran MJ. Availability analysis: a guide to efficient energy use. ASME press. 1st edition. 1989. pp. 146-180.

[11] Sisman N. Kahya E. Aras N. Aras H. Determination of optimum insulation thicknesses of the external walls and roof (ceiling) for Turkey's different degree-day regions. Energy Policy, 35 (10) 5151-5155, 2007

Optimization of a Hybrid Ground Source Heat Pump using the Response Surface Method

Honghee Park[1], Wonuk Kim[1], Joo Seoung Lee[1] and Yongchan Kim[2*]

[1] *Graduate School of Division of Mechanical Engineering, Korea University, Anam-Dong, Sungbuk-Gu, Seoul, 136-713, Korea*
[2] *School of Mechanical Engineering, Korea University, Anam-Dong, Sungbuk-Gu, Seoul, 136-713, Korea*
** Corresponding author. Tel.: +82 2 3290 3366, Fax: +82 2 921 5439, E-mail: yongckim@korea.ac.kr*

Abstract: A hybrid ground source heat pump (HGSHP) has been recommended as a low cost alternative of a ground source heat pump (GSHP) which has higher initial costs with increasing the size of ground heat exchanger (GHX) for imbalanced load conditions. HGSHP systems incorporate both GHX and supplemental equipments, such as cooling towers and/or boilers. The main issues of HGSHP are the optimal size design and control strategies of supplemental equipments. The objective of this paper is to optimize the size and control strategies using an optimization methodology called as the response surface method (RSM) to decrease the system's total initial cost (IC) and/or life cycle cost (LCC) and/or annual energy use (AEU) of HGSHP systems. The simulation data used in this research was originated from Yavutzurk et al. and integrated with the RSM. Commercial software, which is Minitab 15, has been adopted to draw contour plots, surface plots and overlaid contour. With using response optimizer, the optimal size design and control strategies of supplemental equipments were determined individually and the results were compared with the results of Yavutzurk et al. The optimal size and control strategies have been successfully determined using the optimization tool of the RSM.

Keywords: *Hybrid ground source heat pump, Supplemental equipment, Optimization, Response Surface Method*

Nomenclature

EFT	*entering fluid temperature.....K*	*IC*	*initial cost.....$*
ExFT	*exiting fluid temperature .....K*	*LCC*	*life cycle cost .....$*
GHXL	*ground heat exchanger length.....ft(m)*	*PV*	*present value cost.....$*

1. Introduction

The remarkable advantage of a ground source heat pump (GSHP) is its energy saving potential. The GSHP can save up to 50% of the energy that would be used by conventional systems [1]. The prominent disadvantage of GSHP is higher initial costs which make short-term economics unattractive, although long-term economics is attractive because of lower operating costs caused by higher system performance. Furthermore, for imbalanced load conditions, it is inevitable to increase the size of ground heat exchanger (GHX) or the distance between adjacent GHX boreholes to postpone heat buildup caused by the difference between cooling and heating. A hybrid ground source heat pump (HGSHP) has been recommended as a low cost alternative of GSHP, which can reduce GHX size and give more efficient operation. The HGSHP can effectively balance the ground thermal loads by incorporating supplemental equipments, such as cooling towers and/or boilers into the GSHP system. The design and operation of HGSHP are more complex than GSHP. Fig. 1 shows the schematic diagram of HGSHP system comprising serial and parallel arrangement of GHX and supplement equipment such as cooling tower and/or boiler. In this paper, the comparison between serial and parallel arrangement would not be conducted.

ASHRAE [2] sizes the supplemental heat rejecter capacity based on the difference between monthly average heating and cooling loads of the building rather than the peak loads. General

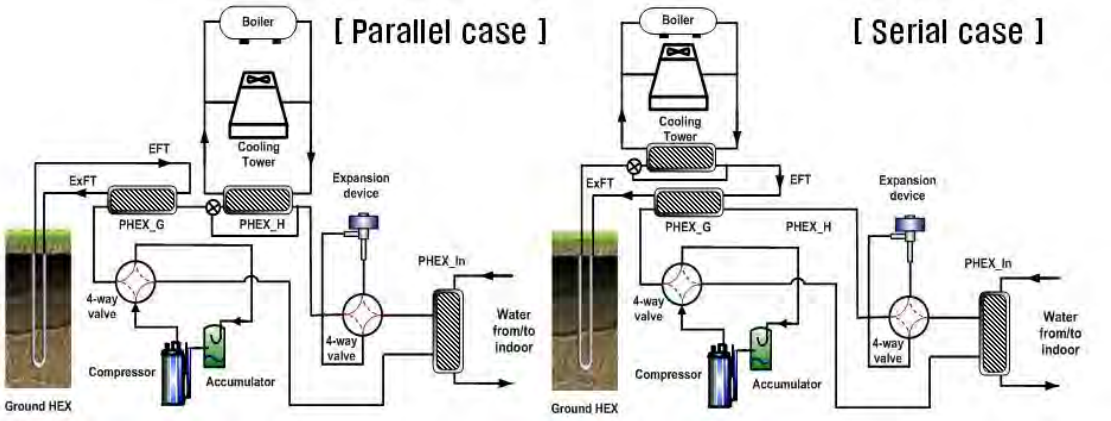

Fig. 1. Schematic diagram of hybrid ground source heat pump system.

guidelines for the integration of the heat rejecter into the system piping were presented. Kavanaugh and Rafferty [3] discuss HGSHP systems within the framework of GHX design alternatives. The sizing of the supplemental heat rejecter is based on the peak block load at the design condition. The nominal capacity is calculated based on the difference between the GHX length required for cooling and heating. Kavanaugh [4] revises and extends the existing design procedures as recommended in the above two publications. In addition, a control method is proposed for balancing the cooling and heating loads on the ground heat exchanger to limit long-term temperature rise. The revised procedure is applied to an office building in three climates, and initial cost and operating cost issues are discussed. Yavutzurk and Spitler [5] present a comparative study investigating several control strategies for HGSHP systems. The strategies investigated include set point control (operating the supplemental rejecter whenever the heat pump entering or exiting fluid temperature exceeds a set temperature, differential temperature control (operating the supplemental rejecter whenever the difference between heat pump fluid temperature and ambient air temperature exceeds set value), and operation of the supplemental rejecter to remove heat from the GHX field during nighttime hours. A 20-year life-cycle cost (LCC) analysis is conducted to compare each control strategy. Singh and Foster [6] explored first-cost savings resulting from HGSHP designs in two building-an office building and an elementary school. Ramamoorthy et al. [7] reported on a similar study that used a cooling pond as a supplemental heat rejecter. Using a differential temperature control strategy, a limited optimization of GHX size and pond size was performed. Chiasson and Yavutzurk [8] used the same system simulation approach to identify scenarios where the HGSHP system with a supplemental heat source is beneficial, in particular schools in heating-dominated climates, where the school was not operated during the summer. The supplemental heat sources investigated were solar thermal collectors and the approach was shown to be economically feasible.

Therefore, the main issues of HGSHP are the optimal size design and control strategies of supplemental equipments to minimize total initial cost or life-cycle cost or operating cost with satisfying designed range of entering or exiting fluid temperature to or from heat pump respectively which assures high performance of HGSHP. To size design of supplemental equipment depends on the size of GHX and its operating hours, and it means that smaller supplemental equipment should operate itself for longer hours. To size supplemental equipments and select its control strategies are coupled.

The objective of this paper is to optimize the size and control strategies using an optimization methodology called as the response surface method (RSM) to decrease the system's total

initial cost (IC) and/or life cycle cost (LCC) and/or annual energy use (AEU) of HGSHP systems.

2. Optimization Method

2.1. Control Strategies

The strategies investigated include 3 kinds of control logics. Set point control (Control 1) means that the cooling tower is activated when the heat pump entering or exiting fluid temperature exceeds a set temperature such as 96.5F (35.8C). Differential temperature control (Control 2) means that the supplemental rejecter is operated whenever the difference between heat pump fluid temperature and ambient air temperature exceeds set value such as 3.6F (2.0C) and is turned off when the difference is less than 2.7F (1.5C). Cool storage control (Control 3) means that the cooling tower is operated during nighttime hours to remove heat from the GHX field. For more detailed information, it could be found out in Yavutzurk and Spitler [5].

2.2. Simulated data used

This paper focused on the adoption of RSM as optimization method of HGSHP and so previously published data was used not to verify the building simulation results and to decide whether it is possible to solve this kind of optimization problem with RSM method or not. Used simulation data from TRNSYS simulation were originated from Yavutzurk and Spitler [5] of which building's total area is approximately 14,205 ft^2 (1320 m^2). A 20-year life-cycle cost (LCC) analysis is conducted to compare each control strategy. The detailed information about the annual building loads was skipped. The simulated data is summarized in Table 1.

2.3. RSM method and Objective function

RSM is a kind of optimization methodology determining the range of main factors for optimizing responses and statistical approximation method for coupled design factors problem. Using minitab software, all RSM process can be conducted and several kinds of plots can be drawn. First of all, the definition of design factors and responses should be conducted. In this paper, determined design factors are ground heat exchanger length (GHXL) and control

Table 1. Simulated data used.

Control	GHXL , ft(m)	Total Initial Costs($)	Total Present Value Costs($)	Annual Energy Use(kWh)
1	3000 (914)	26,662	46,075	24,179
	2625 (800)	23,036	40,783	22,200
	2250 (686)	19,505	35,493	19,913
2	3000 (914)	22,427	38,438	19,941
	2625 (800)	19,774	35,254	19,230
	2250 (686)	17,195	32,171	18,563
3	3000 (914)	21,272	41,845	25,623
	2625 (800)	18,175	37,259	23,800
	2250 (686)	15,078	32,672	21,914

Table 2. Coefficients of response surface regression.

Terms	Coefficients		
	Total Initial Costs($)	Total Present Value Costs($)	Annual Energy Use(kWh)
Constant	4417.81	19752.2	17924.8
a (GHXL)	8.40058	12.4643	6.14636
b (CONTROL)	-4061.50	-14267.7	-13042.8
c (GHXL*GHXL)	0.000217625	0.00018660	-2.37487E-04
d (CONTROL*CONTROL)	825.103	3742.74	3714.60
e (GHXL*CONTROL)	0.642000	-0.939333	-0.371333

strategies with which supplemental equipment such as cooling tower is operated, and selected responses are the size of supplemental equipment, total initial costs, total present value costs and annual energy use. The objective function was defined as minimization of total initial costs and/or total present value costs and/or annual energy use. After analyzing design of experiment, response surface analysis was conducted and several kinds of plots such as contour plots, surface plots and overlain plots for multiple responses were drawn as well as response surface regression. Finally, the optimized values of GHXL and Control strategy were obtained to satisfy the objective function.

3. Results and Discussions

3.1. Response surface regression

Response surface regression was conducted using software of Minitab 15 as shown in Eq. 1. The regression curves were deducted in terms of 'GHXL' and 'CONTROL' comprising second order terms such as 'GHXL*GHXL' and 'CONTROL* CONTROL' and interaction term of 'GHXL* CONTROL' for the responses (Y) such as total initial cost, total present value costs and annual energy use. The regression coefficients are listed in Table 2. The calculated R-Square values of total initial costs, total present value costs and annual energy use are 99.28%, 97.61%, 96.51% respectively.

$$\begin{aligned} Y = \text{Constant} + a\times(\text{GHXL}) + b\times(\text{Control}) + c\times(\text{GHXL}\times\text{GHXL}) \\ + d\times(\text{Control}\times\text{Control}) + e\times(\text{GHXL}\times\text{Control}) \end{aligned} \quad (1)$$

3.2. Surface plots and Contour plots

As it is shown in Fig. 2, Surface plots and Contour plots for 3 responses were drawn. Contour plot is two dimensional and Surface plot is three dimensional. With these plots, optimization direction could be obtained. To decrease total initial costs, total present value costs and annual energy use, GHXL size should be decreased which means increasing cooling tower size in all cases. As for the control strategies, in the case of total initial costs, control strategy should approach Control 3 which means cool storage control to minimize total initial costs, and in the case of total present value costs, control strategy should come close to the middle point between Control 2 which means differential control and Control 2.5 which means the mixed control of 50% Control 2 and 50% Control 3 for minimizing total present value costs. As we can see, the control strategy for annual energy use should approach Control 1.8 to minimize annual energy use.

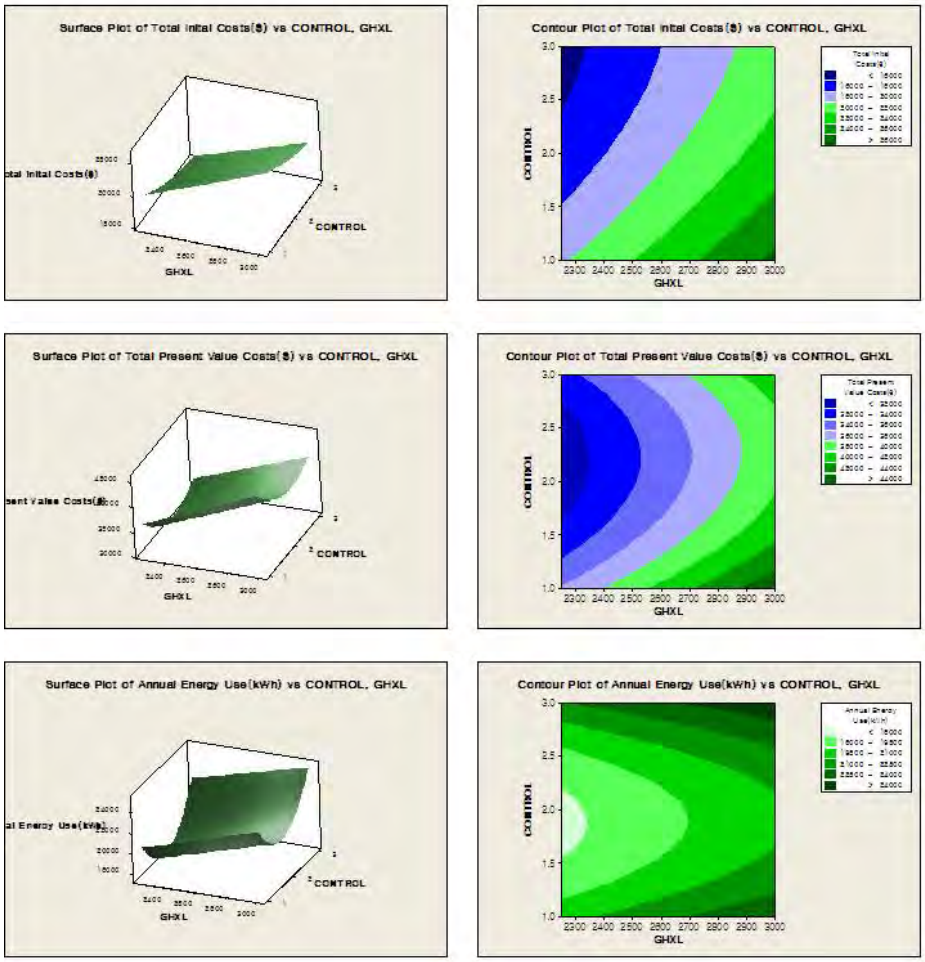

Fig. 2. Surface plots and Contour plots for 3 responses.

3.3. Overlaid contour

To draw overlaid contour, the ranges of 3 responses were determined as it is in Fig. 3 such as 15,000~18,000 ($) for total initial costs and 32,000~35,500 ($) for total present value costs and 18,500~19,900 (kWh) for annual energy use.

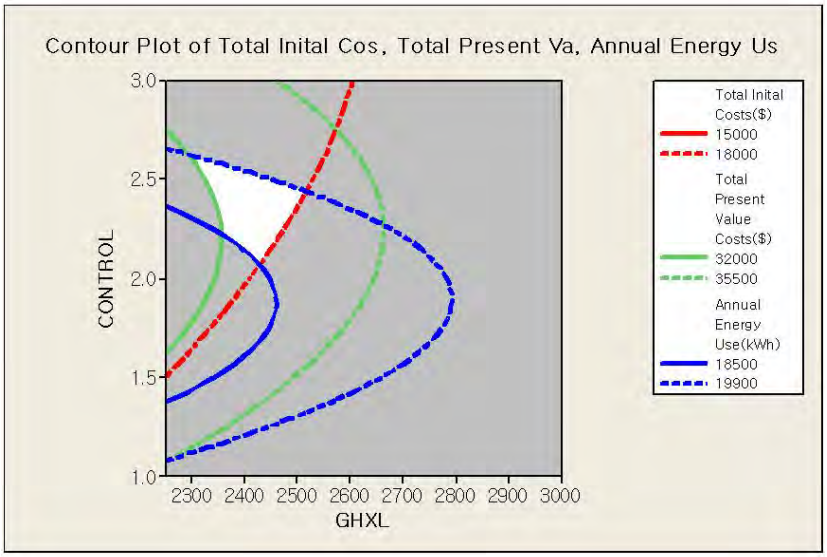

Fig. 3. Overlaid contour for 3 responses.

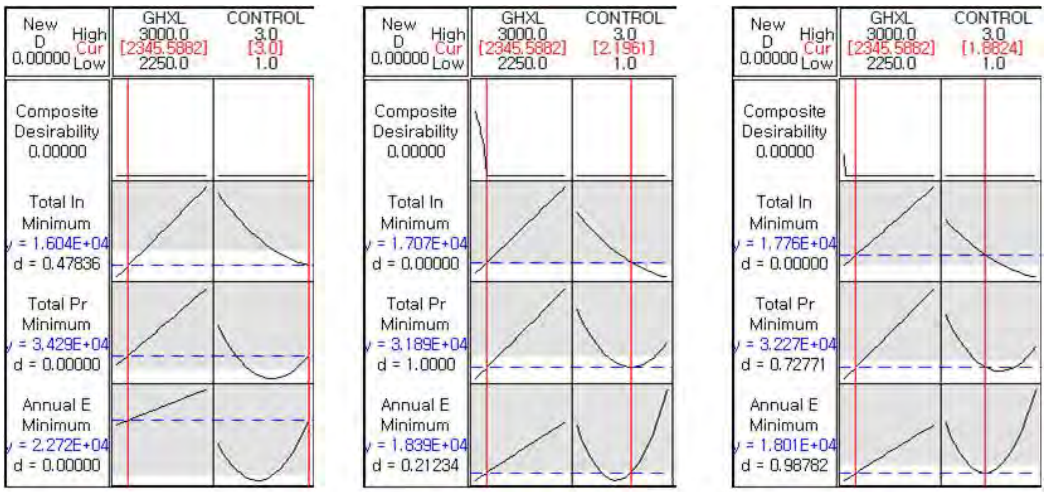

Fig. 4. The result of response optimizer for minimizing 3 responses

In Fig. 3, the bright region enclosed 3 pair of curves satisfies 3 conditions given and it means that the optimal values of factors and responses are within the bright region. For the purpose of determining optimum value of GHXL and Control to minimize individually each response, the response optimizer should be conducted.

3.4. Results from Response optimizer

In Fig. 4 the left figure presenting response optimizer result is for total initial costs and optimum value of GHXL and Control strategy are 2,345 ft (715 m), 3.0 respectively and minimum total initial cost is 16,040 $. The middle figure is for total present value costs and optimum value of GHXL and Control strategy are 2,345 ft (715 m), 2.2 respectively and minimum total present value cost is 31,890 $. The right figure is for annual energy use and optimum value of GHXL and Control strategy are 2,345 ft (715 m), 1.9 respectively and minimum annual energy use is 18,010 (kWh). The individual desirability and composite desirability were checked. These results are listed in Table 3 and compared with the previous results from Yavutzurk and Spitler [5]. With RSM, 17% decrease of total present value costs and 10% of annual energy use compared with Yavutzurk and Spitler [5] were obtained, though there was 7% increase of total initial costs.

4. Conclusions

The objective of this paper was to optimize the size and control strategies using an optimization methodology called as the response surface method (RSM) to decrease the system's total initial cost and/or life cycle cost and/or annual energy use of HGSHP systems.

Table 3. Results Comparison between RSM and Yavutzurk and Spitler [5].

Terms	RSM	Yavutzurk and Spitler [5]	Difference (±%)
Total Initial Costs ($)	16,140 ($)	15,078 ($)	+1,062 (+7%)
Total Present Value Costs ($)	31,890 ($)	38,438 ($)	-6,548 (-17%)
Annual Energy Use (kWh)	18,010 (kWh)	19,941 (kWh)	-1,931 (-10%)

In this paper, determined design factors were ground heat exchanger length (GHXL) and control strategies with which supplemental equipment such as cooling tower is operated, and selected responses were the size of supplemental equipment, total initial costs, total present value costs and annual energy use. The objective function was defined as minimization of total initial costs and/or total present value costs and/or annual energy use. Using minitab software, all RSM process was conducted and response surface regression and several kinds of plots such as surface plots, contour plots and overlaid contour were drawn.

With RSM, 17% decrease of total present value costs and 10% of annual energy use compared with Yavutzurk and Spitler [5] were obtained, though there was 7% increase of total initial costs. The optimal size and control strategies have been successfully determined using the optimization tool of the RSM.

Acknowledgement

This research was sponsored by the Korea Institute of Energy and Resources Technology Evaluation and Planning (Grant No. 2008NBLHME0900002008).

References

[1] United States Department of Energy, Energy Efficiency and Renewable Energy homepage, September 2007, http://www1.eere.energy.gov/geothermal/history.html.

[2] ASHRAE, Commercial/institutional ground-source heat pumps engineering manual, Atlanta: American Society of Heating, Refrigerating and Air-Conditioning Engineers, Inc., 1995.

[3] S.P. Kavanaugh and K. Rafferty, Ground-source heat pumps: Design of geothermal systems for commercial and institutional buildings, Atlanta: American Society of Heating, Refrigerating and Air-Conditioning Engineers, Inc., 1997.

[4] S.P. Kavanaugh, A design method for hybrid ground source heat pumps, ASHRAE Transactions 104 (2), 1998, pp. 691-698.

[5] C. Yavuzturk and J.D. Spitler, Comparative Study to Investigate Operating and control Strategies for Hybrid Ground Source Heat Pump Systems Using a Short Time-step Simulation Model, ASHRAE Transactions 106(2), 2000, pp.192-209.

[6] J.B. Singh and G. Foster, Advantages of Using the Hybrid Geothermal Option, The Second Stockholm International Geothermal Conference, The Richard Stockton College of New Jersey, 1998.

[7] M. Ramamoorthy et al., Optimal Sizing of Hybrid Ground- Source Heat Pump Systems that use a Cooling Pond as a Supplemental Heat Rejecter – A System Simulation Approach, ASHRAE Transactions 107(1), 2001, pp. 26-38.

[8] A.D. Chiasson and C. Yavuzturk, Assessment of the Viability of Hybrid Geothermal Heat Pump Systems with Solar Thermal Collectors, ASHRAE Transactions 109(2), 2003, pp. 487-500.

Experimental ground source heat pump system to investigate heat transfer in soil

Hakan Demir*, Ş. Özgür Atayılmaz, Özden Ağra

Yıldız Technical University, Istanbul, Turkey
** Corresponding author. Tel: +90 212 383 28 20, Fax: +90 212 261 66 59, E-mail: hdemir@yildiz.edu.tr*

Abstract: The earth is an energy resource which has more suitable and stable temperatures than air. Typical values for Coefficient of Performance (COP) of Ground Source Heat Pumps (GSHPs) are up to 8 while it is 4 of air source heat pumps. GSHPs were developed to use ground energy for residential heating. The most important part of a GSHP is the Ground Heat Exchanger (GHE) that consists of pipes buried in the soil and is used for transferring heat between the soil and the heat exchanger of the GSHP. Soil composition, density, moisture and burial depth of pipes affect the size of a GHE. Design of GSHP systems in different regions of US and Europe is performed using data from an experimental model. However, there are many more techniques including some complex calculations for sizing GHEs. An experimental study was carried out to investigate heat transfer in soil. Measured fluid inlet temperatures were used in the numerical simulation and the fluid outlet temperatures were calculated. A parametrical study was conducted to investigate effects of soil thermal properties and geometrical parameters on heat transfer from ground heat exchanger. It is seen that the soil thermal conductivity has great importance on heat transfer. Also, burial depth and distance between pipes are other parameters to be considered for sizing GHEs.

Keywords: *Ground source heat pump, Parallel pipe horizontal ground heat exchanger, Numerical solution*

1. Introduction

The GHE is an important part of GSHP systems and its dimensions and burial depth should be calculated with an effective method. Particularly, the cost of assembly of GHE affects the choice of these systems. In the literature, there are two kinds of analytical approaches: Kelvin Line Source Theory and Cylindrical Source Theory. In addition, there are many studies using two or three dimensional steady state and time dependent numerical techniques [1-7], [8-11, 12]. Kelvin Line Source and Cylindrical Source theories find only symmetrical soil temperature distributions around the pipe. Metz [7] has been suggested an analytical model to find temperature distribution in the soil by dividing ground into blocks around the coil and done some modifications to Line Source theory. Mei [6] has been included the effects of seasonal ground temperature variation, pipe material, circulating liquid properties and compared his work with modified line source and simple line source models. A simplification of boundary conditions to solve equations analytically causes some error on results especially shorter simulation times. Analytical models do not consider the temperature change of soil by depth and the surface effects such as radiation, convection and surface cover. The effects of the convection on the ground surface were included in some of the models [1, 2]. A more complicated model for heat transfer of buried pipes was performed by Negiz, Hastaoglu and Heidemann for petrol transferring pipes [4, 9, 10]. Piechowsky was included mass transfer in his model to take into account the effects of the soil moisture [11, 13]. In this study, a numerical model was suggested with realistic boundary conditions. In order to validate the new model a big scale experimental set area was built.

2. Experimental study

A GSHP having 4 kW heating and 2.7 kW cooling capacity is used for experimental study. The ground heat exchanger consists of three parallel pipes which have 40 m length and ½" diameter buried in soil at 1.8 m depth. The distance between the parallel pipes is 3 m. Experimental GSHP system is installed at Yıldız Technical University Davupaşa Campus on

800 m^2 surface area with no special surface cover. Temperature data were collected using T-type thermocouples buried in soil horizontally and vertically at various distances from the pipe center and at the inlet and outlet of the ground heat exchanger. All the thermocouples are connected to a 64 c hannel PLC system capable of saving data of hourly temperature measurements for 8 days. Figure 1 and 2 represents the experimental setup.

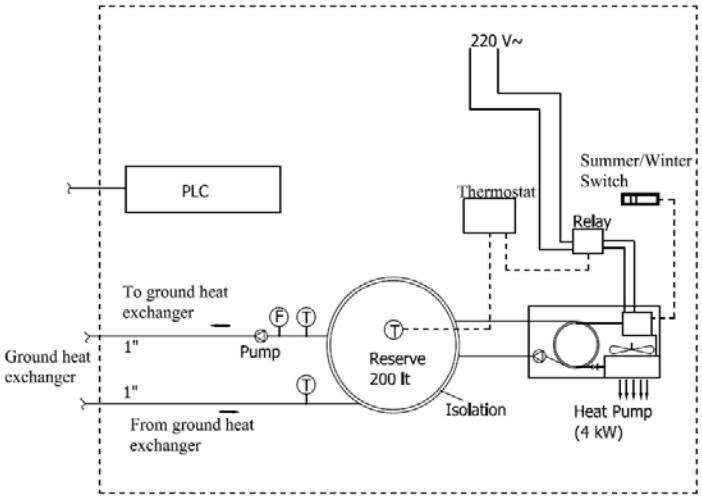

Figure 1 Experimental setup (heat pump and measuring system) [14]

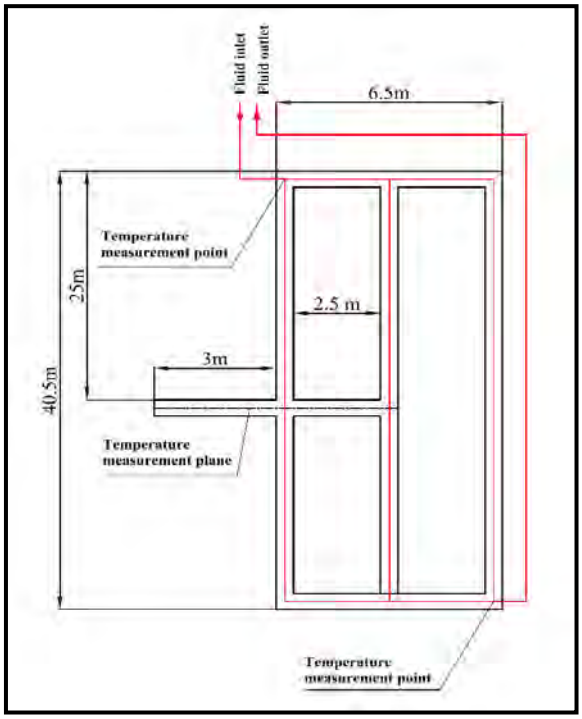

Figure 2 Experimental setup (ground heat exchanger and thermocouple locations) [14]

3. Numerical study

Aiming to find three dimensional temperature distributions in the soil, a new model with realistic boundary conditions was suggested. Heat transfer in the soil is time dependent three dimensional heat conduction. Temperature gradient along the pipe axis is so small that it can be neglected and the heat conduction equation can be solved using dynamical boundary conditions in two-dimensional geometry. The solution domain and boundary conditions was prepared as in Figure 3.

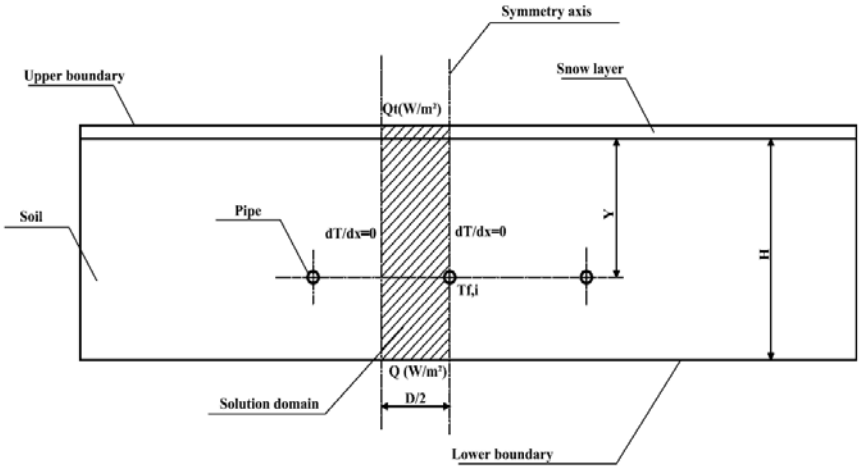

Figure 3 Parallel pipe horizontal GHE and solution area in the soil [14]

The model consists of parallel pipes buried at the depth of Y. Distance between pipes is D. Region shown in Figure 4 is taken as solution domain. This is two dimensional and presented in Cartesian coordinate system.

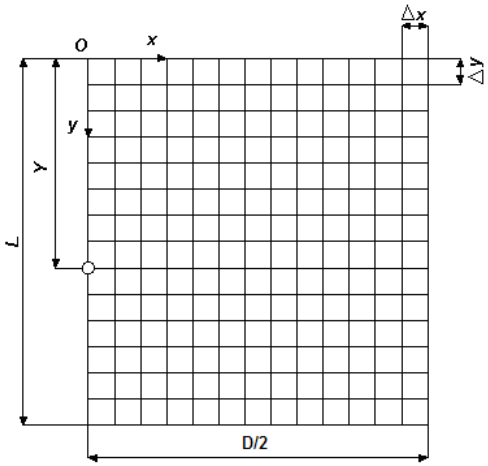

Figure 4 Computational solution domain [14]

Two-dimensional time dependent heat conduction and boundary conditions of problem are of the form;

$$\frac{\partial^2 T}{\partial x^2} + \frac{\partial^2 T}{\partial y^2} = \frac{1}{\alpha}\frac{\partial T}{\partial t} \tag{1}$$

$$T_i = T(x,t) \quad @t = 0 \tag{2}$$

$$\left.\frac{\partial T}{\partial x}\right|_{x=D/2} = 0 \tag{3}$$

$$\left.\frac{\partial T}{\partial x}\right|_{x=0} = 0 \tag{4}$$

$$Q(W/m^2) \quad @y = L \tag{5}$$

$$Q_t(W/m^2) \quad @y = 0 \tag{6}$$

$$T_{f,i} = C \tag{7}$$

Where Q_t is total heat transfer rate at the surface and $T_{f,i}$ is the fluid inlet temperature. Because of the complexity of the boundary conditions, the heat conduction equation has been solved numerically using Alternating Direction Implicit (ADI) Finite Difference formulation. ADI method is stable for every time step and grid size and the resulting matrix system is tri-diagonal. Tri-diagonal matrix systems can be solved easily using the Thomas algorithm. For this purpose, software was developed in MATLAB environment and the effects of solution parameters on the results were investigated. Details of the numerical model and solution procedure can be found in Demir et.al. [14]. The simulation results were acceptable when a mesh size of 0.1 m in x and y directions, 1 m in z direction and 1800 s as time step were used. Parameters from experimental study used in numerical simulation as below:

- Start date 13th December
- Volumetric flow rate, $V_f = 0.42768$ m^3/h
- Soil thermal conductivity, $k_s = 2.18$ W/m K
- Soil thermal diffusivity, $\alpha_s = 0.00000068$ m^2/s
- Pipe outer/inner diameter, $d_o/d_i = 20/14.6$ mm
- Pipe thermal conductivity, $k_p = 0.8999$ W/m K
- Length of parallel pipes, L = 40 m
- Distance between pipes, D = 3 m
- Burial depth, Y = 1.8 m
- Working fluid is water
- Pipe material = PPRC
- Number of parallel pipes, n = 3

4. Results

The experimental fluid inlet/outlet and theoretical fluid outlet temperatures are shown in Figure 5. It is seen that the experimental and numerical results are in good agreement.

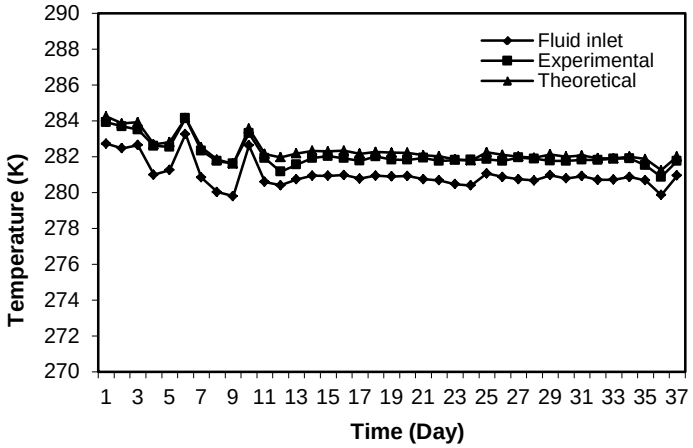

Figure 5 Experimental fluid inlet and experimental/theoretical fluid outlet temperatures [14]

The effects of the parameters, soil thermal conductivity, burial depth and distance between pipes were investigated numerically. Figure 6 and 7 s how the effects of soil thermal conductivity on fluid outlet temperature and horizontal temperature distribution in soil. Fluid outlet temperature increases with increasing thermal conductivity while has no e ffect on horizontal temperature distribution after 250 h of simulation time.

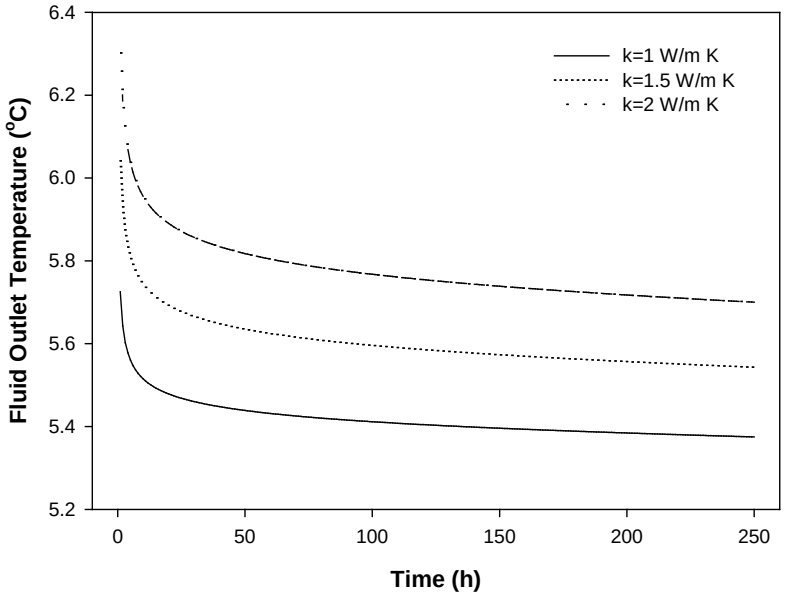

Figure 6 Effects of the soil thermal conductivity on fluid outlet temperature

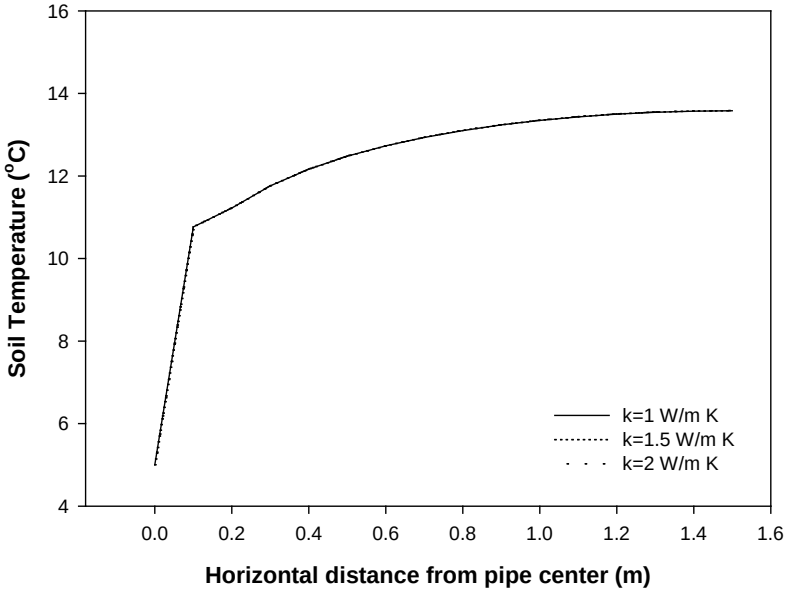

Figure 7 Effects of the soil thermal conductivity on horizontal temperature distribution in soil

In Figure 8 and 9, the effects of the distance between pipes on fluid outlet temperature and horizontal temperature distribution in soil are presented. Fluid outlet temperature increases with increasing distance. Also, it is seen from Figure 9 that increasing the distance between pipes affects the unaffected soil region and heat transfer characteristics. Smaller distances cause decrease of the temperature of the soil in the vicinity of the pipes and reduces heat transfer rate.

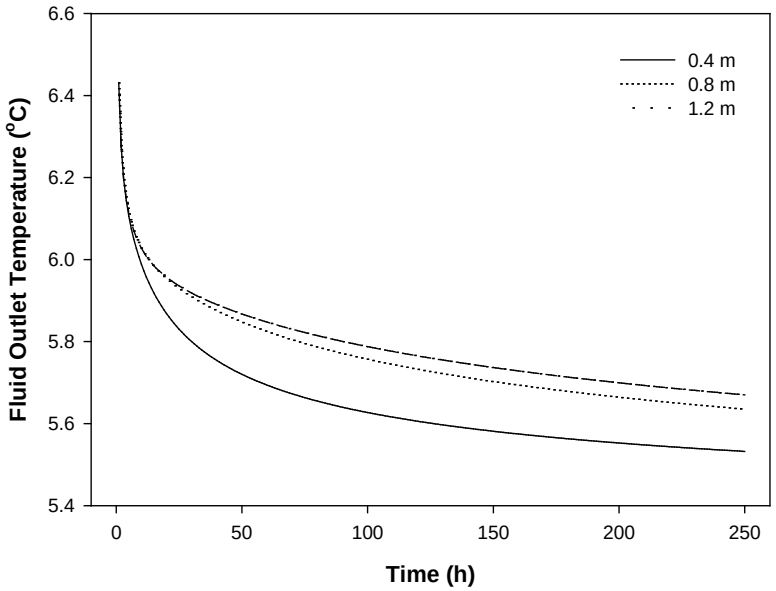

Figure 8 Effects of the distance between pipes on fluid outlet temperature

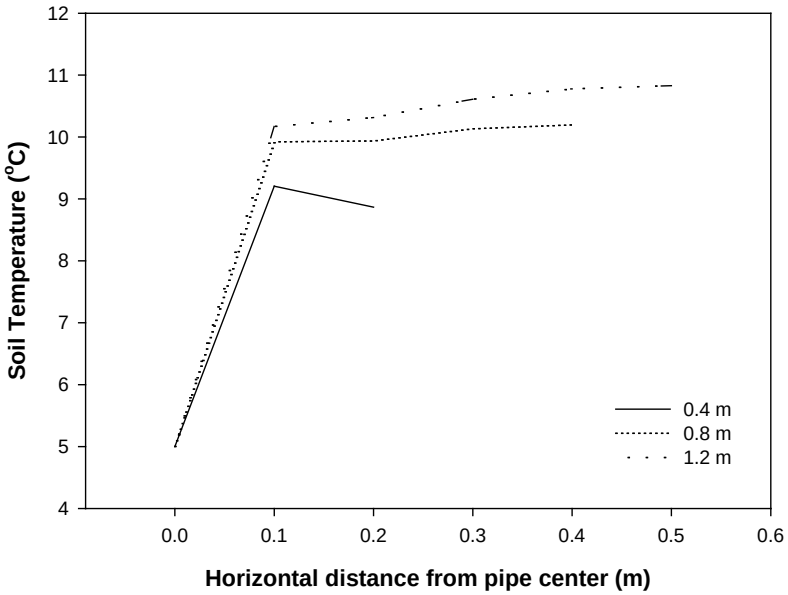

Figure 9 Effects of the distance between pipes on horizontal temperature distribution in soil

In Figure 10 and 11, the effects of the burial depth on fluid outlet temperature and horizontal temperature distribution in soil are shown. Fluid outlet temperature increases with increasing burial depth. It is easily seen the effects of surface temperature variations on the fluid outlet temperature for the burial depth of 0.5 m. Therefore, it is recommended that the minimum burial depth must be 1 m for horizontal ground heat exchangers. Also, increasing the burial depth increases the fluid outlet temperature as the temperature of the soil increase with depth.

5. Conclusions

In this study, the numerical model including all weather conditions was suggested and verified with the experimental study. The most important advantage of the model is implementation of meteorological data to numerical model. It is seen that the maximum deviation between calculated and experimental fluid outlet temperatures is 10.5%. It is

possible to simulate whole year operation of ground heat exchanger providing the meteorological data.

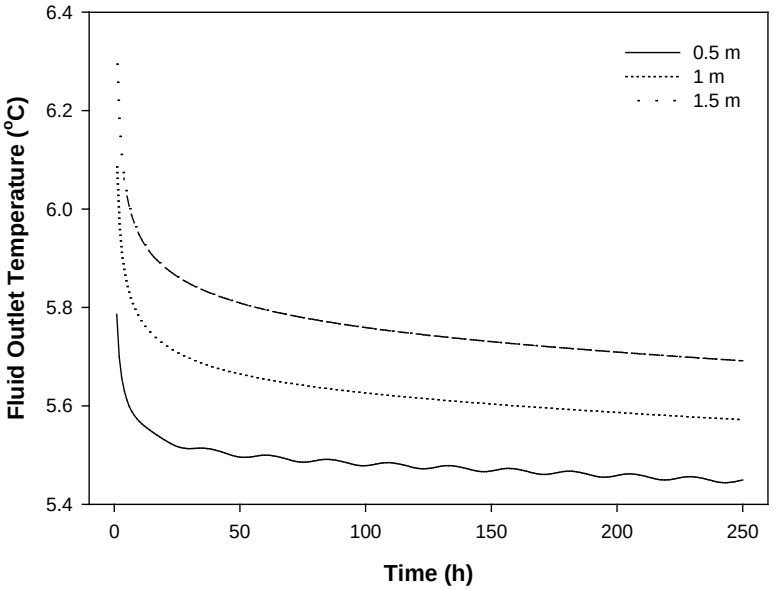

Figure 10 Effects of the burial depth pipes on fluid outlet temperature

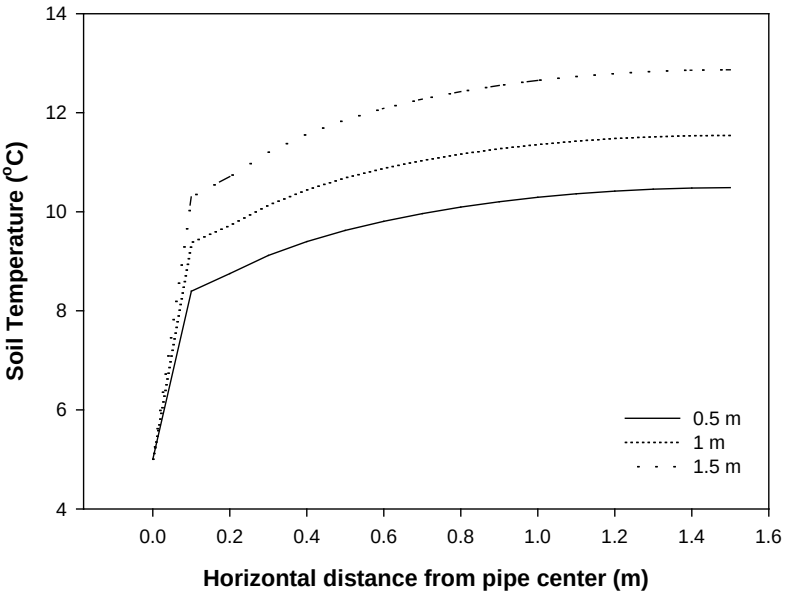

Figure 11 Effects of the burial depth pipes on horizontal temperature distribution in soil

After validating the numerical model, a parametrical study was conducted to investigate effects of the geometrical parameters and soil properties. It is determined that the fluid outlet temperature is strongly depends on soil thermal conductivity. The heat transfer characteristics of the soil in the vicinity of the pipes can be improved by using backfill material. Other important parameters are burial depth and distance between the pipes. Pipes should be buried in the soil below 1 m from the free surface in order to eliminate surface effects such as temperature variation, radiation, snow and rainfall. Also, the distance between pipes should not less than 0.8 m considering the required surface area.

To improve the accuracy of the model neural network approach may be used for modeling soil, air temperature and solar radiation. Also, moisture transfer and variation of soil thermal conductivity with soil moisture content and temperature can be modeled for further studies.

References

[1] B. Bohm, On transient heat losses from buried district heating pipes, Int. Journal of Energy Research 24 (2000), pp. 1311-1334

[2] M. Chung, P.S. Jung, R.H. Rangel, Semi-analytical solution for heat transfer from a buried pipe with convection on t he exposed surface, Int. Journal of Heat and Mass Transfer 42 (1999), pp. 3771-3786

[3] Y. Gu, D.L. O'Neal, An analytical solution to transient heat conduction in a composite region with a cylindrical heat source, Transactions of the ASME 117 (1995), pp. 242-248

[4] M.A. Hastaoglu, A. Negiz, R.A. Heidemann, Three-dimensional transient heat transfer from a buried pipe – part III comprehensive model, Chemical Engineering Science 50 (1995), pp. 2545-2555

[5] T.K. Lei, Development of a computational model for a ground-coupled heat exchanger, ASHRAE Transactions: Research 99 (1993), pp. 149-159

[6] V.C. Mei, Heat transfer of buried pipe for heat pump application, Journal of Solar Energy Engineering 113 (1991), pp. 51-55

[7] P.D. Metz, A Simple computer program to model three-dimensional underground heat flow with realistic boundary conditions, Transactions of the ASME 105 (1983)), pp. 42-49

[8] S. Mukerji, K.A. Tagavi, W.E. Murphy, Steady-state heat transfer analysis of arbitrary coiled buried pipes, Journal of Thermophysics and Heat Transfer 11 (1997), pp. 182-188

[9] A. Negiz, M.A. Hastaoglu, R.A. Heidemann, Three-dimensional heat transfer from a buried pipe – I. laminar flow, Chemical Eng. Science 48 (1993), pp. 3507-3517

[10] A. Negiz, M.A. Hastaoglu, R.A. Heidemann, Three-dimensional transient heat transfer from a buried pipe: solidification of a stationary fluid, Numerical Heat Transfer 28 (1995), pp. 175-193

[11] M. Piechowsky, Heat and mass transfer of a ground heat exchanger: theoretical development, Int. Journal of Energy Research 23 (1999), pp. 571-588

[12] A.D. Chiasson, Advances in Modeling of ground source heat pump systems, MSc Thesis, Oklahoma State University, 1999

[13] M. Piechowski, A ground coupled heat pump system with energy storage, PhD Thesis, The University of Melbourne, 1996

[14] H. Demir, A. Koyun, G. Temir, "Heat Transfer of Horizontal Parallel Pipe Ground Heat Exchanger and Experimental Verification", Applied Thermal Engineering 29 (2009), pp. 224-233

Influence of Undisturbed Ground Temperature and Geothermal Gradient on the Sizing of Borehole Heat Exchangers

Tomislav Kurevija[1,*], Domagoj Vulin[1], Vedrana Krapec[1]

[1] *Faculty of Mining, Geology and Petroleum Engineering, University of Zagreb, Zagreb, Croatia*
** Corresponding author. Tel: +385 1 5535843, Fax: +385 1 4836074, E-mail: tkurevi@rgn.hr*

Abstract: Undisturbed ground temperature is one of the most crucial thermogeological parameters needed for shallow geothermal resources assessment. Energy considered to be geothermal is energy stored in the ground at depths where solar radiation has no effect. At depth where undisturbed ground temperature occurs there is no influence of seasonal variations in air temperature from surface. Exact temperature value, and depth where it occurs, is functionally dependent on surface climate parameters and thermogeologic properties of ground. After abovementioned depth, increase of ground temperature is solely dependent on geothermal gradient. Accurately determined values of undisturbed ground temperature, and depth of occurrence, are beneficial for proper sizing of borehole heat exchangers and ground source heat pump system as a whole.
On practical example of building being heated and cooled with shallow geothermal resource, via heat pump system, influence of undisturbed ground temperature and geothermal gradient on size of borehole heat exchanger is going to be presented. Sizing of borehole heat exchanger was calculated with commercial software Ground Loop Designer (GLD), which uses modified line source and cylinder source solutions of heat conduction in solids.

Keywords: *Borehole heat exchanger, Shallow geothermal energy, Geothermal heat pump, Undisturbed ground temperature, Geothermal gradient*

1. Introduction

Today most of the commercially available simulation software packages that are used for sizing of geothermal heat pumps systems with borehole heat exchangers apply one of two (or both) theoretical heat transfer models. The first model is based on the cylindrical source model and allows for quick but accurate length or temperature calculations based on limited data input. The second model is based on a simple line source theory, but is more detailed in its ability to generate monthly temperature profiles over time given monthly loads and peak data. Although the solutions of the two models do not always agree, and strongly differ on valuation of thermal interferences effect, they do give the engineer more information on which to base a final borehole heat exchanger system design.

The vertical bore length equations used in the first model, also known as ASHRAE/Kavanaugh model, are based upon the solution for heat transfer from a cylinder buried in the earth. The method was developed and tested by Carslaw and Jaeger (1946). The solution gives a temperature difference between the outer cylindrical surface and the undisturbed ground temperature. Ingersoll suggested using the equation and its solution for the sizing of borehole heat exchangers in cases where the extraction or rejection of heat occurs in periods of less than six hours, where the simple line source model fails (Ingersoll, 1954). The model was further improved by solution of Kavanaugh and Deerman (1991) who arranged the methods of Ingersoll to account for U-pipe layout and hourly heat variations. For the first model, the most complete description of method and input data can be found in reference Kavanaugh and Rafferty (1997).

The second model, also known as Lund/Swedish model, is based on the solution to the solely heat conduction in a homogenous medium, which was solved by approximating the borehole as a finite line sink using superposition principle (Eskilson, 1987). The steady state solution

relates to the case where heat is extracted continuously from the borehole without ever exhausting the heat source, making it a fully renewable source of energy. The difference between the second model and the first one is that with the second model it is possible to calculate the evolution of the borehole wall temperature over time when a constant heat rate is extracted from the borehole. It makes use of a dimensionless *g-function* method to model the temperature variations, taking into account the ratio of the borehole radius and length and the physical layout of the bore field.

However, both of those models are not particularly considering geothermal gradient in their analysis, claiming that impact of geothermal gradient on overall borehole length needed for heat transfer is rather small and therefore should be neglected. This paper will discuss difference in results of borehole grid array design, obtained by applying Eskilson/Lund model in simulation process of geothermal heat pump system. Model will include two separate ground temperature inputs: one with entering solely undisturbed ground temperature at the site, and the other by entering effective ground temperature with applied geothermal gradient.

2. Influence of Undisturbed Ground Temperature and Geothermal Gradient

Ground surface is exposed to the solar radiation effect to the certain depth. The intensity of solar radiation is different because of geographic location, morphology and plant diversity. Ground temperature is generally a function of solar heat transferred by radiation, convection and conduction. Undisturbed ground temperature could be considered to occur at depth where annual ground temperature amplitude becomes as low as 0,1°C. Undisturbed ground temperature in fact represents temperature at the depth where exists equilibrium from solar radiation from surface and geothermal heat flow from Earth's crust.

Eskilson (1987), states that only an average undisturbed ground temperature is of importance for the heat extraction analysis while geothermal gradient and surface variations are neglected. This average temperature is normally with good accuracy equal to the undisturbed ground temperature at the mid-depth of the borehole. Experimentally, it is determined by circulating the heat carrier fluid without heat extraction or injection (prior Thermal Response Test). The circulating fluid assumes after a short transient period a steady temperature. Heat is then flowing to the lower half of the borehole from the surroundings, which have a temperature above average undisturbed ground temperature, and the same amount of heat is flowing from the borehole to the somewhat colder surroundings in the upper half. Ekilson (1987) also shown that the errors in heat extraction performance, when the simplified initial and boundary conditions are used (average undisturbed ground temperature on mid-depth of bore) instead of more precise ones which include geothermal gradient and temperature variations at surface, are characteristically less than 1%. This analysis was carried out with geothermal gradient of 0,0162°C/m which is common value for northern regions of Europe. Question emerges what would be effect of geothermal gradient on heat transfer in areas where this value is significantly higher. As shown on Figure 1, northern part of the Republic of Croatia posses much higher geothermal gradients in range between 0,04 - 0,07 °C/m. For example, capital city Zagreb, which is located in northwest part of Croatia has average gradient of 0,05 °C/m.

To also include surface temperature variations in analysis of determining average ground temperature through the borehole and simulate heat transfer between geothermal heat pump systems it is necessary to determine real depth where undisturbed ground temperature occurred. Long-term temperature measurements from 2 cm up to 100 cm are conducted on the points of observation by the Meteorological and Hydrological Service of the Republic of

Croatia (DHMZ). Maximum yearly amplitudes (25,1°C) in the ground temperature were observed at the depth of 2 cm in city of Zagreb. Annual amplitudes are decreasing to 15,1°C at 100 cm depth. By analyzing damping of temperature amplitudes, analytical solution by means of extrapolation of a ground temperature versus depth is possible, as published in previous research paper (Kurevija 2010.). If there are no measured data, yearly temperature oscillation at some depth can be estimated with sinusoidal function solving the differential equation as described by Hillel (1982).

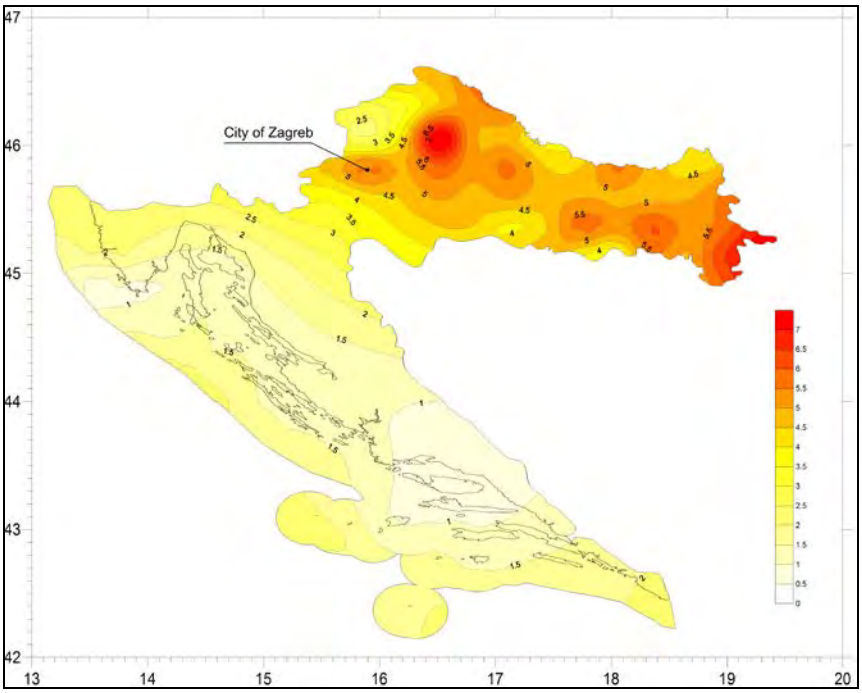

Fig. 1. Geothermal gradients in the Republic of Croatia

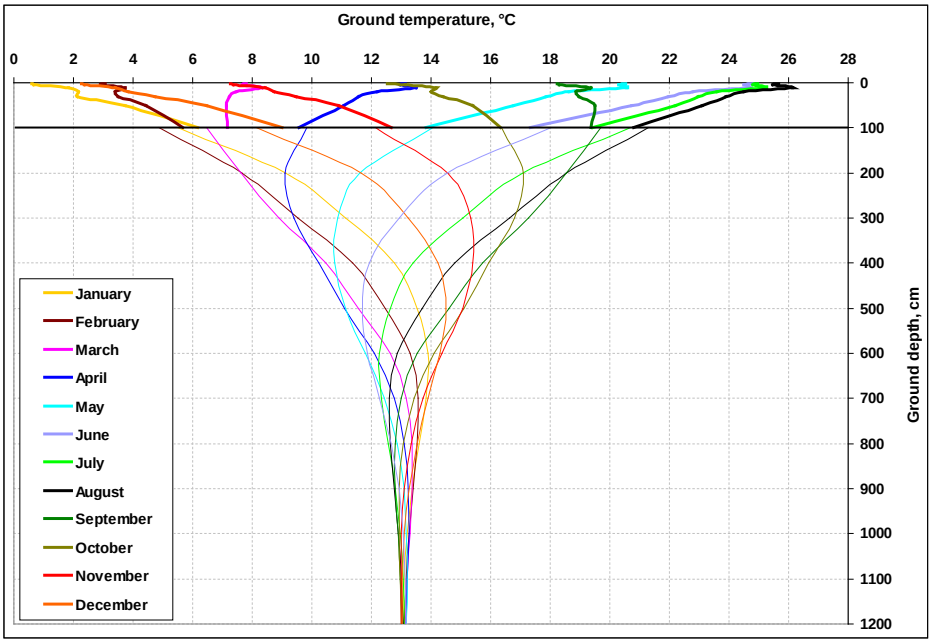

Fig.2. Measured average monthly ground temperatures up to 100 cm and calculated monthly ground temperature oscillations (100-1200 cm) for a meteo station Zagreb-Maksimir (Kurevija, 2010)

By solving the sinusoidal temperature amplitude damping function it can be perceived from Fig.2. that for depth of 1200 cm ground temperature amplitude amounts 0,1°C, and undisturbed ground temperature equals 13,1°C. This value is one of the most important parameters in modeling of borehole heat exchanger.

3. Analysis of Geothermal Heat Pump with Borehole Heat Exchanger Field

After determining undisturbed ground temperature and geothermal gradient in Zagreb location, analysis of ground heat exchanger will be carried out to determine impact of those two parameters. As an example, building with total area of 2500 m^2 and completely heated and cooled with shallow geothermal resource will be discussed. Numerical computation and sizing of borehole heat exchanger will be done with commercially available software *Ground Loop Designer (GLD)* which uses both heat transfer models described in introduction chapter. Second model will be applied (simplified line source heat transfer theory - Swedish/Lund method) because it gives more detailed evolution of the borehole wall and carrier fluid temperatures over long-term period.

Analysis will be based on fixed number of bores in borehole heat exchanger field. Two boreholes array grid will be discussed to determine effect of thermal interferences over long-term period of utilization, one rectangular shaped and compactly arranged in form 5x4, which is presumed to have significant borehole thermal interference effect on loop sizing, and one rectangular shaped in form of 10x2 which is presume to have smaller interferences. Both grids will be simulated in two modes: first one by importing only undisturbed ground temperature (if there is lack of data from circulating carrier fluid through bores prior Thermal Response Test - this is usually done for first approximation in pre-feasibility studies) and second one by importing effective ground temperature (mean ground temperature through the bore depth calculated by including surface variations in first few meters of soil and geothermal gradient which describes temperature rise versus depth). Table 1 shows input data from building annual energy consumption. This was simulated using building energy balance software *KI Expert* which incorporates Croatian directives regarding rational use of energy in buildings and prescribes allowable thermal conductivity factors.

Table 1. Building energy balance

Month	**Heating**	**Cooling**
January	40 633	195
February	25 544	311
March	13 288	764
April	4 003	2 499
May	418	6 403
June	14	10 190
July	0	13 170
August	3	10 261
September	398	4 392
October	6343	1 284
November	21 831	341
December	37 859	289
Total, kWh	**150 355**	**50 096**
Heating/Cooling ratio	3,00	
Peak load 8 hours, kW	99,2	95,8
Annual full load hours	1 516	523

From Table 1 it can be seen that the ratio between energy used during heating season and energy used during cooling season is 3,0. This indicates that more heat would be extracted to the ground than it would be rejected to it (in cooling mode total rejected heat to the ground is the sum of heat rejected from the building and the heat of compression from heat pump) which doubtlessly would cause some cooling of the ground in long-term period of utilization. Borehole input parameters and thermogeological characteristics of the ground at the location can be seen from Table 2. Value of ground thermal conductivity was taken from in-situ measurements conducted on 100m bore (Soldo 2010). Table 3. shows example of designed input parameters for the heat pump system (Waterfurnace EKW130 was used for purpose of this analysis). Building is presumed to have floor heating system with leaving load temperature (LLT) of 40,8°C with entering load temperature (ELT) to the heat pump of 37,8°C. Loop side is set with entering source temperature (EST) of 0°C and leaving source temperature (LST) of -2,3°C.

Table 2. Borehole heat exchanger and thermogeological ground parameters at the site

Loop solution properties	**-Water 76,5% - Propylene glycol 23,5% mixture;** **-Freezing point: -9,4°C** **-Specific heat capacity: 3,992 kJ/kg°C;** **-Density 1024,5 kg/m^3**
Polyethylene single U-pipe parameters	-Pipe size 1" (27,41mm ID/33,40mm OD); -Pipe type SDR11; -Thermal resistance: 0,060 m °C/W; -Average radial pipe placement inside bore
Borehole parameters	-Diameter 130 mm; -Grout thermal conductivity: 2,13 W/m °C; -Borehole eq. thermal resistance: 0,121 m °C/W -Separation distance in grid array: 6,0 m
Ground properties	-Lithology: mostly brown wet clay and unconsolidated coarse sand with thin layers of gravel and marl -Mean volume-specific heat capacity: 2,77 MJ/m^3°C -Undisturbed ground temperature: 13,1°C -Mean thermal conductivity: 1,70 W/m°C -Mean thermal diffusivity: 0,053 m^2/day

Table 3. Example of heat pump system designed input parameters used in ground loop simulation for grid array 5x4 with geothermal gradient included in analysis

Grid array 5x4 with included geothermal gradient	**Heating**	**Cooling**
Source side fluid temperatures, °C	0/-2,3 (EST/LST)	23,6/27,4 (EST/LST)
Load side fluid temperatures, °C	37,8/40,8 (ELT/LLT)	12,0/8,5 (ELT/LLT)
Total unit capacity, kW	99,2	114,6
System peak load, kW	99,2	95,8
Compressor peak demand, kW	28,3	18,8
Heat pump COP, kW/kW	3,5	5,1
Heat extracted/rejected from/to ground	70,9	114,6
Heat pump partial load factor	1,00	0,85

Investigations carried out in relevant literature (Kavanaugh 1984, Eskilson 1987) suggest that geothermal heat pump systems should be sized for at least 30 years period of operation to minimize thermal interferences effects and account sub-cooling of the ground. Principle of multi-year sizing is not to allow minimum temperature of the carrier fluid during peak-load conditions to approach its freezing point during that time and to assure that average fluid temperature of the solution inside the loop be near designed 0°C even after 30 years of operation. If the geothermal system is designed just for 1 year operation, result would be rather small and 'economic' loop size but after multi year of operation loop solution temperature would significantly drop, due to thermal interferences and sub-cooling of the ground, resulting in that way in very inefficient and troublesome system.

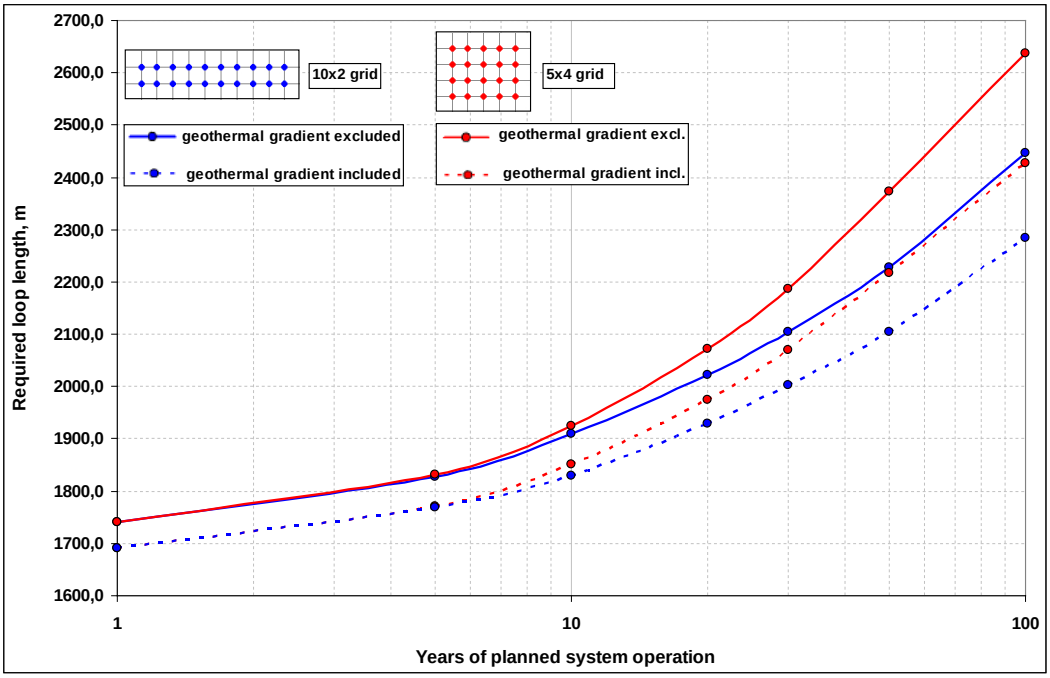

Fig.3. Results of sizing ground loop according to years of planned system operation and various array grids with input data presented in Tables 1,2 and 3 with borehole spacing distance of 6,0m

On Fig.4. results of ground loop simulation are presented. As mentioned, ground loop was simulated for two different grids, compact rectangular 5x4 grid and rectangular 10x2 grid. For both grids variations where calculated inserting in model firstly undisturbed ground temperature of 13,1°C for Zagreb location and then secondly effective ground temperature, which was influenced by geothermal gradient. Variations for different borehole separation distances were introduced to evaluate effect of thermal distances. It can be seen that for low separation distances (below 6,0 m) loop size drastically arises to compensate effect of thermal interferences of an adjacent bores. Also, it can be perceived that geothermal gradient, if introduced in effective ground temperature calculation, significantly influences loop size. For instance, if 5x4 array grid with bores separation distance of 6,0 m is observed, as shown in results from Table 4, it can be seen that analysis which included geothermal gradient in effective ground temperature calculation has 5,3% reduction in loop length, as oppose to analysis which included only undisturbed ground temperature.

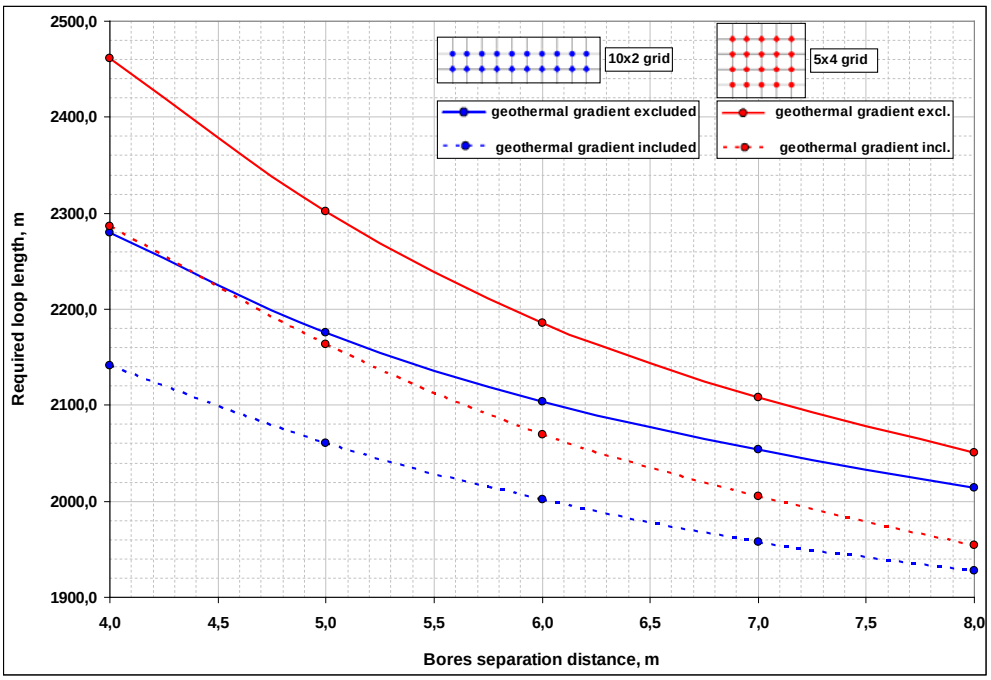

Fig.4. Results of sizing ground loop according to different borehole separation distances and various array grids with input data presented in Tables 1,2 and 3 for 30 years of operation

Table 4. Results of sizing borehole ground loop with calculated changes in loop size due to influence of geothermal gradient

Borehole spacing distance, m	Loop size (Gradient excluded 13,1°C), m	Loop size (Gradient included), m	Change in loop size, %	Depth per bore, m	Effective ground temperature with gradient included, °C	Ground temperature difference, °C
5x4 Borehole Array Grid						
4,0	2460,9	2286,3	7,1	114,3	14,15	1,05
5,0	2301,8	2163,1	6,0	108,2	13,99	0,89
6,0	2186,1	2069,5	5,3	103,5	13,89	0,79
7,0	2107,7	2005,7	4,8	100,3	13,82	0,72
8,0	2050,9	1954,7	4,7	97,7	13,73	0,63
10x2 Borehole Array Grid						
4,0	2279,9	2141,4	6,1	107,2	13,97	0,87
5,0	2175,1	2060,4	5,3	103,0	13,89	0,79
6,0	2103,7	2001,8	4,8	100,1	13,81	0,71
7,0	2053,8	1957,2	4,7	97,9	13,78	0,68
8,0	2014,2	1927,5	4,3	96,4	13,73	0,63

On Fig.5. results of long-term ground loop operation simulation are presented. It can be seen that if loop is sized for 30 years of operation, first years of operation would be most efficient for the geothermal system, as it benefits from 'oversized' loop. After 30 years some indication of steady state appearance can be noticed in loop solution temperatures.

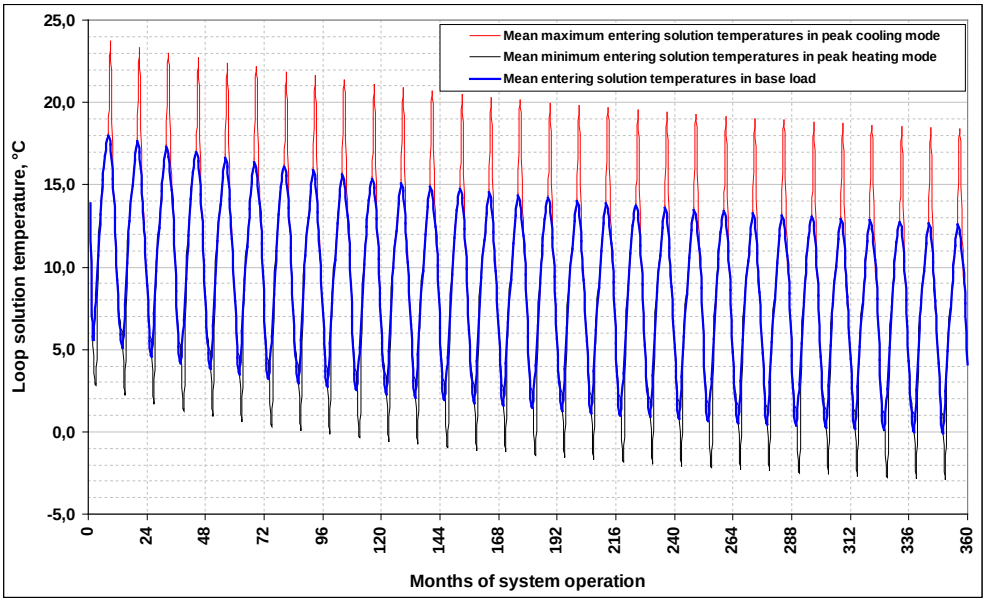

Fig.5. Changes in loop solution temperatures for 30 years of operation for array grid 5x4 and included geothermal gradients, with input data seen in Tables 1 to 4.

4. Conclusion

Analysis of geothermal gradient influence on borehole heat exchanger system showed that for regions where gradients are significantly higher than average, as it is case for northern part of Republic of Croatia, special care should be taken when defining parameters for simulation software input file. As seen from presented results in Fig.4 and Table 4. if only undisturbed ground temperature is entered, which in case of Zagreb location is equal to 13,1°C, and not effective ground temperature that for same location, in 5x4 array grid with 6,0 m bores spacing distance and 103,5m per bore depth, is equal to 13,9°C loop length differs 5,3%. Therefore, this percentage could not be neglected in pre-feasibility project analysis.

References

[1] Carslaw, H. S.; Jaeger J. C. 1946. Conduction of Heat in Solids, Oxford,Claremore Press.

[2] Ingersoll, L.R.; Zobel, O.J.; Ingersoll, A.C. 1954. Heat Conduction with Engineering, Geological and Other Applications. Madison, WI: The University of Wisconsin Press.

[3] Kavanaugh, S.P.; Rafferty, K. 1997. Ground-source Heat Pumps: Design of Geothermal Systems for Commercial and Institutional Buildings. American Society of Heating, Refrigeration and Airconditioning Engineers, Inc., Atlanta, GA.

[4] Eskilson, P. 1987. Thermal Analysis of Heat Extraction Boreholes. Doctoral Thesis, University of Lund, Department of Mathematical Physics. Lund, Sweden.

[5] Kurevija, T.; Vulin, D. 2010. Determining Of Undisturbed Ground Temperature As The Part Of Shallow Geothermal Resources Assessment, The Mining-Geological-Petroleum Bulletin, Faculty of Mining, Geology and Petroleum Engineering, Vol.22, p.27-36

[6] Soldo, V.; Rusevljan, M.; Curko, T.; Grozdek, M. 2010. Ground-source heat pump with a 100 m deep borehole heat exchanger – start up and first results, IIR/Eurotherm Sustainable Refrigeration and Heat Pump Technology Conference, Stockholm

Utilization of geothermal heat pumps in residential buildings for GHGs emission reduction

Farideh Atabi[1*], Seyed Mohammad Reza Heibati[2], Arash Rasouli[3], Ali Poursaeed[4]

[1*] *Assistant Prof., Graduate School of Energy and the Environment, Science & Research Branch, Islamic Azad University, Tehran, Iran*
[2] *Faculty Member of Islamic Azad University, Pardis Branch, Iran*
[3] *B.Sc. Student in Mechanical Engineering, Science & Research Branch, Islamic Azad University, Tehran, Iran*
[4] *B.Sc. Student in Mechanical Engineering, University of Tehran, Iran*
[*] *Corresponding author: Tel: +9821 22292909, E-mail: far-atabi@jamejam.net*

Abstract: This study aims to reduce energy consumption by application of geothermal heat pumps in residential buildings and reduction of Greenhouse Gases (GHGs) emissions under Clean Development Mechanism (CDM) project. In this approach, the required thermal load of a typical four-floor 12-units residential building located in Tehran city has been considered and calculated separately based on the actual operational data. According to the thermal properties of soil and the annual average temperature of the area, the appropriate geothermal heat pump system has been taken into consideration. Subsequently, three scenarios based on transaction of Certified Emission Reductions (CERs) as Primary, Secondary and Unilateral types of CDM projects were created considering the primary costs of purchase and installment of geothermal heat pump system and its electricity consumption. Technical, economical and environmental feasibility study of this project has been assessed through using Proform software in three different scenarios based on global carbon credit market.

The results show that in the optimum scenario in case of replacing the boiler system with vertical geothermal heat pump system in the residential building, could conserve 67,000 GJ of natural gas during the project implementation period and 3,759 tons of CO_2 equivalent emissions would be reduced. Results demonstrate also the favorable economic and environmental impacts that can be achieved by CDM.

Keywords*: Geothermal Heat Pump, GHGs Emission, Residential Building, Carbon Credit*

1. Introduction

Geothermal energy use avoids the problem of acid rain, and it generally reduces greenhouse gas emissions and other forms of air pollution. A continuing strong market for geothermal heat pumps is anticipated as a result of the increasing interest in controlling atmospheric pollution because of the spreading concern about global warming and because of their reliability, high level of comfort, low demand, and low operating costs. Ground source heat pumps (GSHPs), also known as geothermal heat pumps (GHPs), are attractive alternatives for both conventional heating and cooling systems because of their higher energy efficiencies. However, GSHP systems have recently been applied to many residential and a few commercial buildings for heating/cooling purposes [1,2]. These systems have had the largest growth since 1995, almost 59 or 9.7% annually in the United States and Europe. The installed capacity is 6850 MW and annual energy use is 23,214 TJ/year in 26 countries. The actual number of installed units was around 500,000 in 2000. It is also estimated that there are over a million today (e.g. [3,4-9]).

GSHPs have several advantages over air source heat pumps, as given by Lund and Freeston [10]: (a) they consume less energy to operate; (b) they tap the earth or groundwater, a more stable energy source than air; (c) they do not require supplemental heat during extreme low outside temperature; (d) they use less refrigerant; (e) they have a simpler design and consequently less maintenance; and (f) they do not require the unit to be located where it is exposed to weathering. The main disadvantage is the higher initial capital cost, being about 30-50% more expensive than air source units. This is due to the extra expense for burying heat exchangers in the earth or providing a well for the energy sources. However, once

installed, the annual cost is less over the life of the system, resulting in a net savings. In a comprehensive study conducted by Lund et al. [11], it is reported that GSHPs have the largest energy use and installed capacity according to the 2005 data, accounting for 54.4% and 32.0% of the worldwide capacity and use. The installed capacity is 15,384 MW_t and the annual energy use is 87,503 TJ/year, with a capacity factor of 0.18 (in the heating mode) [12].

The concept of GHP is not new. However, the utilization of GHPs in residential buildings is very new in Iran, although they have been in use for years in developed countries and the performance of the components is well documented. Worldwide GSHPs account for 12% of the geothermal energy used for direct applications, amounting to approximately 16,500 TJ (4580 GWh) annually. Present estimates indicate that there are over 150,000 groundwater and 250,000 ground coupled (55% vertical) heat pump installations in the USA [13]. According to the Kyoto Protocol, industrialized countries have agreed to reduce their overall emission of greenhouse gases (GHGs) by at least 5 percent below 1990 levels in the commitment period 2008–2012 (United Nations, 1998). In order to minimize the compliance cost, three flexible mechanisms are defined: the Clean Development Mechanism (CDM), Joint Implementation (JI), and Emission Trading (ET). CDM is the only mechanism applicable to the developing countries. Certified Emission Reductions (CERs) is a unit of GHGs reductions issued pursuant to the Clean Development Mechanism of the Kyoto Protocol, and measured in metric tons of carbon dioxide equivalent. One CER represents a reduction in greenhouse gas emissions of one metric ton of carbon dioxide equivalent. Primary CDM is the transaction of CERs between the original owner of the carbon asset and a buyer in the market. Depending on the amount of risks taken by the buyer and the seller, the price of CERs is agreed upon, which is lower than the secondary CDM prices. Secondary CDM is the transaction where the seller is not the original owner of the carbon asset. Usually, the seller and the buyer of secondary CDM are Annex I countries. Secondary CERs have higher prices than primary CERs due to its minimal risks imposed on the buyer. Unilateral CDM is the type of CDM project that an Annex I country is not involved and the developing country accepts all the risks and expenses in order to sell the CERs with higher prices in the market [14]. However, the developing country requires past experience in development and marketing of CDM projects. The present study deals with technical, economical and environmental feasibility assessment of a four-floor 12-units residential building, located at east of Tehran city, capital of Iran in which a boiler system is replaced by vertical ground source heat pump system under Primary, Secondary and Unilateral CDM projects.

2. Methodology

The residential building under study is a 12-unit complex located at east of Tehran city with four floors and the area of 565m^2 at each floor. The required heating and cooling loads of the building was calculated based on number of residents. Then considering the geographical position, thermal properties of the soil and the climate conditions, for supply of air and water heating, a vertical GSHP system was introduced to replace the present boiler. The reasoning for choosing the vertical type was land limitation, the necessity of keeping the private boundaries of the neighbors and also having the possibility of penetration into depth under ground in order to achieve a rather stable temperature all throughout the year. Then based on the global carbon market, by using Proform software, three scenarios based on Primary, Secondary and Unilateral types of CDM projects were created considering the primary costs of purchase and installment of GSHP system to replace the boiler system. Table (1) shows the specifications of the present heating system of the building.

Table 1. Specifications of the present heating system (boiler)

System Type	Efficiency (%)	Fuel Type	Annual Gas Consumption (GJ/y)
Boiler	75	Natural Gas	16750

For replacing the boiler system by GSHP system and in order to supply the required heating loads in the residential building, some required information and specifications are shown in Table (2).

Table 2. Required information and specifications for choosing proper geothermal heat pump for the desired building

Isentropic Compressor Efficiency (%)	75	Heating load(kW)	220
Electrical Compressor Efficiency (%)	80	Cooling l(kW)	184.4
Pump Efficiency (%)	80	total time of heating operation mode (h/y)	2880
Pump motor Efficiency (%)	80	System function of time for full time(h/y)	1350
Condenser internal diameter (m)	0.0318	System lifetime (year)	10
Condenser external diameter (m)	0.0348	Interest rate (%)	10
Thermal conductivity coefficient of condenser tube (kW/m°C)	0.398	Coefficient of thermal conductivity of soil (W/m°C)	4.2
Inner diameter tube evaporator(m)	0.0318	Earth temperature (°C)	16
Outer diameter tube evaporator (m)	0.0348	Overall heat transfer coefficient in soil (W/m2°C)	12
Heat pipe thermal conductivity coefficient (W/m°C)	0.3979	Thermal conductivity coefficient of evaporator tubes (kW/m°C)	0.398

According to Table (2) and the specifications provided by the manufacturer of different types of geothermal heat pumps [15], and by applying the correlations offered in the reference No.16, the vertical GSHP system with the specifications given at Table(3) was chosen for supplying the required air and water heating.

Table3. Technical specifications and costs of the chosen GSHP system in the building under study

Vertical pipe length converter (m)	9000	Compressor power consumption (kW)	3900
Type of pipe	polyethylene	Power pump (kW)	5.5
The initial investment cost (US$)*	28073.67	Deep wells (m)	111.8
Electricity consumption (MWh/y)	60	Coefficient of performance(COP)**	4.94

*Cost of initial investment is: cost of pump + cost of compressor + cost of operator + cost of condenser + cost of excavation + cost of piping + cost of vertical land converter + cost of installation and launching.

**The temperature dependence of the efficiency has been neglected.

2.1. Technical, Economical and Environmental Assessment of GSHP System

Technical, economical and environmental feasibility study of the chosen GSHP system in the residential building has been implemented by Proform software. Some required information about the present boiler system and new system (GSHP) are offered at Tables (4) and (5). Based on the international carbon credit market, three scenarios were created according to the data on Table (6) and compared by Proform software.

Table 4. Technical data provided as input for Proform software

Depreciation period (Years)	GSHP Capacity (kW)	Coefficient of performance (%) GSHP	Life time GSHP (Years)	GSHP energy consumption (MWh/y)	Boiler efficiency (%)	Type of fuel consumed by the boiler	Old system energy consumption (boiler) (MWh/y)
10	220	4.95	10	60.053	75	Natural gas	465.2

Table 5. Financial and economical data provided as input for Proform software

Discount rate (%)	Income tax rate (%)	Initial investment cost of the GSHP system (US$)	Inflation rate* (%)	Annual interest rate of electricity price (%)	Annual interest rate of natural gas price (%)	Natural gas consumption ** (US$/Gj)	Electricity price (US$/kWh)
16	15	28073.67	20.2	21	5.6	0.271	0.011

*Annual inflation rate based on the report of Central Bank of Islamic Republic of Iran, General Director of Economic Statistics, May 2009.
** Energy Balance, 2008, each m^3 of natural gas GJ 0.03726 and price of natural gas [17].

Table 6. Scenario Analysis based on carbon credit defined by World Bank

Scenarios	Value of carbon credits reduction CO_2 (US$/ton CO)	Price Growth Rate (%)	Sales income tax (%)
Scenario A	10	15	0
Scenario B	15	15	0
Scenario C	20	20	0

As shown in Table (6), carbon credit in scenario A (Primary CDM) is US$ 10/tonCO_2, in scenario B (Secondary CDM) is US$ 15/tonCO_2 and in scenario C (Unilateral CDM) is US$ 20/tonCO_2. In case of taking no action for sale of carbon credit, the results of such case was also compared with the scenario analysis results. The depreciation rate considered in accordance with statistics of balance sheet in the year 2008 is equivalent to 16%. Also income tax rate was considered to be 15%, but the income generated by sales of carbon credit is free from any tax.

3. Results and Discussions

Replacing the boiler system by GSHP system could conserve 67,000 GJ of natural gas (601 MWh/10yr electricity). In Table (7), the amounts of GSHP electricity consumption and decrease in fossil fuel consumption caused by implementation of the project have been shown.

Table7. Amounts of electricity consumption and decrease in fuel consumption over the life of the GSHP system

	Power consumption by GSHP (MWh)	Natural gas consumption rate (GJ000)
Average Annual	60.053	7
Total Project (10 yr)	601	67

As shown in Table (8), in scenario A, taking all the initial investment costs as well as the installment and operation costs fro replacing the boiler by GSHP system into account , the pay back period is 3.9 years. Moreover, net present value (NPV) without tax is estimated to be about US $ 17,000 and the internal rate of return (IRR) is about 27.45%. In case of tax being included, NPV is US$ 15,000, the IRR is 25.88%. In scenario B, the pay back period is 3.1 years. Taking tax into account, the NPV is US$ 30,000 and IRR is 34.66%, however without considering tax, NPV is US $ 33,000 and IRR is 36.11%. In scenario C, before tax, NPV is US $ 62,000 and the pay back period is in 2.6 years and the IRR is 47.66%. In case of considering tax, NPV is US $ 59,000 and IRR is 46.38%. Since the IRR is more than the interest rate (16%), the project is proven to be cost-effective in this case. In case of taking no action for sale of carbon credit, the results show minus profit.

Table 8. Economic assessment of different scenarios A, B, C

Scenarios	Before tax			After Tax	
	Simple pay back (year)	Net present value (NPV) (US$)	Internal rate of return (IRR) (%)	Net present value (NPV) (US$)	Internal rate of return (IRR) (%)
Scenario A	3.9	17000	27.45	15000	25.88
Scenario B	3.1	33000	36.11	30000	34.66
Scenario C	2.6	62000	47.66	59000	46.38
Without considering the sale of carbon credit	8.8	-14000	2.74	-16000	-

Net present values in different scenarios before and after tax have been compared over the life of the GSHP system (10 years) and according to Fig. (1) The scenario C in comparison to other scenarios has higher profit making.

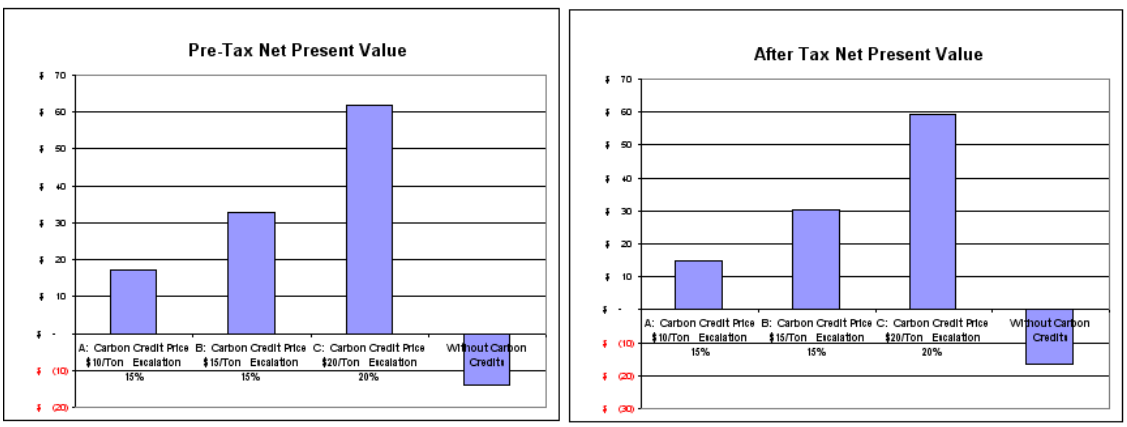

Fig.1. Comparing net present values in different scenarios before and after tax

Table (9) shows the annual income gained by sales of carbon credit in the three scenarios, so that if in the first year (year 0) the amount of US $ 30,000 is invested in the project, the amount of profit during the next year (year 1) in scenario A will be US $ 7,000, in scenario B will be US $ 9,000 and in scenario C will be US $ 10,000. While, in case of non selling of carbon credit, only US $ 3,000 profit in one year will be gained which makes the implementation of the whole project economically non feasible and non profitable. Furthermore, in the next coming years over the life of the project (10 years) the annual cash flow is compared and shown in the Table(9).

Table 9. Annual profit gained by sale of carbon credit in three scenarios during 10 years

Annual Cash Flow (US$000) Before Taxes				
	Without sale of Carbon Credit	Carbon Credit (Scenario A)	Carbon Credit (Scenario B)	Carbon Credit (Scenario C)
Year 0	-30	-30	-30	-30
Year 1	3	7	9	10
Year 2	3	7	10	12
Year 3	3	8	11	14
Year 4	3	9	12	16
Year 5	3	10	13	19
Year 6	4	11	15	22
Year 7	5	12	17	26
Year 8	5	14	19	31
Year 9	5	16	21	36
Year 10	6	17	24	43

Results of Proform software show that the elimination of natural gas consumption in the building reduces green house gases emission by 658 tons of CO_2 equivalent per year and by 3759 tons of CO_2 equivalent during the whole period of implementing the project. As shown in Fig. (2), the rate of CO_2 emission reduction is going up over the time.

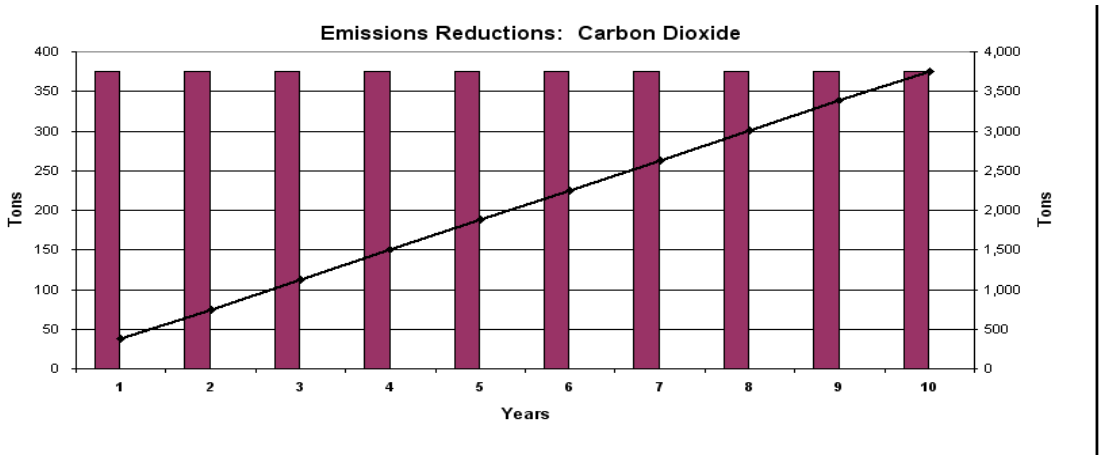

Fig. 2. CO_2 emission reduction during different years of the project implementation

4. Conclusion

In the present study a four-floor 12 unit residential building located at east of Tehran was assessed in the case of replacing the present boiler system by a vertical geothermal heat pump system. Based on the global carbon credit market, by using Proform software, three scenarios were considered on the basis of the primary costs of purchase and installment of GSHP

system to replace the boiler system. In scenario A considering all the investment expenses as well as the installment and operation costs of the geothermal heat pump and replacing boiler with it, the pay back period is 3.9 years. Moreover, considering tax, NPV is estimated to be US $ 15,000 and the internal rate of return (IRR) is about 25.88%. In scenario B the pay back period is 3.1 year. Considering tax, NPV is US $ 30,000 and IRR is 34.66%. In case of implementing scenario C, the NPV is US $ 59,000 and the pay back period is 2.6 years. Furthermore, IRR is 46.38%. Therefore, it is suggested that this project be implemented according to scenario C in which IRR is more than the other two scenarios. The results show that in the optimum scenario in case of replacing the boiler system by vertical geothermal heat pump system under the CDM project in the residential building could conserve 67,000 GJ of natural gas during the project implementation period (10 years) and 3,759 tons of CO_2 equivalent emissions would be reduced. Thus, the results clearly demonstrate that increasing geothermal utilization results to GHG emission reduction while helping to meet increasing power demand. It demonstrates also the favorable economic and environmental impacts that that can be achieved by CDM. The message is that the utilization of GSHP without carbon credit is economically not feasible. However, significant opportunities for GSHP CDM projects are likely to extend into future decades.

References

[1] Kavanaugh SP. Field test of vertical ground-coupled heat pump in Alabama. ASHRAE Transactions, 1992,98:60716.

[2] Hepbasli A, Akdemir O. Energy and exergy analysis of a ground source (geothermal) heat pump system. Energy Conversion and Management 2004,45:73753.

[3] Lund J.W. Ground source (Geothermal) heat pumps. Course on heating with geothermal energy: conventional and new schemes, Convener Paul J Lienau, WGC 2000 Short Courses Kazuno, Thoku District, Japan 810 June, 2000, p. 20936.

[4] Lund J. W. Geothermal heat pumps-trends and comparisons. Geo-Heat Center Q Bull 1989,12(1):16.

[5] Lund JW, Freeston DH. World-wide direct uses of geothermal energy 2000. Proceedings world geothermal 587 congress 2000, Kyushu-Tohoku, Japan, May28 - June 10, 2000, p. 121.

[6] Lund JW, Freeston DH. World-wide direct uses of geothermal energy 2000. Geothermics, 2000,30:2968.

[7] Lund JW. Direct use of geothermal energy in the USA. Appl Energy 2003,74:3342.

[8] Lund JW. Geothermal heat pump utilization in the United States. Geo-Heat Center Q Bull 1988,11(1):507.

[9] Lienau PJ, Lund JW. Geothermal direct use. Testimony presented at the house subcommittee on environment, July 30. Geo-Heat Center, Klamath Falls, OR; 1992.

[10] Lund JW, Freeston DH. World-wide direct uses of geothermal energy 2000. Proceedings world geothermal congress 2000. Kyushu-Tohoku, Japan, May 28June 10, 2000. p. 121.

[11] Lund JW, Freeston DH, Boyd TL. Direct application of geothermal energy: 2005 worldwide review. Geothermics 2005,34(6):691727.

[12] Akpinar E. .K , Hepbasli A., A comparative study on exergetic assessment of two ground-source (geothermal) heat pump systems for residential applications, Building and Environment, 2007, 42 :20042013

[13] Lund JW. Geothermal heat pump utilization in the United States. Geo-Heat Center Q Bull 1988,11(1):507.

[14] United Nations Development Program (UNDP), Human & Income/Poverty in Developing Countries, 2008.

[15] http://www.fhp-mfg.com/aecinfo/1/company/09/09/81/company_1.html

[16] Sanaye S., Niroomand B., "Thermal economic modeling & optimization of vertical ground coupled heat pump", Energy Conversion & Management, 2000, 50, 1136 - 1147.

[17] Ministry of Energy, Energy Balance, Iran Energy optimization Organization, 2008.